

DOSAGE-SENSITIVE MODIFIERS OF *SLIT* FUNCTION

**DOSAGE-SENSITIVE MODIFIERS OF *SLIT* FUNCTION IN THE
DROSOPHILA EMBRYONIC CNS**

by

ADRIENNE L. STEVENS, B.Sc (Honours)

A Thesis
Submitted to the School of Graduate Studies
in Partial Fulfillment of the Requirements
for the Degree
Master of Science

McMaster University

© Copyright by Adrienne L. Stevens, July 2000

MASTER OF SCIENCE (2000)
(Biology)

McMaster University
Hamilton, Ontario

TITLE: Dosage-sensitive modifiers of *slit* function in the *Drosophila*
embryonic CNS

AUTHOR: Adrienne L. Stevens, B.Sc. (Honours), Mount Allison University

SUPERVISOR: J. Roger Jacobs, Ph.D., Associate Professor, McMaster University

Number of Pages: xvii, 248

ABSTRACT

Genetic screens provide information on phenotype interactions as a step to uncovering functional interactions in vivo. In this study, I conducted genetic modifier screens in *Drosophila* that might reveal genes expressed in the embryonic CNS that interact genetically with *slit*. These screens include a blind genetic screen, stable line double mutant analysis, transheterozygote interactions and a dosage-sensitive dominant modifier screen. Differences in CNS phenotypes between the blind screen and the double mutant analysis were uncovered for some of the crosses, indicating background effects of genotype can influence phenotypes observed.

A group of candidate genes were chosen based on motif composition for potential interaction with *slit*, and spatial and temporal expression patterns coinciding with Slit. The majority of these genes show a mutant CNS phenotype on their own. *slit*-interacting genes were identified by their ability to alter midline axon guidance, as assayed with antibodies specific to CNS-expressing proteins. The interacting genes include those encoding receptor and second messengers thought to function in growth cones, integrins and extracellular matrix proteins. From these interactions, I could then propose models of function in axon guidance.

The first model I propose adds to a currently known repressor-derepressor model of axon guidance at the midline of the CNS, involving the Netrin, Commissureless and Robo signaling molecules, whereby Slit is locally suppressed by Netrin function to allow axons to cross the midline via Commissureless-mediated internalisation of Robo. In my second model, Slit may also be involved in integrin signaling, especially through the α PS3 and β PS integrins, in concert with the Laminin molecule. Included in this model is the intersection of cytoplasmic Dock signaling within the growth cone. Thirdly, I demonstrate a genetic interaction with other molecules expressed by the midline glia, Masquerade, Toll and Neurexin. Masquerade and Toll may function in a common pathway, but in parallel to Slit function. Likewise, Neurexin may function in a parallel pathway to Slit.

Slit has shown to interact genetically with a number of molecules that appear to be involved in different aspects of axon guidance. This study was meant to provide a survey

of molecules that may functionally interact with Slit and provides a good basis upon which to explore the interactions in detail in future work.

ACKNOWLEDGEMENTS

First, I would like to thank my supervisor, Dr. J. Roger Jacobs, for providing me with the opportunity to complete a Master's degree in his lab. Roger, I appreciate the time you took to help me develop this project and troubleshoot through a difficult analysis process. This experience has no doubt prepared me for what lies ahead. Roger, I wish you all the best and continued success in this research.

Next, I want to thank my defence chair and committee member, Dr. Ana Regina Campos. Ana, I appreciate the time you set aside to assist in developing my project as a committee member, and your encouraging voice as I examine my future goals and prospects. I wish you the very best in your research. I would also like to thank Dr. Morton for your time and energy spent on examining my thesis as my third defence committee member.

Next, to all of those lab people who have touched and contributed to my life over the past (almost) three years! First, I need to thank Robin Battye for his knowledge, advice and sense of humour that has very much helped - and entertained - me over the past few years. I wish you all the best in your future career and successes. To Allison MacMullin and Amanda Hawley, thanks for your friendships and good luck finishing your degrees. I hope you both have realised the impression that you have made on my life over the past two years. To all others over the past years, Brad Lanoue, Amber Wenstob, Michael Gordon, Mythili Nadella, Sean Reichheld, and to the new kids on the block, Yvonne Sinniah, Mark Settle and Roni Gordon, thanks for adding and contributing to lab life. To members of the Campos Lab, especially Marta Boszko, Dorothy DeSousa and Jana Hassan, thanks for the laughs and encouragement. To the soccer team, the "fish people", and so many others around this department, I have thoroughly enjoyed getting to know you over the years.

To my husband, Chris, your encouragement and support have been fundamental in the successful completion of this degree. I hope you know that a portion of this degree belongs to you for all that you have been and done for me. I look forward to the adventures that await us in the future.

Finally, to my Lord and Saviour, Jesus Christ. To You, I credit all that I have accomplished. Thank-you for being by my side and continually showing me the plans You have for me, to give me a hope and a future (Jeremiah 29:11).

TABLE OF CONTENTS

	PAGE
Title Page	i
Descriptive Note	ii
Abstract	iii
Acknowledgements	v
Table of Contents	vi
List of Illustrations	ix
Abbreviations	xv
Chapter 1 INTRODUCTION	
1.1 Development of the <i>Drosophila</i> CNS	1
1.11 Overview of neurogenesis and gliogenesis	1
1.12 Axonogenesis	6
1.2 Molecules and mechanisms involved in axon guidance	7
1.21 Overview of strategies and mechanisms	7
1.22 Attractive function of the midline	11
1.23 Repulsive function of the midline	12
1.3 Slit family of proteins	14
1.31 <i>Drosophila</i> Slit	14
1.32 Other Slit family members	21
1.33 Slit and Robo1 function together in the repulsion pathway	22
1.4 Research strategy	23
Chapter 2 METHODS	
2.1 <i>Drosophila melanogaster</i> fly stocks	25
2.2 Mutations and deficiency lines	25
2.3 Antibodies	25
2.4 Embryo collections	25
2.5 Fixation protocol	31
2.6 Immunocytochemistry protocol	32
2.7 Mounting and photography	33
2.8 Experimental design and data analysis	34
2.81 Blind screen	34
2.82 Double mutant analysis	34
2.83 <i>slit/robo1</i> transheterozygote interaction	35
2.84 <i>slit/wrapper</i> deficiency transheterozygote interaction	35
2.85 <i>slit/scab</i> transheterozygote interaction	35
2.86 Dosage-sensitive dominant modifier screen	36
2.87 Nerve cord length	36

Chapter 3	SINGLE MUTANT ANALYSIS	
3.1	Introduction to analysis	37
3.2	Mutant phenotypes of genes involved in axon pathfinding	40
3.3	Other genes implicated in axon guidance	49
3.4	Mutations in genes that encode extracellular matrix proteins	50
3.5	Mutations in the integrin gene family	51
3.6	Mutation in a gene encoding a cell adhesion receptor	53
3.7	Mutations in genes present at septate junctions	54
Chapter 4	BLIND GENETIC SCREEN EXPERIMENT	
4.1	Introduction to blind genetic screen	55
4.2	Control crosses and <i>slit</i> alleles form the baseline comparison	56
4.3	Blind test experiments reveal some candidate genes for interaction with <i>slit</i>	59
Chapter 5	DOUBLE MUTANT ANALYSIS	
5.0	Problem of verification of phenotypes	71
5.1	Slit interacts genetically with other axon guidance molecules	71
5.11	Slit interacts genetically with Roundabout	71
5.12	Slit interacts genetically with Netrin	74
5.13	Slit interacts genetically with Commissureless	77
5.14	Slit interacts genetically with Dreadlocks	81
5.2	Slit interacts with extracellular matrix proteins and cell surface receptors	82
5.21	Slit allele interacts with LamininA	82
5.22	Slit shows a genetic interaction with Tiggrin	88
5.23	Slit interacts genetically with Masquerade	91
5.24	Slit displays a weak genetic interaction with alphaPS1 integrin, Mew	94
5.25	Slit interacts genetically with the alphaPS2 integrin, Inflated	98
5.26	Slit interacts genetically with betaPS integrin, Mys	98
5.27	Slit interacts genetically with Toll	104
5.28	Slit interacts genetically with Neurexin	107
5.3	Slit does not interact genetically with Discs-Large or Central Body Defect	110
5.31	Slit does not interact genetically with Discs-Large	110
5.32	Slit does not interact genetically with Central Body Defect	110
Chapter 6	TRANSHETEROZYGOUS AND DOMINANT MODIFIER SCREENS	
6.1	Slit alleles show different degrees of crossover penetrance in trans to Robo	113

6.2	Slit interacts genetically with deficiencies that uncover Wrapper	115
6.3	Genetic interactions with Scab	121
6.31	Scab interacts genetically with <i>slit</i> , <i>robo1</i> and <i>dock</i> mutants	121
6.32	Deficiency crosses show genetic interactions between <i>slit</i> and <i>scab</i>	124
6.4	Dosage-sensitive dominant modifier screen	131
6.41	Robo does not interact genetically with LamA or enhance the sensitised background	132
6.42	LamininB1 deficiencies enhance the <i>slit/+</i> ; <i>lamA/+</i> phenotype	132
6.43	LamininB2 deficiency strongly enhances the <i>slit/+</i> ; <i>lamA/+</i> phenotype	139
6.44	<i>scab</i> interacts to enhance the <i>slit/+</i> ; <i>lamA/+</i> phenotype	142
6.45	Netrin interacts genetically in a triple mutant combination	145
Chapter 7 DISCUSSION		
7.1	Genetic screens - critical assessment of results from different screens and experimental strategy	149
7.01	Genetic screens in flies display potential for genetic interactions to predict functional relevancy	149
7.02	Blind test strategy may provide false results in uncovering genetic interactions	150
7.03	Critical assessment of experimental strategy: modifications for future use	153
7.2	Slit alleles show similar functional interaction with Robo	155
7.3	Slit function repressed by Netrin to allow axons to cross the Comm-mediated Robo down-regulation	156
7.4	Dock may function as an intermediate player in growth cone signaling	157
7.5	Slit interacts genetically with integrins	159
7.6	Slit, Comm, Robo/Integrins/Dock pathways may intersect downstream	159
7.7	Slit and Wrapper function in parallel pathways	162
7.8	Neurexin may indirectly signal to a common Slit-binding RPTP on neurons	162
7.9	Toll may conserve its PNS repellent function in the CNS	168
7.10	Slit and Masquerade have opposing functions in different pathways	169
7.11	Toll and Mas may function together in vivo as a parallel pathway to Slit	170
7.12	Slit may not interact with Tenascin proteins	171
7.13	Dlg1 does not function downstream of Slit	172
7.14	Future projects	172
REFERENCES		174

LIST OF ILLUSTRATIONS

Chapter 1

	PAGE
Figure 1.1 Early CNS development gives rise to neural and glial precursors.	3
Figure 1.2 CNS axon tract architecture and glial positioning.	5
Figure 1.3 Downstream signaling of attractive and repulsive axon guidance cues leads to differential growth cone behaviour.	10
Figure 1.4 Current model of molecular mechanisms of growth cone guidance across the midline.	16
Figure 1.5 Motif composition of Slit and location of mutations in <i>slit</i> alleles.	19

Chapter 2

Table 2.1 Mutants and deficiencies used for genetic screens.	26
Table 2.2 Primary and secondary antibodies used for immunocytochemical analysis.	30

Chapter 3

Figure 3.1 CNS phenotype typical of wildtype embryos.	39
Figure 3.2 (A-J) Most of the candidate genes display a mutant CNS phenotype in a homozygous or hemizygous state, as visualised with mAb 1D4.	42
Figure 3.2 (K-R) Most of the candidate genes display a mutant CNS phenotype in a homozygous or hemizygous state, as visualised with mAb 1D4.	44

Figure 3.3 (A-J).	Some of the candidate genes display a mutant CNS phenotype in a homozygous or hemizygous state, as visualised with mAb BP102.	46
Figure 3.3 (K-R).	Some of the candidate genes display a mutant CNS phenotype in a homozygous or hemizygous state, as visualised with mAb BP102.	48
Chapter 4		
Figure 4.1	Control lines for <i>slit</i> blind genetic test experiment.	58
Figure 4.2 (A-J)	Blind genetic test experiment attempts to identify candidate genes for genetic interaction with <i>slit</i> .	61
Figure 4.2 (K-T)	Blind genetic test experiment attempts to identify candidate genes for genetic interaction with <i>slit</i> .	65
Figure 4.2 (U-DD)	Blind genetic test experiment attempts to identify candidate genes for genetic interaction with <i>slit</i> .	68
Chapter 5		
Figure 5.1	Immunocytochemical analysis of <i>slit</i> ²⁹⁹⁰ , <i>robo1</i> ³ stable double mutant fly line.	73
Figure 5.2	Immunocytochemical analysis of <i>netrin</i> ; <i>slit</i> stable double mutant fly lines.	76
Figure 5.3	Immunocytochemical analysis of <i>slit</i> ; <i>commissureless</i> stable double mutant fly line.	80
Figure 5.4	Immunocytochemical analysis of <i>dreadlocks</i> , <i>slit</i> stable double mutant fly lines.	84
Figure 5.5	Immunocytochemical analysis of <i>slit</i> / <i>lamininA</i> stable double mutant fly lines.	87
Figure 5.6	Immunocytochemical analysis of <i>tiggrin</i> , <i>slit</i> stable double mutant fly lines.	90

Figure 5.7	Immunocytochemical analysis of <i>slit; masquerade</i> stable double mutant fly lines.	93
Figure 5.8	Immunocytochemical analysis of <i>multiple edematous ings; slit</i> stable double mutant fly lines.	96
Figure 5.9	Immunocytochemical analysis of <i>inflated; slit</i> stable double mutant fly lines.	100
Figure 5.10	Immunocytochemical analysis of <i>mysospheroid; slit</i> stable double mutant fly lines.	103
Figure 5.11	Immunocytochemical analysis of <i>slit; Toll</i> stable double mutant fly line.	106
Figure 5.12	Immunocytochemical analysis of <i>slit; neurexin</i> stable double mutant fly lines.	109
Figure 5.13	Immunocytochemical analysis of <i>discs-large; slit</i> stable double mutant fly lines.	112
 Chapter 6		
Table 6.1	Percent segmental crossovers shown in <i>slit/robo1</i> ¹ trans-heterozygotes.	114
Figure 6.1	Immunocytochemical analysis of <i>slit/robo1</i> genetic interaction.	117
Figure 6.2	Immunocytochemical analysis of <i>slit/wrapper</i> genetic interaction.	120
Figure 6.3	Immunocytochemical analysis of gene interactions with <i>scab</i> .	123
Figure 6.4 (A-H)	Immunocytochemical analysis of <i>slit/scab</i> genetic interaction visualised with mAb 1D4.	127
Figure 6.4 (I-O)	Immunocytochemical analysis of <i>slit/scab</i> genetic interaction visualised with mAb BP102.	129
Figure 6.5	Immunocytochemical analysis of a triple mutant genetic screen involving <i>robo</i> , <i>slit</i> and <i>lamininA</i> genes.	134

Figure 6.6	Immunocytochemical analysis of a triple mutant genetic screen involving <i>lamininB1</i> locus, <i>slit</i> and <i>lamininA</i> genes.	137
Figure 6.7	Immunocytochemical analysis of a triple mutant genetic screen involving <i>lamininB2</i> locus, <i>slit</i> and <i>lamininA</i> genes.	141
Figure 6.8	Immunocytochemical analysis of a triple mutant genetic screen involving <i>scab</i> , <i>slit</i> and <i>lamininA</i> genes.	144
Figure 6.9	Immunocytochemical analysis of a triple mutant genetic screen involving <i>netrin</i> , <i>slit</i> and <i>lamininA</i> genes.	147
 Chapter 7		
Figure 7.1	Selective model of axon guidance involving Slit/Robo, Integrin and Dock signaling pathways that may influence actin cytoskeleton.	164
Figure 7.2	Integrin ligand affinity is influenced by cytoplasmic factors.	166
 Appendix Illustrations		
Figure 1	Genetic crosses for blind screen experiment - X chromosome	184
Figure 2	Genetic crosses for blind screen experiment - 2nd chromosome	185
Figure 3	Genetic crosses for blind screen experiment - 3rd chromosome	186
Figure 4	Genetic crosses for blind screen experiment - control crosses	187
Figure 5	Genetic crosses for stable double mutant fly lines - create a line with X chromosome balancer and balanced <i>slit</i> allele.	188
Figure 6	Genetic crosses for stable double mutant fly lines - create double mutant lines for X chromosome mutant and <i>slit</i> allele.	189
Figure 7	Genetic crosses for stable double mutant fly lines - create a recombined chromosome for <i>slit</i> and another mutant on the 2nd chromosome	191

Figure 8	Genetic crosses for stable double mutant fly lines - create a double mutant line for <i>slit</i> and 3rd chromosome balanced marker	192
Figure 9	Genetic crosses for stable double mutant fly lines - create double mutant lines for 3rd chromosome and <i>slit</i> allele.	193
Figure 10	Genetics for deficiency crosses.	196
Figure 11	Genetic crosses for dominant modifier screen.	197
Figure 12	Upper and lower comparison limits for all <i>slit</i> alleles demonstrate some differences between proportional nerve cord lengths.	200
Figure 13	Control lines demonstrate balancer staining pattern and <i>slit</i> only phenotypes	202
Figure 14	Other phenotypes observed in single mutant embryos.	204
Figure 15	Other phenotypes observed with <i>netrin/FM7cβ;slit /CyO[eng]</i> stable double mutant fly lines.	206
Figure 16	Other phenotypes observed with <i>slit/CyO;commissureless /TM3</i> double mutant fly lines.	208
Figure 17	<i>robo1</i> and <i>dock</i> demonstrate a weak genetic interaction in trans.	210
Figure 18	Other phenotypes observed with <i>dreadlock,slit/CyO[eng]</i> stable double mutant fly lines.	212
Figure 19	Other phenotypes observed with <i>slit/CyO; lamininA/TM3</i> stable double mutant fly lines.	214
Figure 20	Other phenotypes observed with <i>slit/CyO; masquerade/TM3</i> stable double mutant fly lines.	216
Figure 21	Other phenotypes observed with <i>multiple edematous wings/FM7cβ; slit /CyO[eng]</i> stable double mutant fly lines.	218
Figure 22	Other phenotypes observed with <i>inflated/FM7cβ;slit /CyO[eng]</i> double mutant fly lines.	220
Figure 23	Other phenotypes observed with <i>mysospheroid/FM7cβ; slit /CyO[eng]</i> double mutant fly lines.	222

Figure 24	Another phenotype observed with <i>slit/CyO;Toll/TM3</i> stable double mutant fly lines.	224
Figure 25	Another phenotype observed with <i>slit/CyO; neurexin/TM3</i> stable double mutant fly lines.	226
Figure 26	Immunocytochemical analysis of <i>central body defect/FM7cβ; slit/CyO[eng]</i> stable double mutant fly lines.	228
Figure 27	Other phenotypes observed in <i>slit/wrapper</i> genetic interaction.	230
Figure 28 (A-E)	Other phenotypes observed in <i>scab</i> genetic interactions.	232
Figure 28 (F-J)	Other phenotypes observed in <i>scab</i> genetic interactions.	234
Figure 29	Other phenotypes observed in <i>slit/scab</i> genetic interaction visualised with mAb 1D4.	236
Figure 30	Other phenotypes observed in <i>slit/scab</i> genetic interaction visualised with mAb BP102.	238
Figure 31 (A-F)	Other phenotypes observed in the triple mutant genetic screen involving the <i>lamininB1</i> (Df(2L)Trf-C6R31), <i>slit</i> (<i>slit</i> ²) and <i>lamininA</i> (<i>lamA</i> ⁹⁻³²) genes.	240
Figure 31 (G-K)	Other phenotypes observed in the triple mutant genetic screen involving the <i>lamininB1</i> (Df(2L)XE-2750), <i>slit</i> (<i>slit</i> ²) and <i>lamininA</i> (<i>lamA</i> ⁹⁻³²) genes.	242
Figure 31 (L-O)	Other phenotypes observed in the triple mutant genetic screen control cross involving the <i>slit</i> (<i>slit</i> ²) gene and <i>lamininAB1</i> (Df(2R)XE-2750) locus.	244
Figure 32	Other phenotypes observed in the triple mutant genetic screen involving the <i>lamininB2</i> (Df(3L)AC1) locus, <i>slit</i> (<i>slit</i> ²) and <i>lamininA</i> (<i>lamA</i> ⁹⁻³²) genes.	246
Figure 33	Other phenotypes observed in the triple mutant genetic screen involving the <i>netrin</i> (Df(1)NP5), <i>slit</i> (<i>slit</i> ²) and <i>lamininA</i> (<i>lamA</i> ⁹⁻³²) genes.	248

ABBREVIATIONS

Abl - abelson tyrosine kinase
AC - anterior commissure
aCC - anterior corner cell
ALPS - agrin, laminin, perlecan, slit (motif)
ANOVA - Analysis of Variance
BIO - biotinylated
C-terminal - carboxyl-terminal portion of protein
caspr - contactin-associated transmembrane receptor
cbd - central body defect
CNS - central nervous system
comm - commissureless
CS-P - Canton-S p-element free
CyO - Curly of Oster
DAB - diaminobenzidine
DCC - deleted in colorectal cancer
Df - deficiency
dlg - discs-large
dock - dreadlocks
ECM - extracellular matrix
EF - expected frequency
EG - exit glia
EGF - epidermal growth factor
EMS - ethylmethane sulfonate
eng - engrailed
ERK - extracellular signal-regulated kinase
ex - expanded
F1, F2 - first generation progeny, second generation progeny
FAK - focal adhesion kinase
FasII - Fasciclin II
FGN - fibrinogen
FM7c β - First Multiple 7c, LacZ transposon
FN - fibronectin
ftz - fushi tarazu
GDP - guanosine 5'-diphosphate
Gp1b - platelet glycoprotein 1b
GPI - glycosylphosphatidylinositol
GTP - guanosine 5'-triphosphate
HRP - horseradish peroxidase

if - inflated
Ig - Immunoglobulin
ILK - integrin-linked kinase
ISG - intersegmental glia
ISN - intersegmental nerve
kDa - kiloDaltons
L1 - neural cell adhesion molecule in vertebrates
lam - laminin
Lbm - Late bloomer
LC - longitudinal connectives
LG - longitudinal glia
LRR - leucine-rich region
mAb - monoclonal antibody
MAPK - mitogen activated protein kinase
mas - masquerade
Mer - Merlin
mew - multiple edematous wings
MG - midline glia
MNB - median neuroblast
MP - midline precursor
Msn - Misshapen
mys - myospheroid
N-terminal - amino-terminal portion of protein
NetA - NetrinA
NetB -NetrinB
NMJ - neuromuscular junction
nrx - neurexin
PBS - phosphate buffered saline
PBT - phosphate buffered saline with Triton-X detergent
PC - posterior commissure
pCC - posterior corner cell
PDZ - postsynaptic density-95/discs-largeA/zona occulens-1
pers.comm. - personal communication
PG - peripheral glia
pKa-C1 - cyclic AMP-dependent protein kinase A
PNS - peripheral nervous system
PS - position-specific
PTP - protein tyrosine phosphatase
PXXP - proline/any amino acid/any amino acid/proline
R1, R6 - photoreceptor cell 1, 6
RGD - arginine/glycine/aspartic acid

robo - roundabout
RPTP - receptor protein tyrosine phosphatase
RTK - receptor tyrosine kinase
scb - scab
sev - sevenless
SG - segmental glia
SH2 - Src homology 2 (domain)
SH3 - Src homology 3 (domain)
SN - segmental nerve
Sos - Son of sevenless
 β -gal - β -galactosidase
Std - standard deviation
TAG-1 - a neuronal cell adhesion molecule in vertebrates
ten-a - tenascin-accessory
ten-m - tenascin-major
tig - tigrin
Tl - Toll
TM3 - Third Multiple 3
UAS - upstream activation sequence
UMI - unpaired median interneuron
VNC - ventral nerve cord
VUM - ventral unpaired median neurons
YIGSR - tyrosine/isoleucine/glycine/serine/arginine

CHAPTER 1 INTRODUCTION

1.1 DEVELOPMENT OF DROSOPHILA CNS

1.1.1 Overview of neurogenesis and gliogenesis

The presumptive mesoderm invaginates during gastrulation to bring together two rows of mesectodermal cells, which separate the two lateral neurogenic regions of the ventral neuroepithelium (Figure 1.1). The mesectodermal cells then invaginate and give rise to precursors of the ventral midline. Expression of the *sim* gene distinguishes these cells from neighbouring cells of the neuroepithelium (Crews et al. 1998, Thomas et al. 1988).

During germ band elongation the 8 midline precursors give rise to the glia and neurons of the midline. Fate determination of these precursors appears to have greater plasticity than originally thought. Three experimental approaches suggest different patterns of fate determination for some of these precursors (Jacobs, 2000). At least 3 of the precursors generate neuronal lineages (MP1, UMI and MNB) and the remainder may generate midline glia (MG). The MG lineage produces the posterior (MGP), middle (MGM) and anterior (MGA) glia, respectively (Figure 1.2; Klambt and Goodman 1991a). These cells undergo morphogenetic movements during development (described later), resulting in the characteristic MGA, MGM and MGP positions by the end of embryogenesis. The MG are involved in axon guidance and ensheathment (Jacobs 2000), midline cytoarchitecture (Jacobs and Goodman 1989), and establishment of the blood-brain barrier (Baumgartner et al. 1996).

From the lateral neurogenic regions, neuroblasts and glioblasts delaminate and give rise to other CNS neurons and the longitudinal glia (LG) (Schmid et al. 1999). Lateral CNS glia include the nerve root, exit and peripheral glia, and the glial cells A and B near the MGA and MGP glia, respectively (Figure 1.2; Klambt and Goodman 1991a).

Figure 1.1 Early CNS development gives rise to neural and glial precursors.

This schematic depicts ventral midline development of *Drosophila* embryos adapted from Klambt and Goodman (1991b). All show a cross-section of the body plan during progressive stages of development (dorsal is up). The top left shows the embryo during the cellular blastoderm stage. The mesoderm (shown in black) is located at the ventral side of the embryo and is flanked on either side by the mesectoderm (arrow) that separates the mesoderm from the prospective neurogenic regions. During gastrulation, (top right) the mesoderm invaginates to bring the flanking mesectoderm regions (two rows of 4 cells per segment) together. During germ band elongation (bottom right) these two mesectoderm rows intermingle to form a single row of 8 cells per segment at the midline. From the mesectoderm, midline neuronal and glial precursors delaminate into an inner layer that is populated laterally by neuroblasts (NBs) and glioblasts that delaminate from the ventral neuroectoderm. The midline neuronal and glial precursors eventually give rise to the neurons and glia of the midline, while the neuroblast and glioblasts give rise to other CNS/PNS neurons and glia.

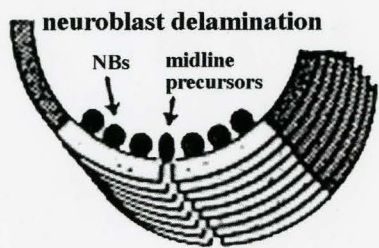
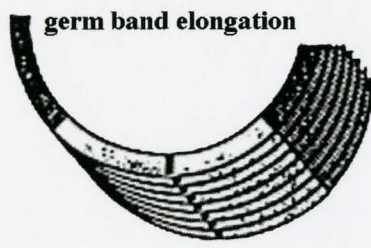
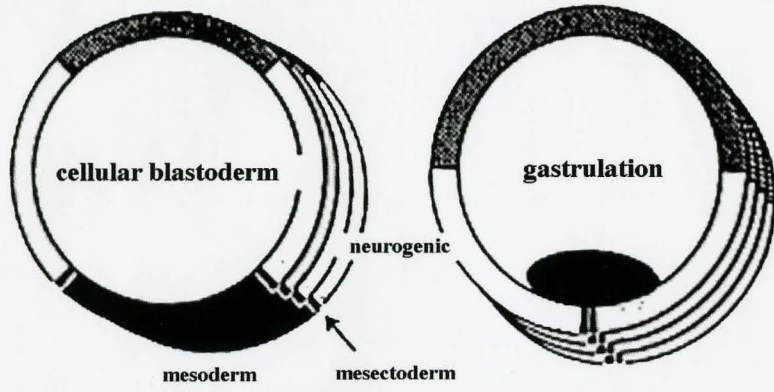
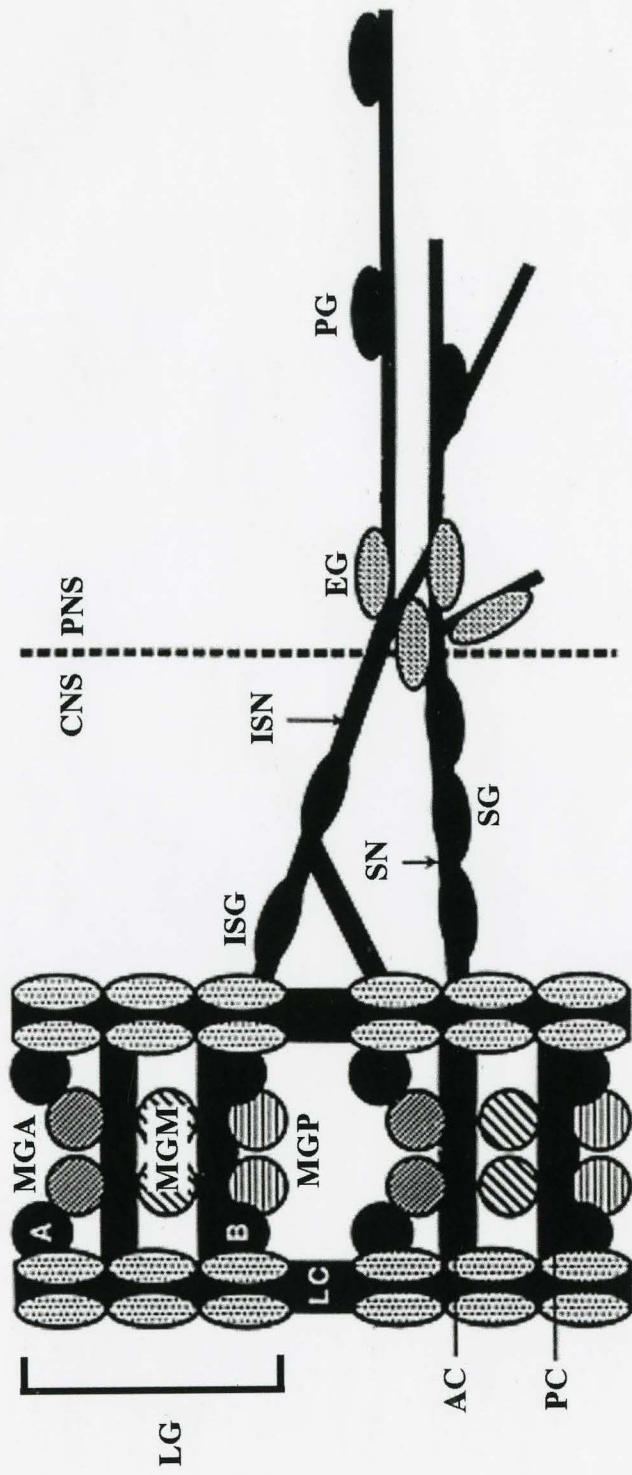


Figure 1.2 CNS axon tract architecture and glial positioning.

CNS and PNS glial positioning and CNS axon tract architecture are shown to represent a mature *Drosophila* embryo. 3 pairs of midline glia populate the anterior (MGA), middle (MGM) and posterior (MGP) regions that separate the anterior commissure (AC) and posterior commissure (PC) in each segment. Lateral to the MGA and MGP lie glial cells A and B, respectively. 3 pairs of longitudinal glia (LG) overlie the longitudinal axons tracts (LC) in each hemisegment. Emerging from the lateral face of the LC are the intersegmental nerve (ISN) and segmental nerve (SG), which project into the PNS. The intersegmental glia (ISG) and segmental glia (SG) overlie the nerve roots. The ISN and SN make axonal exchanges as these nerve roots enter the PNS, where they contact the exit glia (EG). These nerve roots also contact the peripheral glia (PG) as they extend to make contacts with their targets in the periphery (targets not shown). This schematic is adapted from Klambt and Goodman (1991a).



1.12 Axonogenesis

The first pioneers of the CNS begin extending their growth cones at stage 12/5 (around 8.5 hours) of embryonic development. They are the pioneers of the posterior commissure, directed toward the anterior-most VUM cells, the V cells. These pioneers direct their path around the anterior end of the V cells and fasciculate with their contralateral homologs at this point before continuing their respective journeys across the midline to the other side (Klamt et al. 1991). At stage 12/3 (9 hours), the anterior commissure is pioneered, acquiring twice the number of axons as the posterior commissure by the end of embryogenesis. The MG intimately contact these commissural axons and undergo one round of apoptosis after commissural connections have been established (Sonnenfeld and Jacobs 1995). At stage 12/0, the MGM migrate posteriorly over the MGA and move between the two commissures, establishing commissure separation initially formed by the VUM neurons. The VUM neurons remain associated with the MGM through to the end of embryogenesis. Finally, the MGP of the next posterior segment migrate anteriorly across the segment boundary and come to rest just posterior to the posterior commissure. Once MG migrations have been completed, all MG enwrap the axons of the commissures. By the end of embryogenesis, at least one MGM will be present between the commissures, one or both MGA are present, but both MGP undergo apoptosis (Jacobs 2000).

As commissural events are taking place during stage 12, the longitudinal connectives are also being pioneered beginning at stage 12/3. At this stage 4 LG precursors are present and lie dorsally, overtop of the neuronal cell bodies (Jacobs and Goodman 1989). LG positioning was originally thought to precede the development of axonal pathways (Jacobs and Goodman 1989), but it has now been suggested that glia take the lead while migrating with neuronal growth cones (Hidalgo and Booth 2000). Both LG and pioneer axons are required for proper formation of longitudinal pathways and the LG are required for proper fasciculation patterns of longitudinal axons (Hidalgo and Booth

2000). However, it is uncertain whether growth cones of follower axons use only the pioneers to navigate upon, or if they use both the pioneers and glia (Hidalgo and Booth 2000). By 12 hours of development (stage 15) the LG ensheath the tracts at the developing neuropil (region where commissural and longitudinal axon pathways intersect) (Jacobs and Goodman 1989) a function they share with the MG.

As the longitudinal tracts are forming, motoneurons that originate in the CNS send their projections out the intersegmental nerve root (ISN) and the segmental nerve root (SN) to make their peripheral connections; likewise, sensory neurons that originate in the periphery send their axons into the CNS via the nerve roots.

By the end of embryogenesis; the CNS cytoarchitecture takes the form of a ladder with 2 rungs of commissures per neuromere and longitudinal connectives run the length of the CNS, connecting adjacent neuromeres (Figure 1.2). Approximately 40 motoneurons, 5 neurosecretory neurons and 150 interneurons per hemisegment are produced (Goodman and Doe 1993).

1.2 MOLECULES AND MECHANISMS INVOLVED IN AXON GUIDANCE

1.21 Overview of strategies and mechanisms

Since interneurons comprise a majority of the neurons that partake in the establishment of the CNS and greater than 90% of these neurons make contralateral projections across the midline (Kidd et al. 1998a), it is important to determine the cues and guidance mechanisms involved in proper pathfinding of these neurons. An axon's decision whether to cross the midline appears to be determined by a balance of attractive and repulsive cues produced by the midline (reviewed in Van Vactor and Flanagan 1999).

Large-scale genetic screens have identified key components of this system and have classified gene function based on phenotype (Seeger et al. 1993; Hummel et al. 1999a). These phenotype classes have been clearly defined by Hummel et al. (1999a) and include: mutations affecting the formation of commissures; mutations leading to a collapse of all

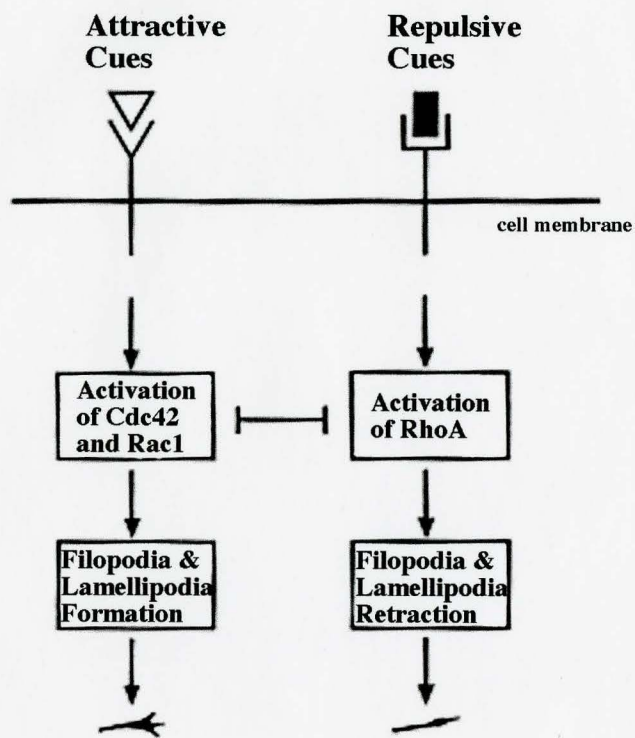
CNS axon tracts; mutations affecting the separation of commissures; mutations affecting fasciculation within the commissures; and, phenotypes novel to these classes. This classification does not distinguish between mutations that influence only glia, neurons, or both.

It is thought that four basic mechanisms work to guide axons appropriately to their targets (reviewed in Goodman 1996, Tessier-Lavigne and Goodman 1996). Chemoattraction (long-range/diffusible cues) and contact-mediated attraction (short-range/nondiffusible cues) are two means by which growth cones are attracted or permitted to explore a particular region of the nervous system. Chemorepulsion (long-range/diffusible cues) and contact-mediated repulsion (short-range/nondiffusible cues) are mechanisms by which growth cones are repelled or inhibited from projecting into a region expressing those molecules. Not all cues fall discretely into one of the four mechanisms; some molecules, such as the Netrins, appear to work bifunctionally to produce attractive responses in some neurons and repulsive responses in others (reviewed in Tessier-Lavigne and Goodman 1996; Mueller 1999). There are several molecules involved in some aspect of axon guidance for both central and peripheral nervous systems. These molecules are reviewed in greater detail elsewhere (see Tessier-Lavigne and Goodman 1996; Mueller 1999). Of particular interest in this present study are the molecules involved in guidance of axons with the midline of the CNS as intermediate target.

The binding of extracellular guidance cues to receptors leads to downstream signaling and behavioural response of the growth cone. A simplified model of signaling involves the activation of Rho-like GTPases (Figure 1.3; reviewed in Mueller 1999). Attractive cues control activation of Cdc42 and Rac GTPases, leading to formation of filopodia and lamellipodia. Conversely, repulsive cues lead to retraction of filopodia and lamellipodia by activation of RhoA GTPase.

Figure 1.3 Downstream signaling of attractive and repulsive axon guidance cues leads to differential growth cone behaviour.

On a simplistic level, axon guidance cues signal through their receptors present on the growth cone to influence guidance decisions by the mechanisms shown here. The guidance decisions are mediated by small GTPase proteins located in the cytoplasm that in turn signal downstream to the cytoskeleton. Attractive cues activate Cdc42 and Rac1 GTPases which lead to filopodia and lamellipodia formation. Repulsive cues activate RhoA GTPase which lead to filopodia and lamellipodia retraction. Activation of either pathway inhibits the other pathway. This schematic was adapted from Mueller (1999).



1.22 Attractive function of the midline

Netrins are secreted, diffusible proteins that are classically known as long-range attractants of axons to the midline. The N-terminal portion of netrins are related to laminin domain VI and three EGF-like repeats of domain V. Their C-terminal portion diverges from the laminins but remains similar between Netrin family members. *Drosophila* Netrin-A (NetA) and Netrin-B (NetB) are more similar to each other than either is to their Netrin relatives in other species (netrin-1 and netrin-2 in chick, UNC-6 in *C. elegans*) (Mitchell et al. 1996). These two genes are redundant in function and are expressed by MG during axonogenesis. NetA is initially expressed at stages 12 and 13 in MGA and MGM, by VUM neurons and in MNB, and although VUM expression fades MG expression remains strong throughout embryogenesis. NetB is expressed in the MG and not by the VUMs or MNB (Mitchell et al. 1996). Both are also expressed in some MP neurons, in muscles, imaginal discs but only NetB is expressed in cardioblasts (Mitchell et al. 1996). NetA and NetB protein is detected on MG and axons of first commissural pathways (stages 12 to 15) while NetB is also found on a lateral group of neurons (Harris et al. 1996). Embryos deficient for both genes demonstrate thin or absent commissures with occasional breaks in longitudinal tracts (Mitchell et al. 1996; Harris et al. 1996). Pan-neural overexpression of NetA or NetB leads to a phenotype reminiscent of the mutant phenotype with bundles of axons projecting laterally toward the nerve roots (Mitchell et al. 1996). Precise distribution of Netrins appears to be crucial for proper axon pathfinding and makes way for a model based on Netrins functioning instructively, instead of just permissively, to guide particular axons to the midline (Mitchell et al. 1996).

Frazzled was identified as the Netrin receptor. Frazzled is a member of the Immunoglobulin (Ig) superfamily of receptors, consisting of 4 Ig domains and 6 FN type-III repeats in the extracellular domain (Kolodziej et al. 1996). Frazzled is expressed at high levels on commissural and longitudinal axons in the developing CNS and on peripheral

motor axons that extend in the ISN and SN pathways (Kolodziej et al. 1996). Both commissures are weakly affected by this gene.

Hummel et al. (1999a,b) recently discovered two genes also involved in the attractive pathway, *schizo* and *weniger*. The posterior commissure is most often affected in *weniger* mutants (as in *netrin* mutants) whereas *schizo* mutants tend to have the anterior commissure most affected (Hummel et al. 1999a). Double mutants of *frazzled/schizo*, *frazzled/weniger* and *schizo/weniger* produce synergistic results, indicating it is likely *schizo* and *weniger* act independent of *netrin* pathway to function in attraction.

1.22 Repulsive function of the midline

Drosophila Roundabout (Robo1) is a likely candidate to be involved in repulsion of axons away from the midline. Robo1 is also included in the Ig superfamily of proteins. Robo1 has 5 Ig and 3 FN type-III domains, a transmembrane domain and a long cytoplasmic domain. The cytoplasmic domain contains conserved motifs with potential for SH3 adaptor protein binding, suggesting it is a receptor and signaling molecule (Kidd et al. 1998a). Robo1 family members include *C. elegans* sax-3, rRobo1, rRobo2, hRobo1, hRobo2 and a putative dRobo2 (Kidd et al. 1998a). Robo1 was first discovered in a genetic screen and displays a mutant phenotype characterised by poorly defined commissures and abnormal crossing and recrossing of the MP1 neuronal pathway across the midline (Seeger et al. 1993). Closer examination of *robo1* mutants reveals abnormal midline crossing of the pCC and MP1 neuron, abnormal midline crossing of the vMP2 neuron, normal crossing and abnormal midline recrossing of the SP1 neuron (Seeger et al. 1993; Kidd et al. 1998b). Robo1 expression is first seen at stage 12 on growth cones that project ipsilaterally (the pCC, aCC, MP1, dMP2 and vMP2 neurons) (Kidd et al. 1998a). Little to no expression is detected on commissural axons as they extend toward and across the midline but levels of protein are upregulated as these axons reach the contralateral side and begin to project longitudinally (Kidd et al. 1998a). Robo1 is also expressed at low

levels throughout the epidermis and at higher levels at sites of muscle attachment (Kidd et al. 1998a). Pan-neural overexpression of Robo1 demonstrated only subtle fasciculation defects, interpreted to reveal strong regulation of Robo1 expression by axons (Kidd et al. 1998a). When expressed by pCC axons that are misrouted in *robo1* mutants (using *ftz-GAL4*), the *robo1* transgene rescued the midline crossing phenotype in all segments, indicating that Robo functions in a cell autonomous manner, consistent with its classification as a receptor (Kidd et al. 1998a). These results then led to the idea of Robo1 functioning as a receptor in contact-dependent repulsion, with its ligand unknown.

Commissureless (*Comm*) was another signaling protein uncovered in the earlier genetic screen (Seeger et al. 1993). *Comm* is a single-pass transmembrane domain protein (Tear et al. 1996). Transcript and protein studies reveal *Comm* is present on MGA and MGM beginning at stage 12 through to stage 16. Transient expression occurs in some neurons lateral to the midline, including the RP1 and RP3 neurons. At stage 12, the first axons to cross the midline have been shown to be closely associated with *Comm*-expressing glia. These glia export *Comm* protein to the passing growth cones (Tear et al. 1996). It is then believed that *Comm* is internalised in the growth cone as vesicles containing *Comm* protein were detected in many neuronal cell bodies within the nerve cord (Tear et al. 1996). Severe hypomorphs of *comm* produce a non-functional protein that is still transferred to commissural growth cones but these axons fail to cross the midline, and instead turn and project longitudinally. Immunolabeling these mutants revealed a nerve cord completely lacking commissures, demonstrating the importance of this gene in commissure formation.

Double mutants for *robo1* and *comm* have a nerve cord with a *robo1*-like phenotype (Seeger et al. 1993). Overexpression of *comm* gives a range of dosage-sensitive, *robo1*-like nerve cord phenotypes, making the *comm* gain-of-function phenotype similar to the *robo1* loss-of-function phenotype (Kidd et al. 1998b). It was also shown that once pan-

neural Comm overexpression was turned-off employing the GAL4-UAS system, Robo1 protein began to accumulate within the nervous system (Kidd et al. 1998b). These results led to the idea that Comm functions to downregulate Robo1 at the midline.

A recent genetic screen revealed another candidate involved in contact-dependent repulsion, *karussel*. *karussel* mutants demonstrate a phenotype similar to *robo* mutants whereby axons recross the midline (Hummel et al. 1999b). In *karussel/comm* double mutant embryos, some segments demonstrate midline crossovers but, in most, the *comm* phenotype is epistatic to *karussel* (Hummel et al. 1999b). This indicates that *karussel* functions in parallel to the Robo1-Comm system, or acts downstream in a common repulsive pathway.

A model interpreting these results (Figure 1.4) depicts commissural axons being attracted to the midline via the Netrin pathway, and Comm protein transferred to those axons as they pass by the MG. Comm present on the growth cones maintains down-regulation of Robo1 expression until they finish crossing the midline. Once reaching the contralateral side, Robo1 expression would then be upregulated and keep those axons from crossing the midline again. *karussel* may be involved in keeping axons from recrossing the midline. As a matter of clarity, Netrins on their own cannot attract axons since *comm* mutants demonstrate lack of commissures, thus allowing Robo1 repulsion to override Netrin attraction. Since it was established that Robo1 is a receptor, and the receptor for the Netrins was discovered, then it was of interest to determine which ligand bound Robo1. Slit was determined to be this ligand (Kidd et al. 1999).

1.3 SLIT FAMILY OF PROTEINS

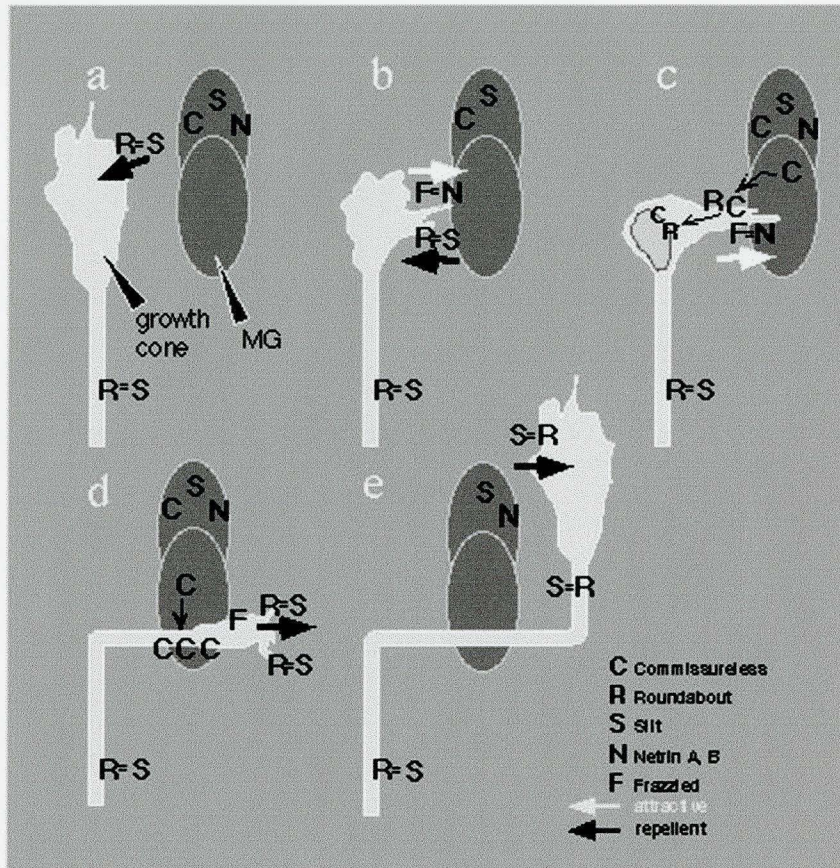
1.31 *Drosophila* Slit

Slit is a secreted extracellular matrix protein that is produced by the midline glia. Located at 52D on chromosome 2, *slit* was uncovered in a genomic library screen using the coding sequence for the EGF-like amino acid region of the *Notch* gene (Rothberg et al.

Figure 1.4 Current model of molecular mechanisms of growth cone guidance.

(a) The current model of growth cone guidance involves commissural axons being attracted to the midline via Netrin proteins secreted by the MG. (b) Frazzled receptors expressed on the surface of the growth cone are responsive to Netrins. (c) Commissureless proteins (Comm) also expressed by the MG and are transferred locally to the growth cone by a mechanism not yet understood. Internalisation of Comm into the growth cone results in simultaneous internalisation of Robo receptors from the growth cone surface.

(d) Commissural axons express low-level Robo, but they uptake Slit from the surface of the MG, where it is expressed. (e) These growth cones then continue projection across the midline to the contralateral side, where they turn either anteriorly or posteriorly (depending on the identity of the axon) and project longitudinally. These axons never recross the midline due to upregulation of Robo which allows the repulsive pathway to remain the stronger influence than attraction at the midline. Axons that are not destined to cross the midline retain high levels of Robo on their growth cone surface from the outset. (Reprinted from Jacobs 2000, with permission.)



1988). Although this screen also uncovered other loci, *in situ* hybridisation and protein localisation demonstrated the presence of Slit in the ventral nerve cord (Rothberg et al. 1988).

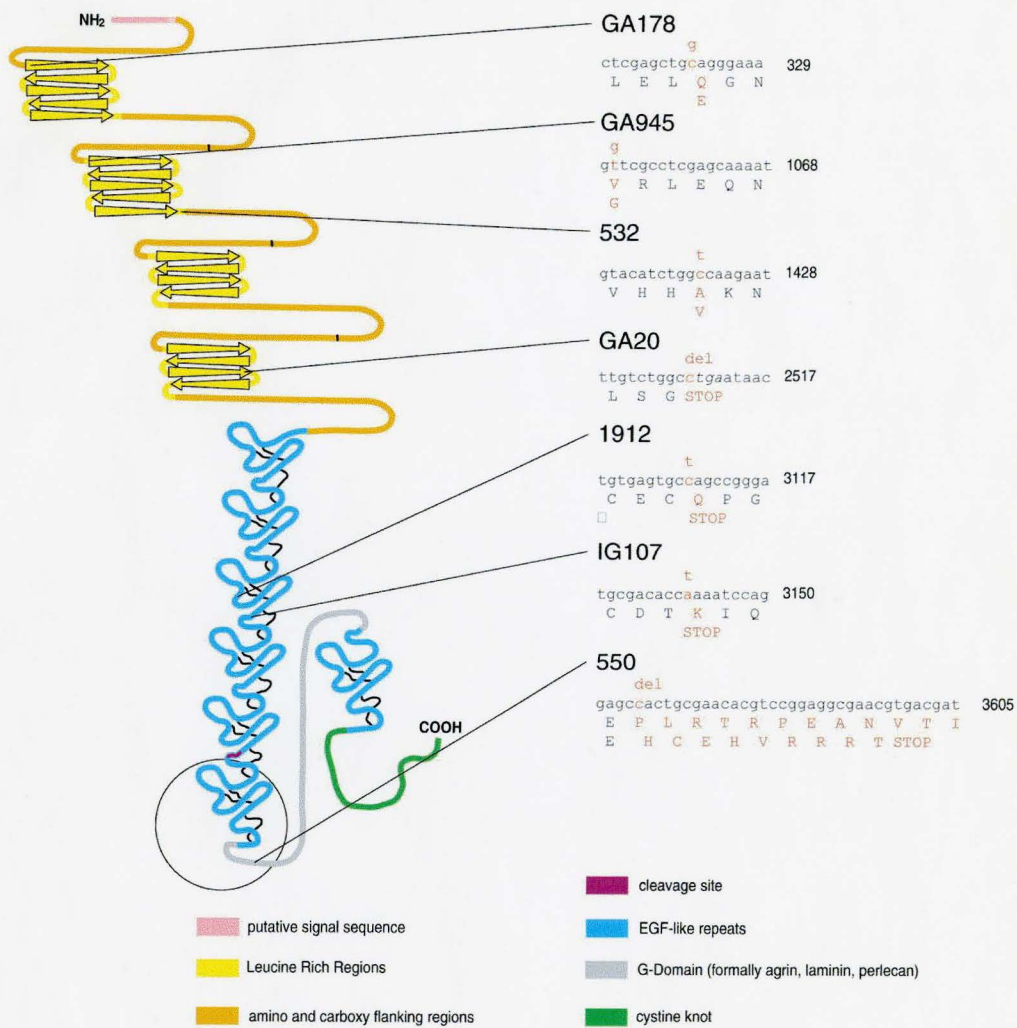
Initial *slit* transcripts are observed during stage 6 (cellular blastoderm stage) where expression is restricted to the ectodermal precursors. During germ band extension (stage 10) transcripts are labeled continuously in the midline and periodically in the lateral ectoderm, from anterior to posterior. By stage 13 (shortened germ band) the signal is located predominantly along the midline of the CNS and persists to the end of embryogenesis (stage 17).

Protein expression is in accordance with transcript studies, indicating the highest expression on the MG cell surface and weaker expression on axon tracts (Rothberg et al. 1990). Based on this pattern, Slit is hypothesised to be secreted by the MG onto axon tracts as they cross the midline (Rothberg et al. 1990). Slit is absent from lateral neurons, the nerve roots and peripheral axon tracts. Looking beyond the CNS, Slit is also expressed in the heart, specifically in cardioblasts during dorsal closure, and also at sites of muscle attachment to the epidermis (Rothberg et al. 1990).

Slit contains leucine-rich repeats (LRR), epidermal growth factor (EGF)-like repeats, a laminin-like G domain and a cystine rich region within its protein structure (Figure 1.5). Based on known functions of these domains, we may postulate possible Slit function in the nervous system. LRR domains are thought to be required for binding other proteins (Hocking et al. 1998). EGF repeats are also implicated in protein-protein interactions as they have been shown to mediate Notch and Delta binding (Lieber et al. 1992). The laminin-like G domain (also known as the ALPS motif, Rothberg and Artavanis-Tsakonas [1992]) is also proposed to be involved in protein-protein interactions, as mammalian Laminin was shown to mediate binding of Syndecan to integrins via this motif (Hoffman et al. 1998). Cystines have shown to be involved in dimerisation events

Figure 1.5 Motif composition of Slit and location of mutations in *slit* alleles.

This schematic depicts the structural motifs of Slit protein. Located at the N-terminus is a putative signal sequence followed by 4 leucine-rich regions (LRR). The first two LRR domains contain 5 repeats of the LRR sequence, while the remaining two contain 4 sequential repeats. Each LRR domain is bordered by conserved amino and carboxy flanking regions. Following the LRR domains are 7 EGF-like motifs, with the 6th and 7th repeat separated by a G-domain also found in other proteins (see legend). Slit is predicted to be cleaved between the 5th and 6th EGF repeats. At the C-terminus is a cysteine-rich region that may form a knotted structure. Also shown are the molecular characterisation of lesions in alleles *slit*^{GA178}, *slit*^{GA945}, *slit*⁵³², *slit*^{GA20}, *slit*¹⁹¹², *slit*^{IG107} (aka *slit*²) and *slit*⁵⁵⁰. The lesions produced in alleles *slit*³¹⁴⁹ and *slit*²⁹⁹⁰ could not be located by sequence analysis (Battye 2000). Alleles *slit*^{E158}, *slit*^{F119} and *slit*^{F81} were previously characterised to be P-element insertions upstream of the start codon (Rothberg et al. 1990). (Reprinted from Battye 2000, with permission).



(Voorberg et al. 1991), although dimerisation has not been demonstrated for Slit.

An earlier screen (Nusslein-Volhard et al. 1984) first identified the *slit* locus based on a cuticular phenotype. Later studies revealed the dramatic nervous system phenotype, as severe *slit* mutants display a full collapse of axon tracts to the midline (Rothberg et al. 1988; Rothberg et al. 1990; Sonnenfeld and Jacobs 1994). Prior to axonogenesis, MP2 neurons and others are displaced ventrally (Sonnenfeld and Jacobs 1994). At stage 12, the pCC neuronal cell body abnormally enters the midline and fasciculates with its contralateral homolog and remains in the midline, extending in the anterior direction (Battye et al. 1999; Kidd et al. 1999). Likewise, the SP1 neuron enters but does not leave the midline (Kidd et al. 1999). The aCC neuron abnormally extends toward and across the midline (Kidd et al. 1999). The MG normally enwrapping these axon tracts fail to undergo proper differentiation and are displaced ventrally. They still maintain contact with commissural axons, which form on the ventral side (Sonnenfeld and Jacobs 1994; Battye et al. 1999). *slit* mutants have also shown defects in muscle development, whereby the ventral oblique muscles abnormally cross the dorsal surface of the nerve cord in lieu of inserting ventrally (Battye et al. 1999). Preliminary work has suggested defects in heart development as well (Battye 2000). These detailed analyses have shown repulsion of axons and muscle pioneers away from sources of Slit, although its role in heart development is still uncertain.

From a genetic perspective, 12 alleles of *slit* show a range of phenotypes, including defects in axon tract morphology, nerve cord length and muscle development (Battye 2000; this work). Molecular characterisation of most alleles was completed recently (Battye 2000). Most alleles were confirmed to be single amino acid changes. Previous characterisation of enhancer trap alleles revealed P-element insertion upstream of the start codon (Rothberg et al. 1990).

1.32 Other Slit family members

Recently, the existence and characterisation of *Drosophila* Slit (dSlit) homologs has been investigated. Mammalian, avian, amphibian and other invertebrate Slits have now been reported and shown to be important in nervous system development .

Itoh et al. (1998) and Brose et al. (1999) have reported human Slit forms (hSlit1, hSlit2 and hSlit3). They are 40% similar to dSlit and 60% similar to each other in amino acid sequence (Brose et al. 1999). They contain an additional LRR in the 3rd repeat and two extra EGF-like repeats. hSlit2 (190 kDa) has been shown to be proteolytically cleaved *in vitro* into a 140 kDa N-terminal fragment and an 55-60 kDa C-terminal fragment, indicating a potentially conserved processing mechanism *in vivo*, as dSlit has also shown to be cleaved *in vitro* (Brose et al. 1999). Northern blot analysis revealed their distributions exclusively in the brain, spinal cord and thyroid (Itoh et al. 1998).

Rat Slit forms rSlit1, rSlit2 and rSlit3 have different tissue expression, although all three forms are expressed at the ventral midline of the nervous system (Holmes et al. 1998; Itoh et al. 1998; Brose et al. 1999). rSlit1 is expressed broadly by floor plate cells (midline cells of the vertebrate spinal cord), rSlit2 is restricted to the most basal and medial region of the floor plate and weakly in region of commissural neurons, and rSlit3 is expressed by the floor plate at lower levels than rSlit1 and rSlit2 (Brose et al. 1999).

Mouse mSlit1, mSlit2 and mSlit3 forms are all expressed in the floor plate, limb and other organs (Li et al. 1999; Yuan et al. 1999). mSlit1 and mSlit2 have 40% amino acid sequence similarity to dSlit and 60% amino acid sequence similarity to each other (Holmes et al. 1998).

Other Slit forms also described in literature include chicken, *Xenopus* and *C. elegans* Slit. Chicken Slit is a partial sequence, containing only 1 LRR region and 3 EGF repeats, and is expressed in the floor plate, motor neurons and roof plate (Li et al. 1999).

Xenopus Slit shares structural features with dSlit and mSlits (Li et al. 1999). *C. elegans* Slit shares the same LRR and EGF signature as dSlit (Itoh et al. 1998).

1.33 Slit and Robo1 function together in the repulsion pathway

Slit was a prime candidate for signaling through Robo1. Their distribution patterns coincide and they show a dominant genetic interaction. *robo/slit* transheterozygotes had defects in 35.3%-74% of segments, depending on the severity of the *slit* allele used (Battye et al. 1999; Kidd et al. 1999; this work). In *slit¹/+*, *robo1¹* embryos, *slit* dominantly enhances the *robo* phenotype by showing greater constriction of axons toward the midline (Kidd et al. 1999).

Evidence of a direct interaction between Robo1 and Slit was demonstrated with in vitro experiments. COS cells expressing *Drosophila* Robo (dRobo1) bound dSlit from Schneider-2 cell supernatants (Brose et al. 1999). COS cells expressing rRobo1 or rRobo2 bound hSlit2 (Brose et al. 1999). Secreted *Xenopus* Slit in culture bound to cells expressing Robo (Li et al. 1999). Likewise, mSlit1 bound Robo in a Western blot (Yuan et al. 1999). Cross-species experiments showed weak binding, although specific, as hSlit2 and dSlit did not bind DCC, TAG-1 or L1 controls (Brose et al. 1999). Similarly, rRobo1, rRobo2 and dRobo did not bind other cell surface proteins such as F-spondin, Netrin1 or Semaphorin III (Brose et al. 1999).

The role of Slit as a Robo-binding ligand is an important one; however, this may not be its only function. Very recent work has demonstrated the region of Slit responsible for binding to and signaling through Robo1 may lie with the LRR repeats found near the N terminus of the protein (Battye 2000). Slit has domains that have importance in other proteins, leading to the idea that Slit may be a multifunctional protein within the nervous system. Given that it is cleaved in vitro and only the N terminal portion (LRRs and 5 EGF-like repeats) is thought to bind Robo1, this leaves the C terminal portion (2 EGF repeats, G domain and Cystine knot) to be distributed and potentially used elsewhere within the nerve

cord. In vitro experiments have shown that hSlit2 binds to Laminin1 but not Fibronectin in culture (Brose et al. 1999). Netrin1 bound to COS cells expressing hSlit2 (Brose et al. 1999). rSlit1 and rSlit2 from rat brain extracts bound a heparin sulfate proteoglycan fusion protein, glypican, by affinity chromatography (Liang et al. 1999). The domains by which Slit bind to Laminin, Netrin or Glypican are not yet known, although Slit may bind glypican via both its core protein and heparin sulfate chains (Liang et al. 1999).

1.4 RESEARCH STRATEGY

Genetic interactions are defined by a change in phenotype associated with a change in genotype. By reducing the gene dosage of two candidate genes, their combined function may be sufficiently impaired to produce a phenotype, if they interact genetically. This analysis has been useful in determining various ligand-receptor pairs, including Delta and Notch (Artavanis-Tsakonas et al. 1995) and semaphorin/plexin A (Winberg et al. 1998).

Genetic screens have been useful in uncovering genes that interact with a gene of interest. Price et al. (1997) conducted an EMS mutagenesis screen on wing phenotypes to uncover mutations in genes that were dominant enhancers of the background mutation in the EGF receptor. Wessendorf et al. (1992) conducted a genetic screen whereby dominant enhancers and suppressors of integrin wing phenotypes were discovered by examining F1 flies mutant in the integrin gene *inflated* and a candidate gene. Boubé et al. (1997) tested for dose-sensitive modifiers of *proboscipedia* (*pb*) in development of adult mouthparts by examining F1 progeny of flies with a *pb* transgene mated to flies with deficiencies.

This study has examined the possibility of Slit interacting with other proteins that are present in the nervous system with similar spatial and temporal distribution. These candidate proteins would also contain motifs involved in protein-protein interactions. The objective of this study was to undertake a genetic screen to identify candidate genes that may interact genetically with *slit*.

I conducted a blind screen that involved generating embryos mutant for a hypomorphic allele of *slit*, *slit*²⁹⁹⁰, and a mutation in another gene. This would potentially test for both dominant and recessive modifiers of *slit* as different combinations of heterozygous and hemi- or homozygous genotypes would be present within a population of embryos. *slit*²⁹⁹⁰ was chosen as genetic modifiers functioning either by enhancement or suppression would be easily identified by changes in *slit*²⁹⁹⁰ CNS phenotype. *slit*²⁹⁹⁰ mutants display a less severe midline collapse and midline crossing of axon tracts than shown for the severe hypomorph *slit*².

In attempts to confirm the results from the first screen, I then created stable double mutant lines, using a procedure similar to that described in Hummel et al. (1999b). A double mutant line carrying dominant markers on two chromosomes was used to introduce the genes of interest (*slit* plus candidate) into the chromosomes. These double mutant lines were then assessed for phenotypic changes in CNS architecture.

Finally, I conducted a dose-sensitive dominant modifier screen with some of the candidate genes. Since it was shown that Laminin and Slit bind to each other, at least *in vitro*, I generated a *slit*²; *lamininA* double mutant line to be used as a sensitised background for this screen. I generated triple mutant transheterozygous embryos by mating *slit*²; *lamininA* double mutant flies with flies either mutant in a candidate gene or deficient in a candidate locus. This screen attempts to uncover genes that interact genetically with *slit* and *lamininA* as revealed by changes in CNS phenotype of F1 progeny as a result of a reduction in gene function.

CHAPTER 2 METHODS

2.1 DROSOPHILA MELANOGASTER FLY STOCKS

Fly stocks were obtained from the Bloomington Stock Centre, unless indicated otherwise. All flies were maintained on sucrose-salts-yeast agar medium in polypropylene shell vials (Fisher Scientific) or glass culture tubes (Fisher Scientific) at room temperature (22-25°C). The wild type strain Canton-S P-element free (CS-P) was used as a control for CNS phenotype. Most single mutant lethal lines examined were maintained over a balancer chromosome containing a P[*fushi tarazu-LacZ* (*ftz-LacZ*)] reporter transposon for X chromosome mutations, a P[*engrailed-LacZ* (*eng-LacZ*)] for 2nd chromosome mutations, and either a P[*Ultrabithorax-LacZ* (*Ubx-LacZ*)] or P[*actin-LacZ*] to balance mutations on the 3rd chromosome. Homozygous mutants were identified as embryos lacking LacZ labeling. Mutants for *scab* were identified by the presence of dorsal blisters due to defects in dorsal closure associated with this gene (Stark et al. 1997).

2.2 MUTATIONS AND DEFICIENCY LINES

All mutants and deficiencies used are reported in Table 2.1.

2.3 ANTIBODIES

All primary and secondary antibodies used are outlined in Table 2.2.

2.4 EMBRYO COLLECTIONS

Adult flies were mated in plastic tri-pour beakers with respiration holes and capped with 60x15 mm plastic petri dishes. Petri dishes were filled with solidified apple juice agar and supplemented with yeast paste for flies to feed on. Females would oviposit fertilised eggs onto the surface of the agar. Typically, plates would be changed twice daily: morning collections (09h00) would develop at room temperature (22-25°C) for 8 hours and then placed at 18°C in the evening (17h00) for overnight development to approximately stage 17; evening collections (17h00) would develop overnight at room temperature. Both sets

Table 2.1 Mutants and deficiencies used for genetic screens.

Gene (Allele/Df)	Cytological Location*	Genetics	Protein Type/Motifs	Proposed Function	Reported Phenotype	Protein Distribution**	Reference
NetrinA,B [Df(1)NP5, Df(1)KA9] <i>Source: M.Seeger</i>	12E10-F1, 12F1-4 12E9;12F2-5 12E6;13A2-5	uncovers NetA and NetB genes on X chromosome	secreted; contain domain VI of laminin, 3 EGF-like repeats in domain V and novel C-terminal domain	attraction/repulsion to and from midline	commissures thin, sometimes absent; occasional breaks in longitudinal tracts	NetA: MGA/M, VUMs, some neurons, some muscles NetB: MGA/M, some neurons, some muscles, cardioblasts	Mitchell et al. (1996)
Central body defect (cbd ¹)	11A1-7	uncovers tenascin ^a gene (11A6-9); generated by EMS mutagenesis; homozygous viable	secreted ECM protein: 8 tenascin-type EGF-like repeats; lacks FN type III repeats and FGN globe present in vertebrate tenascins	cell-substrate repulsion during axon guidance	data not available	perinuclear; CNS, brain, near muscle insertion sites (embryos); eye (pupae) associated with growing axons	Baumgartner and Chiquet-Ehrismann (1993)
Discs-large (dlg1 ⁶)	10B8	EMS mutagen, late larval, recessive	guanylate kinase domain; SH3 domain; PDZ domain; cytoplasmic	links septate junction to cytoskeleton; septate junction structure formation	no CNS phenotype reported; overgrowth of imaginal discs	synapse of NMJ at position of septate junction in neurons	Woods and Bryant (1991); Woods et al. (1996)
Multiple edematous wings (mew ^{M6})	11E9	EMS mutagen, recessive	alpha-PS1 integrin	cell adhesion receptor; receptor for laminin	axon guidance errors	punctate expression in dorsal part of nerve cord (stg. 12); low levels on axons presumed; transcript expression on midline cells	Wehrli et al. (1993); Hoang and Chiba (1998)
Inflated (if ^{k27c})	15A6	EMS amorph, recessive	alpha-PS2 integrin	cell adhesion receptor; receptor for tigrin	axon guidance errors	low levels on axons presumed; transcript expression on cells adjacent to midline	Hoang and Chiba (1998)
Myospheroid (mys ¹)	7 D5	³² P mutagen, loss of function, recessive	beta-integrin	cell adhesion receptor	herniation of midgut and nervous tissue; muscles retract from sites of attachment; axon guidance errors	longitudinal tracts; ISN, SN; transcript expression on midline cells	Newman and Wright(1981) MacKrell et al. (1988); Hoang and Chiba (1998)

*locations are given for gene loci and breakpoints are provided for deficiencies in adjacent column

**limited to nervous system, muscle and heart regions which also express Slit

Gene (Allele/Df)	Cytological Location	Genetics	Protein Type/Motifs	Proposed Function	Reported Phenotype	Protein Distribution	Reference
Slit (slit ² [aka slit ^{IG1071}], slit ²⁹⁹⁰) Df(2R)Jp4 <i>Source: C. Goodman</i>	52D1-8 51F13; 52F8-9	EMS and enhancer trap alleles; range in severity	4 LRR motifs with conserved flanking regions, 7 EGF-like repeats, laminin G domain, cystine knot	ligand for Robo; axon repulsion	collapsed nerve cord; muscles extend over dorsal portion of nerve cord; cardiac cells fail to adhere	MG, nerve cord, muscle, heart	Rothberg et al. (1988, 1990); Batty et al. (1999); Kidd et al. (1999)
Roundabout (robo ¹ , robo ³) <i>Source: G. Tear</i>	59A1	EMS; amorph; recessive	5 Ig + 3 FN domains, transmembrane, cytoplasmic region; axon guidance receptor	receptor for Slit; axon repulsion	MP1 fascicle aberrantly crosses and recrosses midline; fuzzy commissures	high levels: longitudinal axons, muscle attachment sites low levels: commissures, throughout epidermis	Seeger et al. (1993); Kidd et al. (1998a, b)
Dreadlocks (dock ^{P1} aka dock ⁰⁴⁷²³)	21D3-4	P-element insert, amorph, recessive	3 SH3 domains, 1 SH2 domain; cytoplasmic; adapter protein	facilitates RP3 synapse formation; guidance of some interneurons	wavy fascicles; occasional breaks in longitudinals; delay in synapse formation by RP3 motoneuron	most neurons in CNS and cell bodies, especially motor neurons	Desai et al. (1999)
Tiggrin (tig ^x) <i>Source: T. Bunch</i>	26D1-2	P-element insertion, lethal, recessive	secreted PS2 ligand; N-terminus: 1 Cys residue, 16 repetitive segments (novel); RGD at C-terminus	adhesion/cell spreading; maintain muscle-muscle attachments in larvae	detachment of some body wall muscles; gaps between muscles	muscle apodemes, hemocytes, basement membrane, commissures, muscle attachment sites	Fogerty et al. (1994); Bunch et al. (1998)
Scab (scb ²) Df(2R)XTE-18 Df(2R)Jp1	51F4-5 51E3; 52C9-D1 51D3-8; 52F5-9	EMS, recessive	PS3 integrin	cell adhesion; signal transduction; short-term memory	dorsal closure defects; germ band twists laterally; mislocalisation of pericardial cells	high levels (stg 14-16) in MG; lower levels throughout nerve cord, dorsal vessel	Stark et al. (1997); Grotwiell et al. (1998)
LamininB1 [Df(2L)XE-2750, Df(2L)Trf-C6R31]	28D1-2 28B2; 28D1 28DE (within)	no mutations within locus isolated	beta chain of cruciform complex; EGF motifs	see LamininA	unknown	see LamininA	see LamininA

Gene (Allele/Df)	Cytological Location	Genetics	Protein Type/Motifs	Proposed Function	Reported Phenotype	Protein Distribution	Reference
Wrapper [Df(2R)X58-3, Df(2R)X58-12]	58D6 58C3-7;58D6-8 58D1-2;59A	uncovers wrapper locus on 3 rd chromosome; recessive	Ig superfamily: 3 Ig domains, 1 FN III repeat, GPI linkage	Late MG survival; enwrapping commissures proper separation of commissures	stg 16: commissures fail to separate; MGs die prematurely	stg 12: MGs throughout embryogenesis stg 17: lateral glia, brain glia	Noordermeer et al. (1998)
LamininA (lamA ^{9,32})	65A12	Δ 2-3 mutagen; loss of function; recessive; collagen binding domain, heparin-binding	alpha chain of 3-chain complex; EGF motifs, Cystine rich	heart ultrastructure; pathfinding of pioneer interneurons; binding to integrins	heart "broken", pericardial cells dissociate from cardioblasts; ventral oblique muscles never reach attachment sites; fragmented basement membrane	basement membranes (esp. muscles and nervous system); high levels in mesectodermal strand, in and around axon pathways and in glial cells (CNS + PNS)	Montell and Goodman (1989); Yarnitzky and Volk (1995); Garcia-Alonso et al. (1996)
Toll (Tl ^{R3})	97D8	EMS, hypomorph, conditional temperature sensitive	transmembrane receptor; LRRs in extracellular portion	inhibit synaptogenesis of specific motoneuron growth cones; cell adhesion	improper innervation of RP motoneuron or loss of RPs in segments, esp. RP3 motoneuron	ventral somatic muscle clefts; stg 10: border between mesectodermal cells at midline; dorsal vessel; midline glia	Hashimoto et al. (1991); Halfon et al. (1995); Rose et al. (1997)
Masquerade (mas ^{x124}) <i>Source: W. Chia</i>	64B1	double P-element excision of gene, null, loss of function	secreted; serine protease-like domain	somatic muscle attachment; taste behaviour; axon pathfinding; acts as inhibitor of serine protease activity; cell-matrix adhesion	stalling of aCC and pCC axons; commissure problems	MG; longitudinal connectives	Murugasu-Oei et al. (1995, 1996)
Commissureless (comm ^{a490} ; aka comm ¹) <i>Source: C. Goodman</i>	71E3-5	EMS; strong hypomorph; recessive	transmembrane protein; no motifs similar to other known proteins	downregulates Robo-mediated repulsion on commissural axons	commissures absent; fasciculation errors of longitudinals; MG displaced laterally (Seeger et al. 1993)	stg 12-16: MGA/M (surface and Golgi), some neurons lateral to midline, commissural axons in contact with MG, neuronal vesicles (internalised)	Seeger et al. (1993) Tear et al. (1996)
Neurexin (nrx ⁴³⁰⁴)	68 F5-6	hypomorph.; EMS mutagenised; recessive	transmembrane; discoid-like domain, lamininG, EGF, fibrinogen, band 4.1-/PDZ-binding domains	establish and maintain blood-brain barrier at glial and epithelial cells; speculative role in signaling	paralysed; breakdown in blood-brain barrier	septate junctions, MGs	Baumgartner et al. (1996); Peles et al. (1997)

Gene (Allele/Df)	Cytological Location	Genetics	Protein Type/Motifs	Proposed Function	Reported Phenotype	Protein Distribution	Reference
Hem (P{lacZ}Hem ⁰³³³⁵ aka. kette)	79E1-2	P-element insertion in intron region downstream of start codon; recessive	conserved Cystine residues; >1 transmembrane domain; rich in Leucine residues	in CNS, uncertain	fusion of commissures; frequent disruption of longitudinal connectives	restricted to brain and nervous system in late embryogenesis; oocytes	Baumgartner et al. (1995); Hummel et al. (1999a); Hummel et al. (2000)
Tenascin-major [Df(3L)Ten ^{m=AL1})	79E3-4 79E1-E4;79E3-79E8	Xray mutagen; disrupts tenascin-major	secreted proteoglycan; attached moiety likely of chondroitin sulfate or dermatan sulfate; 8 EGF-like repeats, 'CC' domain highly related to Ten ^a , 11 FN III-like repeats, RGD motif and various sites for glycosaminoglycan attachment	based on vertebrate studies and presence of homologous domains, likely involved in growth cone repulsion;	no reported phenotype in CNS, heart or muscle; only reported phenotype is that of a pair-rule phenotype	stg 12: cell bodies of certain neurons, lateral to midline stg 13-15: AC and PC pioneers, longitudinal connectives; cardiac cells stg 16: muscle attachment sites (All seen for mRNA and protein)	Baumgartner et al. (1994)
LamininB2 [Df(3L)AC1]	67B5-6 67A2; 67D7-13 or 67A5; 67D9-13	no mutations isolated yet for this gene	see LamininA	see LamininA	see LamininA	see LamininA	see LamininA

Table 2.2 Primary and secondary antibodies used for immunocytochemical analysis.

Primary Antibody	Type	Source	Dilution	Features/Distribution
BP102	Mouse, monoclonal	C. Goodman	1:4	Labels an uncharacterised carbohydrate moiety found on all CNS axons. In wild-type embryos, labeling exhibits a ladder-like pattern.
mAb 1D4 (anti-Fasciclin II)	Mouse, monoclonal	C. Goodman	1:4	Labels Fasciclin II, an axonal glycoprotein present on surfaces of axons that form the three longitudinal connectives. In wild-type embryos, three bilaterally symmetrical longitudinal bundles are labeled from anterior to posterior of the nerve cord.
anti-beta-galactosidase	Rabbit, polyclonal	Cappel	1:200	Labels any P{LacZ} element expressed in the embryo; here, used to identify balancer chromosomes. Expression pattern depends on the reporter transposon present in the construct.
Secondary Antibody				
Goat anti-Mouse HRP	Peroxidase-conjugated	Jackson Immunological	1:200	Cross-reacts to any antibody raised in a mouse.
Goat anti-Rabbit HRP	Peroxidase-conjugated	Jackson Immunological	1:200	Cross-reacts to any antibody raised in a rabbit.
Goat anti-Mouse BIO	Biotinylated	Jackson Immunological	1:100	Cross-reacts to any antibody raised in a mouse

of plates were placed at 4°C to ensure development was arrested until the time of fixation (no later than 72 hours post-oviposition). Agar plates from double mutant lines and crosses for the genetic screens were placed at 18°C for a few additional hours to approximate development to stage 16-17.

For lines raised in culture tubes (16x100), a housing unit was constructed (design adapted from A. Brand) with 10 plastic tubes emerging from a Plexiglas platform. A Plexiglas plate was also constructed and fitted with nytex material to collect for embryos and use for the fixation protocol.

Embryos were staged according to Campos-Ortega and Hartenstein (1985). Stages are identified according to gut morphology, the degree of extension of the head and the length of the nerve cord.

2.5 FIXATION PROTOCOL

Plates collected and temporarily stored at 4°C were placed at room temperature for one hour prior to fixation. This allowed microtubules to repolymerise to resume embryogenesis, and consequently, nerve cord development. Commercial bleach diluted in water to half concentration (2.82 sodium hypochlorite p/v) was generously added to agar plates to dechorionate embryos over a period of 5 minutes. Embryos were then rinsed with distilled water into a nytex sieve chamber and blotted dry with Kimwipes. After drying, embryos were then transferred into scintillation vials containing a 1:1 mixture of heptane and 3.7% formaldehyde in 1x phosphate-buffered saline (PBS, pH 7.4). Embryos were rotated in this solution for 25 minutes.

After fixation, the bottom layer (PBS + fixative) was removed with a Pasteur pipette and discarded. The top layer (heptane + embryos) remained within the vial and submitted to forced influxes of methanol, reaching equal volume of heptane. The vial was then capped and shaken violently to crack the embryos out of their vitelline membrane.

Devitellinised embryos then fell to the bottom of the vial, in the methanol phase, while the vitelline membrane remained at the interphase. These embryos were transferred to clean glass culture tubes (12x75) for repeated washings in methanol, transferring to a new glass tube after every third methanol wash. Washes were completed after 3 changes of glassware. Embryos destined for future use (within a two-week period) were stored in methanol at 4°C.

2.6 IMMUNOCYTOCHEMISTRY PROTOCOL

Embryos ready for antibody labeling were then hydrated by replacing methanol with PBT (1x PBS and 0.5% Triton-X detergent). Tubes were rinsed again in PBT, capped and rotated for 20 minutes. After rotating, embryos were allowed to settle and the PBT removed to a level where embryos remained submerged. Embryos were then blocked with normal goat serum (NGS; Jackson Immunological) in PBT (1:15 dilution) and placed on an orbital shaker for 1 hour at room temperature. After blocking, primary antibody was added to each tube (refer to Table 2) and incubated on the orbital shaker for either 6 hours at room temperature or overnight at 4°C.

After incubation, embryos were rinsed 5 times with PBT and placed on a rotator overnight at 4°C. The next morning, embryos were re-blocked in NGS (same dilution as above) for 1 hour and incubated in peroxidase-conjugated (HRP 2°) or biotinylated secondary (BIO 2°) antibody (refer to Table 2.2) for 2 hours at room temperature. Embryos in HRP 2° were then rinsed 5 times and placed on a rotator for either 4 hours at room temperature or overnight at 4°C. Embryos in BIO 2° were rinsed for a few hours, then PBT was removed and 2% A+B VectaStain Reagents (VectaStain) were added. These reagents were allowed to incubate for 1 hour and then tubes were rinsed 5 times in preparation for the peroxidase reaction.

To begin the peroxidase reaction, embryos were incubated in DAB/PBT solution (0.33 mg/mL) with NiCl₂/ CoCl₂ for 2 minutes. Hydrogen peroxide was added to the tube

at 0.03% concentration to begin the peroxidase colourimetric reaction. The reaction was monitored visually through a compound microscope and stopped by diluting the reaction with PBT. Embryos were subsequently rinsed 3 times to rid of DAB substrate. For embryos destined to be double labeled with another antibody (usually α - β -*galactosidase* for balancer identity), embryos would be reblocked with NGS/PBT solution and repeat the protocol beginning with the primary antibody. For the second label, NiCl₂/ CoCl₂ is not added to DAB/PBT solution.

Embryos labeled with a single antibody or completing a double label were then dehydrated with successive ethanol gradients (30%, 50%, 70%, 90%, 95% and 3x 100%). Finally, 100% ethanol was replaced in the tube with methyl salicylate (Canadawide Scientific). For long term storage, embryos in methyl salicylate were transferred to 1.5 mL screwcap microtubes and labeled for recording purposes.

2.7 MOUNTING AND PHOTOGRAPHY

Embryos were viewed in wells with a Zeiss compound dissecting microscope. Selected embryos were placed on glass slides for either whole mount observation (ventral view) or for dissection. Nerve cords were removed from the rest of the embryo tissue with an electrolytically sharpened Tungsten wire mounted within a syringe-needle apparatus. The tissue was surrounded by Permout (Fisher) prior to placing of the glass coverslip; Permout is used to avoid dessication of the sample. These slides were allowed to set for a minimum of 24 hours prior to examination under the Zeiss Axiophot microscope.

Whole mount embryos were examined and photographed at 400x magnification, filleted nerve cords at 630x magnification. Colour slide film (Fuji RTP Tungsten or Kodak EPY Ektachrome) was developed commercially.

2.8 EXPERIMENTAL DESIGN AND DATA ANALYSIS

2.81 Blind Screen

Flies mutant for a gene of interest were crossed with flies mutant for a hypomorphic allele of slit (*slit*²⁹⁹⁰) and F1 progeny were intercrossed in a house to analyse second generation embryos. A full account of the genetics involved in the rationale of this cross is outlined in Appendix Figures 1-4. Wildtype, control crosses and single mutant lines were included in this screen.

Embryos involved were immunolabeled with α -Fas II and set aside for blind identification by another person. Embryos were then visualised under a compound microscope and screened qualitatively for axon phenotypes present in each tube. Of interest were embryos that exhibited phenotypes worse or different than that demonstrated by homozygous *slit*²⁹⁹⁰ embryos or embryos homo-/hemizygous for each candidate gene. Representative embryos within the collections were mounted and photographed.

2.82 Double Mutant Analysis

Double mutant lines were generated with the use of balanced lines also generated during this study. The genetics involved for each type of cross are outlined in Appendix Figures 5-9. Flies of the genotype FM7cB; *slit*²⁹⁹⁰/CyO[*eng-LacZ*] and FM7cB; *slit*²/CyO[*eng-LacZ*] were created and used to generate double mutant lines for X chromosome mutants in combination with *slit*. Fly lines with a recombined 2nd chromosome were generated using *yw*-; *Sco*/CyO[*eng-LacZ*] to screen against. Flies of the genotype *yw*-; *Star*/CyO; *D*/TM3 were used to generate flies of the genotypes *yw*-; *slit*²⁹⁹⁰/CyO; *D*/TM3 and *yw*-; *slit*²/CyO; *D*/TM3.

Embryos double labeled with either BP102 or α -Fas II and α - β -galactosidase (α - β -gal) were observed under the compound microscope in wells. Embryos in a given

population were scored for phenotype and compared to phenotype(s) exhibited by the single homo-/hemizygous mutants. The expected frequency of occurrence was also taken into account as a means to determine the genotype of the embryos. Representative embryos were then mounted and photographed as a record of the phenotype.

2.83 Slit/Robo Transheterozygote Interaction

Flies mutant for all alleles of *slit* were mated to flies mutant for *robo1* (*robo1*¹) in a house. This cross produced 1/4 embryos with a mutant copy for both genes. Their embryos were labeled for α -Fas II and α - *β -gal*. Embryos used for analysis were selected based on the lack of α - *β -gal* labeling. Nerve cords were filleted from embryos and mounted on glass slides. Thoracic and abdominal segments were counted at 630x magnification for presence/absence of midline crossovers for each transheterozygous combination. Each combination was expressed as a percentage of segmental crossover +/- standard deviation exhibited in the population.

2.84 Slit Wrapper Transheterozygote Interaction

Flies mutant for the alleles *slit*² and *slit*²⁹⁹⁰ were mated to flies deficient in the *wrapper* gene. This cross produced 1/4 embryos with a reduced copy of each the *slit* and *wrapper* genes. These embryos were immunolabeled with α -Fas II or BP102 and α - *β -gal*. Nerve cords were filleted from embryos and mounted on glass slides. This cross is outlined in Appendix Figure 10a.

2.85 Slit Scab Transheterozygote Interaction

Flies mutant for *slit*² and *scab* were mated with flies mutant for deficiencies that uncover the *slit* locus, the *scab* locus and both loci. Embryonic progeny were immunolabelled with α -Fas II or BP102 and α - *β -gal*. Nerve cords were filleted from embryos and mounted on glass slides. This cross is outlined in Appendix Figure 10b.

2.86 Dosage-sensitive Dominant Modifier Screen

Flies with a genomic deficiency or mutation were crossed to flies doubly mutant for *slit* and *lamA*. F1 embryos were double labeled for both BP102/ α - β -gal and α -Fas II/ α - β -gal combinations. Embryos were scored for percentage of occurrence within a population of embryos and compared with control crosses (when possible) and expected frequencies. An outline of the genetics involved in these crosses is detailed in Appendix Figure 11.

2.87 Nerve Cord Length

Embryos from all *slit* alleles were assessed for phenotypic variations based on nerve cord length. It was qualitatively observed that the more severe *slit* alleles exhibited nerve cords (and thus germbands) that failed to condense as wildtype embryos do. This analysis was an attempt to uncover quantitative differences between the alleles and compare them to their CNS phenotype.

22 embryos (stage 17) were mounted ventrally on glass slides and examined with a cameralucida microscope. The recorded features for measurement were: the anterior and posterior tips of the embryo, the anterior and posterior tips of the nerve cord, as visualised by BP102. Nerve cord length was then expressed as a ratio of the length of the nerve cord to the length of the anterior tip of the nerve cord to the posterior tip of the embryo. ANOVA analysis and post-hoc Tukey upper and lower limit intervals were calculated to identify differences between the alleles. These results were not central to the thesis and placed in Appendix Figure 12.

CHAPTER 3 SINGLE MUTANT ANALYSIS

The candidate genes selected to test for genetic interactions with Slit were based on particular criteria. First, they need to be expressed in a similar temporal and spatial distribution as Slit in the nervous system. Secondly, they must contain motifs, such as EGF-like and/or LRR regions, that are involved in protein-protein interactions that suggest a mechanism for interacting with Slit, as Slit also contains these motifs. With these criteria in mind, I selected 19 candidates to test, 18 of which are explored here. The remaining candidate, *wrapper*, was tested using a deficiency line. The homozygous phenotype of this deficiency was not examined.

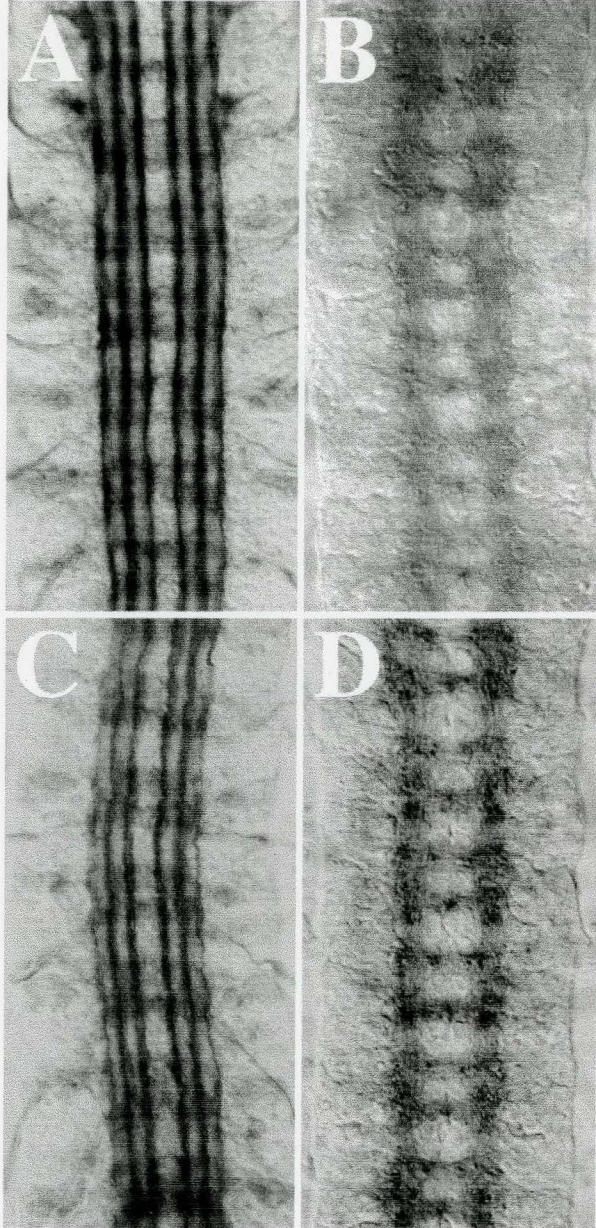
3.1 INTRODUCTION TO ANALYSIS

Table 2.1 lists each mutant or deficiency used and pertinent information for selection as a candidate interacting gene. Information provided was limited to distribution and function as related to Slit.

Canton-S p-element-free (+/+) and *yw*⁻; +; + flies were used as controls for CNS axon tract architecture, as assayed by mAb 1D4 (anti-Fas II monoclonal antibody) and mAb BP102. Both fly lines show a typical wildtype phenotype when visualised with either antibody. When labeled with mAb 1D4, they label 3 characteristic bilaterally symmetrical FasII-positive fascicles extending the length of the ventral nerve cord (Figure 3.1 A, C). With BP102 labeling, the “ladder-like” phenotype typical of wildtype embryos is observed in these fly lines (Figure 3.1 B, D). The ladder consists of 2 rungs per neuromere (nervous system segment), the anterior and posterior commissures, connected by longitudinal axons between segments. These wildtype phenotypes will form the basis of comparison for all experiments.

Figure 3.1 CNS phenotype typical of wildtype embryos.

Canton-S p-element free (A, B) and *yw*⁻ (C, D) embryos were stained with antibodies to compare wildtype CNS cytoarchitecture. Each panel shows late stage 16 VNC dissections in frontal view with anterior at the top. All panels for figures will be shown this way, unless otherwise specified. Embryos stained with mAb 1D4 (A, C), directed against the FasciclinII (FasII) protein, display three bilaterally symmetrical longitudinal tracts that project the length of the embryo on each side of the midline. Embryos stained with mAb BP102 (B, D), directed against a carbohydrate moiety present on all CNS axons, have the characteristic ladder-like phenotype of two rungs of commissures per neuromere, connected by a longitudinal bundle of axons on each side.



3.2 MUTANT PHENOTYPES OF GENES INVOLVED IN AXON PATHFINDING

*slit*² mutants display a severe collapse of longitudinal and commissural axon tracts at the midline (Figure 3.2A). Commissures still form in these mutants (Battye et al. 1999), although they are fused at the midline (Figure 3.3A). The phenotypes observed in these mutants is consistent with reports in literature (Rothberg et al. 1988; Sonnenfeld and Jacobs 1994; Battye et al. 1999; Kidd et al. 1999). A hypomorphic allele of *slit*, *slit*²⁹⁹⁰, displays a less severe collapse of longitudinal connectives toward the midline (Figure 3.2B). Collapse appears to involve the two medial FasII-positive fascicles, leaving the lateral fascicle unaltered. Commissures appear fuzzy (poorly defined) in these mutants and longitudinal axons between segments are thinned or missing (Figure 3.3B). The phenotype of *slit*²⁹⁹⁰ has not previously been reported, although bears a close resemblance to another hypomorphic allele, *slit*⁵³² (Battye et al. 1999).

*robo1*¹ mutants display a prominent circling phenotype of medial axons across the ventral midline (Figure 3.2C). This abnormal crossing of axons does not involve the middle and lateral fascicles (Seeger et al. 1993; Kidd et al. 1998 a,b). These mutants also display fuzzy and thicker commissures and thinned longitudinal axons between segments (Figure 3.3C), consistent with previous findings (Seeger et al. 1993; Kidd et al. 1998a,b).

No mutations in the *netrin* genes have been reported to date. However, a few deficiencies exist that uncover the function of both *netrinA* and *netrinB* genes. Df(1)NP5/Y embryos exhibit altered fasciculation patterns when visualised with mAb 1D4 (Figure 3.2D). When examined with mAb BP102, they have thinned or absent commissures and thinned or absent longitudinal connections (Figure 3.3D). This phenotype is consistent with published findings (Mitchell et al. 1996), although this deficiency had not previously been examined with mAb 1D4.

Figure 3.2 (A-J) Most of the candidate genes display a mutant CNS phenotype in a homozygous or hemizygous state, as visualised with mAb 1D4.

*slit*² severe hypomorphs (A) have fully collapsed axon tracts and *slit*²⁹⁹⁰ weak hypomorphs (B) demonstrate a partial collapse. *robo1*¹ mutants (C) have a unique circling phenotype that involves only the medial-most fascicle. Altered selective fasciculation patterns of FasII-positive axons are observed in netrin-deficient (Df(1) NP5/Y, D) and *comm*^{a490} mutant (E) embryos. *dock*^{P1} mutants (F) display gaps in the outer fascicle (arrows). *Hem*⁰³³³⁵ mutants (G) display a similar, but less severe, narrowing of axon tracts and midline crossovers as compared to *slit* mutants. *lamA*⁹⁻³² mutants (H) have a near wildtype phenotype with occasional gaps in the lateral fascicle. *tig*^x mutants (I) display gaps in the outer fascicle (arrow) more severe than *dock*^{P1} mutants. *mas*^{x124} mutants (J) display a near or complete fusion of the inner fascicle between segments (arrowhead).

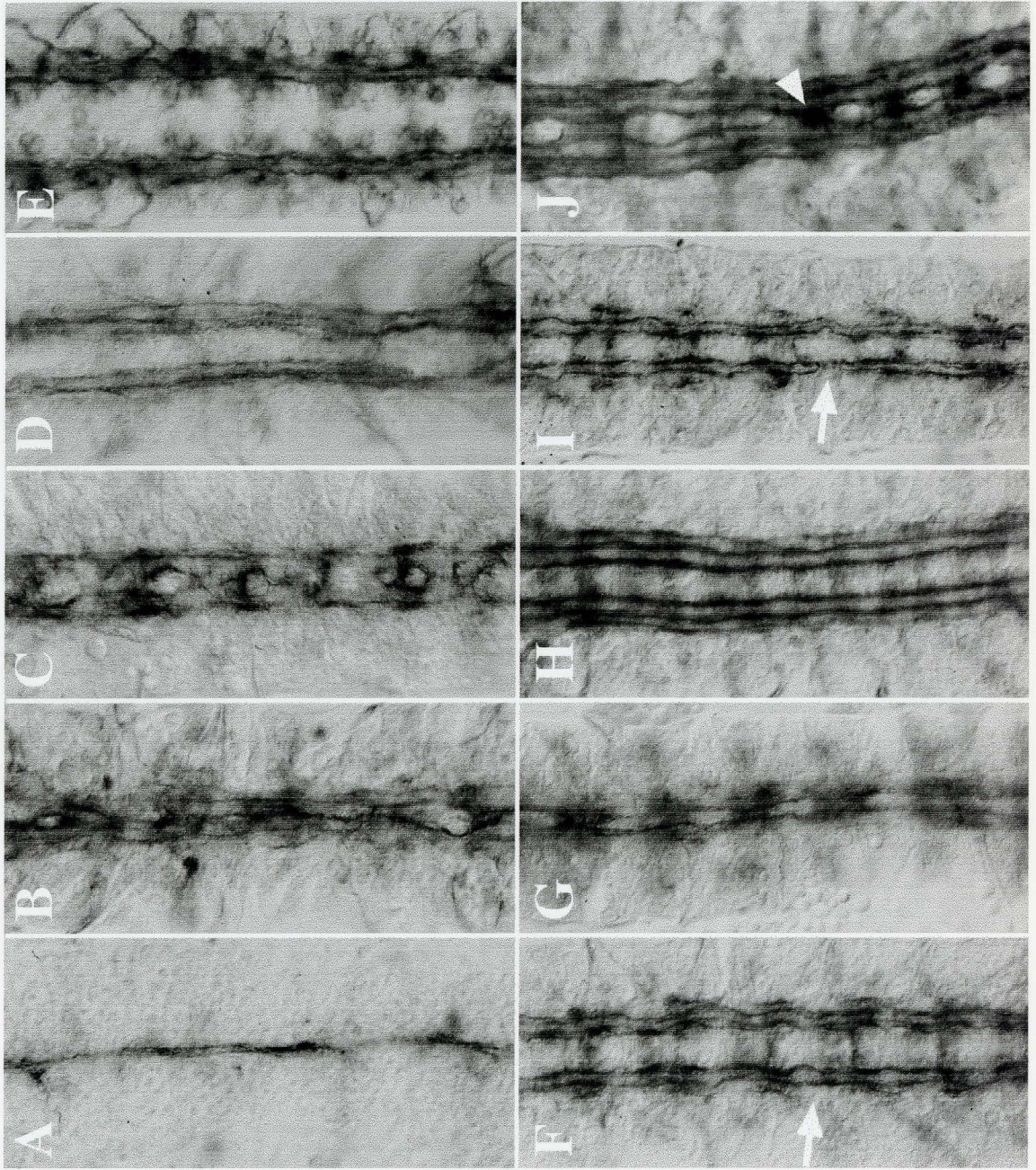


Figure 3.2 (K-R) Most of the candidate genes display a mutant CNS phenotype in a homozygous or hemizygous state, as visualised with mAb 1D4.

ten-m^{AL1} mutants (K) display altered defasciculation between the lateral two fascicles, and frequent absence of the lateral-most fascicle. *mew^{M6}/Y* mutants (L) appear more severe and defasciculated and narrowed toward the midline in some segments (arrow). *ifk^{27e}/Y* mutants (M) demonstrate axons crossing the midline in some segments (arrow) and gaps in the lateral fascicle (arrowhead). *scb²* mutants (N) and *mys^l/Y* mutants (O) display medial fusion in middle segments (arrow), although *mys^l* mutants are more severe. *Tl^{R3}* mutants (P) display selective defasciculation errors in the two lateral fascicles and occasional absence of the lateral-most fascicle. *dlg1⁶* mutants (Q) have a wildtype FasII pattern, although FasII expression is reduced (see text). Lateral displacement of axons in segments is evident (arrow) as well as aberrant axons projection (arrowhead) across the midline in *nrx⁴³⁰⁴* mutants (R).

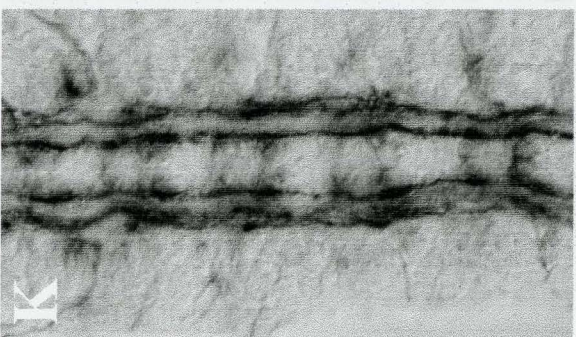
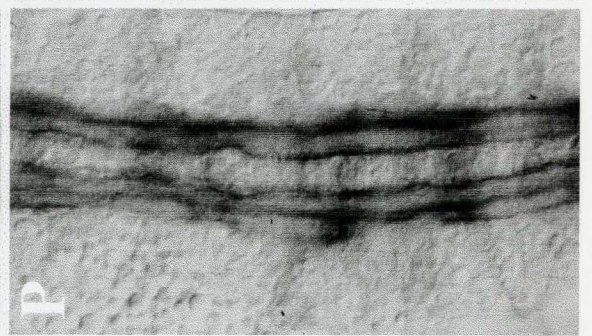
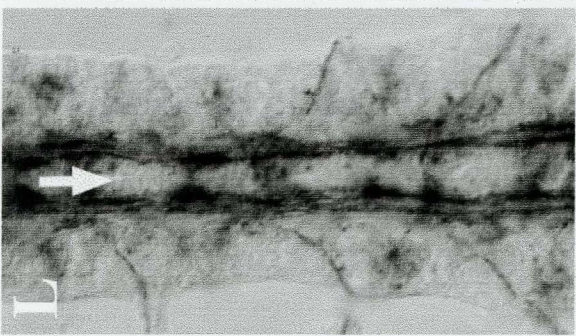
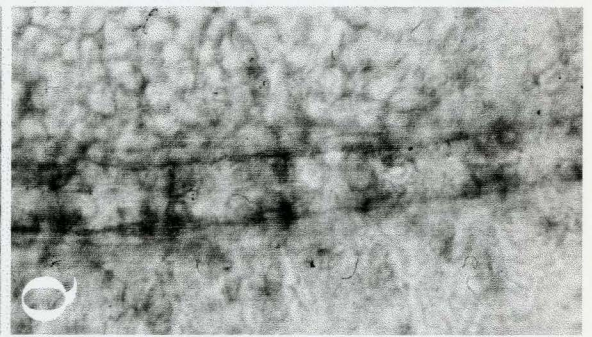
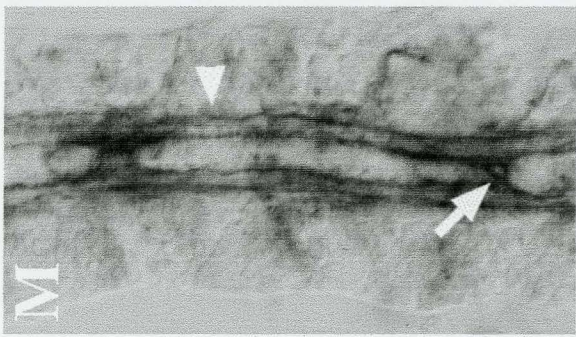
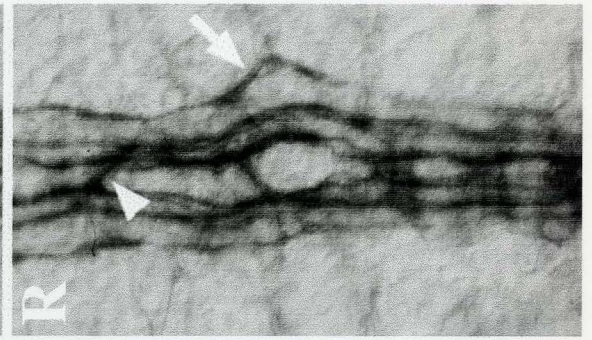
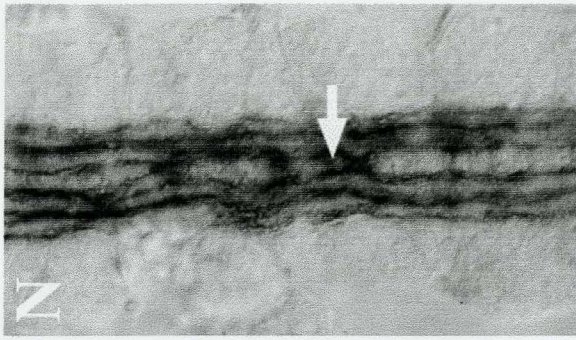


Figure 3.3 (A-J) Some of the candidate genes display a mutant CNS phenotype in the homozygous or hemizygous state, as visualised with mAb BP102.

*slit*² severe hypomorphs (A) have collapsed axon tracts and commissures at the midline. *slit*²⁹⁹⁰ weak hypomorphs (B) are partially collapsed with fuzzy commissures and thinned connections between segments (arrow). *robo1*¹ mutants (C) display a partial collapse similar to *slit*²⁹⁹⁰, although commissures are still not well separated (arrow) and intersegmental connections are thinned. *netrin*-deficient (Df(1) NP5/Y, D) embryos display frequent thinning or absence of the posterior commissure (arrowhead) and longitudinal axon tracts (arrow). *comm*^{a490} mutants (E) do not form commissures. *dock*^{P1} mutants (F) and show few defects although the nerve cord is slightly narrowed compared to wildtype. *Hem*⁰³³³⁵ mutants (G) have fuzzy commissures and narrow axon tracts. *lamA*⁹⁻³² mutants (H) and *tig*^x mutants (I) appear wildtype. *mas*^{x124} mutants (J) display some segments with fused commissures (arrowhead), while others have aberrant commissure formation (arrow).

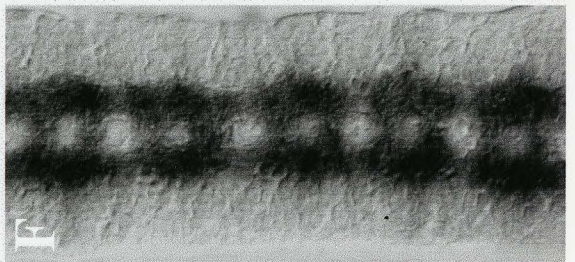
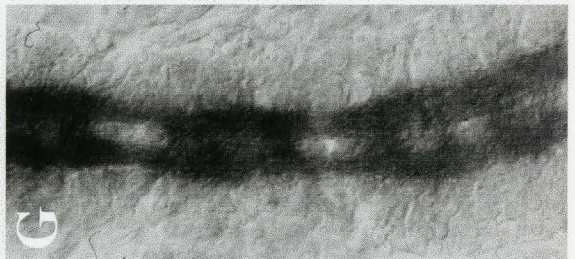
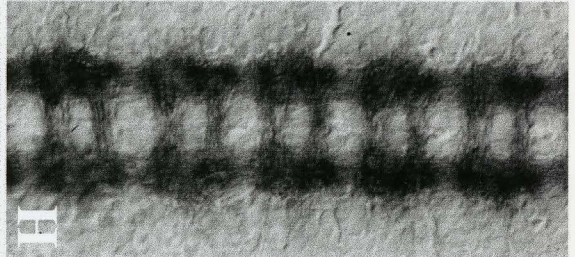
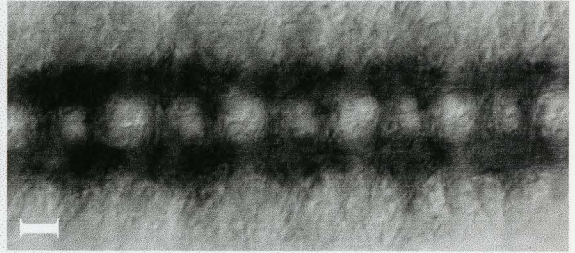
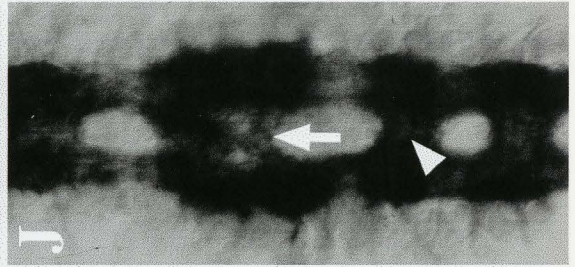
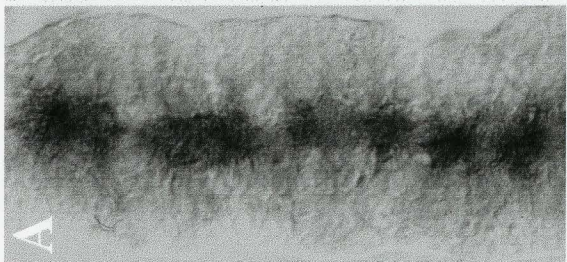
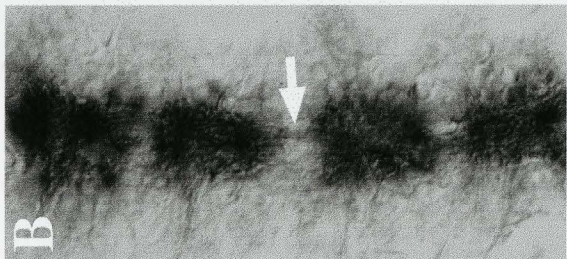
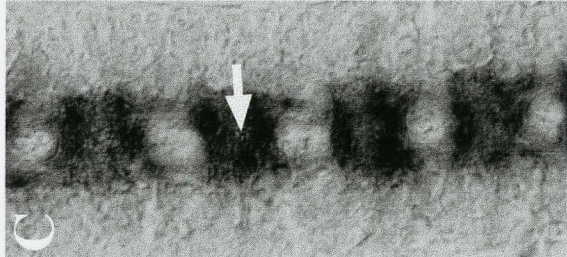
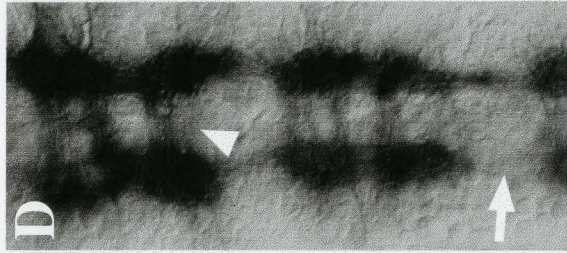
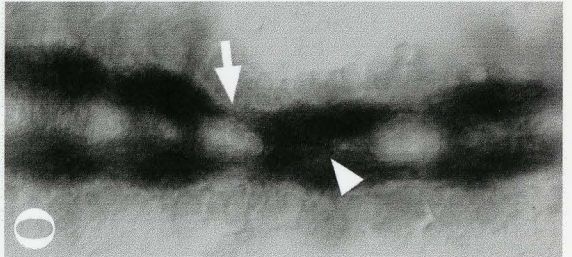
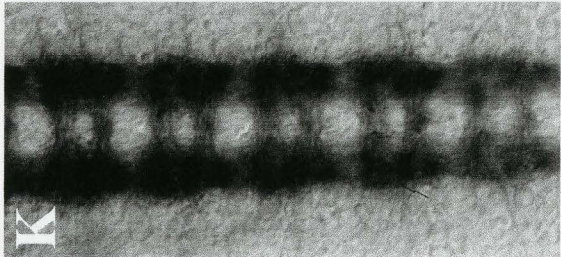
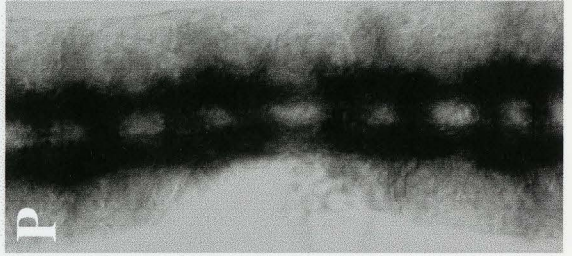
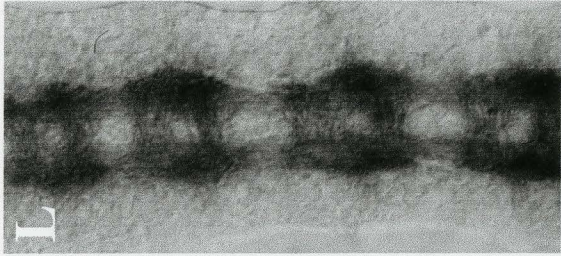
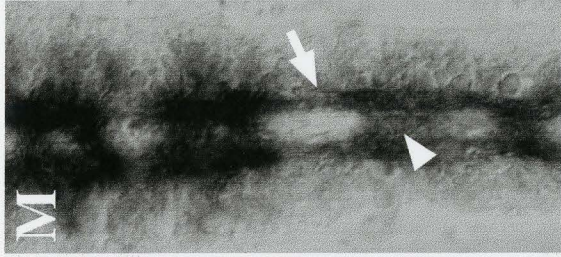
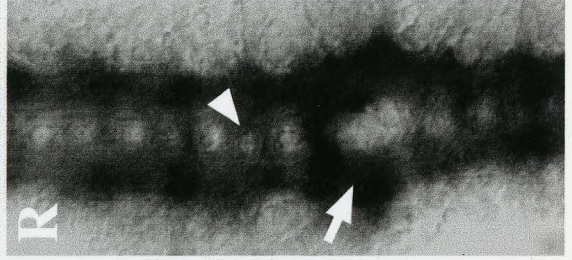
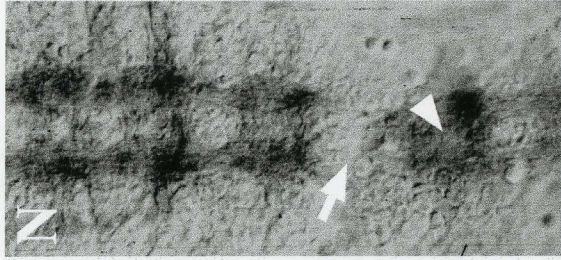


Figure 3.3 (K-R) Some of the candidate genes display a mutant CNS phenotype in the homozygous or hemizygous state when visualised with mAb BP102.

ten-m^{ALI} mutants (K) are indistinguishable from wildtype. *mew^{M6}/Y* mutants (L) demonstrate slight narrowing of axons tracts toward the midline. *ij^{27e}/Y* (M), *scb²* (N) and *mys^l/Y* (O) mutant embryos demonstrate fuzzy commissures in some segments (arrowhead) and thinned longitudinal tracts between some segments (arrow). *Tl^{R3}* mutants (P) demonstrate slight narrowing of axon tracts toward the midline. *dlg1⁶* mutants (Q) are indistinguishable from wildtype. *nrx⁴³⁰⁴* mutants (R) demonstrate poor commissure separation (arrowhead) and lateral displacement of axons combined with lack of commissures in at least one segment (arrow).



comm^{a490} mutants have been well characterised (Seeger et al. 1993; Tear et al. 1996). These mutants display defasciculation defects when observed with mAb 1D4 (Figure 3.2E) and complete lack of commissures when stained with mAb BP102 (Figure 3.3E).

3.3 OTHER GENES IMPLICATED IN AXON GUIDANCE

Dreadlocks (Dock) is a cytoplasmic molecule recently identified as an adapter protein involved in axonal guidance and synapse formation (Clemens et al. 1996; Desai et al. 1999). *dock*^{P1} mutants display mildly wavy FasII-positive fascicles and frequent gaps in the lateral fascicle (Figure 3.2F), consistent with literature reports (Desai et al. 1999). These mutants, however, do not show mutant a CNS phenotype when observed with mAb BP102 (Figure 3.3F). No previous reports have investigated a commissural phenotype for this allele, although thinned longitudinal tracts between segments with a different allele has been described (Hummel et al. 2000). An embryo lacking both maternal and zygotic Dock protein demonstrate a discontinuous lateral fascicle and FasII-positive axons crossing the midline (Desai et al. 1999).

DHem-2 is transmembrane protein originally examined for function in oogenesis (Baumgartner et al. 1995). Recently, however, dHem-2 has been shown to be involved in axon guidance in the CNS (Hummel et al. 1999a, 2000). *Hem*⁰³³³⁵ mutants (allelic to *kette*; Hummel et al. 2000) display a narrowed axon tract and midline crossovers when visualised with mAb 1D4 (Figure 3.2G). These mutants are also narrowed toward the midline and display poorly defined commissures and thinned longitudinal tracts, as revealed with mAb BP102 (Figure 3.3G). The phenotypes observed here reflect a P-element insertion in an intron near the start codon (Hummel et al. 2000). Hummel et al. (1999a, 2000) describe a similar, but more severe, phenotype with a *kette* allele mutated within an exonic region.

3.4 MUTATIONS IN GENES THAT ENCODE EXTRACELLULAR MATRIX PROTEINS

Laminin is a fundamental part of basement membranes of the extracellular matrix. All laminin forms are composed of three helical subunits (α , β and γ) that associate to form a cruciform complex. *Drosophila* laminin has been characterised and found to be required for heart, somatic muscle and gut development (Yarnitzky and Volk 1995). *Drosophila lamininA* gene is one of two α -subunits characterised. The other α -chain gene, *wing blister*, was only recently characterised (Martin et al. 1999) and not known at the time of this analysis. *lama*⁹⁻³² demonstrates only a mild CNS phenotype with occasional gaps in the lateral fascicle, but otherwise looks wildtype (Figure 3.2H). With mAb BP102, this mutant looks wildtype (Figure 3.3H). No mutations have been isolated for the LamininB1 (β -subunit) and LamininB2 (γ -subunit) chains to date.

Tiggrin is another extracellular matrix component in *Drosophila*. Tiggrin has been shown to play an important role at sites of muscle insertion by binding to α -PS2 integrins at these sites (Fogerty et al. 1994; Bunch et al. 1998). Of importance here is its reported expression around commissures (Fogerty et al. 1994). *tig*^x mutants (Figure 3.2I) display a phenotype similar to *dock*^{P1} mutants, whereby fascicles are somewhat wavy down the length of the nerve cord and appear to show large gaps in the lateral fascicle. However, with mAb BP102, these embryos do not show a mutant phenotype (Figure 3.3I).

Masquerade is a secreted extracellular matrix protein expressed by the midline glia and has been shown to be required for somatic muscle attachment (Murugasu-Oei et al. 1995, 1996). *mas*^{x124} mutants demonstrate fusion of medial fascicles at the midline (Figure 3.2J) and aberrant commissure formation in some segments while others appear poorly separated (Figure 3.3J). The observed BP102 phenotype is consistent with that reported in literature (Murugasu-Oei et al. 1996), although *mas* mutants were not previously examined at later stages of development with mAb 1D4. Murugasu-Oei et al. (1996) reported stalling of some aCC and pCC axons at earlier stages of axonogenesis, around stage 13.

Tenascin proteins are also secreted extracellular matrix proteins. Four different tenascin proteins have been characterised in vertebrates (Faissner 1997) while only two have been discovered in *Drosophila*, Tenascin-m and Tenascin-a. Tenascin-m is the major tenascin protein and has been localised to commissural and longitudinal axons of the CNS (Baumgartner et al. 1994). *ten-m^{ALI}* mutants are defasciculated between the two lateral fascicles and frequent absence of the lateral-most fascicle (Figure 3.2K). These mutants do not show a phenotype with mAb BP102 (Figure 3.3.K). No mutation has been isolated in the *tenascin-a* (accessory tenascin protein) gene.

3.5 MUTATIONS IN THE INTEGRIN GENE FAMILY

Integrins are a class of transmembrane cell receptors classically involved in cell adhesion and cell-matrix communication events. They are heterodimers comprised of an α -subunit and a β -subunit. Three α -subunit genes and two β -subunit genes have been cloned in *Drosophila*, and are tagged as “position-specific” (PS) based on their restricted patterns of expression in imaginal discs (Gotwals et al. 1994).

multiple edematous wings (mew) is the gene that encodes the α PS1-subunit in flies. *mew* has been shown to be involved in muscle attachment (Brower et al. 1995) and is also expressed in the nervous system in a cluster of cells at the midline (Hoang and Chiba 1998). 89% of *mew^{M6}* mutants (n=98) demonstrate defasciculation of all three longitudinal pathways and narrowing toward the midline (Figure 3.2L). A less representative proportion of these mutants (11%) display occasional crossing of the medial fascicle and gaps in some longitudinal axons (Appendix Figure 14C). When observed with mAb BP102, these mutants demonstrate slight narrowing of axon tracts toward the midline (Figure 3.3L). Hoang and Chiba (1998) characterises *mew* mutants with a midline fusion of medial FasII-positive axons or gaps in the lateral fascicle.

inflated (if) was cloned as the gene encoding the α PS2-subunit in *Drosophila*. This integrin subunit was shown to be located at sites of muscle attachment, apposed to the

α PS1-subunit (Brown 1994). Inflated is expressed in a cluster of midline cells and in bilaterally paired mediolateral clusters of cells adjacent to the midline (Hoang and Chiba 1998). 31% of *if^{k27e}* mutants (n=39) display axons crossing the midline in some segments and gaps in the lateral fascicle (Figure 3.2M). Other embryos (38%) in this collection display only gaps in the lateral fascicle (Appendix Figure 14A), while the remainder (31%) show no mutant phenotype (data not shown). When visualised with mAb BP102, the majority of embryos display poorly defined commissures in some segments and thinned longitudinal connections between segments (Figure 3.3M). A less representative proportion of *if^{k27e}* mutants show a more severely collapsed commissure in some segments (Appendix Figure 14B). Hoang and Chiba (1998) report a midline fusion of medial FasII-positive axons or gaps in the lateral fascicle in these mutants.

Scab is the third known integrin α -subunit known to date and thus denoted as α PS3. *scab* (*scb*; aka *Volado*) was recently cloned and shown to be localised to tissues undergoing invagination, tissue movement and morphogenesis, including the CNS midline and the heart (Stark et al. 1997), and has also shown to be involved in short-term memory (Grotewiel et al. 1998). *scb²* mutants are easily identified by a prominent dorsal hole at later embryonic stages (Appendix Figure 14D) as they fail to undergo dorsal closure (Stark et al. 1997). 54% of *scb²* mutants (n=171) do not display a mutant CNS phenotype (data not shown). Medial fascicles of some *scb²* mutants (22%) are fused at the midline in some segments (Figure 3.2N). Other mutants (24%) have a twisted nerve cord, making it difficult to identify midline crossovers (Appendix Figure 14D and E). As a result the percentage of mutants exhibiting crossovers can be viewed as a conservative representation. It was difficult to identify the presence of mutant phenotypes with mAb BP102, but of those mutants seen, they demonstrated thinned longitudinal connections and

occasional fuzzy commissures (Figure 3.3N). No other studies known to date have examined *scb* mutants for a CNS phenotype.

myospheroid (*mys*) is the gene that encodes one of the two integrin β -subunits. This subunit, β PS, associates with each of α PS1, α PS2 and α PS3 *in vivo*. The other β subunit, β_v , is expressed only in the midgut (Yee and Hynes 1993). Mutant phenotypes observed in the β PS integrin are more severe than α PS integrins (Roote and Zusman 1995). Consistent with this observation, I observed mutant phenotypes in 50% of *mys*¹ mutant embryos (n=361) that were worse than the α PS integrins. These mutants displayed medial fascicles fused at the midline in the middle segments (Figure 3.2O), medial fascicles that were closely apposed at the midline in some segments and laterally displaced in other segments (Appendix Figure 14F), or, fascicles that were no longer selectively fasciculated and showed midline crossing (Appendix Figure 14G). The other half of *mys*¹ mutants showed no CNS mutant phenotype (data not shown), although all *mys*¹ mutants were dorsally herniated as was also observed in *scb* mutants. With BP102, *mys*¹ mutants demonstrated fuzzy commissures and thinned longitudinals (Figure 3.3O), or a more obvious collapse of axons tracts toward the midline in some segments (Appendix Figure 14H). However, the majority of these mutants did not have a CNS mutant phenotype (data not shown). Hoang and Chiba (1998) report a similar phenotype for *mys* mutants (visualised with mAb 1D4) as was shown here (Figure 3.2O) and another phenotype displaying gaps in the lateral-most fascicle.

3.6 MUTATION IN A GENE ENCODING A CELL ADHESION RECEPTOR

Toll is a transmembrane protein classically studied for its role in dorsal-ventral pattern formation (Hashimoto et al. 1991). Toll has also been shown to be involved in proper motoneuron and muscle development during embryogenesis (Halfon et al. 1995). With great interest to this study, Toll is another protein expressed by the midline glia

(Halfon et al. 1995) and is involved in cell adhesion (Keith and Gay 1990). Tl^{R3} mutants display selective fasciculation errors in the two lateral fascicles and occasional absence of the lateral-most fascicle (Figure 3.2P), consistent with a phenotype presented in previous work (Halfon et al. 1995). With BP102, these mutants show slight narrowing of axon tracts toward the midline (Figure 3.3P).

3.7 MUTATIONS IN GENES PRESENT AT SEPTATE JUNCTIONS

Discs-large (Dlg1) is known for its role in tumor suppression in *Drosophila* (Woods and Bryant 1989). This gene encodes a cytoplasmic protein which has been localised to septate junctions between epithelial cells and glia and also synaptic junctions in neurons (Woods and Bryant 1991; Woods et al. 1996; Hough et al. 1997). Existence of an SH3 domain in Dlg1 opens the possibility for a role in signal transduction (Woods and Bryant 1991). This was an appropriate avenue to examine as Dlg1 protein is localised to CNS neurons (Woods and Bryant 1991). $dlg1^6$ mutants appear wildtype in CNS architecture with mAbs 1D4 and BP102 (Figures 3.2Q and 3.3Q). Dlg1 has shown to be directly responsible for recruiting FasII to the surface of the presynaptic membrane as mutants in $dlg1$ result in abnormal FasII distribution (Thomas et al. 1997). Thus, this accounts for the reduced FasII labelling observed in these mutants (Figure 3.2Q).

Drosophila Neurexin (Nrx IV) is a transmembrane protein found at septate junctions. Nrx IV is not a true homolog of vertebrate neurexins. It exhibits greater amino acid similarity to vertebrate Caspr, a protein proposed to be involved as a signaling component between glia and neurons (Peles et al. 1997). Nrx IV has been shown to be required for septate junction and blood-brain barrier formation and is expressed on MG (Baumgartner et al. 1996). nrx^{4304} mutants demonstrate a consistent CNS phenotype, characterised by lateral displacement of axons in at least one segment (Figures 3.2R, 3.3R) and occasional midline crossing or midline fusion (Figure 3.2R) and absence of commissures in the segment exhibiting lateral displacement of axons (Figure 3.3R).

CHAPTER 4 BLIND GENETIC SCREEN EXPERIMENT

4.1 INTRODUCTION TO BLIND GENETIC SCREEN

The first goal of this study was to determine if a *slit* hypomorph with a mild CNS phenotype could be affected by a mutation in another gene, such that it would alter the *slit* CNS phenotype by either enhancing it (making it more severe) or suppressing it (making it less severe, more toward wildtype). I chose the *slit*²⁹⁹⁰ allele, as these homozygotes demonstrate a mild CNS phenotype that can be used to test for either enhancement or suppression (refer to Chapter 3). Mutations in 15 candidate genes were located on the X, 2nd and 3rd chromosomes. Double mutant embryos were collected and stained for mAb 1D4 to assay for severity of crossover phenotypes. This screen was used only as a qualitative test for candidate genes that may interact genetically with *slit*. Quantitative results will be provided where possible. All counts shown are a percentage of mutants scored, not a percentage of the whole embryo population. No counts were scored in collections that did not demonstrate a genetic interaction.

To generate a population of embryos that include double mutant genotypes for *slit*²⁹⁹⁰ and an X chromosome candidate gene, female flies mutant on the X chromosome were mated en masse to male *slit*²⁹⁹⁰ flies. Selective F1 progeny were then intermated en masse in an egg collection house to collect F2 embryos. Refer to Appendix Figure 1 for an illustration of the genetics for this cross.

To generate *slit*²⁹⁹⁰ and 2nd chromosome mutation transheterozygotes, flies from each mutant fly line were mated en masse in an egg collection house to create transheterozygous F1 embryos in the collection. Refer to Appendix Figure 2 for an illustration of the genetics for this cross.

To generate a population of embryos that include double mutant genotypes for *slit*²⁹⁹⁰ and a 3rd chromosome candidate gene, flies from each mutant fly line were mated en

masse. Selective F1 progeny were then intermated en masse in an egg collection house, to collect F2 embryos. Refer to Appendix Figure 3 for an illustration of the genetics for this cross.

Control crosses were also included in this screen. Since lethal mutations on the X chromosome produced lethal embryos in males, all males in the F1 generation were of the genotype FM7c β /Y on the 1st chromosome. As a result, the presence of balancer chromosomes in the blind test may introduce another factor affecting CNS phenotype, I crossed FM7c[ftz-lacZ] flies to *slit*²⁹⁹⁰ flies to create double heterozygotes for the balancer and *slit*²⁹⁹⁰. This mating allowed me to both collect F1 embryos and to intermate F1 flies to collect F2 embryos that were homozygous on both chromosomes. Refer to Appendix Figure 4 for an illustration of the genetics of this cross.

Embryos were immunolabeled and stored in tubes prior to examination. These tubes were blindly coded by another individual and examined under such conditions. Identification of these tubes was made known after analysis was complete.

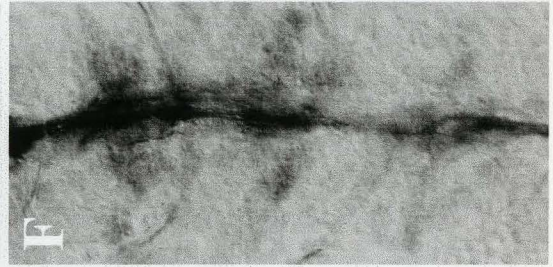
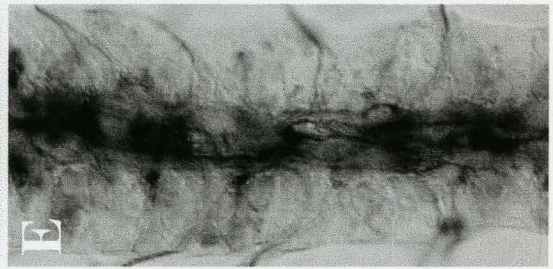
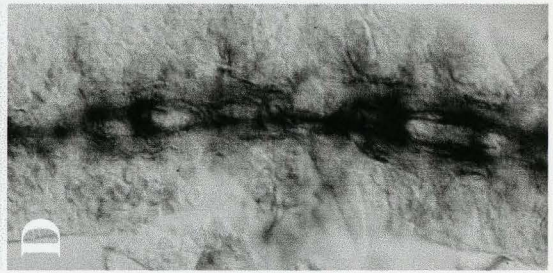
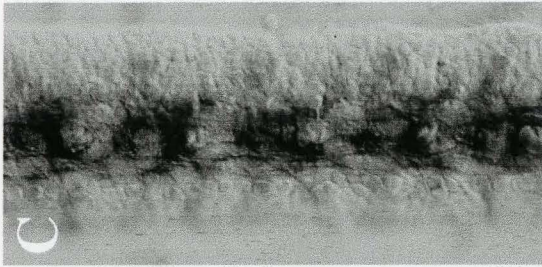
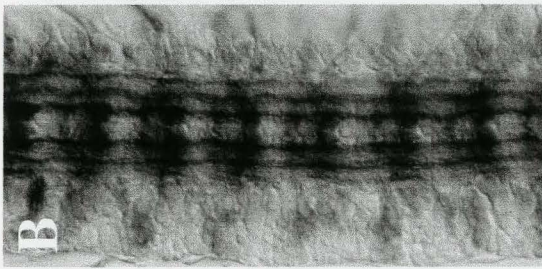
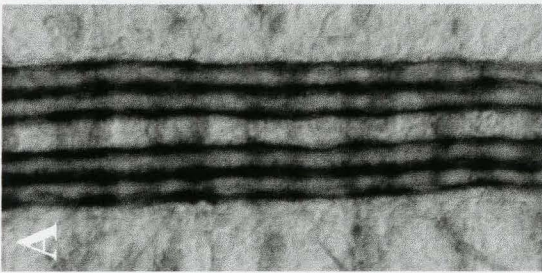
4.2 CONTROL CROSSES AND SLIT ALLELES FORM THE BASELINE COMPARISON

Wildtype CS-P CNS phenotype is shown in Figure 4.1A. Embryos heterozygous for the balancer chromosome FM7c[ftz-lacZ] (aka FM7c β) and the allele *slit*²⁹⁹⁰ demonstrated a wildtype-like phenotype (Figure 4.1A), although staining in the lateral fascicle is faint in this example. Embryos homozygous or hemizygous for FM7c[ftz-lacZ] and homozygous for *slit*²⁹⁹⁰ (Figure 4.1C) displayed the crossover phenotype previously shown for the single mutant *slit*²⁹⁹⁰ (compare to Figure 3.2B).

Also included in this blind test were a subset of *slit* alleles that represent differing severities of CNS phenotype previously characterised (Battye 2000). *slit*^{E158} is an allele produced by P element insertion into a site upstream of the start codon is (Rothberg et al. 1990), which may affect the levels of transcript and, subsequently, levels of Slit protein

Figure 4.1 Control lines for *slit* blind genetic test experiment.

Tubes of mAb 1D4 immunolabelled embryos were blindly coded prior to examination (see text). CS-P (A) and FM7c[ftz-lacZ]/+; *slit*²⁹⁹⁰/+ (B) embryos exhibit wildtype axon tract morphology. FM7c[ftz-lacZ]/Y; *slit*²⁹⁹⁰ and FM7c[ftz-lacZ]; *slit*²⁹⁹⁰ embryos display only a *slit*²⁹⁹⁰ phenotype (C). Included in this screen were *slit*^{E158} (D), *slit*²⁹⁹⁰ (E), *slit*¹⁹¹² (F) and *slit*² (G) mutants for comparison.



produced by the MG. These homozygotes produce a phenotype displaying variation in severity along the length of the nerve cord: some segments show midline crossovers and fusion, while others do not demonstrate any crossovers (Figure 4.1D). *slit*²⁹⁹⁰ mutants are shown again in Figure 4.1E. *slit*¹⁹¹² mutants were generated through an EMS mutagenesis screen and produce a fully collapsed nerve tract at the midline (Figure 4.1F) similar to *slit*² mutants (Figure 4.1G).

Assessments of genotypes of these crosses are difficult, as balancer chromosomes were not stained for (X and 2nd chromosome crosses) or were selected against (3rd chromosome crosses). As a result, I will attempt to identify the genotypes of these embryos based on comparing expected and observed frequencies of the genotypes expected in the population.

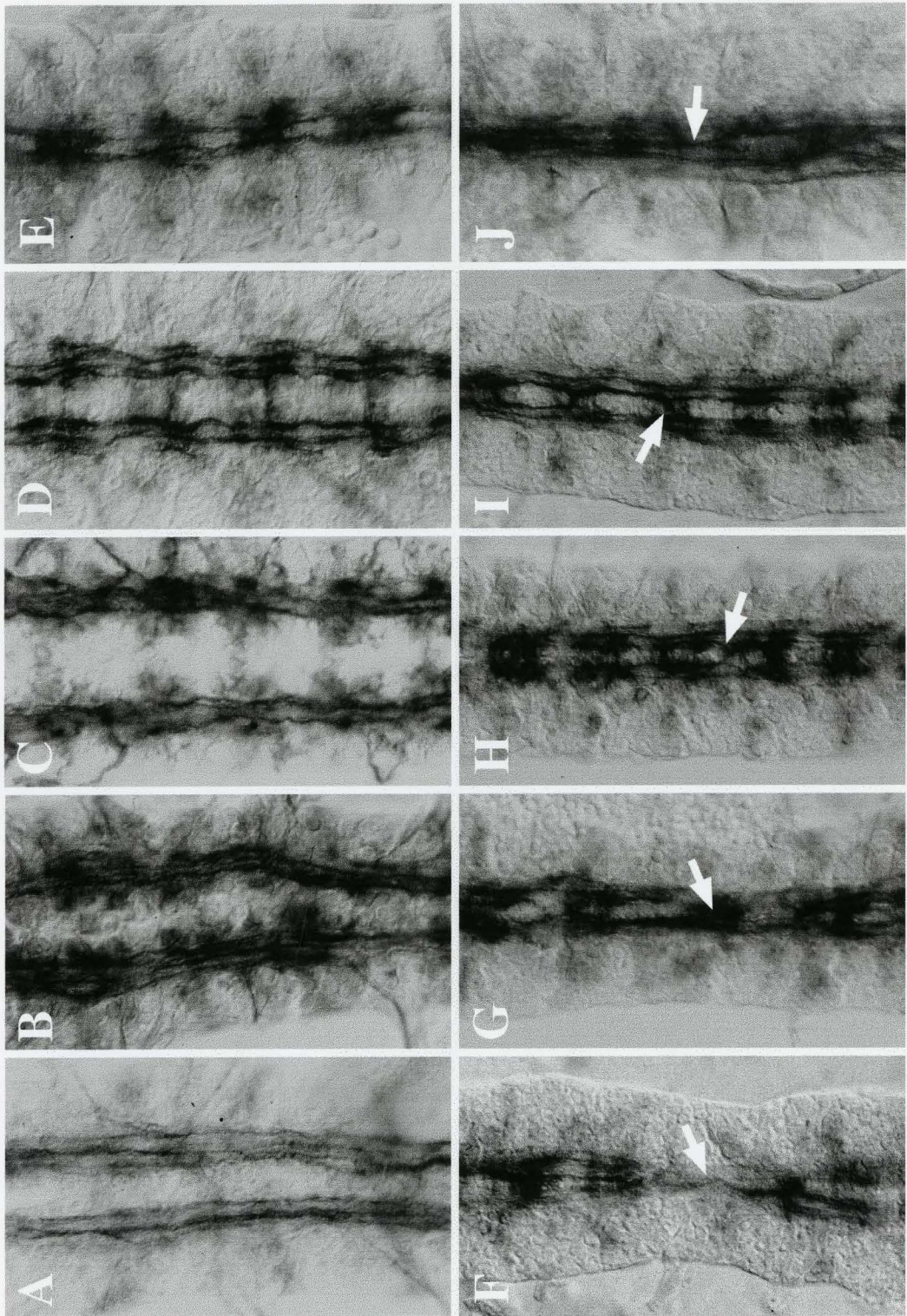
4.3 BLIND TEST EXPERIMENTS REVEAL SOME CANDIDATE GENES FOR INTERACTION WITH *SLIT*.

Single mutant embryos were also included in this screen and their phenotypes are shown in the upper row of panels within each figure for phenotypic comparison (Figure 4.2 A-E, K-O, U-Y). Phenotypes for most of these mutants were described previously in Chapter 3. The *netrin* deficiency Df(1)KA9/Y (not described previously; Figure 4.2B) produces a similar phenotype to the *netrin* deficiency Df(1)NP5/Y (Figure 4.2A). *central body defect (cbd)*, a mutant gene that maps near the *tenascin-a* locus, was not described previously, but was included in this screen. Embryos from the *cbd*¹ collection appear wildtype (Figure 4.2N).

Middle segments of embryos from a Df(1)NP5 and *slit*²⁹⁹⁰ cross display midline fusion of medial fascicles, while other segments had midline crossovers, and a few were unaffected (Figure 4.2F). These embryos may represent the Df(1)NP5/+; *slit*²⁹⁹⁰/+ genotype. Mutants similar to this from the Df(1)KA9 and *slit*²⁹⁹⁰ cross also showed midline crossovers and fusion in 28% of mutants (n=78; Figure 4.2G). Likewise, these

Figure 4.2 (A-J) Blind genetic test experiment attempts to identify candidate genes for interaction with slit.

Late stage 16 embryos were immunolabelled with mAb 1D4 prior to dissection. Included in this screen were the netrin deficiencies Df(1)NP5/Y (A) and Df(1)KA9/Y (B), *comm^{a490}* (C), *dock^{P1}* (D) and *Hem⁰³³³⁵* (E). NP5/+; *slit²⁹⁹⁰*/+ and KA9/+; *slit²⁹⁹⁰*/+ double mutant embryos display midline aberrations in most segments (arrows), ranging from medial fusion of axons to midline crossovers (compare F and G). *slit²⁹⁹⁰*/+; *comm^{a490}*/+ mutant embryos (H) demonstrate crossovers of the medial longitudinal fascicle (arrow), reminiscent of *slit²⁹⁹⁰* mutants. *slit²⁹⁹⁰*/*dock^{P1}* transheterozygote embryos display mild crossovers in a few segments (arrow, I). *slit²⁹⁹⁰*/+; *Hem⁰³³³⁵*/+ mutant embryos demonstrate fusion of the medial axon tracts (arrow, J).



embryos may represent the double heterozygous phenotype, $Df(1)KA9/+; slit^{2990}/+$ genotype. The expected frequency (EF) for these genotypes is 22%. This is likely representative of a genetic interaction between the *netrin* and *slit* genes. Also seen in this collection were *netrin* (17%) phenotype, representing the genotypes $KA9/Y; slit^{2990}/+$ (EF=22%) and $KA9/Y; +$ (EF=11%), and *slit*²⁹⁹⁰ (55%) phenotype, representing the genotypes $KA9/+; slit^{2990}$ (EF=11%), $KA9/Y; slit^{2990}$ (EF=11%), $+; slit^{2990}$ (EF=11%) and $+/Y; slit^{2990}$ (EF=11%) (data not shown).

A subset of mutants from the *slit*²⁹⁹⁰ and *comm*^{a490} cross displayed a narrowed nerve cord with crossovers in some segments (45% of mutants, n=61; Figure 4.2H). This phenotype may represent the *slit*²⁹⁹⁰ /+; *comm*^{a490} /+ genotype (EF=36%), although further analysis using double mutant lines would need to be done to support this data. Also seen in this collection were the *comm*^{a490} (16%) phenotype, representing the *slit*²⁹⁹⁰ /+; *comm*^{a490} (EF=18%) and $+; comm^{a490}$ (EF=9%) genotypes, and the *slit*²⁹⁹⁰ (39%) phenotype, likely representing the *slit*²⁹⁹⁰; *comm*^{a490} (EF=9%), *slit*²⁹⁹⁰; *comm*^{a490} /+ (EF=18%) and *slit*²⁹⁹⁰; + (EF=9%) genotypes (data not shown).

From the *dock*^{P1} /*slit*²⁹⁹⁰ transheterozygous cross, embryos with defects showed midline crossovers of medial axon tracts in several segments (Figure 4.2I), indicating these genes interact genetically. Other embryos in this collection (likely *dock*^{P1} /+ and *slit*²⁹⁹⁰ /+ genotypes) appeared wildtype (data not shown).

52% (n=142) of phenotypic mutants from the *slit*²⁹⁹⁰ and *Hem*⁰³³³⁵ cross appeared medially fused down the length of the nerve cord, with little spacing at the midline (Figure 4.2J). Based on frequency, these embryos may be of the genotype *slit*²⁹⁹⁰ /+; *Hem*⁰³³³⁵ /+ (EF=36%), thereby indicating a genetic interaction between *slit* and *Hem*. However, as the collapse of the medial axon tract seen in these mutants is greater than in *slit*²⁹⁹⁰ embryos, these embryos may be representative of *slit*²⁹⁹⁰; *Hem*⁰³³³⁵ (EF=9%) or *slit*²⁹⁹⁰; *Hem*⁰³³³⁵ /+ (EF=9%) genotypes (data not shown).

(EF=18%) genotypes. At this point, I cannot be certain. Other mutants in this collection were of the *Hem*⁰³³³⁵ (16%) phenotype, representing *slit*²⁹⁹⁰/+; *Hem*⁰³³³⁵ (EF=18%) and +; *Hem*⁰³³³⁵ (EF=9%) genotypes, and *slit*²⁹⁹⁰ (32%) mutant phenotype, possibly representing the *slit*²⁹⁹⁰; *Hem*⁰³³³⁵ (EF=9%), *slit*²⁹⁹⁰; *Hem*⁰³³³⁵/+ (EF=18%) and *slit*²⁹⁹⁰; + (EF=9%) genotypes (data not shown).

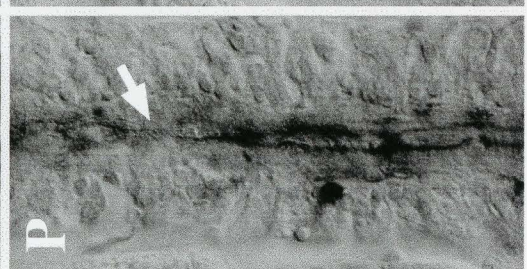
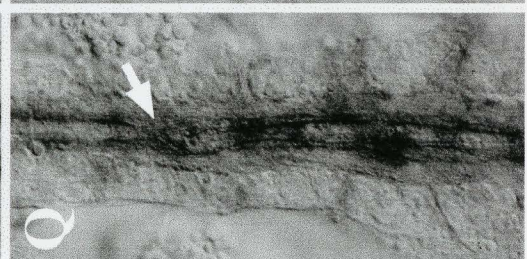
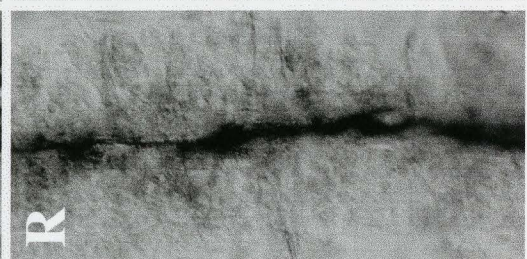
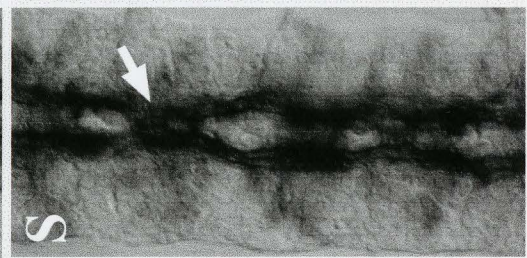
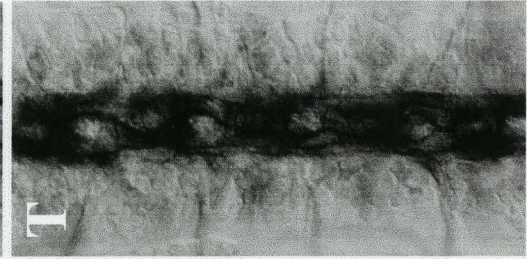
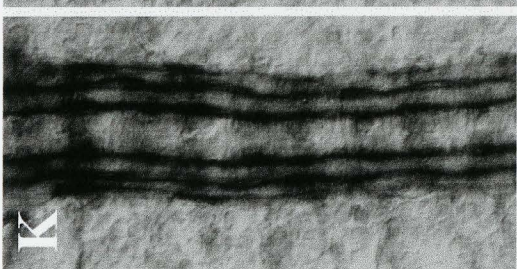
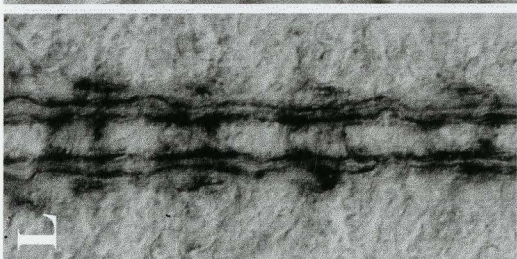
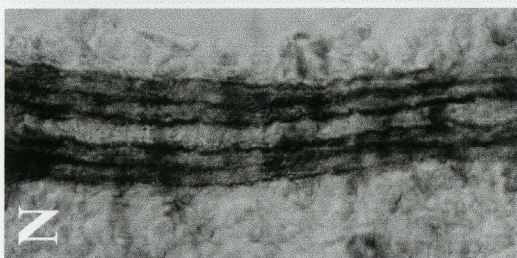
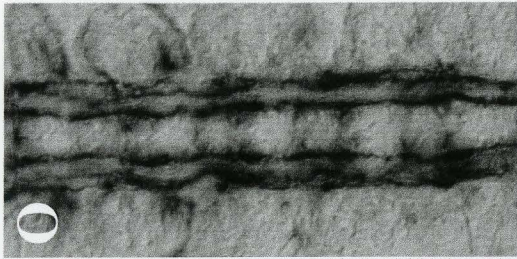
Mutants from the *slit*²⁹⁹⁰ and *lamA*⁹⁻³² cross appear to have the same phenotype as that of *slit*²⁹⁹⁰ mutants, demonstrating crossover of the medial axon tract across the midline, while the other fascicles remained unaffected. (Lateral fascicles here are faintly stained, although they do not cross the midline.) Occasionally, embryos would display medial fusion of axons at the midline (Figure 4.2P). This suggests that *slit* and *lamA* may interact genetically, if the latter phenotype is representative of a genotype different than that of the *slit*²⁹⁹⁰-like phenotypes observed in the collection. No counts in this collection were scored as all originally appeared like *slit*²⁹⁹⁰ mutants. This difference would need to be resolved upon examination of the stable double mutant lines as I cannot predict what the genotype is. Other embryos in this collection appeared wildtype (data not shown).

tig^x/*slit*²⁹⁹⁰ transheterozygotes show occasional crossovers across the midline (Figure 4.2Q). This suggests a genetic interaction between *tig*^x and *slit*²⁹⁹⁰, as an aberrant midline crossing phenotype is observed with a reduced gene copy for both genes. Other embryos in this collection (likely *slit*²⁹⁹⁰/+ and *tig*^x/+) appear wildtype (data not shown).

Mutants from a *slit*²⁹⁹⁰ and *mas*^{x124} cross demonstrate the first evidence of enhancement of the *slit*²⁹⁹⁰ mutant phenotype. These mutants are fused at the CNS midline with occasional looping of axons within segments (Figure 4.2R). Again, it is difficult to predict the genotype attributed to this phenotype, but could be representative of *slit*²⁹⁹⁰; *mas*^{x124}/+ or *slit*²⁹⁹⁰; *mas*^{x124}. The elucidation of dominant versus recessive enhancement of the *slit*²⁹⁹⁰ phenotype by *mas*^{x124} awaits the results of the stable double mutant line.

Figure 4.2 (K-T) Blind genetic test experiment attempts to identify candidate genes for interaction with slit.

Other gene candidates included in this screen were: *lamA*⁹⁻³² (K), *tig^x* (L), *mas^{x124}* (M), *cbd¹* (N) and *ten-m^{ALI}* (O). Embryos from a *slit*²⁹⁹⁰ and *lamA*⁹⁻³² double mutant cross (P) display phenotypes similar to *slit*²⁹⁹⁰ mutants, evidenced by midline crossing of medial axons while the other fascicles remained unaffected. Occasionally, embryos would show evidence of medial fusion (arrow, P). *slit*²⁹⁹⁰/*tig^x* transheterozygotes (Q) display mild midline crossovers (arrow). *slit*²⁹⁹⁰; *mas^{x124}* or *slit*²⁹⁹⁰; *mas^{x124}*/+ (R) mutants appear more severely collapsed than *slit*²⁹⁹⁰. *cbd¹*/Y; *slit*²⁹⁹⁰/+ or *cbd¹*/+; *slit*²⁹⁹⁰/+ mutants (S) show occasional midline crossing of FasII-positive axons (arrow). Mutant embryos from a *slit*²⁹⁹⁰ and *ten-m^{ALI}* cross (T) show only a *slit*²⁹⁹⁰-like phenotype.

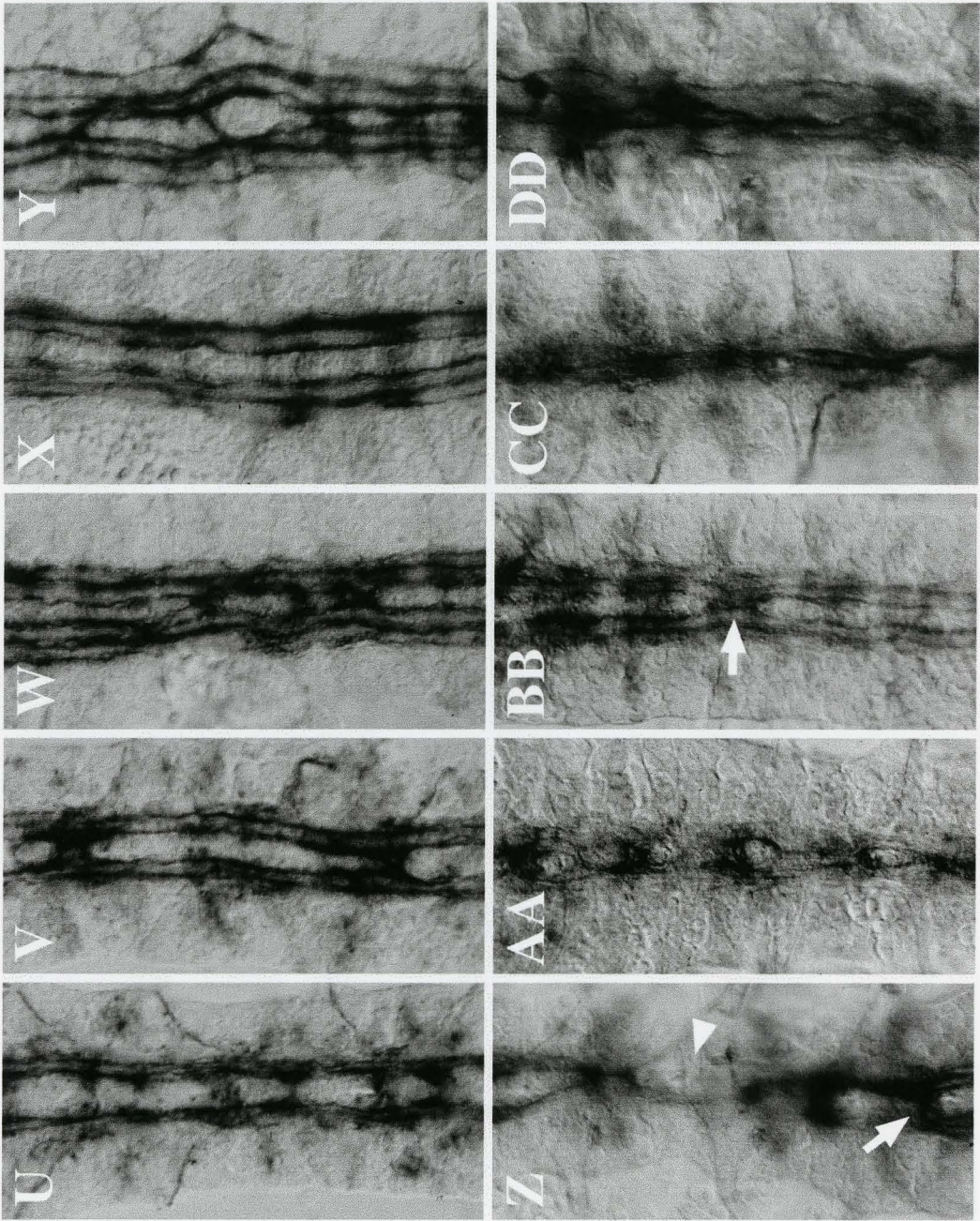


Interaction of *slit* with *tenascin* genes was also investigated. *cbd¹; slit²⁹⁹⁰* mutants display midline crossovers in some segments in 23.5% of mutants (n=51) (Figure 4.2S). Fascicles in these mutants also lose selective fasciculation and are narrower toward the midline in non-crossing segments. These embryos may be either *cbd¹/+; slit²⁹⁹⁰/+* (EF=25%) and/or *cbd¹/Y; slit²⁹⁹⁰/+* (EF=25%) but the frequencies do not hold true to expected values. Whether or not this is a true genetic interaction between *cbd¹* and *slit²⁹⁹⁰* is difficult to determine as the *cbd¹* fly line was homozygous viable and other genetic markers were recombined out. Other mutant phenotypes in this collection were of *slit²⁹⁹⁰* phenotype (76.5%), representing at least the *cbd¹/+; slit²⁹⁹⁰*, *cbd¹/Y; slit²⁹⁹⁰*, *+; slit²⁹⁹⁰* and *+/Y; slit²⁹⁹⁰* genotypes (all EF=12.5%) but perhaps *cbd¹/Y; slit²⁹⁹⁰* (EF=25%) as well, if not representative of the crossover phenotype. When introducing the *ten-m* allele, *slit²⁹⁹⁰; ten-m^{AL1}* mutants exhibit a *slit²⁹⁹⁰* phenotype (Figure 4.2T), indicating these genes do not interact genetically.

The α -integrin genes were also incorporated into this blind screen. Mutant phenotypes in the *mew^{M6}; slit²⁹⁹⁰* double mutant collection exhibited crossing of midline axons and axons missing in some segments in 15% of mutants (n=48) (Figure 4.2Z), indicating these genes likely interact. This phenotype could be representative of either *mew^{M6}/+; slit²⁹⁹⁰/+* (EF=25%) or *mew^{M6}/Y; slit²⁹⁹⁰/+* (EF=25%) genotypes. Other mutant phenotypes in this collection were of *slit²⁹⁹⁰* phenotype (85%), possibly representing *mew^{M6}/+; slit²⁹⁹⁰* (EF=12.5%), *mew^{M6}/Y; slit²⁹⁹⁰* (EF=12.5%), *+; slit²⁹⁹⁰* (EF=12.5) or *+/Y; slit²⁹⁹⁰* (EF=12.5%) genotypes. Mutant embryos in the *if^{k27e}; slit²⁹⁹⁰* double mutant collection display a *slit²⁹⁹⁰*-like phenotype although the medial axon tract is not as collapsed toward the midline (Figure 4.2AA). These embryos may represent the *if^{k27e}/Y; slit²⁹⁹⁰* or *if^{k27e}/+; slit²⁹⁹⁰* genotypes. The remainder in the collection look wildtype. *scb²/slit²⁹⁹⁰*

Figure 4.2 (U-DD) Blind genetic test experiment attempts to identify candidate genes for interaction with slit.

Other gene candidates included in this screen were: *mew^{M6}* (U), *ifk^{27e}* (V), *scb²* (W), *Tl^{R3}* (X) and *nrx⁴³⁰⁴* (Y). *mew^{M6}/Y; slit²⁹⁹⁰/+* or *mew^{M6}/+; slit²⁹⁹⁰/+* mutants (Z) exhibited an alternate phenotype of midline crossing of medial axons (arrow) and axons missing in some segments (arrowhead). *ifk^{27e}/Y; slit²⁹⁹⁰/+* or *ifk^{27e}/+; slit²⁹⁹⁰/+* mutants (AA) were indistinguishable from *slit²⁹⁹⁰* embryos. *scb²/slit²⁹⁹⁰* transheterozygotes (BB) demonstrated crossing of medial axons at the midline. *slit²⁹⁹⁰/+; Tl^{R3}/+* or *slit²⁹⁹⁰/+; Tl^{R3}* mutants (CC) exhibited a near *slit²⁹⁹⁰* phenotype, but with greater collapse of axons to the midline. Embryos from a *slit²⁹⁹⁰* and *nrx⁴³⁰⁴* double mutant cross (DD) were indistinguishable from *slit²⁹⁹⁰* mutants.



transheterozygotes demonstrated crossing of medial axons at the midline (Figure 4.2BB). These genes likely interact as a phenotype was shown with a mutant copy in each gene.

Mutant embryos in the *slit*²⁹⁹⁰; *Tl*^{R3} collection appeared slightly more collapsed toward the midline than *slit*²⁹⁹⁰ mutants (Figure 4.2CC) and may represent the *slit*²⁹⁹⁰; *Tl*^{R3} or *slit*²⁹⁹⁰; *Tl*^{R3}/+ genotypes. This may reveal a genetic interaction between these genes, but would need to be further supported by analysis of the stable double mutant line. No counts were done on this collection as phenotypes were scored as the *slit*²⁹⁹⁰ phenotype.

*slit*²⁹⁹⁰; *nrx*⁴³⁰⁴ double mutant embryos displayed only those phenotypes resembling *slit*²⁹⁹⁰, *nrx*⁴³⁰⁴ and wildtype within the collection. These genes likely do not interact genetically, although the phenotype in Figure 4.2DD appears to have greater medial fusion at the midline than *slit*²⁹⁹⁰ mutants. Further analysis is need to confirm these results.

From this blind double mutant screen *dock*, *Hem*, *tig*, *mas*, *mew* and *scb* genes appear to interact genetically with *slit*²⁹⁹⁰. It is also likely that *netrin*, *comm*, *lamA*, *cbd* and *Tl* interact genetically with *slit*²⁹⁹⁰, although further investigation with the stable double mutant lines is required. It is not likely that *if* and *nrx* genes interact genetically with *slit*²⁹⁹⁰ to produce an altered CNS phenotype. However, most of these genetic combinations will be examined from stable double mutant fly lines generated during this study and presented in the next chapter.

CHAPTER 5 DOUBLE MUTANT ANALYSIS

A total of 23 double mutant lines were established, out of 26 attempted (unable to generate stable, viable lines with 3 candidates in combination with *slit*²). The double mutant analysis proved to be more difficult to analyse than originally anticipated. Double mutant fly lines involving X chromosome mutants and *slit* (*slit*² and *slit*²⁹⁹⁰) were balanced by a *ftz-lacZ* reporter transposon on the X and with *eng-lacZ* on the 2nd. *ftz* striped expression declines at the stage of germ band elongation and thus β -galactosidase activity is not expressed at late embryogenesis. This impaired my ability to detect the presence of a balanced X chromosome within most collections. However, the *eng-lacZ* expression remained strong through to stage 17. Identification of balanced chromosome in recombinants on the 2nd was readily identified by *eng-lacZ*.

However, genotyping of double mutant lines involving a *slit* mutant on the 2nd and a mutation on the 3rd chromosome was even more difficult. The fly line used to begin double mutant crosses was a *Star/CyO[eng-lacZ]; D/TM3* stock that had a *lacZ* reporter transposon on the 2nd chromosome balancer and no embryonic marker on the 3rd chromosome balancer. (The *Star/CyO[eng-lacZ]; D/TM3[actin-lacZ]* could not be established as stable, viable lines). However, it was later discovered that the *eng-lacZ* was no longer present on the CyO chromosome when tested for β -galactosidase expression, resulting in no marked chromosomes for embryonic markers. Thus, immunostaining with anti- β -galactosidase antibody resulted only in diffuse background staining. In light of this discovery, I recorded counts of phenotypes observed in each collection and will present those upon discussion of phenotypes.

For all double mutant lines examined, the phenotype(s) observed for each mutant candidate gene are included as panels within each figure for comparison to the double

mutants. An outline of crosses used to generate stable double mutant fly lines are in Appendix Figure 5.

5.0 PROBLEM OF VERIFICATION OF PHENOTYPES

As described above, I encountered problems with verifying the genotypes of embryos within the double mutant stock collections due to lack of labeling balancer chromosomes in most cases. As a result, I could not specifically identify the particular genotype to the phenotypes of observed embryos. With this limitation, I resolved to identifying genotypes based on the frequency of occurrence and the nature or severity of the interaction within the population. By using this strategy, I provide an estimate of the genotypes and begin to assess whether a genetic interaction is occurring between two genes.

5.1 SLIT INTERACTS GENETICALLY WITH OTHER AXON GUIDANCE MOLECULES

5.11 Slit interacts genetically with Roundabout

Recently, Slit has been identified as the ligand for a known repulsive guidance receptor, Robo1 (Kidd et al. 1999; Brose et al. 1999). When visualised with mAb 1D4, *slit²/robo1¹* transheterozygotes display aberrant projection of medial axons across the midline (Battye et al. 1999; Kidd et al. 1999). To confirm these results with double mutant analysis, I created a recombinant fly line double mutant for *slit²⁹⁹⁰* and *robo1³*. *robo1³* is an amorphic allele just as the previously mentioned *robo1¹* is. Expected recombination frequency is 24% based on genetic location, which was approximated using cytological location (FlyBase) and cytogenetic map in Lindsley and Zimm (1992). However, upon completing complementation crosses, only 2 of 76 (2.6%) putative recombinant lines failed to complement both loci, resulting in a recombinant line. Midline crossing of medial axons is apparent in *slit²⁹⁹⁰, robo1³/CyO[eng]* double heterozygous recombinants (Figure 5.1C). This crossing phenotype is different than that shown for *slit²⁹⁹⁰* (Figure 3.2B) or *robo1³*

Figure 5.1 Immunocytochemical analysis of *slit*²⁹⁹⁰, *robo1*³ stable recombinant fly line.

Nerve cords are immunolabelled with mAb 1D4 (A, C, E) and mAb BP102 (B, D, F). The *robo1*³ mutant phenotype is shown in A and B and is similar to that described for *robo1*¹ mutants (refer to Figure 3.2C, 3.3C). *slit*²⁹⁹⁰, *robo1*³/CyO[*eng*] double heterozygous recombinants display midline crossing of the medial fascicle in some segments (arrow, C). These embryos display a commissural phenotype similar to *robo1*³ mutants, although separation is better defined here (arrowhead, D). *slit*²⁹⁹⁰, *robo1*³ homozygotes (E) display a collapse of longitudinal fascicles toward the midline (arrow), although mild separation is still displayed in some segments (arrowhead). These embryos show a commissural phenotype similar to *slit*²⁹⁹⁰ mutants, although some intersegmental connections are missing (arrow, F).

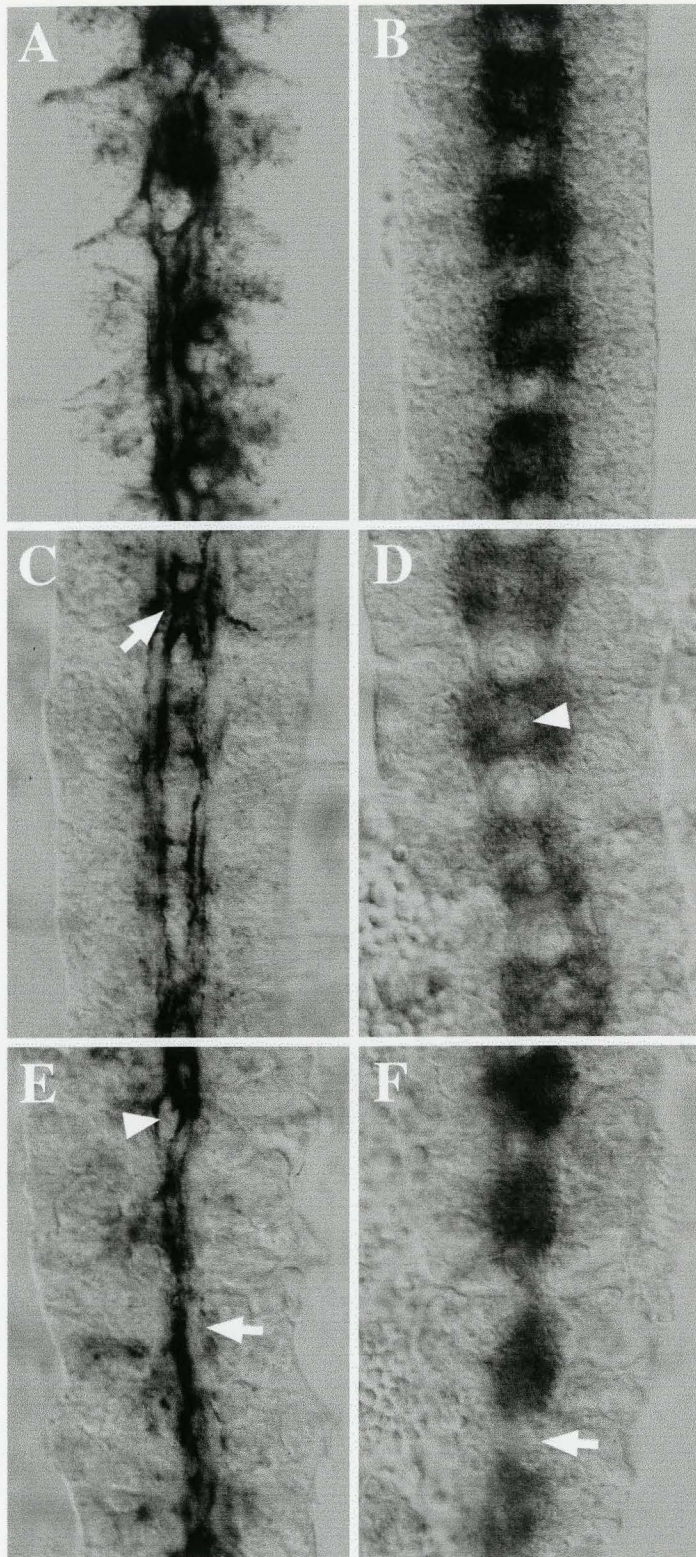


(Figure 5.1A). These mutants stained with mAb BP102 display thinned longitudinal connections between segments and thicker commissures (Figure 5.1D) similar to *robo1*³ mutants (Figure 5.1B), although the double heterozygous commissures are better separated. When examining the double homozygous recombinant nerve cord (ie. *slit*²⁹⁹⁰, *robo1*³), longitudinal axons collapse to the midline with looping of axons around the midline in some segments (Figure 5.1E). These embryos display collapsed commissures with mAb BP102 and longitudinal connections between segments are occasionally absent (Figure 5.1F). Double mutant recombinant lines for the strong hypomorphic allele, *slit*², and *robo1*¹ were attempted but balanced, stable fly lines were not recovered (Battye 2000). These results support the genetic interaction reported between *slit* and *robo1* suggest they likely function in the same repulsive pathway.

5.12 Slit interacts genetically with Netrin

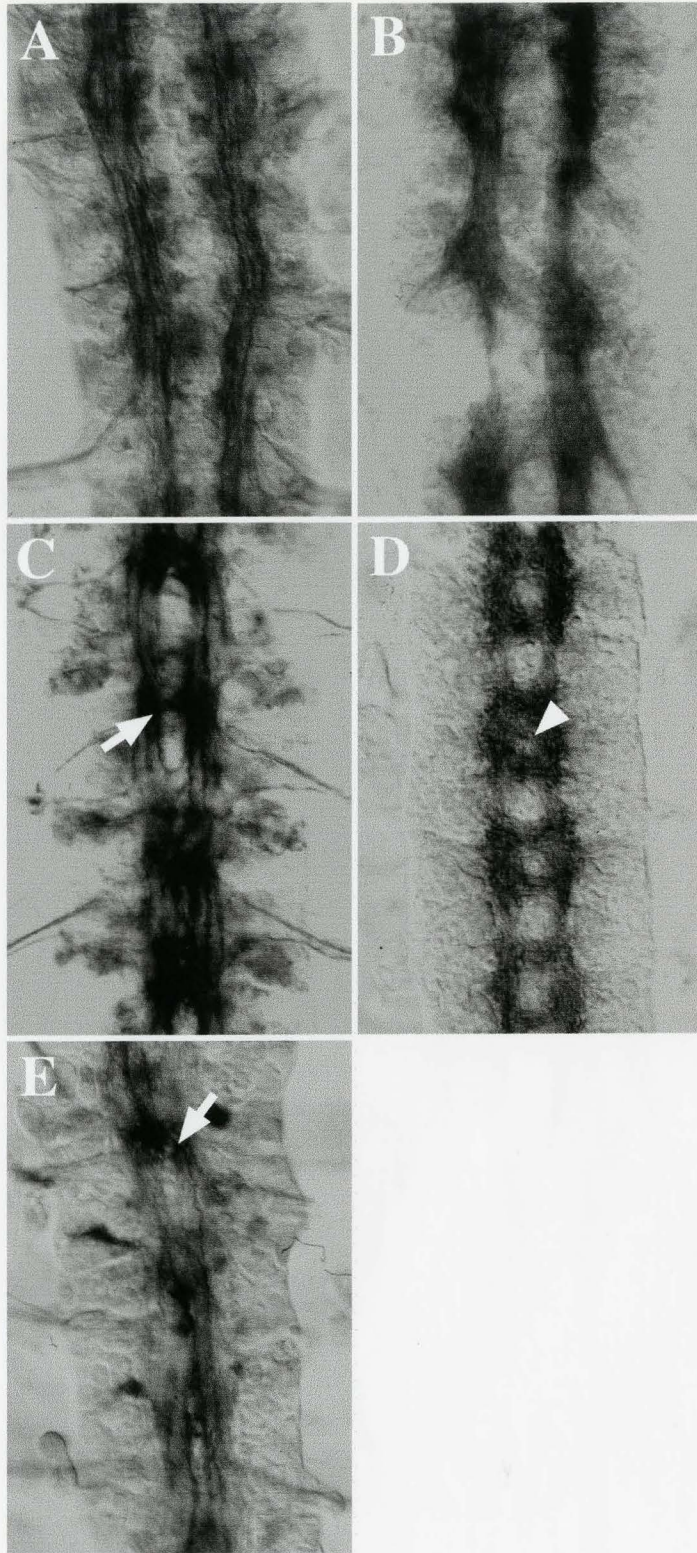
As Netrins form a component of the attractive function of the midline, it was of interest to determine how reduced *netrin* expression combined with reduced *slit* expression (reduced repulsive function) would affect nerve cord phenotype, and thus axon guidance. Stable double mutant fly lines Df(1)KA9/FM7cβ; *slit*²⁹⁹⁰/CyO[*eng*] and Df(1)KA9/FM7cβ; *slit*²/CyO[*eng*] were generated (Figure 5.2). Reduced copies of *netrin* and *slit*² presented a range of phenotypes, including a narrowed nerve cord with persistent midline crossing of medial fascicles (Figure 5.2C), a midline crossover phenotype involving all three longitudinal fascicles (Appendix Figure 15A) and nerve cords with subtle midline crossing (Appendix Figure 15B). These embryos represent either KA9/Y; *slit*²/CyO[*eng*] or KA9/FM7cβ; *slit*²/CyO[*eng*] as they also show the *engrailed* balancer pattern with β-galactosidase staining (balancer staining not shown here). Likewise, crossovers were observed in embryos from the KA9/FM7cβ; *slit*²⁹⁹⁰/CyO[*eng*] fly stock although staining of lateral fascicles was not as well defined (Figure 5.2E). The precise type of genetic interaction occurring in these situations is not clear as the 1D4 collection yielded too few

**Figure 5.2 Immunocytochemical analysis of KA9/FM7c β ;
slit /CyO[*eng*] stable double mutant fly lines.**

Nerve cords are immunolabelled with mAb 1D4 (A, C, E) and mAb BP102 (B, D).

Df(1)KA9/Y (A, B) removes both *netrinA* and *netrinB* genes. Reduced copies of both *netrin* and *slit²* genes in a KA9/FM7c β ; *slit²*/CyO[*eng*] embryo produce nerve cords with midline crossing of the medial fascicle (arrow, C). These embryos display slightly narrowed nerve cords with thinned longitudinal connections between segments, yet commissures remain separated in 16.3% (n=417) of embryos (arrowhead, D).

KA9/FM7c β ; *slit²⁹⁹⁰*/CyO[*eng*] embryos (E) show similar medial crossovers (arrow) as observed in C.



embryos for reliable counts. As the KA9/Fm7c β ; *slit*²/CyO[eng] BP102 collection yielded the greatest number of embryos for counts, I am able to eliminate some possibilities for the type of genetic interaction occurring. 16.3% of embryos (n=417) display slightly narrowed nerve cords, thicker commissure and, subsequently, thinned longitudinal connections between segments (Figure 5.2D). It is unlikely that *netrin* is suppressing the *slit* phenotype as 37.9% (n=417) of embryos are of the *slit*² phenotype (all *slit*² genotypes represent expected frequency, EF, of 25%), making it probable that any combinations of KA9 with *slit*² homozygotes (total EF=12.5%) yield only the *slit*² phenotype, including the double homozygous mutant KA9/Y; *slit*²/*slit*² (EF=6.25%, included in the 12.5%). The *netrin* phenotype was only observed in 15.6% of embryos, representative of at least KA9/Y; CyO[eng] (EF=6.25%) but possibly also KA9/Y; *slit*²/CyO[eng] (EF=12.5%) as the observed frequency is 2.5 times more than expected for only KA9/Y; CyO[eng] alone. Thus the remaining phenotype observed in this collection is of KA9/FM7c β ; *slit*²/CyO[eng] (EF=12.5%, compare to 16.3% observed above). This also indicates that in the KA9/FM7c β ; *slit*²⁹⁹⁰/CyO[eng] collection, the embryo shown in Figure 5.2E is likely a double heterozygote, KA9/FM7c β ; *slit*²⁹⁹⁰/CyO[eng]. However, if the phenotype were indicative of the KA9/Y; *slit*²/CyO[eng], this may reflect suppression of *netrin* phenotype by a half reduction in *slit* expression.

5.13 Slit interacts genetically with Commissureless

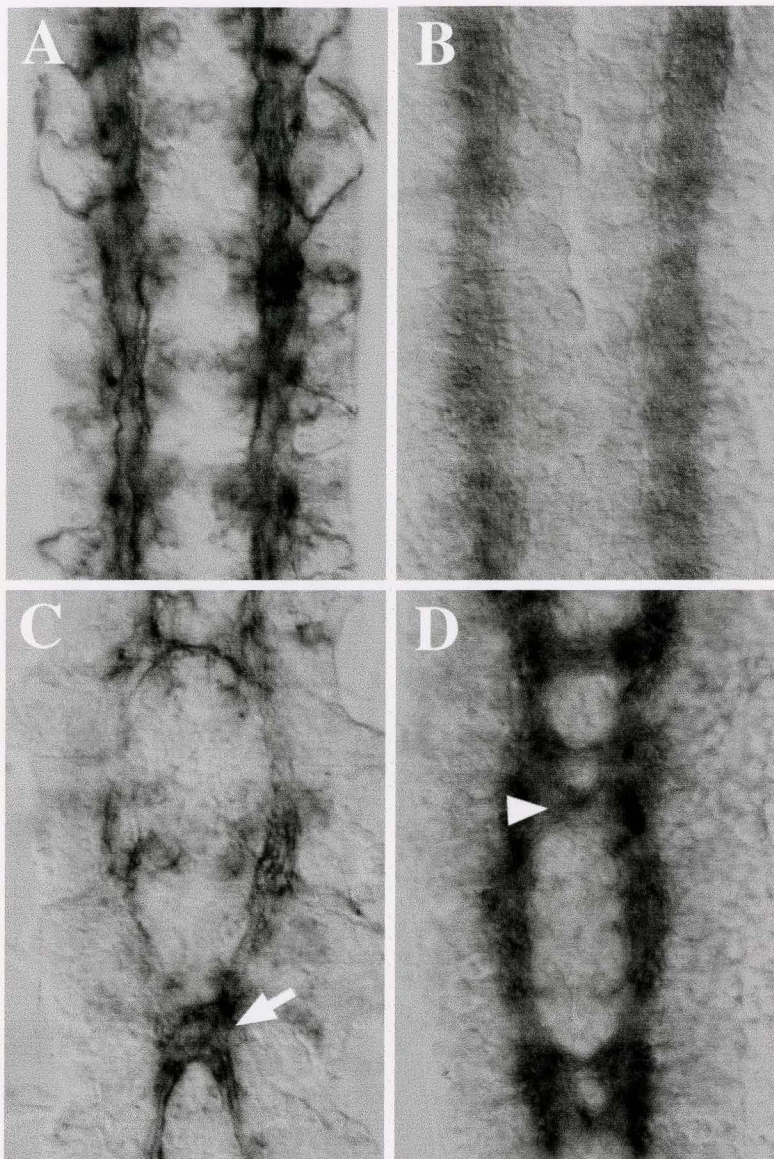
Comm is believed to promote internalisation of the Robo1 receptor. After Comm is picked-up by growth cones passing the MG it is endocytosed into the growth cone which also removes Slit-binding Robo1 from the growth cone surface. If this is so, then how do growth cones respond when Comm and Slit proteins are concomitantly being expressed at reduced levels in the nervous system?

8.8% (n=514) of mutants from *slit*²⁹⁹⁰/CyO; *comm*^{a490}/TM3 double mutant collection display apparent defasciculation and thinned fascicle projection on either side of the midline and extension of misguided axons across the midline in some segments, but not in others (Figure 5.3C). With BP102, 14.6% (n=356) of embryos show 1 or 2 commissures forming only in some segments (Figure 5.3D). It is likely these embryos represent double mutant homozygotes (ie. *slit*²⁹⁹⁰; *comm*^{a490}) for two reasons. First, their frequency of occurrence within the population is relatively low. This is especially true for the 1D4 collection, as they are near as frequent to that expected for double homozygotes, 1/16 or 6.25%. Secondly, this phenotype is also observed in Hummel et al. (1999b). Since they used double LacZ reporter chromosomes to select against in embryo collections, their phenotype is likely representative of a double homozygote, although they do not explicitly say so. These double homozygotes are similar to the phenotype reported for a *comm* hypomorph, *comm*⁸ (Tear et al. 1996). Thus, *slit* weakly suppresses the *comm* phenotype.

Other 1D4-labeled mutants within this collection appear narrower at the midline with occasional crossovers (Appendix Figure 16A) or with thinned longitudinal tracts and multiple crossovers (Appendix Figure 16B) in 38% of observed embryos. Although these two phenotypes were classified under the same category, they may represent two different genotypes. Those of Appendix Figure 16A that exhibit less crossovers may be *slit*²⁹⁹⁰/CyO; *comm*^{a490} (EF=12.5%), again indicative of *slit* suppressing *comm* as some axons cross the midline, which is not seen in *comm* mutants. Embryos with more crossovers (Appendix Figure 16B) may represent an equal reduction of both genes, *slit*²⁹⁹⁰/CyO; *comm*^{a490}/TM3 (EF=25%), evidence of more *slit*-mediated suppression of *comm*, as *comm* is now present in only one mutant copy. BP102-labeled embryos show more variation on the *comm*^{a490} mutant phenotype, whereby 20.5% (n=356) of embryos

**Figure 5.3 Immunocytochemical analysis of *slit*/CyO;
commissureless /TM3 stable double mutant fly lines.**

Nerve cords are immunolabelled with mAb 1D4 (A, C) and mAb BP102 (B, D). *comm^{a490}* mutant phenotype is shown in A and B. 1D4-immunolabelled *slit²⁹⁹⁰; comm^{a490}* double mutant embryos (C) display aberrant midline crossing in some segments (arrow) in 8.8% (n=514) of embryos. Fasciculation in these nerve cords is not selective and fascicles appears thinned. These embryos (D) display commissural connections in some segments (arrowhead), while other segments do not form commissures (14.6% of embryos, n=356). Some segments show only one commissure forming.



display thinned longitudinal connections between segments that either aberrantly form commissures or none at all (Appendix Figure 16C), or, experience breaks in longitudinals between segments or laterally displaced longitudinals in other segments (Appendix Figure 16D). These phenotypes likely represent *slit*²⁹⁹⁰/CyO; *comm*^{a490} (EF=12.5%) because the dominant mutant phenotype is *comm*^{a490}, yet some commissures begin to form but not as well as Figure 5.3D. Another 6.5% of embryos are representative of Appendix Figure 16E, where nerve cords are narrowed and form abnormal commissures and thinned longitudinal connections between segments. These embryos resemble those of Appendix Figure 16B and may represent *slit*²⁹⁹⁰/CyO; *comm*^{a490}/TM3 although their frequency may not approximate that expected for this genotype, 4/16 or 25%. For both the 1D4 and BP102 collections, the *slit*²⁹⁹⁰ phenotype (EF=18.75%) is observed in 25% and 21.3% of embryos, respectively, thereby indicating that *slit*; *comm*/TM3 (EF=12.5%, included in the above mentioned 18.75%) give a *slit*²⁹⁹⁰ phenotype making it unlikely that *comm*/+ suppresses the *slit* phenotype. I attempted to generate *slit*²; *comm*^{a490} stable double mutant fly lines but was unsuccessful to be able to establish noncomplementation at both loci in 4 of 6 lines double mutant lines generated (2 remain untested).

5.14 Slit interacts genetically with Dreadlocks

Dock is an adapter protein known for its potential for signaling in growth cone guidance. Dock is proposed to signal downstream of Robo1 activation as binding is reported in vitro (C. Bargmann, pers. comm.). I wanted to examine the effects of *robo* and *dock* mutants together in the nervous system, so I included a housed collection of *robo1*¹ and *dock*^{P1} mutant flies. In *dock*^{P1}/*robo1*¹ transheterozygotes the lateral two fascicles wander in and out of their respective pathways and absence of the lateral-most fascicle is evident in some segments (Appendix Figure 17A). However, when viewed with BP102, axon tracts appear wildtype (Appendix Figure 17B). As a result of this weak interaction, I decided to test for a genetic interaction between *dock* and *slit*. *dock*^{P1} and *slit*²⁹⁹⁰ mutants

were recombined onto the same chromosome with a frequency of 10.5% (n=19) while *dock*^{P1} and *slit*² mutants were recombined at a frequency of 15.5% (n=58). *dock*^{P1}, *slit*²⁹⁹⁰/CyO[*eng*] recombinant double heterozygotes display midline crossovers in some segments with 1D4 (Figure 5.4C) and very thinned longitudinals with BP102 (Figure 5.4D). *dock*^{P1}, *slit*²⁹⁹⁰ recombinant double homozygotes look similar to *slit*²⁹⁹⁰ homozygotes, although medial fascicles appear fused at the midline in some segments, instead of showing a midline circling phenotype like *slit*²⁹⁹⁰ shows (Appendix Figure 18A). When visualised with BP102, these double homozygotes display a lack of commissure separation, unlike *slit*²⁹⁹⁰, and occasional absence of longitudinal connections, also not seen in *slit*²⁹⁹⁰ (Appendix Figure 18B). *dock*^{P1}, *slit*²/CyO[*eng*] recombinant double heterozygotes display more frequent and severe crossing back and forth across the midline than *dock*^{P1}, *slit*²⁹⁹⁰/CyO[*eng*] embryos (Figure 5.4E) and midline collapse in some segments (Figure 5.4F). However, a range of crossovers and midline collapse was observed (Appendix Figure 18C, D). *dock*^{P1}, *slit*² double homozygotes are indistinguishable from *slit*² mutants [data not shown]. These results suggest Slit and Dock display a genetic interaction in vivo, although this analysis could not establish whether one modifies the mutant phenotype of the other, or vice versa. It is evident that *dock* weakly enhances the *slit*²⁹⁹⁰ phenotype in double recessive condition when observed with BP102 (Appendix Figure 18B), making it likely that they function in a common pathway.

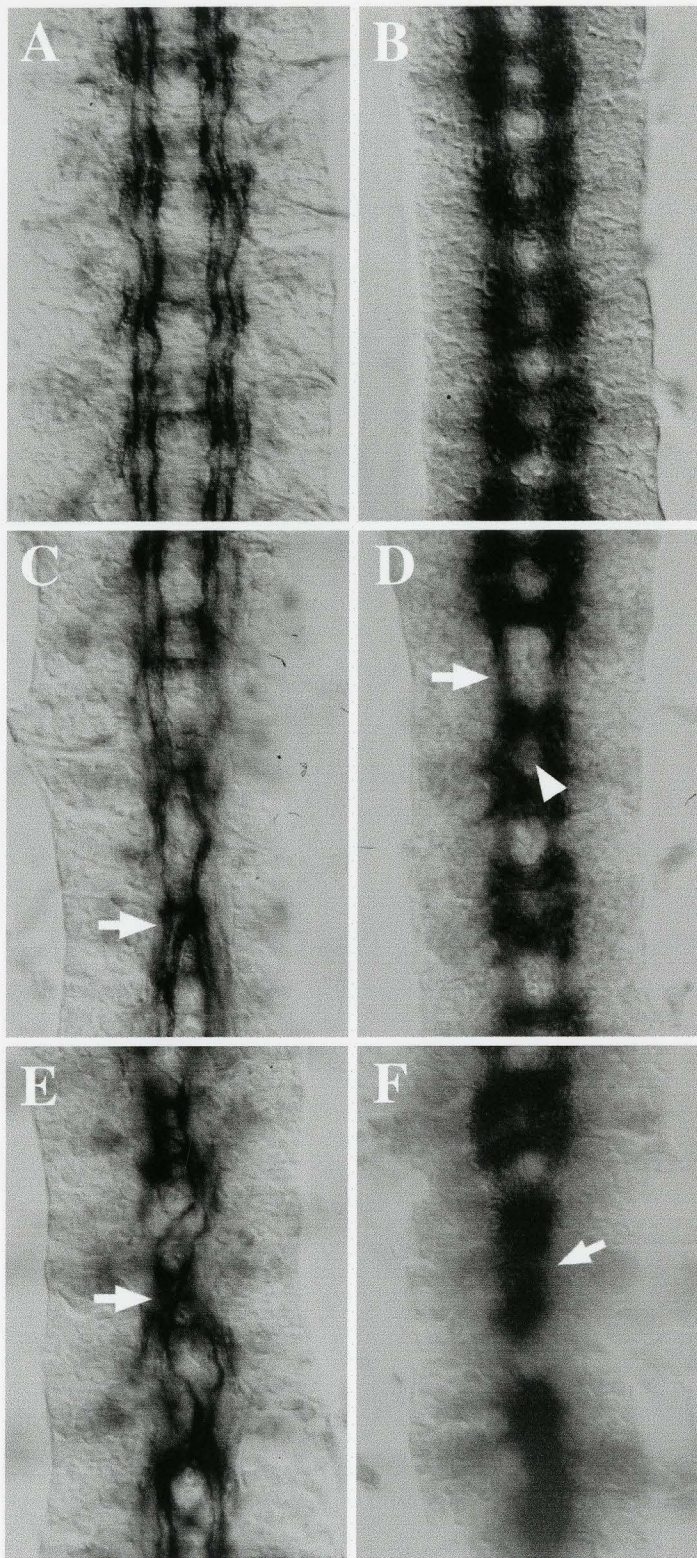
5.2 SLIT INTERACTS WITH EXTRACELLULAR MATRIX PROTEINS AND CELL SURFACE RECEPTORS

5.2.1 Slit allele interacts with LamininA

Laminin is an attractive candidate for involvement in cell-matrix interactions as it forms a fundamental component of basement membranes. Laminin 1 has been shown to bind hSlit2 in vitro (Brose et al. 1999) so the potential for interaction in vivo is promising.

**Figure 5.4 Immunocytochemical analysis of *dreadlocks*, *slit*
/CyO[eng] stable recombinant fly lines.**

Nerve cords are immunolabelled with mAb 1D4 (A, C, E) and mAb BP102 (B, D, F). *dock^{P1}* mutant phenotype is shown in A and B. *dock^{P1}, slit²⁹⁹⁰/CyO[eng]* heterozygous recombinants display midline crossovers in some segments (arrow, C). Thinned longitudinal connections are apparent in these embryos (arrow, D), although commissures remain separated (arrowhead, D). *dock^{P1}, slit²/CyO[eng]* heterozygous recombinants (E) demonstrate greater crossover frequency and severity (arrow) than *dock^{P1}, slit²⁹⁹⁰/CyO[eng]* mutants (compare to C). *dock^{P1}, slit²/CyO[eng]* heterozygous recombinants demonstrate near midline collapse in some segments (arrow, F).



When viewed with mAb 1D4 labeling, *slit*²⁹⁹⁰; *lamA*⁹⁻³² double homozygotes (8.5%, n=175; EF=6.25%) display collapsed axon tracts at the midline (Figure 5.5C), reminiscent of *slit*² mutants. *slit*²⁹⁹⁰/CyO; *lamA*⁹⁻³²/TM3 double heterozygotes (18%; EF=25%) show narrowing of longitudinal axon tracts toward the midline (Appendix Figure 19A). *slit*²⁹⁹⁰/CyO; *lamA*⁹⁻³² genotypic mutants may also represent this phenotype as well. 9% of mutants exhibited a *slit*²⁹⁹⁰ phenotype, representing *slit*²⁹⁹⁰; TM3 (EF=6.25%) and *slit*²⁹⁹⁰; *lamA*⁹⁻³²/TM3 genotypes (EF=12.5%). The remainder of embryos were wildtype in phenotype. When this collection was viewed with BP102, double homozygotes were collapsed at the midline (Figure 5.5D) in 11.6% of embryos (EF=6.25%). In double heterozygotes, the nerve cord is narrowed toward the midline, yet commissures remain defined in 16.1% of embryos (EF=25%; Appendix Figure 19B). The remainder of mutant embryos are of the *slit*²⁹⁹⁰ phenotype and represent 18.6% of population and also represent the *slit*²⁹⁹⁰; TM3 (EF=6.25%) and *slit*²⁹⁹⁰; *lamA*⁹⁻³²/TM3 genotypes (EF=12.5%). These data display a strong genetic interaction, and in particular, recessive enhancement (ie. worsening) of the *slit*²⁹⁹⁰ phenotype by *lamA*⁹⁻³² mutants.

Again, this examination included a double mutant of *slit*² and *lamA*⁹⁻³². A genetic interaction between *slit*²/CyO; *lamA*⁹⁻³²/TM3 double heterozygotes (39.1%, n=197; EF=25%) is apparent as midline crossovers occur with the medial fascicle (Figure 5.5E). Also included in this genotypic group are those exhibiting one medial crossover (Appendix Figure 19C) or with weak midline crossovers and defasciculated axons (Appendix Figure 19D). 30.5% of embryos display a *slit*² phenotype (data not shown), accounting for the *slit*²; *lamA*⁹⁻³², *slit*²; *lamA*⁹⁻³²/TM3 and *slit*²; TM3 genotypes (EF= 6.25%, 12.5% and 6.25%, respectively). When viewed with BP102, the double heterozygote (29.5%, n=278; EF=25%) has well defined segmental commissures but longitudinal axons are thinned between segments (Figure 5.5F). 22.3% of embryos in this BP102 collection

**Figure 5.5 Immunocytochemical analysis of *slit*/CyO; *lamininA*
/TM3 stable double mutant fly lines.**

Nerve cords are immunolabelled with mAb 1D4 (A, C, E) and mAb BP102 (B, D, F).

*lamA*⁹⁻³² mutant phenotype is shown in A and B. Near midline fusion of FasII-positive axons (C) and all CNS axons (D) is evident in *slit*²⁹⁹⁰; *lamA*⁹⁻³² homozygous double mutant embryos, which represent 8.5% (n=175) of embryos. *slit*²/CyO; *lamA*⁹⁻³²/TM3 double heterozygotes demonstrate weak midline crossing in some segments in 39.1% (n=197) of embryos (arrow, E). Commissures remain separated (arrowhead), although they display thinned longitudinal tracts and some narrowed segments (F).

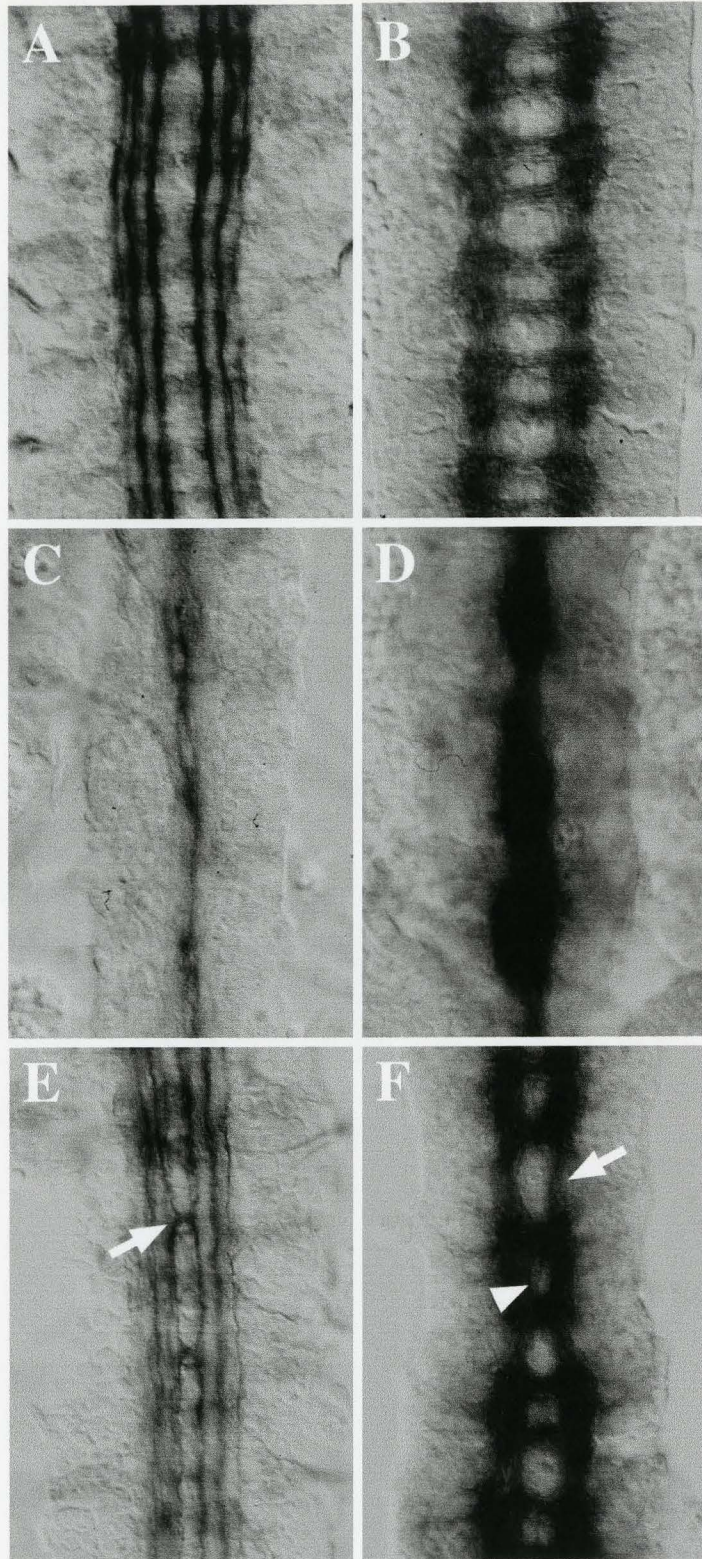


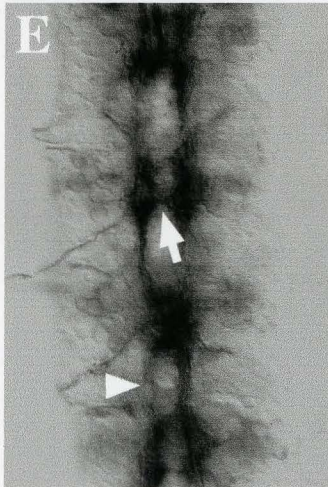
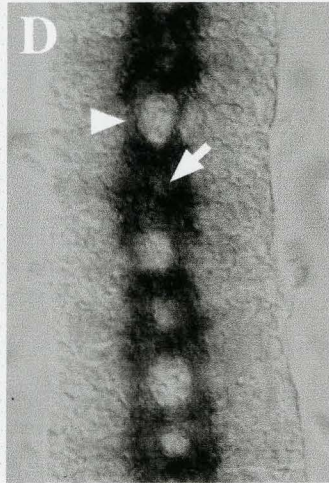
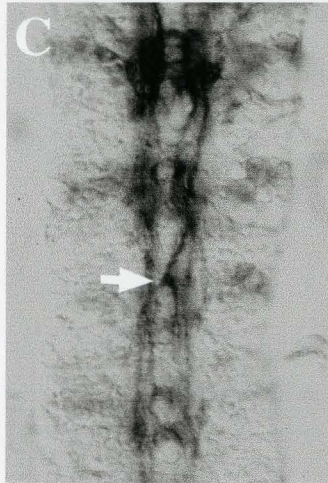
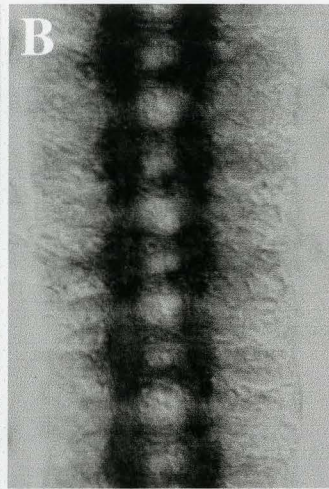
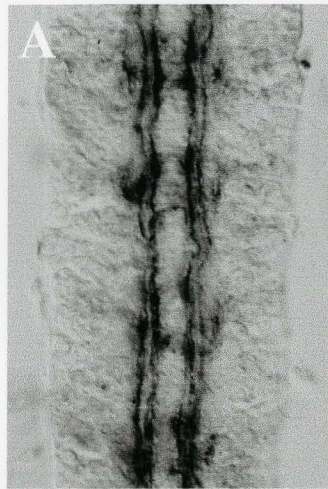
exhibit extreme narrowing in some segments (Appendix Figure 19E) or consistent narrowing down the length of the nerve cord (Appendix Figure 19F), which could be representative of the *slit*²/CyO; *lama*⁹⁻³² genotype (expected frequency 12.5%). 25.2% of mutants exhibit the *slit*² phenotype, indicating *slit*²; *lama*⁹⁻³² double homozygous mutants (EF= 6.25%), *slit*²; *lama*⁹⁻³²/TM3 mutants (EF=12.5%) and *slit*²; TM3 mutants (EF=6.25%) exhibit this phenotype (data not shown). Observing a mild phenotype between *slit*² and *lama*⁹⁻³² as double heterozygotes and enhancement of the *slit*²⁹⁹⁰ phenotype in double homozygotes implies these genes genetically interact in vivo.

5.22 Slit shows a genetic interaction with Tiggrin

Tiggrin is a novel ECM protein that binds specifically to α PS2 integrin via an RGD recognition sequence. *tig*^x was recombined with *slit*². Expected recombination frequency was 55% but observed frequencies were 26% (n=27) for *tig*^x, *slit*²⁹⁹⁰ recombinants and 5% (n=20) for *tig*^x, *slit*² recombinants. *tig*^x, *slit*²⁹⁹⁰/CyO[*eng*] recombinant double heterozygotes exhibit a mild CNS phenotype as shown by few midline crossovers, involving only the medial fascicle (Figure 5.6C). These embryos display thinned longitudinal tracts and poorly defined commissures in some segments (Figure 5.6D). *tig*^x, *slit*²/CyO[*eng*] recombinant double heterozygotes (Figure 5.6E) display more severe and frequent midline crossovers than the hypomorph combination and thinned fascicles in some segments. *tig*^x, *slit*²/CyO[*eng*] recombinant double heterozygotes visualised with BP102 appeared wildtype (data not shown). *tig*^x, *slit*²⁹⁹⁰ and *tig*^x, *slit*² double homozygotes were not different in phenotype from *slit*²⁹⁹⁰ and *slit*² mutants, respectively. These results imply that *tig* weakly interacts with *slit*, although whether they function cooperatively or antagonistically is yet to be determined.

Figure 5.6 **Immunocytochemical analysis of *tiggrin*, *slit*/CyO[*eng*] stable recombinant fly lines.**

Nerve cords are immunolabelled with mAb 1D4 (A, C, E) and mAb BP102 (B, D). *tig^x* mutant phenotype is shown in A and B. *tig^x, slit²⁹⁹⁰/CyO[eng]* heterozygous recombinants demonstrate midline crossovers (arrow) in some segments (C). Commissures are poorly defined in some segments (arrow) and longitudinal tracts appear thinned (arrowhead, D). *tig^x, slit²/CyO[eng]* heterozygous recombinants display mild crossovers between segments (arrow, E).



5.23 Slit interacts genetically with Masquerade

Masquerade, as a novel, secreted protease-like protein, makes for an interesting candidate to study for interaction with *slit* due to its reported CNS phenotype and expression by MG. *slit*²⁹⁹⁰/CyO; *mas*^{x124} mutants may represent the 1D4-labeled phenotype observed in Figure 5.7C. These embryos exhibit crossovers and some midline fusion in 10.3% of the population (n=632). When examining other 1D4-labeled embryos, Appendix Figure 20A may represent the double heterozygote genotypes, *slit*²⁹⁹⁰/CyO; *mas*^{x124}/TM3.

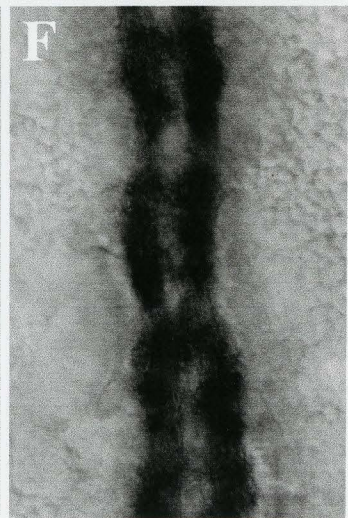
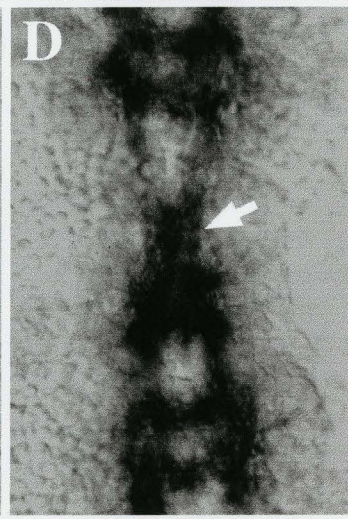
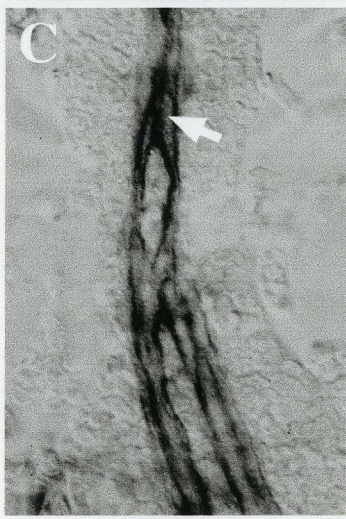
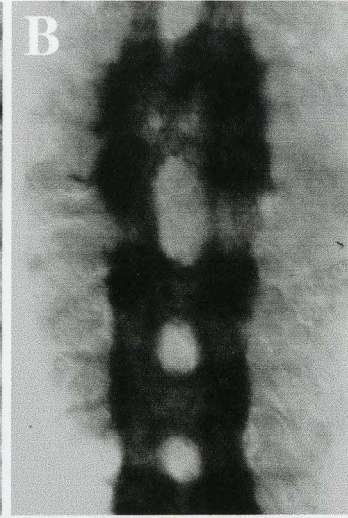
The BP102-labeled phenotype observed in Figure 5.7D may either represent the genotype *slit*²⁹⁹⁰/CyO; *mas*^{x124}/TM3 (Ef=25%) or *slit*²⁹⁹⁰/CyO; *mas*^{x124} (Ef=12.5%). However, the frequency of this phenotype in the population represents only 4.9% (n=426) of embryos, making it difficult to estimate the genotype. 39.4% of this population of embryos exhibit poorly separated commissures (Appendix Figure 20B) and likely represent *slit*²⁹⁹⁰/CyO; *mas*^{x124} (Ef=12.5%) and CyO; *mas*^{x124} (Ef= 6.25%) or a collection containing only CyO; *mas*^{x124} (Ef=6.25%) as *mas*^{x124} single mutants show lack of separation of commissures (compare to Figure 5.7B).

The most interesting phenotypes in both collections were of those shown in Appendix Figure 20C and D. 17.7% of embryos demonstrate the *slit*²⁹⁹⁰ mutant phenotype and enhanced muscle phenotype, that causes the a severely kinked nerve cord that could be due to muscle defects. These embryos are likely *slit*²⁹⁹⁰; *mas*^{x124} homozygous double mutants (Ef=6.25%).

In *slit*²; *mas*^{x124} double mutant collections, midline collapse of fascicles occurs in 4.1% of 1D4-labeled embryos (n=662) and likely represents the *slit*²/CyO; *mas*^{x124}/TM3 genotype (Figure 5.7E; Ef=25%). Other embryos in this collection are not collapsed toward the midline but instead demonstrate persistent crossing back and forth across the midline in 12.2% of embryos (n=662) and are likely the *slit*²/CyO; *mas*^{x124}/+ genotype (Appendix Figure 20E; Ef=12.5%). When visualised with BP102, 4.9% of embryos

Figure 5.7 **Immunocytochemical analysis of *slit*/CyO;
masquerade/TM3 stable double mutant fly lines.**

Nerve cords are immunolabelled with mAb 1D4 (A, C, E) and mAb BP102 (B, D, F). *mas^{x124}* mutant phenotype is shown in A and B. *slit²⁹⁹⁰/CyO; mas^{x124}* mutants (C, D) exhibit midline fusion of axons in some segments (arrows) in 10.3% (1D4, n=632) and 4.9% (BP102, n=426) of embryos. This crossing is more severe in *slit²/CyO; mas^{x124}* mutants (E) representing 4.1% of the population (n=662). *slit²/CyO; mas^{x124}* mutants (4.9%, n=313) show consistent narrowing of axons tracts in (F).



(n=313) display a narrow nerve cord and fuzzy commissures (Figure 5.7F). These embryos likely represent the *slit*²/CyO; *mas*^{x124}/TM3 genotype (expected frequency 12.5%). Like the *slit*²⁹⁹⁰; *mas*^{x124} double mutant line collection, 19.8% exhibit fused anterior and posterior commissures (Appendix Figure 20F). These embryos likely represented the *slit*²/CyO; *mas*^{x124} and CyO; *mas*^{x124} genotypes, or only the CyO; *mas*^{x124} genotype. Homozygous double mutants display the *slit*² CNS phenotype and kinked nerve cord (Appendix Figure 20G and H).

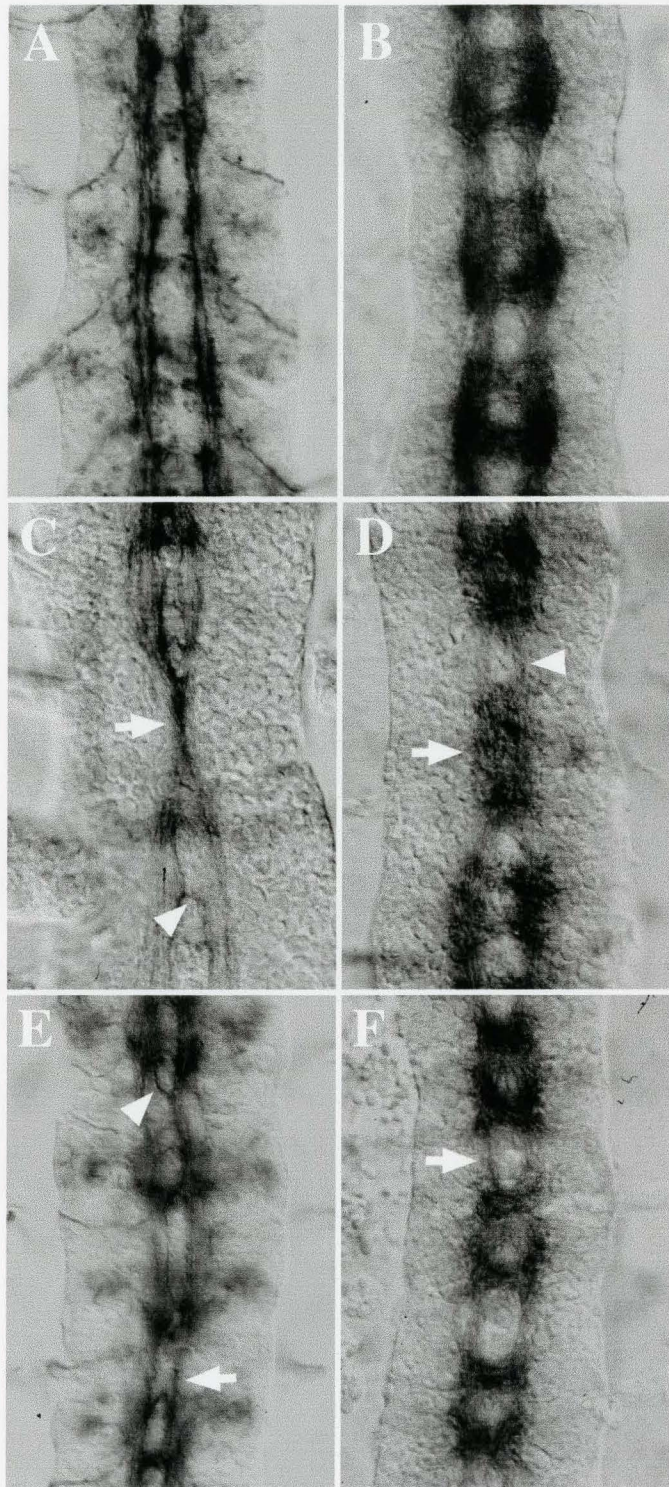
It is difficult to determine what these genotypes are, as I was unable to stain for embryonic markers. However, the double homozygotes were easy to identify based on the mutant phenotype. The other muscle and fused commissure phenotypes were easy to identify as they exhibit the *mas*^{x124} single mutant phenotype. It is likely Slit and Mas functionally interact in the nervous system by enhancement of the *mas* phenotype by *slit* in *slit*/CyO; *mas* genotypes. The presence of enhanced *slit* muscle defects seen by kinks in the nerve cord opens up the possibility of functional interaction there. As a result, *slit* may enhance the *mas* phenotype.

5.24 Slit displays a weak genetic interaction with AlphaPS1 Integrin, Mew

8.3% of 1D4-labeled embryos from a *mew*^{M6}/FM7cβ; *slit*²⁹⁹⁰/CyO[eng] double mutant stock appear medially fused in at least one segment and medial midline crossovers in other segments (Figure 5.8C) or display crossovers, but not midline fusion (Appendix Figure 21A). These phenotypes represent *mew*^{M6}/Y; *slit*²⁹⁹⁰/CyO[eng] mutants (EF=6.25%). I am unsure if *mew*^{M6}/FM7cβ; *slit*²⁹⁹⁰/CyO[eng] mutants exhibit a phenotype. With mAb BP102, 14.7% of embryos display CNS defects. Some, likely *mew*^{M6}/Y; *slit*²⁹⁹⁰/CyO[eng], exhibit a CNS phenotype with segmental collapse that mirrors the 1D4 phenotype (Figure 5.8D). In others, there is occasional midline collapse in a segment while other segments appear wildtype (Appendix Figure 21B). The majority

Figure 5.8 **Immunocytochemical analysis of *multiple edematous wings*/FM7cβ *slit*/CyO[*eng*] stable double mutant fly lines.**

Nerve cords are immunolabelled with mAb 1D4 (A, C, E) and BP102 (B, D, F). *mew^{M6}/Y* mutant phenotype is shown in A and B. 1D4-immunolabelled *mew^{M6}/Y; slit²⁹⁹⁰/CyO[eng]* mutants (C) demonstrate midline fusion of longitudinal axons in at least one segment (arrow) and medial crossovers in other segments (arrowhead). This phenotype is mirrored in the BP102 pattern (D), as some segments appear collapsed toward the midline (arrow). Longitudinal connections are thinner between these segments (arrowhead). *mew^{M6}/Y; slit²/CyO[eng]* mutants demonstrate narrowing (arrow) and crossing of medial axons (arrowhead) in the nerve cord (E). The same embryos labelled with BP102 display a narrowed nerve cord and thinned longitudinal axon tracts between segments (arrow, F).



of mutant phenotypes observed in the *mew^{M6}/FM7cβ; slit²⁹⁹⁰/CyO[eng]* double mutant embryo collection was that of *slit²⁹⁹⁰* (data not shown) for both 1D4 (34.2%, n=228) and BP102 (39.6%, n=313). This group possibly includes the *mew^{M6}/FM7cβ; slit²⁹⁹⁰* and *FM7cβ; slit²⁹⁹⁰* genotypes (EF=6.25%, 6.25% and 12.5%, respectively).

The observed frequencies with *mew^{M6}/FM7cβ; slit²/CyO[eng]* double mutant line is not as straight forward. Of 3 collections examined, 2 scored 55% (n= 121) and 57% (n=49) of mutants exhibiting a crossover phenotype, while the third collection reported 15.1% (n=73) of mutants exhibiting crossovers. I cannot account for the discrepancy of these results. However, the range of this 'class' of phenotype is similar between collections. Defects include narrowing and frequent midline crossing of axons (Figure 5.8E), likely representing *mew^{M6}/Y; slit²/CyO[eng]*, and weaker segmental crossovers and occasional midline fusion (Appendix 21C), likely representing *mew^{M6}/FM7cβ; slit²/CyO[eng]*. 30% of embryos in two of the collections and 64.4% in the third collection display the *slit²* phenotype (data not shown). This group includes the genotypes *mew^{M6}/Y; slit²*, *mew^{M6}/FM7cβ; slit²* and *FM7cβ; slit²* (EF=6.25%, 6.25% and 12.5%, respectively). When visualised with BP102, 5.5% (n=308) of embryos display a narrowed nerve cord phenotype, shown in Figure 5.8F. These nerve cords display thinned longitudinal tracts and thicker anterior and posterior commissures. Other mutants here display one segment that is collapsed toward the midline, although other abdominal segments appear wildtype (Appendix 21D). Genotypes are likely the same as above, *mew^{M6}/Y; slit²/CyO[eng]* and *mew^{M6}/FM7cβ; slit²/CyO[eng]*. In this collection, 26.6% of embryos are of the *slit²* phenotype (data not shown), accounting for the *mew^{M6}/Y; slit²*, *mew^{M6}/FM7cβ; slit²* and *FM7cβ; slit²* genotypes (EF=6.25%, 6.25% and 12.5%, respectively). It is suggested here that *slit* enhances the *mew* phenotype in a dose-sensitive manner, making it likely they have a weak, but cooperative, function.

5.25 Slit interacts genetically with the AlphaPS2 integrin, Inflated

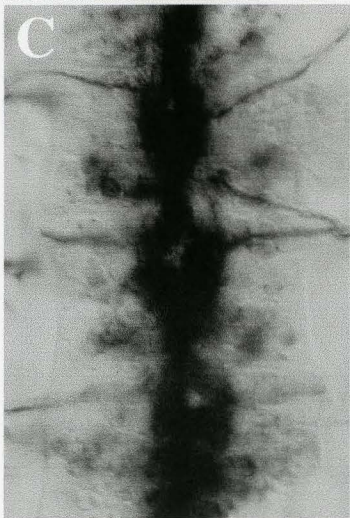
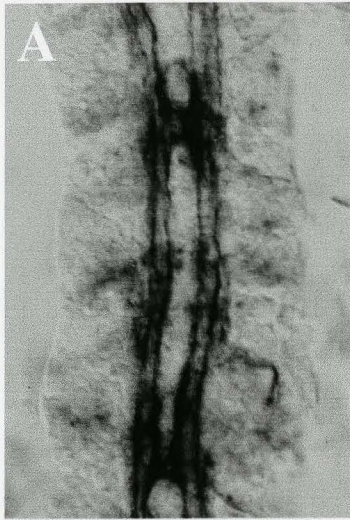
Analysing phenotypes from *if*/FM7c β ; *slit*/CyO[*eng*] fly lines was difficult as they were weakly viable in pairwise tubes and yielded only a few embryos. However, from housed collections, the following phenotypes emerged. For both the *if*^{*k27e*}/FM7c β ; *slit*²⁹⁹⁰/CyO[*eng*] (Figure 5.9B) and *if*^{*k27e*}/FM7c β ; *slit*²/CyO[*eng*] (Figure 5.9C) fly lines, a few embryos displayed midline crossovers less severe than seen for *slit* homozygous mutants. These embryos also showed the presence of β -galactosidase activity in the *engrailed* pattern, indicating that *slit* must have been present in a heterozygous copy in both cases. The question arises: what is the level of expression of *if*^{*k27e*} in this interaction? The embryos displayed a range of phenotypes from midline fusion (Appendix Figure 22A) and heavy midline crossing (Appendix Figure 22B) for *if*^{*k27e*}/Y; *slit*²⁹⁹⁰/CyO[*eng*] embryos, to inconsistent severity of crossover along the length of the nerve cord (Appendix Figure 22C) and weak midline crossing (Appendix Figure 22D) in *if*^{*k27e*}/FM7c β ; *slit*²/CyO[*eng*] embryos. Since the nerve cord shown in Appendix Figure 22D was observed to stain for both LacZ balancer chromosomes and shows a relatively weak crossover phenotype, it is likely representative of *if*^{*k27e*}/FM7c β ; *slit*²/CyO[*eng*]. Therefore, Figure 5.9C likely represents an embryo hemizygous for *if* and heterozygous for *slit*² (ie. *if*^{*k27e*}/Y; *slit*²/CyO[*eng*]). As a result, Figure 5.9B is likely *if*^{*k27e*}/Y; *slit*²⁹⁹⁰/CyO[*eng*]. The displayed weak interaction between *if* and *slit* is consistent with that observed between *slit* and *tig*, as Tiggrin is the ligand for AlphaPS2-integrin in vivo. *slit* may function to weakly enhance *if*.

5.26 Slit interacts genetically with BetaPS-integrin, Mys

As the other two alpha-integrin subunits examined thus far display a genetic interaction with *slit*, it is conceivable that the β -subunit would also. *mys*¹/Y; *slit*²⁹⁹⁰ embryos show an enhanced *slit*²⁹⁹⁰ CNS phenotype as these nerve cords are completely collapsed toward the midline (Figure 5.10C, D) similar to *slit*² mutants. 25% of embryos

Figure 5.9 **Immunocytochemical analysis of *inflated*/FM7c β ; *slit*/*CyO*[*eng*] stable double mutant fly lines.**

Nerve cords are immunolabelled with mAb 1D4. *if^{k27e}/Y* mutant phenotype is shown in A. *if^{k27e}/Y; slit²⁹⁹⁰/CyO[eng]* mutants show midline crossovers involving all three longitudinal fascicles (B). Similarly, *if^{k27e}/Y; slit²/CyO[eng]* mutants (C) show midline crossovers, but more severely narrowed than B.

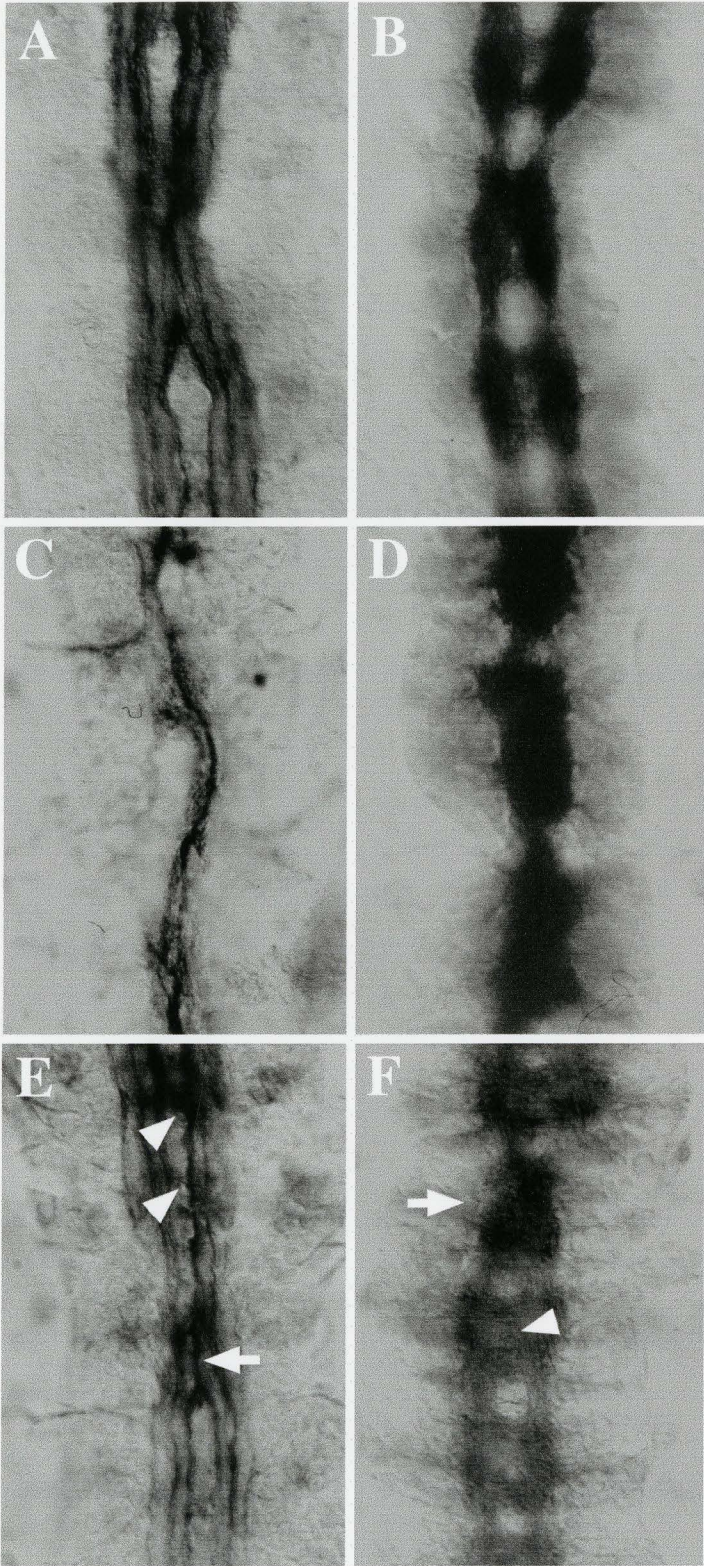


(n=57) are of this phenotype (EF=6.25%). Another 25% of embryos in this collection display midline crossovers with 1D4 that range from mild (Appendix Figure 23A) to several midline crossovers (Appendix Figure 23B). The phenotype shown in Appendix Figure 23A is representative of a *mys¹/Y; slit²⁹⁹⁰/CyO[eng]* genotype (EF=12.5%), as the germband is twisted from *mys* muscle defects and stains weakly for *eng-lacZ*. The embryo in Appendix Figure 23B stains positive for both *ftz-* and *eng-lacZ* balancers and is thus the genotype *mys¹/FM7cB; slit²⁹⁹⁰/CyO[eng]* (EF=12.5%). As another 19% is represented clearly by the *slit²⁹⁹⁰* phenotype, it is likely that a *mys¹* heterozygous genotype does not enhance the *slit²⁹⁹⁰* mutant phenotype (ie. in *mys¹/FM7cB; slit²⁹⁹⁰* embryos, EF=6.25%). When observed with BP102, only the *slit²*-like (Figure 5.10D; a *mys¹/Y; slit²⁹⁹⁰* embryo), *slit²⁹⁹⁰* and wildtype phenotypes are seen. This indicates that reduced dosages of *mys¹* and *slit²⁹⁹⁰* does not create a detectable intermediate phenotype, like that observed with mAb 1D4, when viewed with this antibody.

mys¹ also interacts genetically with *slit²*. Midline crossovers were apparent in 12% of embryos labeled with mAb 1D4 (n=59). 7% stained positive for *eng-lacZ* balancer chromosome, indicating they likely represent the *mys¹/Y; slit²/CyO[eng]* genotype (EF=12.5%). The phenotype is in accordance with this proposed genotype, as nerve cords are fused at the midline in some segments (like *mys¹* mutants), yet display crossovers in other segments not observed in the *mys¹* mutant phenotype (Figure 5.10E). Likewise with BP102, these embryos display fuzzy commissures similar to that of *mys¹* mutants, yet also show midline collapse in at least one segment (Figure 5.10F). 5% of 1D4 mutants exhibited crossovers and stained for both *lacZ* balancer chromosomes. These crossovers are milder than Figure 5.10E and do not display midline fusion (Appendix Figure 23C) and are likely *mys¹/FM7cB; slit²/CyO[eng]* (EF=12.5%). These embryos labeled with BP102 also stain for both *lacZ* balancers and display midline fusion in one segment, while other

Figure 5.10 **Immunocytochemical analysis of *myspheroid*/FM7c β ; *slit*/CyO[*eng*] stable double mutant fly lines.**

Nerve cords are immunolabelled with mAb 1D4 (A, C, E) and mAb BP102 (B, D, F). *mys*¹/Y mutant phenotype is shown in A and B. *mys*¹/Y; *slit*²⁹⁹⁰ double mutants exhibit complete midline collapse (C, D), similar to *slit*² mutants in 25% (n=57) embryos. *mys*¹/Y; *slit*²/CyO[*eng*] mutants (E, F) show midline fusion of the medial fascicle in some segments (arrow, E), although not all segments and fascicles appear as severely affected (arrowhead, E) or affected at all. These embryos represent 7% (n=59) of the population. Similarly, some commissures appear collapsed toward the midline (arrow, F) in some segments, while others display fuzzy commissures (arrowhead, F).



commissural segments appear wildtype (Appendix Figure 23D). The remainder of mutant embryos had the *slit*² phenotype, indicating that *mys*¹ mutants do not suppress or otherwise alter the *slit*² phenotype in *mys*¹/FM7cβ; *slit*² (EF=6.25%) and *mys*¹/Y; *slit*² combinations (EF=6.25%).

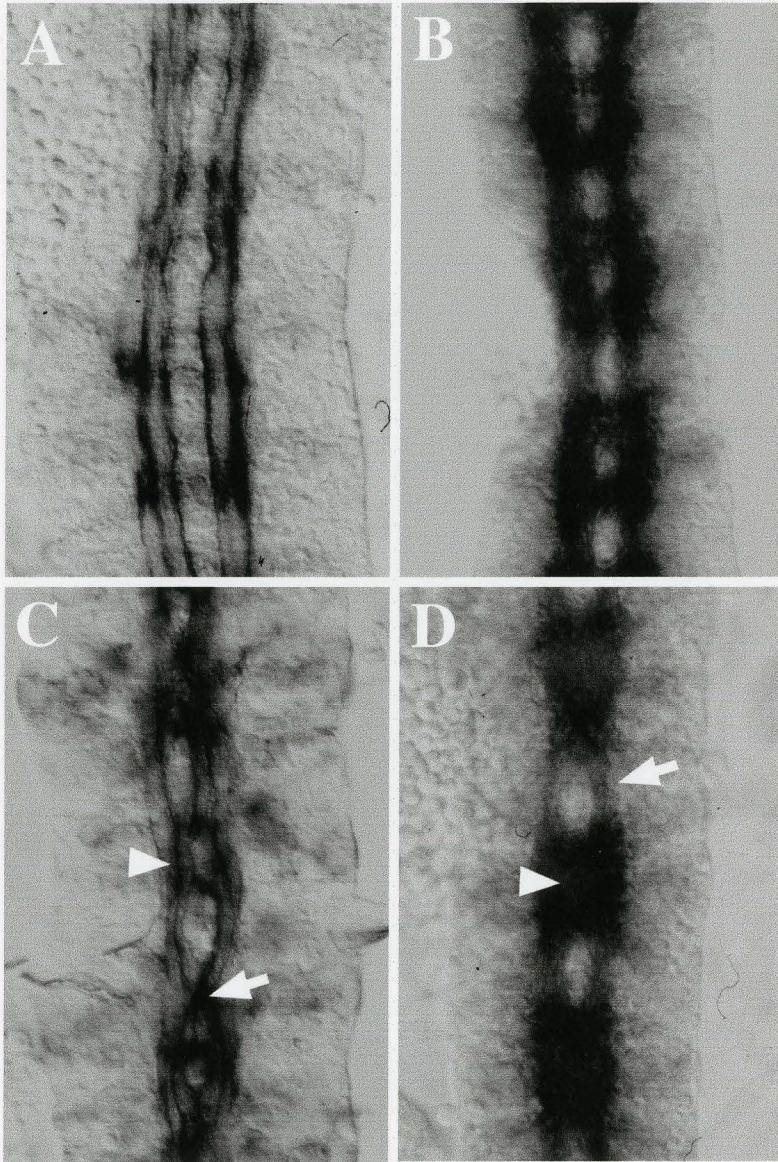
5.27 Slit interacts genetically with Toll

23.3% (n=257) of 1D4-labeled embryos from the double mutant stock display a crossover phenotype that ranges in severity. Figure 5.11C depicts embryos that have midline crossovers involving at least the medial-most fascicle and possibly the next lateral fascicle, and also display midline fusion in other segments. Other embryos display crossovers involving only the medial fascicle (Appendix Figure 24). These embryos likely represent *slit*²⁹⁹⁰/CyO; *Tl*^{R3} (EF=12.5%) and *slit*²⁹⁹⁰/CyO; *Tl*^{R3}/TM3 (EF=6.25%) genotypes, respectively. 31.9% of mutants in the collection display only the *slit*²⁹⁹⁰ phenotypes and include the genotypes *slit*²⁹⁹⁰; *Tl*, *slit*²⁹⁹⁰; *Tl*/TM3 and *slit*²⁹⁹⁰; TM3 with EF= 6.25%, 12.5% and 6.25%, respectively. With BP102, 6.8% of embryos display a narrowed nerve cord with thinned longitudinals and fuzzy commissures (Figure 5.11D), likely representative of the same pool of genotypes mentioned above. The remainder of this collection display *slit*²⁹⁹⁰ (45.1%), representing the same genotypes as mentioned for the 1D4 collection, or, wildtype phenotypes (data not shown).

When the collection was scored, 4.7% of *slit* phenotypes were originally thought to be more severe than that of *slit*²⁹⁹⁰. Closer examination revealed these phenotypes were of the *slit*²⁹⁹⁰ phenotypes like that shown in Figure 4.1E. These data suggest that *slit* severely enhances the *Tl* phenotype. The construction of a stable double mutant fly line with *slit*² and *Tl*^{R3} was attempted, but not successful, as 7 balanced lines complemented either of the two loci and 2 lines could not stably maintain the balancers. *slit*² and *Tl*^{R3} appear to be lethal in a double heterozygous combination. This supports the interaction observed with the *slit*²⁹⁹⁰/CyO; *Tl*^{R3}/TM3 double mutant stock.

Figure 5.11 Immunocytochemical analysis of *slit/CyO*; *Toll/TM3* stable double mutant fly line.

Nerve cords are immunolabelled with mAb 1D4 (A, C) and mAb BP102 (B, D). *Tl^{RS}* mutant phenotype is shown in A and B. *slit²⁹⁹⁰/CyO*; *Tl^{RS}* mutants (23.3%, n=257) exhibit midline crossovers (arrowhead) and midline fusion (arrow) involving the medial fascicle (C). Likewise, fuzzy commissures (arrowhead) and thinned longitudinal tracts (arrow) are evident in these embryos (D), which represent 6.8% of the population (n=366).



5.28 Slit interacts genetically with Neurexin

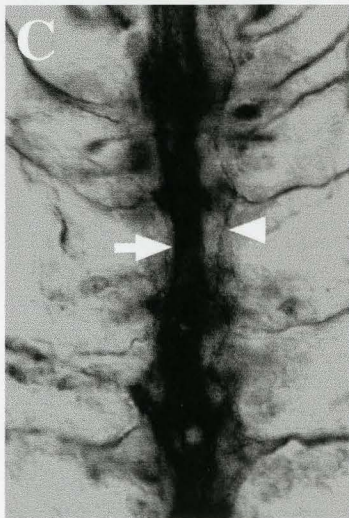
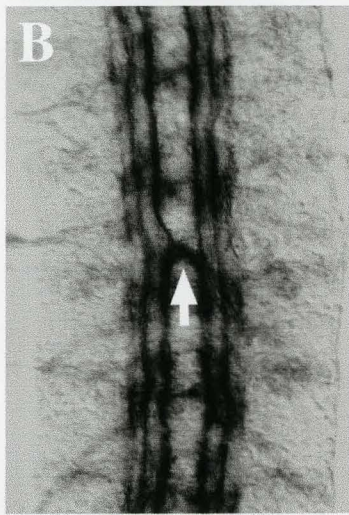
*slit*²⁹⁹⁰/CyO; *nrx*⁴³⁰⁴/TM3 and *slit*²/CyO; *nrx*⁴³⁰⁴/TM3 mutant fly lines were generated and maintained in a few pairwise tubes. As a result, housed collections were prepared but few embryos were collected. Thus, phenotypes shown are not known how frequent they occur in the population, but are helpful to speculate how Slit may be involved with Neurexin in vivo.

Figure 5.12B shows midline crossover of a medial fascicle seen in the *slit*²⁹⁹⁰/CyO; *nrx*⁴³⁰⁴/TM3 double mutant line. Appendix Figure 25 shows a mutant with fusion of medial fascicles in one segment. These phenotypes represent 4 of 30 embryos. Other mutant phenotypes observed in this collection include the *slit*²⁹⁹⁰ (9 of 30) and *nrx*⁴³⁰⁴ (7 of 30) single mutants and wildtype (10 of 30). I can only speculate that the phenotype shown in Figure 5.12B is representative of a double heterozygote (ie. *slit*²⁹⁹⁰/CyO; *nrx*⁴³⁰⁴/TM3) but I cannot rule out the possibility that *nrx*⁴³⁰⁴ mutants could enhance or suppress the phenotype of *slit*²⁹⁹⁰, since this collection did not yield sufficient embryos for reliable counts.

Figure 5.12C displays multiple midline crossovers, involving two of the three longitudinal fascicles, leaving the lateral-most fascicle unaffected (6 of 26 embryos). *slit*²/CyO; *nrx*⁴³⁰⁴/TM3 could represent the genotype associated with this phenotype. *slit*² was observed only once out of 26 embryos. However, 3 embryos were classified as the *slit*²⁹⁹⁰ phenotype, but similar to the crossover phenotype that is different from the *slit*²⁹⁹⁰ phenotype. This may signify suppression of *slit* phenotype by *nrx*. Further study is needed to make a sound conclusion.

Figure 5.12 **Immunocytochemical analysis of *slit/CyO*; *neurexin/TM3* stable double mutant fly lines.**

Nerve cords are immunolabelled with mAb 1D4. *nrx*⁴³⁰⁴ mutant phenotype is shown in A. *slit*²⁹⁹⁰/*CyO*; *nrx*⁴³⁰⁴/*TM3* mutants (B) show weak midline crossing of the medial fascicle in at least one segment (arrow). *slit*²/*CyO*; *nrx*⁴³⁰⁴/*TM3* mutants (C) display a more severe crossover phenotype, involving at least the inner and middle fascicle (arrow). The outer fascicle remains unaffected (arrowhead).



phenotypes observed for both genetic stocks were only of *slit*²⁹⁹⁰ and *slit*², indicating that they do not interact genetically with *dlg1*⁶. However, a reduction in FasII cell surface expression was observed in the double mutant, consistent with Dlg1's proposed role in proper localisation of FasII in neurons (Thomas et al. 1997).

5.32 Slit does not interact genetically with Central Body Defect

*cbd*¹ uncovers the *tenascin-a* locus and was used to test for a genetic interaction between *slit* and *ten-a*. *cbd*¹/FM7cβ; *slit*²⁹⁹⁰/CyO[eng] and *cbd*¹/FM7cβ; *slit*²/CyO[eng] mutant phenotypes are indistinguishable from *slit*²⁹⁹⁰ and *slit*² single mutants (Appendix Figure 26C-F) with 1D4 and BP102. However, *cbd*¹ is known to be homozygous viable and the genetic markers associated with this locus, *wavy* and *dusky*, were not seen in this line. I cannot be certain that the *cbd*¹ mutant is still in this stock and conclude the interaction between *slit* and *tenascin-a* to be unknown.

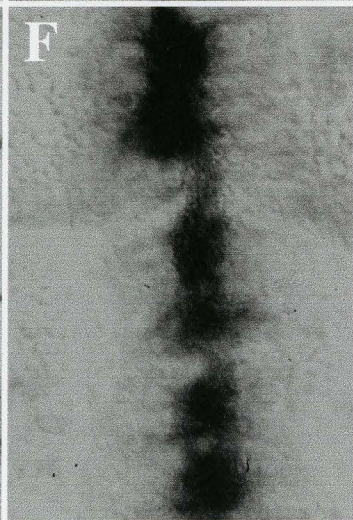
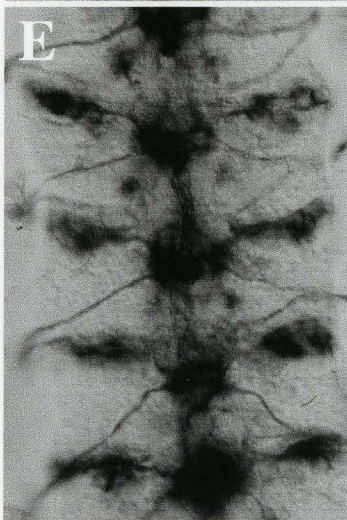
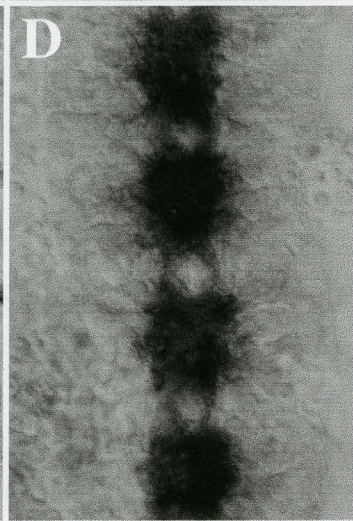
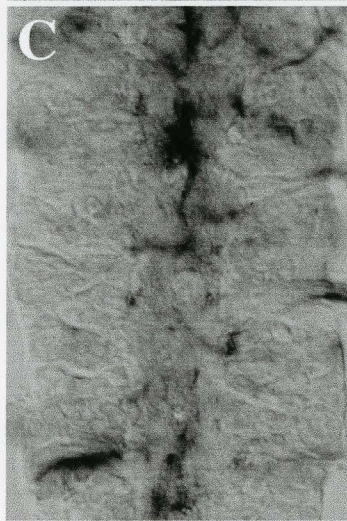
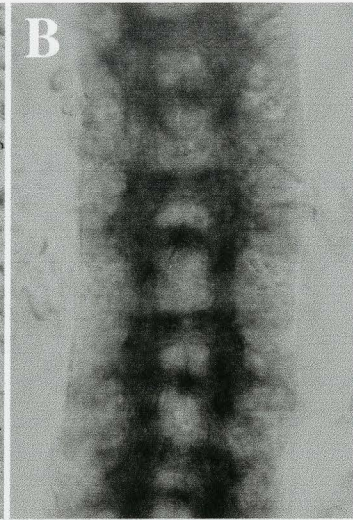
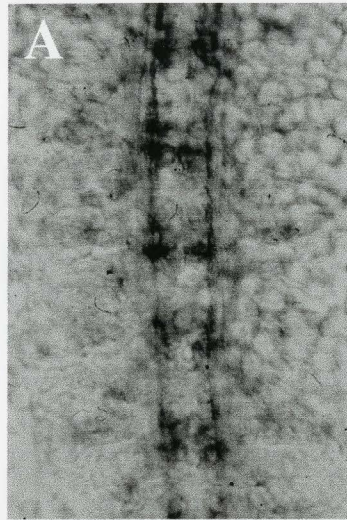
Figure 5.13 **Immunocytochemical analysis of *discs-large/FM7cβ*;
slit/CyO[*eng*] stable double mutant fly lines.**

Nerve cords are immunolabelled with mAb 1D4 (A, C, E) and mAb BP102 (B, D, F).

dlg1⁶ mutants display a wildtype CNS morphology (A, B). *dlg1⁶; slit²⁹⁹⁰* (C, D) and *dlg1⁶;*

slit² (E, F) double mutants are indistinguishable from the *slit²⁹⁹⁰* and *slit²* phenotypes,

respectively.



CHAPTER 6 TRANSHETEROZYGOUS AND DOSAGE-SENSITIVE DOMINANT MODIFIER SCREENS

This chapter outlines genetic tests that were not part of the blind test examination or the double mutant analysis. The first part examines the genetic interaction between all alleles of *slit* and an allele of *robo*. Next, the genetic interaction between *slit* and a deficiency that uncovers *wrapper*, a gene involved in MG survival, is shown. Genetic combinations of *slit/robo* pathway molecules with the α -PS3 integrin *scab* are explored. Finally, a tertiary site genetic modifier screen is conducted using a *slit; lamA* double mutant line as a sensitised background to detect changes in CNS phenotype with a reduction in gene expression of a candidate locus. These are the final experiments conducted to detect other genes that interact genetically with *slit*.

6.1 SLIT ALLELES SHOW DIFFERENT DEGREES OF CROSSOVER PENETRANCE IN TRANS TO ROBO

The initial *slit*²/*robo*¹ genetic interaction (Chapter 1; Battye et al. 1999) was examined for all alleles of *slit* to determine if the genetic interaction was similar among all alleles. Transheterozygous embryos, stained with mAb 1D4, were chosen based on absence of embryonic markers. Table 6.1 summarises the results obtained. All alleles display only midline crossing of the medial FasII-positive fascicle, leaving the other two fascicles unaltered.

*slit*² was originally defined as the most severe *slit* allele, based upon the axon tract phenotype (Battye 2000). When placed in trans to *robo*¹, 44.9% of segments show midline crossovers. This is surprising, because it is not the most severe genetic interaction among the alleles. The alleles exhibiting the most frequent occurrence of crossovers include the alleles *slit*³¹⁴⁹, *slit*^{GA178}, *slit*^{GA20} and *slit*¹⁹¹², representing between 60.2% and 62.9% of segments with midline crossovers. The remainder of alleles include *slit*²⁹⁹⁰, *slit*⁵⁵⁰, *slit*⁵³², *slit*^{GA945} and *slit*², exhibiting between 44.9% and 48.3% segmental

Table 6.1 Percent segmental crossovers shown in *slit/robo1¹* transheterozygotes.

<i>slit</i> Allele	n (embryos)	Segments Counted	Mean % (+/- Std) Crossovers
<i>slit 3149</i>	40	318	62.9 +/- 27%
<i>slit GA178</i>	32	227	61.2 +/- 28%
<i>slit GA20</i>	30	219	60.3 +/- 29%
<i>slit 1912</i>	31	231	60.2 +/- 25%
<i>slit 550</i>	35	284	47.5 +/- 23%
<i>slit 2990</i>	35	267	48.3 +/- 24%
<i>slit GA945</i>	29	215	46.1 +/- 21%
<i>slit 532</i>	35	281	46.3 +/- 26%
<i>slit 2</i>	29	227	44.9 +/- 22%
<i>slit F81</i>	29	232	41.8 +/- 26%
<i>slit F119</i>	28	229	37.6 +/- 28%
<i>slit E158</i>	29	221	35.3 +/- 19%

crossovers. The enhancer trap alleles *slit*^{F81}, *slit*^{F119} and *slit*^{E158}, exhibited between 35.3% and 41.8% of crossovers. Upon examining these means +/- their standard deviations (Table 6.1), these combinations significantly overlap one another, making it likely that a specific allele does not significantly affect the genetic interaction more than another.

*slit*²/+ (Figure 6.1A) and *robo1*¹/+ (Figure 6.1B) heterozygotes do not display midline crossovers. *slit*³¹⁴⁹/*robo1*¹ transheterozygotes showed the most severe interaction, exhibiting 62.9% of segments with crossover (Figure 6.1C). *slit*²⁹⁹⁰/*robo1*¹ transheterozygotes showed 48.3% of segments with midline crossovers (Figure 6.1D). *slit*²/*robo1*¹ transheterozygotes exhibit a 44.9% segmental crossover frequency (Figure 6.1E). The weakest genetic interactions was *slit*^{E158}/*robo1*¹, exhibiting 35.3% of segments with midline crossover.

To test for effects on viability, F1 flies from a *slit*² and *robo1*¹ fly cross were counted for presence/absence of the CyO balancer. These gene complement in trans, as approximately 1/3 of F₁ flies do not carry a balancer. Thus, a half reduction of *slit* and *robo1* gene copies do not affect viability.

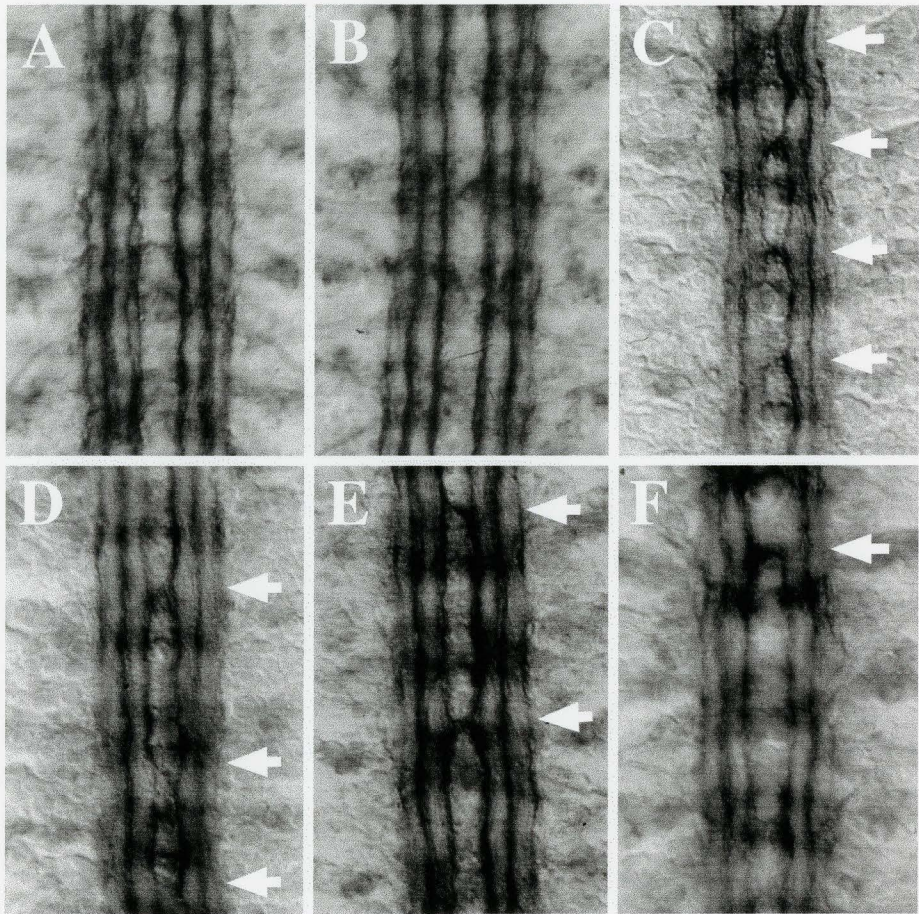
6.2 SLIT INTERACTS GENETICALLY WITH DEFICIENCIES THAT UNCOVER WRAPPER

Wrapper encodes a protein member of the Ig superfamily. Wrapper is expressed by MGA and MGM and appears to be involved in the development and maintenance of commissure separation mediated by contact with commissural axons (Noordermeer et al. 1998). Due to this putative role of Wrapper, I wanted to examine the possibility of *slit* interacting with *wrapper*.

Since no wrapper mutants were available, I used a deficiency, Df(2R)X58-3, in the region that *wrapper* is located (see Table 2.1). Two mutant phenotypes were revealed in

Figure 6.1 Immunocytochemical analysis of *slit/robo1* genetic interaction.

Nerve cords are immunolabelled with mAb 1D4. *slit*^{2/+} (A) and *robo1*^{1/+} (B) heterozygotes reveal a CNS phenotype identical to wildtype. Representative *slit*^{2/robo1} transheterozygotes are shown to demonstrate a genetic interaction as evidenced by midline crossing of axons (arrows). *slit*^{3149/robo1} (C), *slit*^{2990/robo1} (D), *slit*^{2/robo1} (E) and *slit*^{E158/robo1} (F) demonstrate a range of genetic interactions between *slit* alleles and *robo1*.



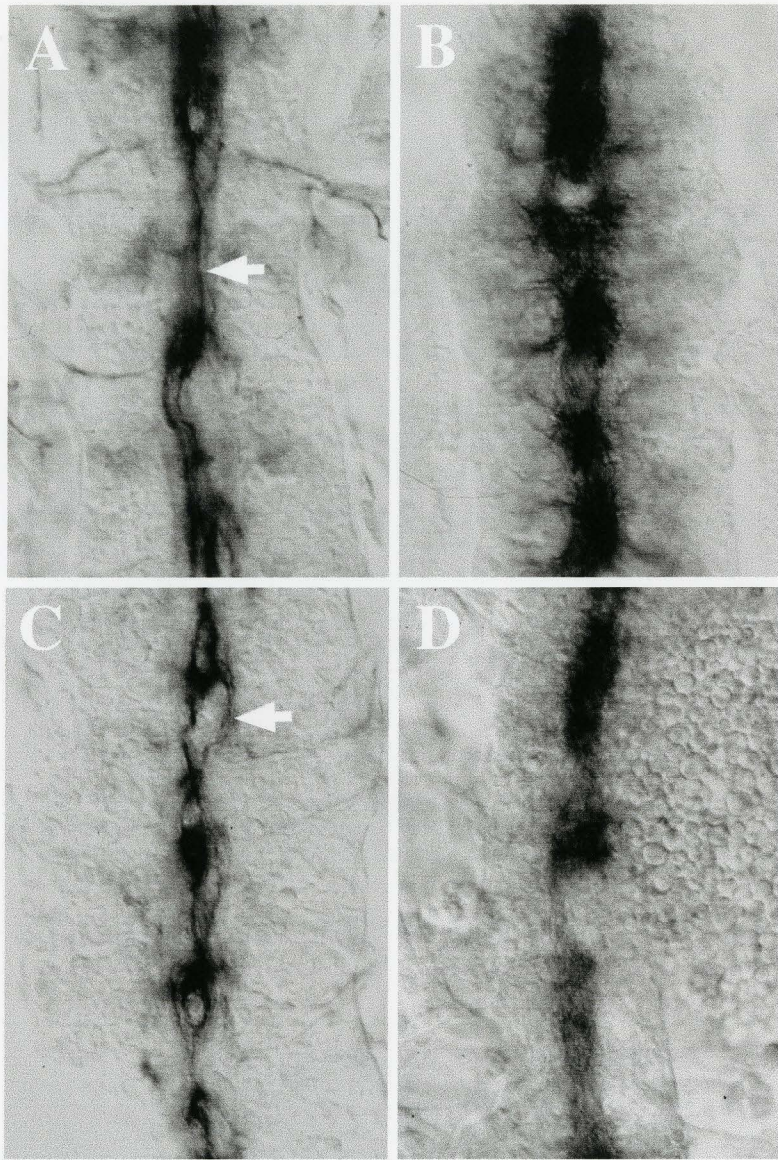
a *slit*²/Df(2R)X58-3 transheterozygous embryo. 22% of phenotypic mutants (n=77) display a collapse of FasII-positive axons at the CNS midline (Figure 6.2A). This phenotype is mirrored in BP102 collection (Figure 6.2B). However, 78% of mutant embryos exhibit occasional midline fascicle fusion (mAb 1D4) and fusion of commissures (BP102) while other segments appear wildtype (Appendix Figure 27A, B). A similar distribution of phenotypes is observed in *slit*²⁹⁹⁰/Df(2R)X58-3 embryo collection. Fascicles (mAb 1D4) are collapsed toward the midline but exhibit persistent crossing and recrossing of axons across the midline in 16.2% (n=37) of mutants (Figure 6.2C). This close association at the midline, however, generates a collapsed BP102 phenotype (Figure 6.2D) similar to *slit*²/Df(2R)X58-3 mutants (compare to B). Other mAb 1D4 phenotypes observed in this collection display midline crossovers in 83.8% of mutants (Appendix Figure 27C). When viewed with BP102, these mutants display a narrowed nerve cord with fuzzy commissures and thinned longitudinals (Appendix Figure 27D). It is not known what phenotype is exhibited by Df(2R)X58-3 homozygotes.

I initially used a larger deficiency, Df(2R)X58-12, which uncovered both the *wrapper* and *robo1* loci. *slit*²⁹⁹⁰/Df(2R)X58-12 transheterozygotes show medial crossovers in some mutants (Appendix Figure 27E), but the presence of *robo1* mutant locus interferes with analysing an interaction between *slit* and *wrapper*. Df(2R)X58-12 homozygotes appear fused at the midline with mAb 1D4 (data not shown). However, with other results shown, it is evident that *slit* and Df(2R)X58-3 interact genetically.

Df(2R)X58-3 uncovers the region 58C3-7; 58D6-8 and Df(2R)X58-12 uncovers the region 58D1-2; 59A. Some genes have been characterised in this region but of those, only a few would be of interest here. *defective proventriculus*, located at 58D2, encodes a homeobox domain protein that is expressed in the ventral nerve cord but no CNS phenotype has been reported. *no endurance*, located within 58E is involved in synaptic

Figure 6.2 Immunocytochemical analysis of *slit/wrapper* genetic interaction.

Nerve cords are immunolabelled with mAb 1D4 (A, C) and BP102 (B, D). *Df(2R)X58-3* uncovers the *wrapper* gene. *slit²/Df(2R)X58-3* transheterozygotes (A, B) display a collapsed midline phenotype (arrow) in 22% (n=77) of phenotypic mutants. *slit²⁹⁹⁰/Df(2R)X58-3* transheterozygotes (C) exhibit a less severe collapsed phenotype (arrow), represented by continuous midline crossing and recrossing of axons, in 16.2% (n=37) of phenotypic mutants. These mutants stained with BP102 (D) demonstrate a similar nerve cord with a collapsed and fused commissure phenotype as observed in B.



vesicle trafficking and mutants display behavioural and movement defects. These genes may also contribute to the phenotype displayed by the X58-3 deficiency in trans to *slit* and cannot be discounted from this analysis. *cyclinB*, located within 59A also has CNS expression but no reported CNS phenotype but may contribute to the collapsed phenotype exhibited by Df(2R)X58-12 homozygotes. Further work would need to be done to determine if these genes display CNS defects.

6.3 GENETIC INTERACTIONS WITH SCAB

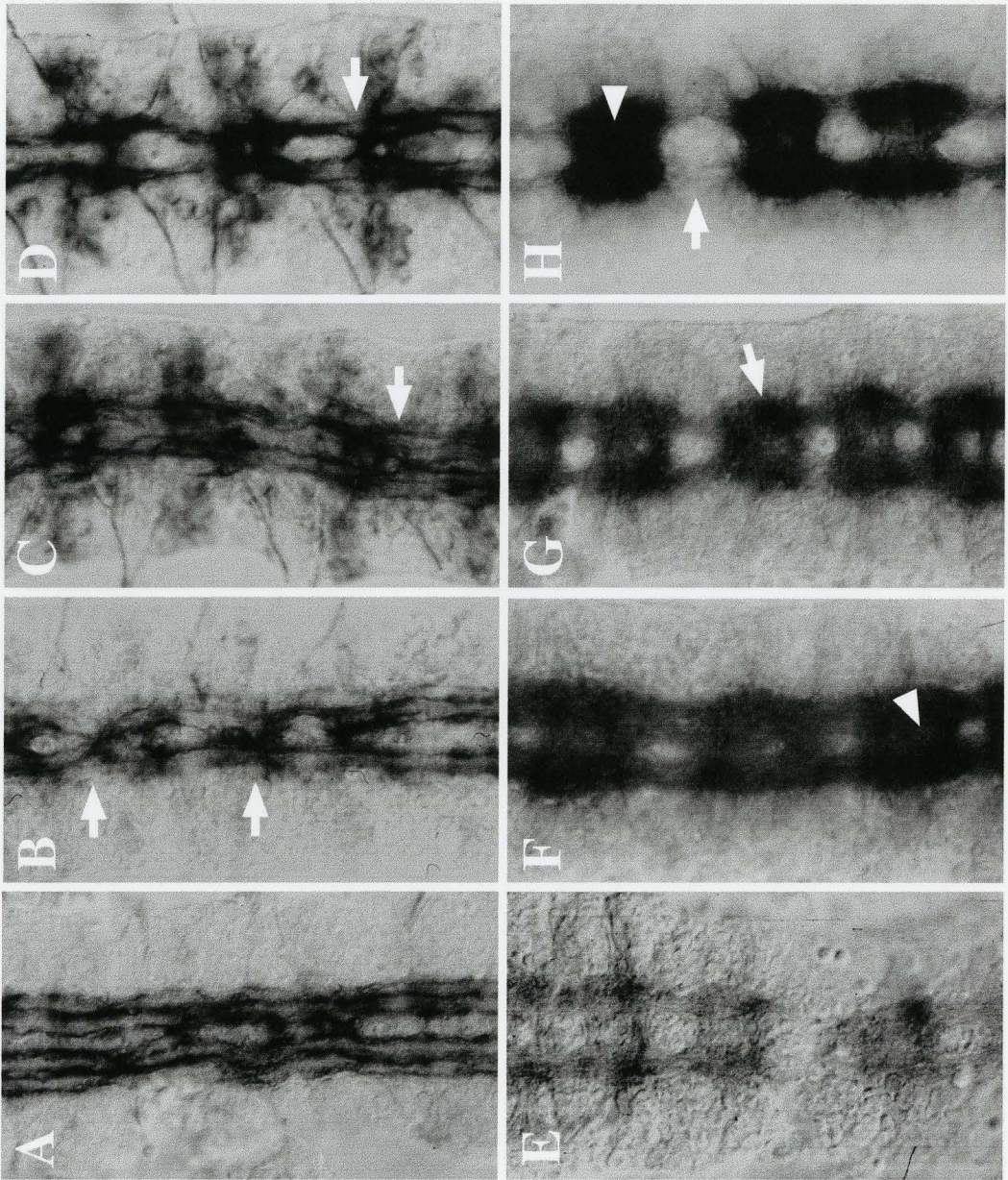
6.31 Scab interacts genetically with *slit*, *robo1* and *dock* mutants

scab (*scb*) was another candidate gene included in this assessment. *scb* maps closely to *slit*, located at 51E10-11. This made a recombination very difficult to attempt, yielding a theoretical recombination frequency at 4%. Thus I used a quick cross to determine if *scb* in trans to *slit*² would interact genetically. I expect 25% of the population of embryos, or 50% of unmarked embryos (lack of β -gal staining) to be the transheterozygous genotype in all crosses conducted here. (The *scb* mutant stock does not carry a LacZ-marked balancer chromosome.)

In a *slit*²/*scb*² transheterozygous cross, 61.2% (n=80) of unmarked embryos labeled with mAb 1D4 show a mutant phenotype. Of these embryos, 50% (n=49) display multiple midline crossovers in the middle segments of the nerve tract (Figure 6.3B). The remainder 50% display one segmental midline crossover (Appendix Figure 28A), crossovers involving at least two fascicles (Appendix Figure 28B) or total midline fusion in some segments (Appendix Figure 28C). When viewed with BP102, 30.8% (n=247) of unmarked embryos displayed a mutant phenotype. Of these embryos, 51.3% (n=76) of transheterozygotes displayed a narrowed nerve cord and poorly defined commissures (Figure 6.3F). 40.8% of these embryos showed 1-2 collapsed segments (Appendix Figure 28D) while a small proportion (7.9%) were fused at the midline in a few segments (Appendix Figure 30E).

Figure 6.3 **Immunocytochemical analysis of gene interactions with *scab*.**

Nerve cords are immunolabelled with mAb 1D4 (A-D) and mAb BP102 (E-H). *scb*² mutants are shown in A and E. 50% (n=49) of *scb*²/*slit*² transheterozygotes demonstrate crossovers (arrow) in the middle segments of the nerve tract (B). When immunolabelled with BP102 51.3% (n=76) display a narrowed nerve tract and poorly defined commissures in some segments (arrowhead, F). 14.5% (n=69) of *scb*²/*robo1*¹ transheterozygotes show frequent midline crossing of medial axons (arrow, C), and narrowing of the tract with poorly defined commissures (arrow, G). *scb*²/*dock*^{P1} transheterozygotes demonstrate more severe crossovers in 18.3% (n=77) of embryos (D), as crossover appears to involve all three longitudinal fascicles (arrow, compare to B and C). These embryos all display fuzzy commissures (arrowhead, H) and thinned or absent longitudinal connections (arrow, H).



Since *scb* exhibited a genetic interaction with *slit*², I then tested *scb* in trans to *robo1*¹ and *dock*^{P1} to determine if *scb* interacts genetically with other putative players in the *slit/robo* signaling pathway.

In a *scb*²/*robo1*¹ transheterozygous cross, 48% (n=144) of unmarked embryos display a mutant phenotype. 14.5% of these embryos (n=69) display multiple (Figure 6.3C) or single (Appendix Figure 30F) midline crossovers with mAb 1D4. The majority (85.5%) display a near to wildtype phenotype, although gaps in the lateral fascicle due to reduced 1D4 staining are present (Appendix Figure 28G). BP102-stained embryos are slightly narrowed toward the midline and commissures are poorly defined (Figure 6.3G). A few embryos display pronounced thinning of longitudinals (Appendix Figure 28H). These results indicate that *scb* and *robo1* interact genetically.

*scb*²/*dock*^{P1} transheterozygotes also show significant CNS phenotypes. The majority of unmarked embryos (81.7%) do not have an apparent mutant phenotype (Appendix Figure 28I) but 18.3% (n=77) of unmarked embryos display multiple midline crossovers and defasciculation of longitudinal tracts (Figure 6.3D). These embryos display thick and fuzzy commissures and thinned or nearly absent longitudinals (Figure 6.3H). Some display a milder phenotype of narrowed nerve cord and poorly separated commissures (Appendix Figure 28J). These results conclude that *slit*, *robo1* and *dock* interact genetically with *scb*.

6.32 Deficiency crosses show genetic interactions between *slit* and *scab*

To further examine the *slit/scb* interaction, I employed deficiencies (Table 2.1) in trans with both *slit* and *scb* to test for dosage sensitive effects. I expect 50% of the *slit* crosses to be unmarked embryos (lack of β -gal staining), and 50% of the unmarked embryos to be the transheterozygote genotype. As neither *scb* nor the deficiencies carry

LacZ chromosomes, all embryos will be counted and I expect 25% of those embryos to be the transheterozygote genotype.

Df(2R)XTE-18 uncovers the *scb* locus and not the *slit* locus. As a result, embryos that carry *scb*² and the deficiency in trans (ie. *scb*²/Df(2R)XTE-18) display dorsal closure defects also observed in *scb*² mutants. 23% (n=139) of embryos exhibit dorsal herniation as a result of failure of dorsal closure. 69% (n=32) of these herniated embryos display mild defasciculation defects and frequent gaps in the lateral fascicle when viewed with mAb 1D4 (Appendix Figure 29A). The remaining 31% exhibit midline crossovers, an example of which is shown in Figure 6.4B. They display midline crossing of at least the two inner fascicles while the lateral fascicle remains unaltered. These phenotypes are like those observed in *scb*² mutants. When stained with BP102, 27.2% (n=125) of embryos exhibit the dorsal herniation defect but have a wildtype CNS phenotype. 4% of embryos are not dorsally herniated but display poorly defined commissures and thinned longitudinal tracts (Figure 6.4J).

Df(2R)XTE-18 has breakpoints that either map adjacent to, or also uncover, the upstream sequence of *slit*. To clarify this breakpoint region, I mated *slit* flies to flies of this deficiency stock. Noncomplementation of these regions would be easily scored by presence of all curly wing F1 progeny. As 28% (n=43) straight wing progeny emerged from this cross, approximating the 1/3 of expected F1 to be transheterozygotes, I concluded the deficiency complements the *slit* locus. This indicates the deficiency does not uncover *slit*.

I also observed the phenotypes exhibited by the *slit*²/Df(2R)XTE-18 transheterozygous cross. 52% of unmarked embryos from this collection exhibited mutant phenotypes (n=73). Of this group of mutant phenotypes (likely the *slit*²/Df(2R)XTE-18 genotype), 76.3% (n=38) of embryos display thinned and defasciculated longitudinal axons with some segmental crossovers (Figure 6.4F). 18.4%

Figure 6.4 (A-H) Immunocytochemical analysis of *slit/scab* genetic interaction visualised with mAb 1D4.

*scb*² and *slit*² mutants are shown in A and E. 31% (n=139) of *scb*²/Df(2R)XTE-18 (B) transheterozygotes demonstrate midline crossing of axons involving at least the two inner longitudinal fascicles (arrowhead) and the lateral fascicle remains unaltered (arrow). 76% (n=38) *slit*²/Df(2R)XTE-18 (F) transheterozygotes demonstrate defasciculated longitudinals and crossovers in segments, that appears to involve all three fascicles (arrow). 22% (n=88) of *scb*²/Df(2R)Jp4 transheterozygotes (C) display midline crossing of the medial fascicle (arrow). *slit*²/Df(2R)Jp4 transheterozygotes display a *slit*² mutant phenotype (G, compare with H). 11.8% (n=127) of *scb*²/Df(2R)Jp1 transheterozygotes (D) display crossing of the medial longitudinal fascicle across the midline (arrow) and occasional fusion in a segment (arrowhead). *slit*²/Df(2R)Jp1 transheterozygotes (H) are indistinguishable from *slit*² mutants (compare with E). Adjacent to the figure is a schematic depicting the relative breakpoints of the *scb*, *slit* and the deficiencies that uncover these loci.

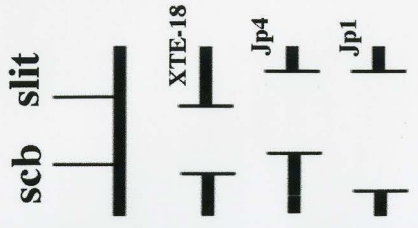
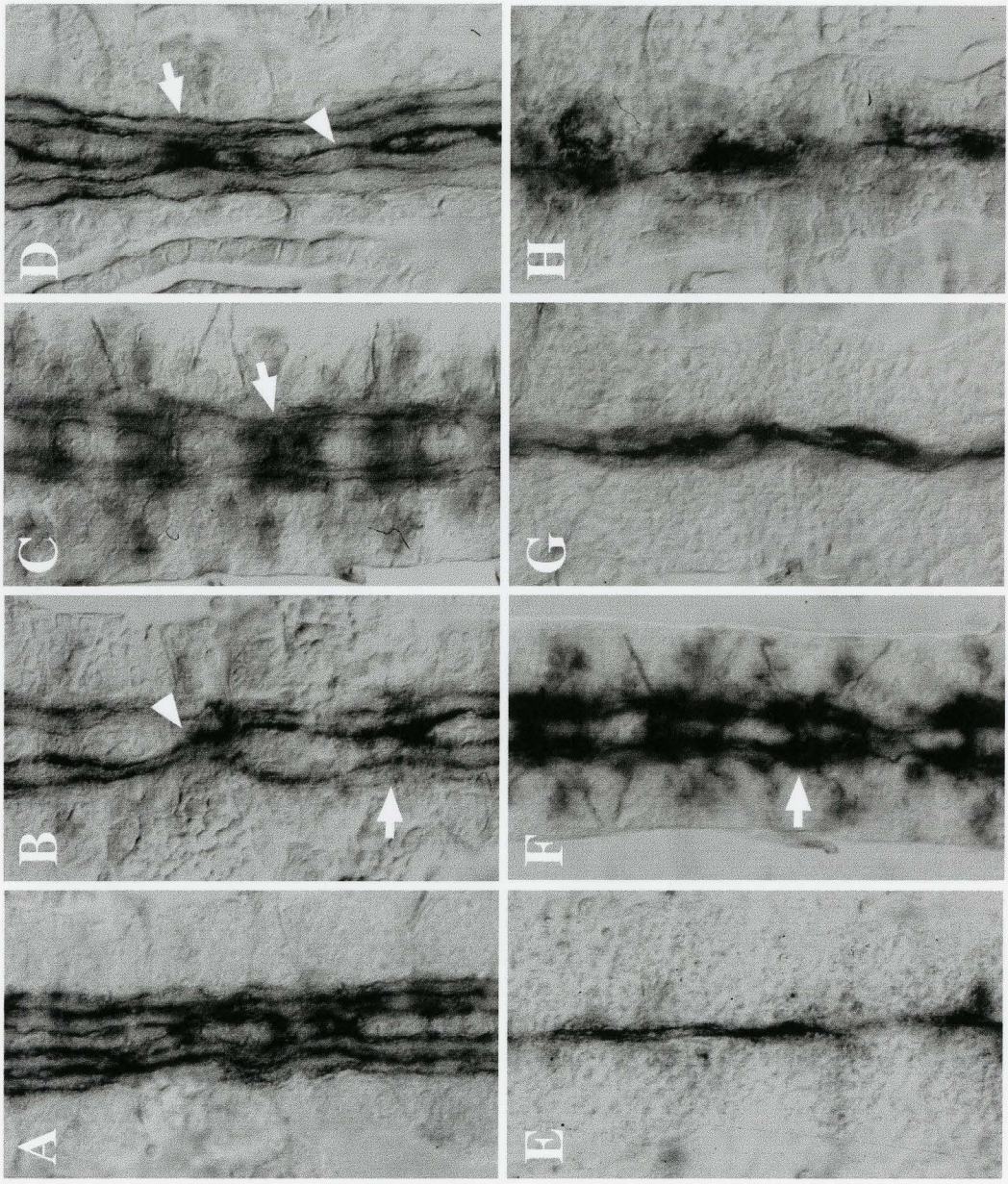
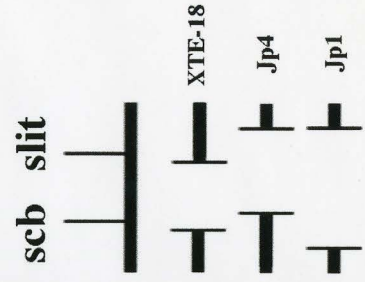
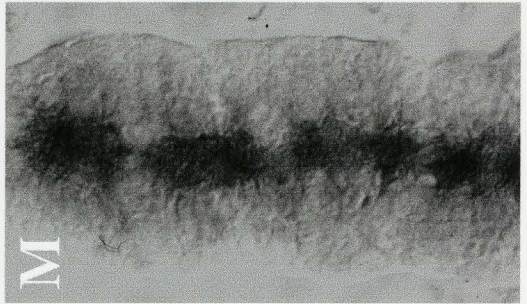
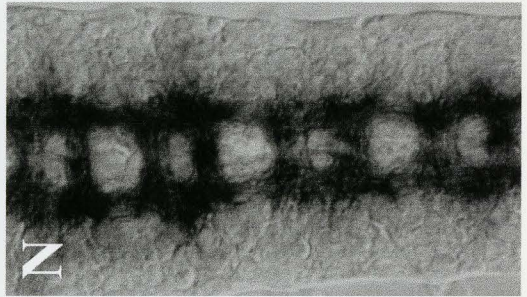
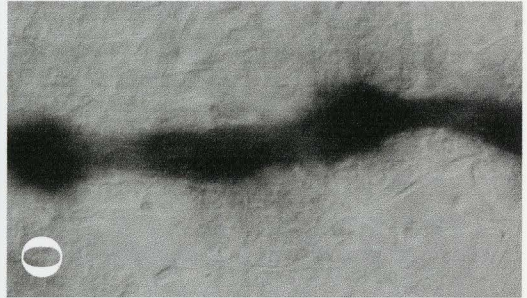
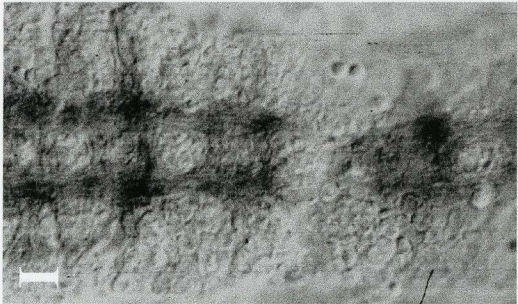
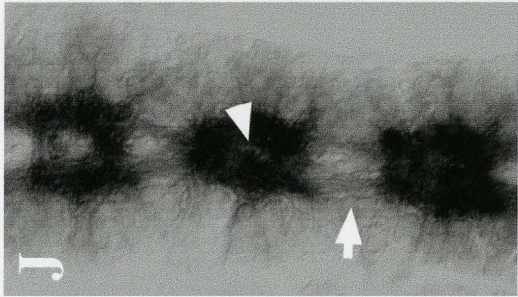
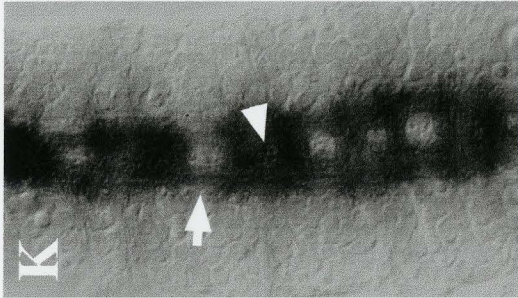
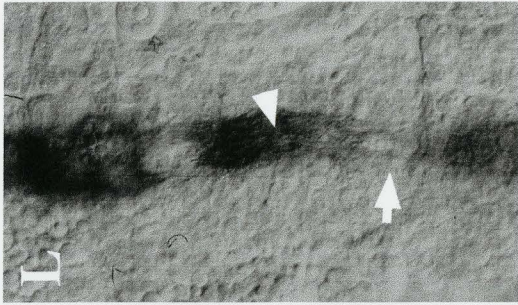


Figure 6.4 (I-O) Immunocytochemical analysis of *slit/scab* genetic interaction visualised with mAb BP102.

*scb*² and *slit*² mutants are shown in I and M. Deficiencies Df(2R)XTE-18, Df(2R)Jp4 and Df(2R)Jp1 uncover the genes *scab*, *slit* and *scab + slit*, respectively. 5% (n=125) of *scb*²/Df(2R)XTE-18 transheterozygotes (J) demonstrate a narrowing toward the midline in some segments, making commissures poorly defined (arrowhead) and longitudinal connections between these segments thinned (arrow). *slit*²/Df(2R)XTE-18 transheterozygotes (15.6%, n=32; N) did not demonstrate obvious defects, although the nerve tract appears narrowed and longitudinals thinned. *scb*²/Df(2R)Jp4 transheterozygotes (33.9%, N=62; K) demonstrate poorly defined commissures (arrowhead) and thinned longitudinals between segments (arrow). *slit*²/Df(2R)Jp4 (O) transheterozygotes are indistinguishable from *slit*² mutants. *scb*²/Df(2R)Jp1 mutants (L) are narrow toward the midline, display poorly defined commissures (arrowhead) and thinned longitudinal tracts (arrow). Adjacent to panel O is a schematic depicting the relative breakpoints of the *scb*, *slit* and the deficiencies that uncover these loci.



display nerve cords with all longitudinal fascicles projecting across the midline (Appendix Figure 29B). 5.3% of these mutants display only 1 midline crossover (Appendix Figure 29C). Commissures remain defined and longitudinals thinned in 15.6% of unmarked BP102-labeled embryos (Figure 6.4N). These results reveal a genetic interaction between *slit* and the region uncovered by Df(2R)XTE-18.

Df(2R)Jp4 uncovers the region encoded by the *slit* locus. 22.7% (n=88) of embryos from a *scb*²/Df(2R)Jp4 transheterozygous cross display several midline crossovers (Figure 6.4C), or one midline crossover (Appendix Figure 29D), or midline narrowing and slight fusion of medial axons at the midline (Appendix Figure 29E). 33.9% (n=62) of BP102-stained embryos have fuzzy commissures and thinned longitudinal axons between segments (Figure 6.4K). Some of these mutants display an obvious segmental collapse toward the midline (Appendix Figure 30A). These phenotypes indicate that *scb* interacts genetically with the region uncovered by Df(2R)Jp4. *slit*²/Df(2R)Jp4 transheterozygotes display a *slit*² phenotype (Figure 6.4G, O).

Df(2R)Jp1 uncovers both *scb* and *slit* loci. I included this deficiency to examine combinations of mutant homozygous and heterozygous loci for *scb* and *slit*. 52.5% (n=242) of embryos from *scb*/Df(2R)Jp1 transheterozygous cross show dorsal herniation evident of *scb* locus. I have interpreted these embryos to be *scb*²/Jp1 and disregarded the remainder of the collection. Of these embryos, 75.6% (n=127) display no mutant nerve cord phenotype (data not shown). 11.8% show frequent midline crossing and midline fusion at the midline (Figure 6.4D). Another 12.6% of embryos display a twisted VNC seen also in *scb*² mutants (Appendix Figure 29F). These embryos may also display midline crossovers but the twisted nerve cord makes this difficult to assess. BP102-labeled embryos display narrowed nerve cord with fuzzy commissures and thinned longitudinal tracts (Figure 6.4L) or a narrowed nerve cord and fuzzy commissures in some segments (Appendix Figure 30B). These results suggest that reduced *slit* enhances the *scb* 1D4 and

BP102 mutant phenotypes to display more midline fusion as compared to *scb* mutants alone.

slit²/Df(2R)Jp1 transheterozygotes (Figure 6.4H) are indistinguishable from *slit²* mutants. Thus, *scb/+* clearly does not function to suppress the *slit²* phenotype, but *slit* and *scb* do interact genetically and likely function in a common or parallel pathway.

6.4 DOSAGE-SENSITIVE DOMINANT MODIFIER SCREEN

Laminin1 was found to bind hSlit2 in cell culture (Brose et al. 1999). As Laminin and Slit proteins are coexpressed in the CNS during axonogenesis (Table 2.1), and they also generate a mutant phenotype when both genes are present in reduced copies (Chapter 5), they likely function in vivo during development. I generated a *slit; lamA* double mutant line to use as a sensitised background for testing other genes that may act as modifiers in this system. A sensitised background is one in which a known weak genetic interaction occurs, but allows an investigator to determine what other factors may interact genetically with it. Since *slit²/+; lamA⁹⁻³²/+* embryos (Figure 5.5E) show a weak genetic interaction in *Drosophila*, other mutants or deficiencies were crossed into it to determine if they would enhance or suppress the genetic interaction. Embryos from this cross would be triple mutants with a heterozygous copy of each gene and deficiency. This genetic interaction could result in phenotypic “enhancement” (worsening of the *slit²/+; lamA⁹⁻³²/+* phenotype) or phenotypic “suppression” (lessening of the *slit²/+; lamA⁹⁻³²/+* phenotype toward wildtype). Examples of this cross and proportions of genotypes expected in the F1 generation are outlined in Appendix Figure 11. For each cross, except that involving *netrin* (X chromosome), I would expect the frequency for each genotype including the triple heterozygote to be 1/8 or 12.5%. For the *netrin* triple mutant cross, I expect each genotype to occur with a frequency of 1/16 or 6.25%.

6.41 Robo does not interact genetically with LamA or enhance the sensitised background.

Robo was the first logical candidate used in this screen due to its genetic interaction with Slit. Triple heterozygotes *slit²/robo1¹; lamA⁹⁻³²/+* (Figure 6.5A) display persistent midline crossing of the medial longitudinal fascicles, while the remainder two fascicles are unaltered. This is the only phenotype observed in the triple mutant collection. With BP102, a narrowing of the nerve cord tract is evident with poorly separated commissures (Figure 6.5B). To directly determine if *robo* interacts with *lamA* in vivo, *robo1¹* mutant flies were mated with *lamA⁹⁻³²* mutant flies and a reduced copy of both genes resulted in wildtype phenotypes with mAb 1D4 (Figure 6.5B) and BP102 (Figure 6.5F). When *slit²* and *lamA⁹⁻³²* are also present in reduced copies (ie. *slit²/+; lamA⁹⁻³²/+*), midline crossing of the medial fascicle is like that observed for the triple heterozygous mutant although not as frequent (Figure 6.5C) and the nerve cord appears narrowed with poorly separated commissures and thinned longitudinals (Figure 6.5G). Likewise with *slit²/robo1¹* transheterozygotes we see the same midline crossover phenotype (Figure 6.5D). It could be argued that the triple heterozygous combination produces an enhanced frequency of segmental crossovers, but does not enhance the type of phenotypic interaction. This enhancement of crossover frequency is likely due to an additive effect of the *slit²/+; lamA⁹⁻³²/+* and *slit²/robo1¹* interactions and not due to an interaction between *robo1¹* and *lamA⁹⁻³²* as they produced no visible phenotype. Thus, whatever functional interaction *slit²* has with *lamA⁹⁻³²* is independent of *robo1¹*, and vice versa for the *slit²/robo1¹* interaction.

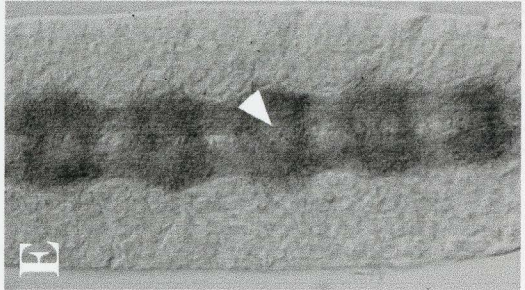
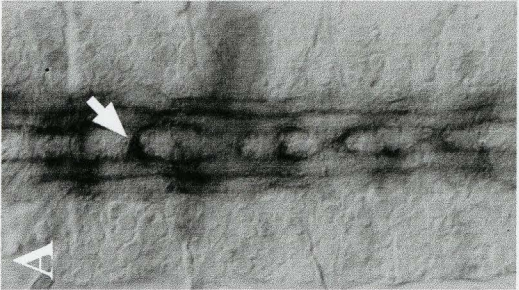
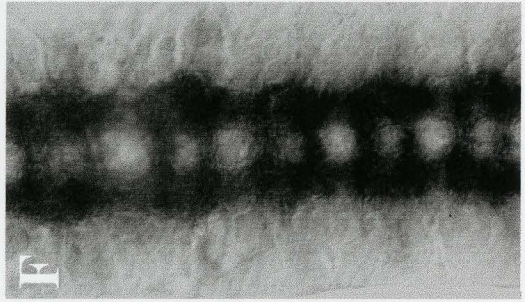
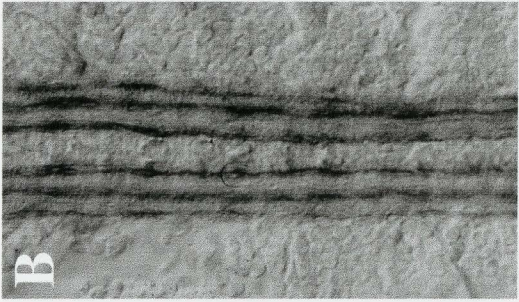
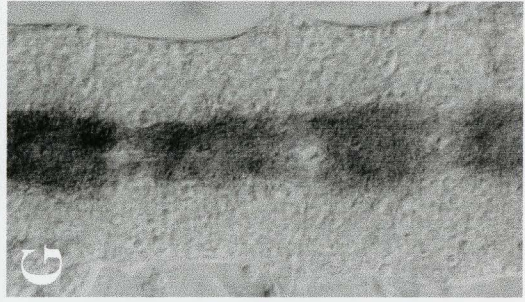
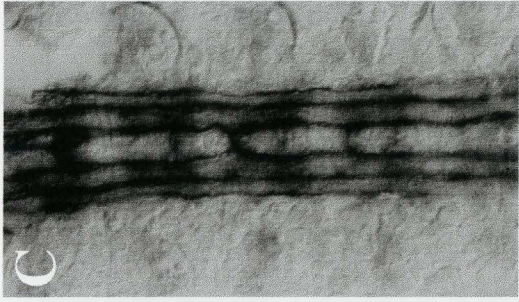
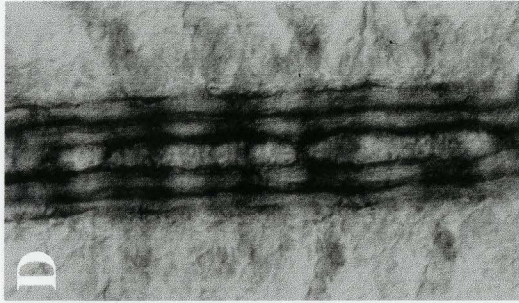
6.42 LamininB1 deficiencies enhance the *slit/+;lamA/+* phenotype

Since a genetic interaction between Slit and LamininA chain was established, I next wanted to determine how a reduced gene dosage of a LamininB1 chain would affect CNS

Figure 6.5 **Immunocytochemical analysis of a triple mutant genetic screen involving *robo1*, *slit* and *lamininA* genes.**

Nerve cords are immunolabelled with mAb 1D4 (A-D) and mAb BP102 (E-G).

Heterozygous embryos triple mutant for *robo1*¹, *slit*² and *lamA*⁹⁻³² (A) demonstrate midline crossing of the medial longitudinal fascicle (arrow). These embryos display poorly defined commissures (arrowhead, E) with BP102. Embryos double heterozygous for *robo1*¹ and *lamA*⁹⁻³² display a wildtype phenotype (B, F). *slit*^{2/+}; *lamA*^{9-32/+} heterozygotes (C, G) display a phenotype similar to the triple mutant (compare to A and E), although the axon tract appears to be collapsed toward the midline in *slit*^{2/+}; *lamA*^{9-32/+} embryos (G). Likewise, *slit*^{2/robo1}¹ transheterozygotes (D) display a crossover phenotype similar to A and C.



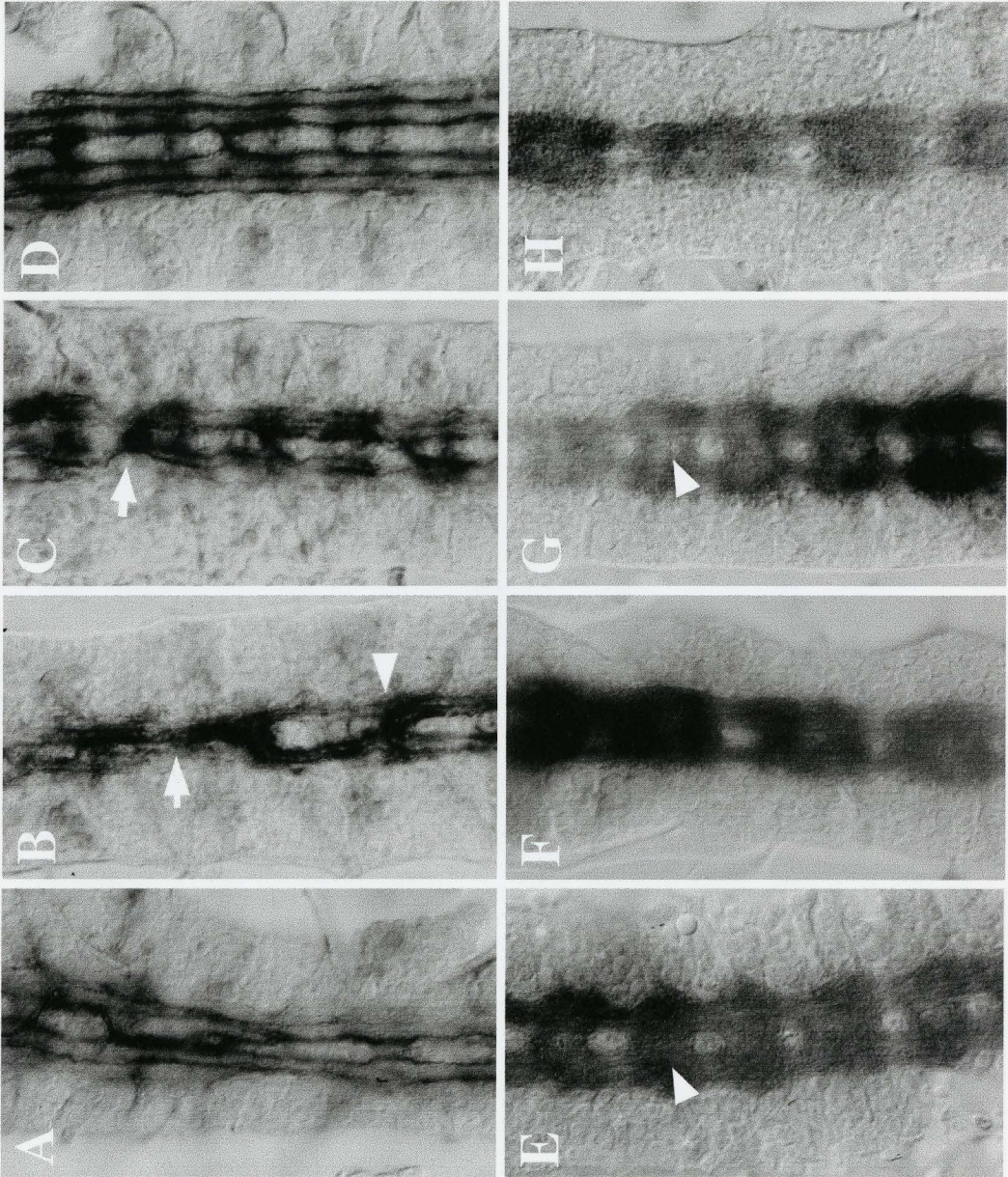
phenotype. Two deficiencies were employed for this, Df(2R)Trf-C631 and Df(2R)XE-2750 (see Table 2.1 for breakpoints) that uncover the lamininB1 locus at 28D.

20% (n=90) of embryos from the triple heterozygous cross containing the *slit*²/Df(2R)Trf-C631; *lamA*⁹⁻³²/+ genotype displayed continuous crossing and recrossing of medial axons and severe narrowing of the nerve cord toward the midline (Figure 6.6A). 17.8% of the collection exhibited clumping of FasII-positive axons at the midline within each segment and lack intersegmental connections (Appendix Figure 31A). Another 16.7% of embryos within this collection displayed a range of CNS phenotypes different from Figure 6.6A. These phenotypes included occasional midline crossovers without narrowing (Appendix Figure 31B), crossing of all fascicles across the midline in one segment (Appendix Figure 31C), and mild midline crossover with little disruption in fascicle projection (Appendix Figure 31D). When viewed with BP102, 6.4% (n=173) of embryos display fuzzy commissures and narrowing toward the midline (Figure 6.6E). 4.6% of the collection display clumps of axons within each segment and little or no intersegmental connections while segmental commissures are poorly defined (Appendix Figure 31 E, F).

When tested with the other deficiency, Df(2R)XE-2750, a similar range of phenotypes is evident. 7.8% (n=129) of the collection display a narrowed nerve cord, occasional midline fusion, and continuous crossing and recrossing of fascicles across the midline (Figure 6.6B). This phenotype is most representative of a *slit*²/Df(2R)XE-2750; *lamA*⁹⁻³²/+ triple heterozygous mutant. Another 10.8% of embryos display a severely narrowed nerve cord with occasional midline separation (Appendix Figure 31G). 6.2% of embryos display a looping crossover phenotype (Appendix Figure 31H) similar to that observed in Appendix Figure 31B. 27.9% of embryos display slight midline narrowing (Appendix Figure 31I) with occasional midline crossovers (not shown) similar to Appendix Figure 31D. With BP102, 7.6% (n=276) of embryos have narrowed nerve cords and

Figure 6.6 **Immunocytochemical analysis of a triple mutant genetic screen involving *lamininB1* locus, *slit* and *lamininA* genes.**

Nerve cords are immunolabelled with mAb 1D4 (A-D) and BP102 (E-H). Heterozygous embryos triple mutant for Df(2L)Trf-C6R31, *slit*² and *lamA*⁹⁻³² (20%, n=90; A) demonstrate crossing and recrossing of the inner two fascicles (arrows) and narrowing of the nerve cord. These embryos (6.4%, n=173) also display fused commissures (arrowhead) although collapse of the nerve cord is not evident with BP102 (E). Heterozygous embryos triple mutant for Df(2L)XE-2750, *slit*² and *lamA*⁹⁻³² (B) display some segments showing fusion of fascicles at the midline (arrow), while other exhibit continuous crossing across the midline in 7.8% (n=129) of embryos (arrowhead). *slit*²/Df(2R)XE-2750 transheterozygotes display midline crossovers that involve at least the inner medial fascicle but involve all three fascicles in some segments (arrow, C) in 24.1% (n=87a) and 13.8% (n=87b) of embryos (a and b denote two separate embryo collections). These differences reflect few changes in commissure morphology, although little separation is apparent in these mutants (arrowhead, G). *slit*²/+; *lamA*⁹⁻³²/+ transheterozygotes display mild crossovers in some segments of the VNC (D). These mutants, however, display a narrow nerve tract and poorly defined commissures (H).



fuzzy commissures (Figure 6.6F) similar to Figure 6.6E. Other embryos (1.8%) in the triple mutant collection display midline fusion in some segments (Appendix Figure 31J). 5.8% of embryos again display clumps of axons within segments and absence or thinning of intersegmental connections (Appendix Figure 31K) similar to that observed in Appendix Figure 31E.

In this screen, I included a cross that tests for a genetic interaction between *slit*² and Df(2R)XE-2750 as I can be certain this deficiency removes part of the *lamininB1* gene (whereas the breakpoints of the other deficiency are uncertain). Two collections (denoted *a* and *b*) were completed for this cross for mAb 1D4. Common to both collections was a persistent crossover phenotype involving at least 1 but sometimes 2 fascicles in 24.1% (n=87*a*) and 13.8% (n=87*b*) of embryos (Figure 6.6C). I deduced this to be the most representative phenotype of *slit*²/Df(2R)XE-2750 transheterozygotes. Other phenotypes seen were nerve cords showing one segmental crossover (Appendix Figure 31L) in 41.3% (n=87*a*) and 13.8% (the same grouping as the above phenotype, n=87*b*) of embryos, and a midline fusion of the medial fascicle (Appendix Figure 31M) or fusion with occasional looping (Appendix Figure 31N) only seen in the second collection (21.8%, n=87*b*). The BP102-labeled collection yielded few embryos, but some displayed poorly separated commissures (Figure 6.6G) or complete midline fusion (Appendix Figure 31O). The *slit*²/+; *lamA*⁹⁻³²/+ double heterozygotes were included for phenotypic comparison (Figure 6.6 D, H).

The observed frequency of phenotypes do not correspond well with expected frequencies. I cannot account for this, even if I consider balancer effects on phenotype. I chose the images in Figure 6.6A and B under two criteria: first, I chose the images as a middle representative of a range of phenotypes; second, I disregarded the embryos that display the severe segmental clumping of axons (Appendix Figure 31A) as they may represent either balancer defects, or the phenotype observed when two arms of the laminin

molecule are reduced in expression. Since laminin is such a fundamental and important component of basement membranes, its partial deficiency would intuitively lead to severe defects.

It appears that *slit* interacts more strongly with the lamininB1 deficiency than it does with the *lamA*⁹⁻³² allele. When all three are present in heterozygous copies, the range is not significantly different than that for *slit/Df(2R)XE-2750* transheterozygotes. This indicates that the functional interaction between *slit* and *lamB1*, or other genes uncovered by this deficiency, affects axon guidance to a greater degree than the interaction *slit* and *lamA*. Not included in this screen was a test for determining if a *lamB1/+; lamA/+* heterozygous combination would yield a CNS phenotype, as this would be important to help determine if some of my phenotypes were not a triple heterozygous mutant but actually this double heterozygous combination.

6.43 LamininB2 deficiency strongly enhances the *slit/+; lamA/+* phenotype.

A deficiency uncovering the *lamB2* gene, *Df(3L)AC1*, was also included in this screen. 16.85% (n=357) of embryos from the triple mutant collection display a severe, *slit*-like phenotype with mAb 1D4 (Figure 6.7A), indicative of a strong genetic interaction. Other phenotypes viewed in the 1D4 collection include narrowing of and midline crossing in most segments (21.8%, Appendix Figure 32A) and slight narrowing with occasional midline crossover (9.2%, Appendix Figure 32B). The severe collapse phenotype is also evident in 8.1% (n=86) of embryos stained with mAb BP102 (Figure 6.7D). 11.6% of BP102-labeled embryos show nerve cord narrowing and inconsistent commissure separation (Appendix Figure 32C).

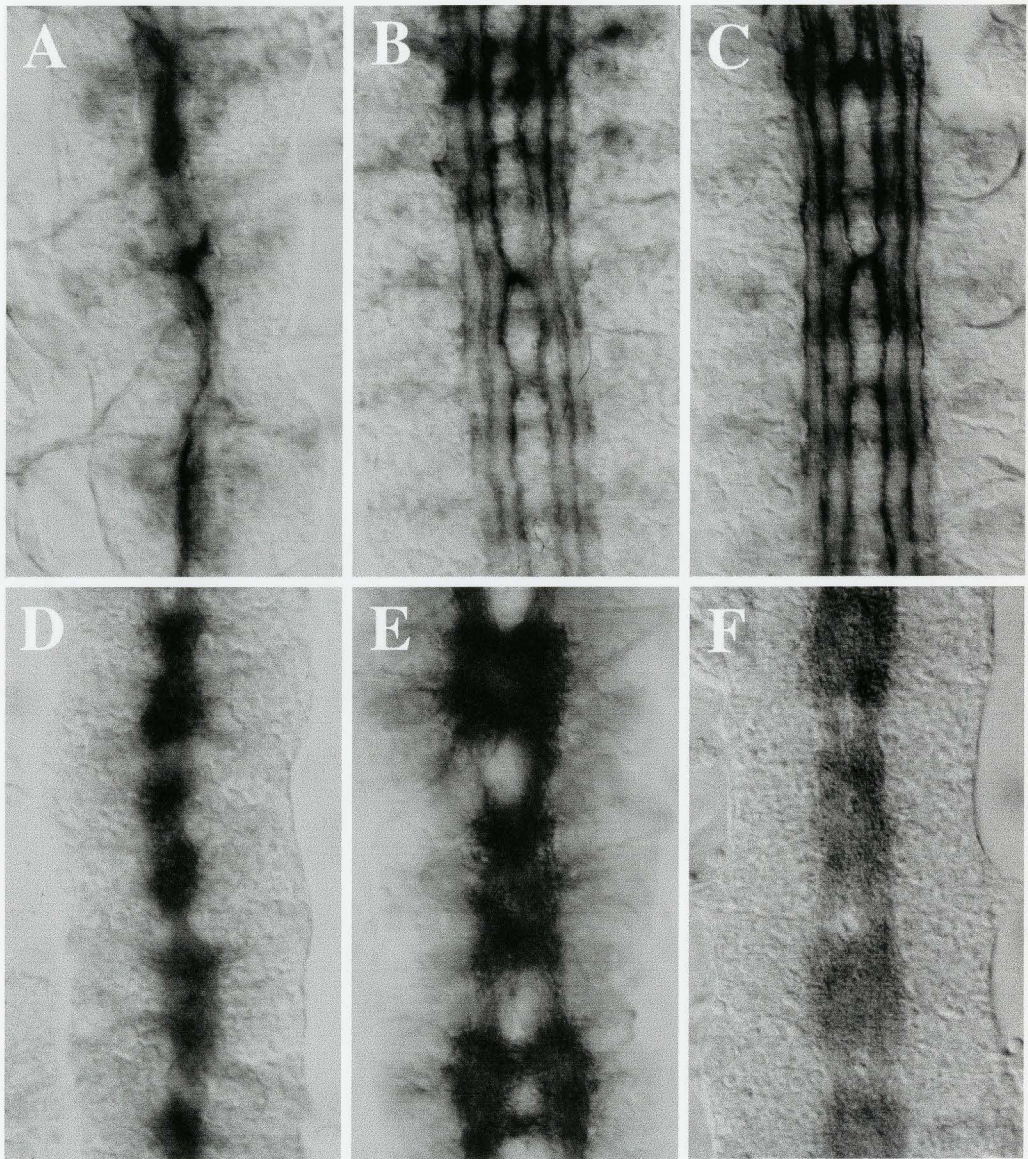
*slit*²/*+*; *Df(2L)AC1/+* double heterozygotes (15.8%, n=183) show occasional midline crossing of the medial fascicle (Figure 6.7B), similar to that observed for *slit*²/*+*; *lamA*⁹⁻³²/*+* heterozygotes (Figure 6.7C). This phenotype was also observed in 9.2% of embryos from the triple mutant collection (Appendix Figure 32B), indicative the *slit*²/*+*;

Figure 6.7 **Immunocytochemical analysis of a triple mutant genetic screen involving *lamininB2* locus, *slit* and *lamininA* genes.**

Nerve cords are immunolabelled with mAb 1D4 (A-C) and mAb BP102 (D-F).

Heterozygous embryos triple mutant for Df(3L)AC1, *slit*² and *lamA*⁹⁻³² demonstrate complete nerve cord fusion at the midline (A) in 16.9% (n=357) of embryos. These embryos (8.8%, n=86) likewise show a phenotype similar to *slit*² mutants with BP102 (D).

Embryos double heterozygous for *slit*²/+; Df(3L)AC1/+ (15.8%, n=183) or *slit*²/+; *lamA*⁹⁻³²/+ demonstrate mild midline crossovers (B, C). Their phenotypes differ when examined with BP102 as *slit*²/+; Df(3L)AC1/+ display a range in segmental collapse among segments (E) in 9.6% (n=177), but *slit*²/+; *lamA*⁹⁻³²/+ embryos display a consistent degree of narrowing along the length of the nerve cord (F).



Df(3L)AC1/+ genotype is present. With BP102, segments are narrowed toward the midline and longitudinals are thinned in 9.6% (n=177) of embryos, somewhat similar to *slit*²/+; *lamA*⁹⁻³²/+ embryos and also similar to Appendix Figure 32C, which could represent the *slit*²/+; Df(3L)AC1/+ in the triple mutant collection.

These results indicate a strong genetic interaction in the triple mutant. It is not known what phenotype is produced from *lamA*/Df(3L)AC1 transheterozygotes, and this is important for final assessment of this genetic interaction.

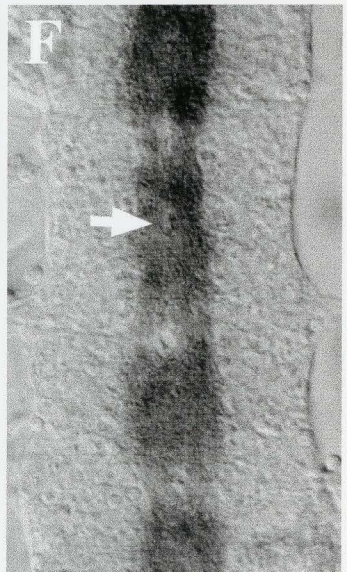
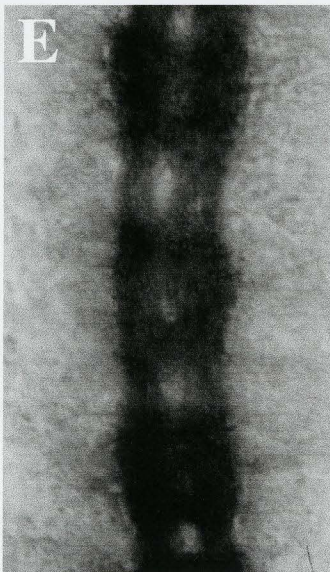
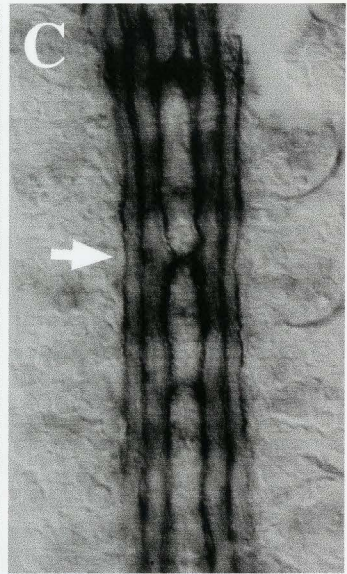
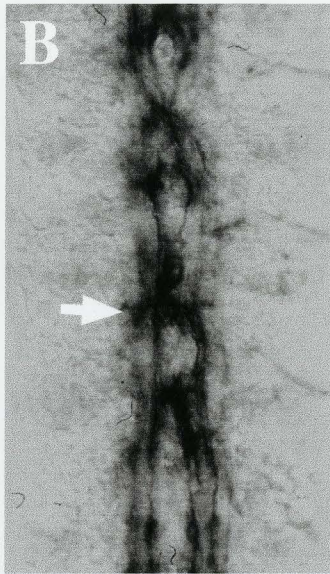
6.44 *scb* interacts to enhance *slit*/+; *lamA*/+ phenotype

scb was another candidate for interaction with *slit* and *lamA* based on the *scb*/*slit* interaction and a putative role of LamininA binding to Scab as a ligand during dorsal vessel formation (Stark et al. 1997).

11.4% (n=525) of embryos from the triple mutant collection show a severely collapsed *slit*-like phenotype (Figure 6.8A) with mAb 1D4. Other embryos observed in the 1D4 collection include *slit*/*scb* transheterozygote (9.5%) shown in Figure 6.8B, *slit*²/+; *lamA*⁹⁻³²/+ double heterozygotes (11.4%) shown in Figure 6.8C and 4.6% with the phenotype observed in other collections consisting of clumps of axons within segments and lack of longitudinal connections between segments (data not shown, similar to Appendix Figure 31A). The severe *slit*-like collapsed phenotype was also observed in 7.3% (n=315) of BP102-stained embryos (Figure 6.8D). 5.1% of BP102-stained mutants had 1-2 segments with midline narrowing (data not shown) and 7.6% of embryos exhibited narrowed nerve cord and thinned longitudinals (data not shown) similar to *slit*²/+; *lamA*⁹⁻³²/+ mutants shown in Figure 6.8F. Another 6.6% also show segments with grouping of axons and lacking intersegmental connections like those observed in Appendix Figure 31E.

Figure 6.8 **Immunocytochemical analysis of a triple mutant genetic screen involving *scab*, *slit* and *lamininA* genes.**

Nerve cords are immunolabelled with mAb 1D4 (A-C) and BP102 (D-F). Heterozygous nerve cords triple mutant for *scb*², *slit*² and *lamA*⁹⁻³² demonstrate a severe collapse of longitudinal fascicles toward the midline (A) in 11.4% (n=525) of embryos. Likewise, no commissures are distinguishable at the midline collapse (7.3%, n=315; D). Embryos transheterozygous for *slit*²/*scb*² demonstrate aberrant segmental crossovers across the midline (arrow, B) and some collapsed segments without distinct commissures (arrow, E). Embryos double heterozygous for *slit*²/+; *lamA*⁹⁻³²/+ display mild midline crossovers (arrow, C) and narrowing of and poorly defined commissures (arrow, F).



Based on these phenotypes it is highly likely a *slit/scb; lamA⁹⁻³²/+* triple heterozygote represents a strong genetic interaction. It is not known what a *scb/+; lamA/+* double heterozygote looks like and would need to be completed for final analysis.

6.45 Netrin interacts genetically in a triple mutant combination

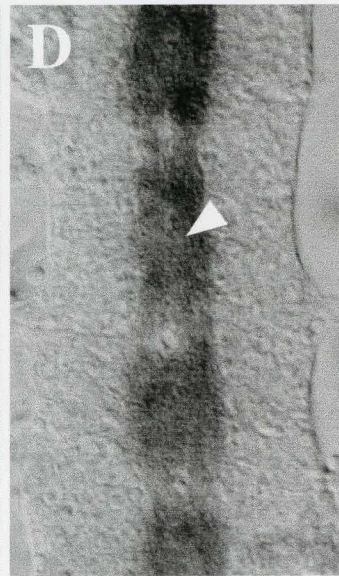
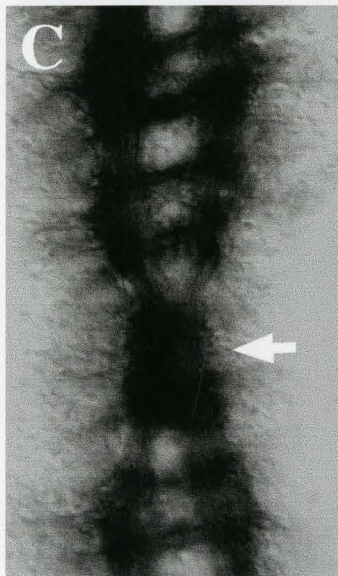
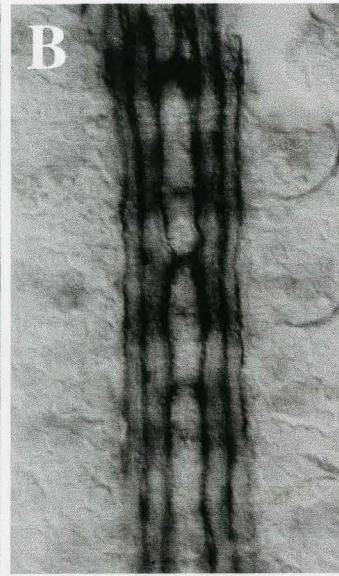
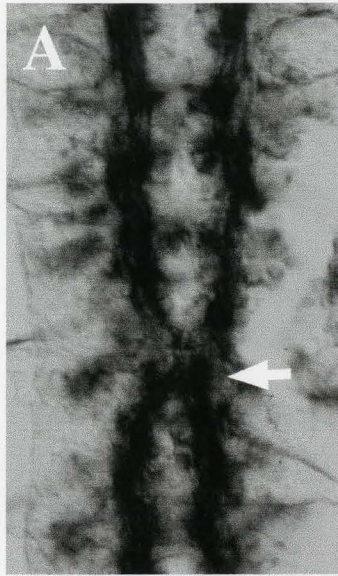
Netrin1 was shown to bind hSlit2 in cell culture (Brose et al. 1999) and to function antagonistically in growth cone guidance to laminin1 (Hopker et al. 1999). These findings led me to investigate whether *netrin* (Df(1)NP5) would interact genetically with *slit/+; lamA/+*.

2.3% (n=171) of embryos in the triple mutant collection display the 1D4-labeled phenotype depicted in Figure 6.9A. These embryos display a *netrin*-like defasciculation of fascicles but exhibit one segmental crossover at the midline. 5.8% of 1D4-labeled embryos exhibit mild midline crossovers like that observed for *slit²/+; lamA/+* heterozygotes (refer to Figure 6.9B). Another 1.8% of embryos display a narrowed nerve cord with segmental crossovers (Appendix Figure 33A) and 2.3% exhibit several midline crossovers (Appendix Figure 33B), although both these phenotypes may be of the same genotype. These latter two phenotypes are very similar to those observed in the *netrin; slit²* double mutant lines (see Appendix Figure 15). Thus, these phenotypes are likely representative of NP5/+; *slit²/+* double heterozygote.

The crossover phenotype observed in Figure 6.9A is mirrored in 6.25% (n=208) of BP102 mutants but the commissural *netrin* phenotype is not present. As a result, Figure 6.9A and C are likely representative of a NP5/+; *slit²/+; lamA⁹⁻³²/+* triple heterozygote or NP5/+; +; *lamA⁹⁻³²/+* double heterozygote. A test for genetic interaction between Df(1)NP5 and *lamA⁹⁻³²* would need to be done to confirm results. The *netrin* phenotype is observed in 19% of embryos labeled with 1D4 and in 16.3% of the BP102 embryo

Figure 6.9 **Immunocytochemical analysis of a triple mutant genetic screen involving *netrin* locus, *slit* and *lamininA* genes.**

Nerve cords are immunolabelled with mAb 1D4 (A, B) and BP102 (C, D). Heterozygous embryos triple mutant for Df(1)NP5, *slit*² and *lamA*⁹⁻³² demonstrate occasional crossing of axons at the midline in 2.3% (n=171) of embryos (arrow, A). Likewise, this crossing mirrors a segmental collapse at the midline when observed with BP102 (arrow, C) in 6.25% (n=208) of embryos. Embryos double heterozygous for *slit*^{2/+}; *lamA*^{9-32/+} display mild midline crossovers (arrow, B) and narrowing of (arrows, D) and poorly defined commissures (arrowhead, D).



collection. I suspect the NP5/Y; *slit*²/+; *lamA*⁹⁻³²/+ genotype is represented in this group of embryos.

CHAPTER 7 DISCUSSION

7.1 GENETIC SCREENS – CRITICAL ASSESSMENT OF RESULTS FROM DIFFERENT SCREENS AND EXPERIMENTAL STRATEGY

7.01 Genetic screens in flies demonstrate potential for genetic interactions to predict functional relevancy.

Genetic screens are useful for identifying other genes that interact functionally with a gene of interest. Most genetic screens in flies attempt to identify second-site modifiers of the mutant phenotype of the gene of interest.

Simon et al. (1991) used a *sevenless* (*sev*) allele where signaling was reduced, but not abolished in such a modifier screen. They tested for other mutations that would either enhance (abolish signaling) or suppress (restore signaling) the *sev* mutant phenotype. Therrien et al. (1995) ectopically expressed activated Ras1, which produces a rough eye phenotype. This allowed them to screen for mutations that either enhanced (again, increased the phenotype) or suppressed (reduced) eye roughness. McCartney et al. (2000) demonstrated mutual enhancement with reduction of gene copies of *Merlin* (*Mer*) and *expanded* (*ex*): heterozygous copy of *ex* enhanced the hemizygous *Mer* rough eyes and wing phenotype, while a heterozygous copy of *Mer* likewise enhanced the *ex* wing phenotype. Strutt et al. (1995) demonstrated dominant suppression of cyclic AMP-dependent protein kinase A (pKa-C1) on weak *hedgehog* phenotype in eye development and proposed pKa-C1 acts downstream or in a parallel pathway. Kennison and Tamkun (1988) conducted an EMS mutagenesis in the background of mutant *Polycomb* and *Antennapedia* alleles to test for enhancement or suppression in search for other homeotic loci. Boube et al. (1997) also conducted a screen for homeotic genes, this time using flies expressing a transgene for the *proboscipedia* gene and mating them to flies with deficiencies to uncover loci that would dominantly reduce transgene function, that is,

transformation of antennae to maxillary palps. Walsh and Brown (1998) also tested for dominant genetic interactions of new loci (X-ray-induced mutations) that are able to enhance the hemizygous phenotypes of the integrins *mew*, *if* and *mys* wing blister phenotypes.

In each of these cases, different strategies were employed to test for second-site mutations that affected the phenotype of the primary site mutation. In this study, I used three different strategies to test for suppressors and/or enhancers of the *slit* phenotype in attempts to reveal other genes that may functionally interact with it. First, I attempted to score for changes in the CNS phenotype using a blind approach to mask the identity of the genotypes. I did this in two ways: first, I eliminated the use of lacZ expression that would identify the presence of balancer chromosomes within some of the embryonic collections; secondly, I allowed another person to mask the identity of each individual collection as to not bias my results. The second strategy used was in establishing stable, balanced fly lines that contained mutations for either of *slit*²⁹⁹⁰ or *slit*² allele and a mutation in a candidate interacting gene. These lines were housed for embryo collections and results were to be compared with blind test results, where possible. Finally, a third strategy was employed to screen for tertiary site mutations that would affect a sensitised background. In this strategy, the double mutant *slit*²; *lama*⁹⁻³² fly line was tested in triple heterozygous condition with another fly line (either mutation or deficiency) to uncover enhancers of the weak *slit*²/+; *lama*⁹⁻³²/+ CNS phenotype.

7.02 Blind test strategy may provide false results in uncovering genetic interactions.

In comparing results from the blind test and the double mutant lines, phenotypes were found to be similar. NP5/+; *slit*²⁹⁹⁰/+ and KA9/+; *slit*²⁹⁹⁰/+ blind test embryos in Figure 4.2F and G, respectively, were similar to KA9/FM7cβ; *slit*²⁹⁹⁰/CyO[*eng*] stable line embryos in Figure 5.2E. KA9/+; *slit*²⁹⁹⁰/+ blind test embryos were also similar in phenotype to that observed in KA9/FM7cβ; *slit*²/CyO[*eng*] stable line embryos in Figure

5.2C. Crossovers were also similar in embryos from the *slit*²⁹⁹⁰/*tig*^x blind test and recombinant lines. With *if*^{k27e}/Y; *slit*²⁹⁹⁰/+ and *if*^{k27e}/Y; *slit*²⁹⁹⁰/CyO[*eng*] mutants, I observed *slit*²⁹⁹⁰-like phenotypes in the blind test and stable line screens. Although I originally described the blind test embryos to be either *if*^{k27e}/Y; *slit*²⁹⁹⁰ or *if*^{k27e}/+; *slit*²⁹⁹⁰, I approximate their genotype to be *if*^{k27e}/Y; *slit*²⁹⁹⁰/+ based on double mutant analysis. With *slit*²⁹⁹⁰/*scb*² transheterozygotes, we can see midline crossing/fusion as also observed, albeit, worse in *slit*²/*scb*² transheterozygotes. *mew*^{M6}/Y; *slit*²⁹⁹⁰/+ and *mew*^{M6}/Y; *slit*²⁹⁹⁰/CyO[*eng*] embryos exhibited variable but similar phenotypes between the blind test and stable lines, although the loss of the longitudinal tracts was not observed in the stable line collection. Although I originally scored these blind test embryos as either *mew*^{M6}/+; *slit*²⁹⁹⁰/+ or *mew*^{M6}/Y; *slit*²⁹⁹⁰/+, I conclude their phenotype to be *mew*^{M6}/Y; *slit*²⁹⁹⁰/+ based on double mutant analysis. In the *slit*²⁹⁹⁰/*dock*^{P1} genetic interaction, crossovers are apparent in both the blind test and recombinant line but crossover phenotype varied between the two. In the transheterozygote, midline crossing is only observed with the inner fascicle, whereas the recombinant demonstrates crossing of both the inner and middle fascicle in some segments and only the inner fascicle in others. This is likely due to recombination effects, as a larger portion of the chromosome than just the *dock* or the *slit* locus was likely recombined and thus may, although weakly, have affected the phenotype observed. *slit*²⁹⁹⁰/+; *Tl*^{R3} and *slit*²⁹⁹⁰/CyO; *Tl*^{R3} mutants revealed *slit*²⁹⁹⁰ mutant phenotype in both screens. Although I originally scored this genotype as either *slit*²⁹⁹⁰; *Tl*^{R3} or *slit*²⁹⁹⁰; *Tl*^{R3}/+ in the blind test, I can conclude this genotype to be *slit*²⁹⁹⁰/+; *Tl*^{R3} based on double mutant analysis.

However, there is also evidence that this blind test strategy provides false results in predicting genetic interactions. *slit*²⁹⁹⁰/+; *comm*^{a490}/+ blind test embryos were similar to one phenotype observed for the stable line embryos (Appendix Figure 16B) although longitudinals are not as disorganised as was seen in the blind test embryos. However,

these embryos from the double mutant line were also thought to represent the *slit*²⁹⁹⁰/CyO; *comm*^{a490}/TM3 genotype. No embryos in the blind test were found to exhibit the double mutant phenotype observed in the stable line collection. *slit*²⁹⁹⁰; *lamA*⁹⁻³² mutant embryos exhibit a *slit*²-like collapse of axon tracts at the midline in stable line collections that is not observed in the blind test collection, although a midline fusion is observed in some segments of these embryos. These blind test embryos do resemble the *slit*²⁹⁹⁰/CyO; *lamA*⁹⁻³²/TM3 embryos and I therefore conclude this is the genotype of the blind test embryos as well. In *slit*²⁹⁹⁰; *mas*^{x124} blind test mutants (either *slit*²⁹⁹⁰; *mas*^{x124} or *slit*²⁹⁹⁰; *mas*^{x124}/+ genotypes), a *slit*²-like phenotype is observed (Figure 4.2R) which is not observed in the stable line collection (Figure 5.7C, Appendix Figure 20). I cannot account for this difference, especially since my stable line embryo collection was examined at a large sample size (n=632). Especially surprising were the results from the *cbd*¹; *slit*²⁹⁹⁰ interaction. Blind test embryos depict a midline crossover phenotype in this collection that is not observed in the stable line collection. This may have to do with the problems previously mentioned with the *cbd* gene, with my inability to detect whether the mutation is still in the stock, as it is homozygous viable and other cis chromosome markers are absent. If the mutation was present in the stock, then either it was “lost” from the stock prior to generation of the stable double mutant line or did not yield a viable line in combination with *slit* if they interacted strongly. In the latter case, this would have allowed flies not carrying *cbd* to become prevalent in the fly population, effectively selecting against flies carrying both *cbd* and *slit* over several generations. Different results were obtained from the blind test and stable line collections when examining a *slit*²⁹⁹⁰ and *nrx*⁴³⁰⁴ interaction. Although few embryos were obtained in the stable line collections, midline crossovers were apparent in several cases, while blind test embryos saw no phenotypes different from *slit* or *nrx* in the collection.

The phenotypic differences observed between these tests likely lies in background differences in genotype. The double mutant lines contained balancer chromosomes that were eliminated in most of the blind test crosses. The presence of balancers very likely account for the differences in variation between these tests. This is readily observed when comparing the *cbd¹; slit²⁹⁹⁰* blind test to the double mutant, as the FM7 balancer was present in the blind test (where crossovers were observed) and absent in the double mutant (where no midline crossovers were scored). Even though I stained control lines for balancer defects and observed only wildtype phenotypes (Appendix Figure 13), this does not discount the possibility that balancers could act to modify phenotypes.

7.03 Critical assessment of experimental strategy: modifications for future use.

Although I found the blind strategy helpful and a first step indicator for genetic interactions, I would argue against its use in accurately predicting in vivo effects of genetic interactions. It would have been better to attempt the screen in the following manner.

X chromosome mutations. First, I would have conducted this blind test initially the same way as I did, except that I would have stained embryos for β -gal expression on the FM7 balancer chromosome to help identify part of the collection. Secondly, after initial crossing of mutant lines to each other to create F1 double heterozygous flies for blind test, these flies should have been crossed back to *slit* mutant stock so these embryos could likewise be stained for LacZ expression on the CyO balancer chromosome. After analysing these collections, I could then compare phenotypes because both collections would theoretically yield the same phenotypes as genotypes differ only in the presence of different balancer chromosomes. These balancer chromosomes, based on my analysis, would have a negligible effect on phenotype. Finally, I would also conduct a quick cross mating to assess whether X chromosome and *slit* mutant genes in a double heterozygous copy alone would produce a phenotype and compare this phenotype to phenotypes observed in the above collections (as this genotype would also be present in them).

2nd chromosome mutations. Not much can be altered when examining F1 embryos from a quick cross mating. To do again, however, I would stain for marked balancer chromosomes to verify that the phenotypes observed are from a transheterozygote and not a heterozygote for either mutation, although I am confident that my observed results are from a transheterozygous combination of genes. I could also attempt to assess modifier effects by crossing the recombinants I generated (*tig*, *dock* and *robo*) back to original stock lines. My approach for *scb* is still limited to transheterozygotes and deficiency crosses, as was done.

3rd chromosome mutations. After initial crossing of mutant lines to each other to create F₁ double heterozygous flies, these flies should have been crossed back to both original mutant lines (thus yielding two separate collections) to test for modification (enhancement or suppression) of one gene (heterozygous) on the other homozygous mutant gene's phenotype. This would have been ideal for two reasons. First, it would allow balancer staining for one chromosome (different for each collection), thus enabling to separate part of the collection. Of this collection, theoretically half of embryos should be expressing β -galactosidase activity. Of this half, a quarter should be of the genotype *slit/+; mas/TM3 β* (which may or may not yield a phenotype) and the remainder would be wild type in phenotype. Of the unbalanced collection, a quarter should be *slit/+; mas/+* (which could be compared to both the *slit/+; mas/TM3 β* for phenotype or balancer defects and also to a one-time mating of *slit* mutant stock to the *mas* mutant stock), a quarter would be of the *mas* phenotype (*+/+; mas/mas*), a quarter would be wild type (*+/+; mas/+*) and a quarter would be *slit/+; mas/mas* to test for modifier effects of a 2-fold reduction of *slit* with no *mas* activity. This would have also increased my chances of obtaining a predictable genetic interaction from 1/16 (blind test) to 1/8 (new strategy). These results could then be compared to the results obtained from crossing the stable double mutant line back to each

original stock to assess for modifier effects. You could then also use the stable double mutant line to compare these results as well as to predict the effect of a homozygous double mutant. This strategy would then effectively determine if frequencies of genotypes were altered as I observed when assessing double mutant lines. This would help me predict contributions of gene function in absence of reliable numbers. Finally, I would also do a quick cross described for the X chromosome mutations, whereby I collect double heterozygous embryos mutant for *slit* and a 3rd chromosome gene and compare the phenotype to the above collections.

The use of stable double mutant lines is the most effective predictor of gene interactions. Since you already have a stock of flies available, it is also easier for doing counts and multiple collections for stains, and you also have the flexibility of doing various genetic manipulations to assess for dosage-sensitive interactions. The downfall of this method is the length of time and amount of crosses required to establish the double mutant lines, especially if in the end these lines are not useful for further experimentation.

7.2 Slit alleles show similar functional interaction with Robo

I fully examined the *slit/robo* interaction by assessing the degree of crossover to determine if the alleles would be able to demonstrate functional differences between them in how they interact with *robo1*. I have shown that the alleles do not show significant differences from each other in crossover frequency with *robo1*.

As the LRR regions of Slit have been shown to be required for binding to Robo, it was of interest to determine which *slit* alleles contained genetic lesions within the LRR repeats. Recent molecular characterisation (Battye 2000) has revealed that alleles *slit*^{GA178}, *slit*^{GA945}, *slit*⁵³² and *slit*^{GA20} were found to be mutated within these regions. Closer examination of the crossover data reveals that the most severe crossover frequencies are not shown by all of these alleles. In addition, axon guidance and muscle phenotypes and

viability data correlate well with the LRR mutants occupying the most severe defects (Battye 2000). Thus, the crossover data does not correlate well with these other data. This may indicate that other regions of Slit are required for signaling through Robo1. As well, the choice of allele for examining genetic interactions may not matter if they show similar degrees of defects.

Slit is proposed to interact and function in vivo with other Robos in this system. Robo2 and Robo3 are proposed to be expressed on the middle and lateral fascicles, respectively, and to have greater binding affinities with Slit than Robo1 (B. Dickinson, pers. comm.). This information accounts for the observed crossing of only the medial fascicle as Robo2 and Robo3 are still functioning in the absence of Robo1. A *robo1 robo2 robo3* triple mutant reveals a *slit*² mutant phenotypes in the nervous system (C. Goodman, pers. comm.)

7.3 Slit function repressed by Netrin to allow axons to cross via Comm-mediated Robo down-regulation

A genetic interaction was shown between the *slit* alleles and the *netrin* deficiency in a double heterozygote combination. Although the exact nature of this genetic interaction could not be identified, a *netrin/+; slit/+; lamA/+* triple heterozygote demonstrated a *netrin*-mediated suppression of the *slit/+; lamA/+* double heterozygote phenotype. This data may identify *netrin* as a suppressor of *slit* function as well. However, this suppression may be a weak one, as suppression was not evident in a *netrin; slit* double mutant. This suppression may function directly in vivo, as Netrin was shown to bind hSlit2 in vitro (Brose et al. 1999).

This data also supports evidence showing Netrin and Laminin may have opposing functions within the nervous system, as netrin attraction was converted to repulsion by laminin1 (Hopker et al. 1999). However, a genetic interaction between netrin and lamininA would need to be demonstrated to confirm this. As YIGSR was the amino acid

sequence shown to mediate the change from attraction to repulsion, Netrin may interact more strongly with the *Drosophila* LamininB1 chain, which contains a sequence similar to the YIGSR sequence, a YSGSR sequence (FlyBase). Testing this is difficult, as no mutations within the LamininB1 gene have been uncovered to date.

In contrast to the above, *slit* was shown to suppress the *comm* phenotype. This data is consistent with opposing roles of Comm and Robo in signaling, as Slit and Robo mediate repulsion.

As a result, I can modify the model introduced in Chapter 1. Netrin acts as a global attractant to attract commissural axons toward the midline. Netrin, expressed by the MG, could act locally to suppress Slit function (also expressed by the MG) to enable Comm to mediate Robo internalisation into the growth cone. The mechanism of transfer or function of Comm to internalise Robo is not known. Slit is also transferred to the growth cones. Once growth cones reach the contralateral side, Slit is no longer suppressed and Robo protein is upregulated on the growth cone surface.

7.4 Dock may function as an intermediate player in growth cone signaling

Slit and Dock also demonstrate a genetic interaction in midline guidance, indicating these proteins may be involved in similar pathways. This interaction, however, is different than that shown for Robo and Dock, as they do not show a midline crossover phenotype. Interpretation is difficult because it appears that although Slit and Robo function in the same pathway, they differ in their genetic interactions with Dock.

Dock has been shown to be involved in growth cone guidance. *dock* mutants in the eye show abnormal fasciculation and projection errors of axons in eye development (Garrity et al. 1996). Specifically, the R1-R6 axons project beyond their normal target, the lamina, and extend into the medulla. This provides evidence that Dock functions in proper targeting. Dock has been shown to bind to Pak, a regulator of actin cytoskeleton formation, via its SH3 domain to the PXXP motif of Pak (Hing et al. 1999). *dock* and *pak*

mutants show the same eye phenotype and likely function in a positive manner. However, Dock has also shown to bind to Misshapen (Msn), a protein that prematurely stops axon growth by signaling to the cytoskeleton when overexpressed (Ruan et al. 1999). The model put forth involves negative regulation of Msn by Dock by preventing Msn from interacting with its substrate, thus enabling axon outgrowth. The SH2 domain of Dock (Ruan et al. 1999) mediates this negative regulation. However, Dock-mediated stop signals are responsible for activating, positioning and releasing Msn to interact with its substrate to activate termination of axon extension (Hing et al. 1999). For this function, Dock binds via its SH3 domain to the PXXP domain of Msn (Ruan et al. 1999). This implies Dock can work as a switch to sequester Msn and activate Pak for axon outgrowth as well as direct Msn function to stop growth cone motility, as it responds to upstream signals.

As a result, Dock may similarly function as a switch in growth cone signaling in the CNS. Exactly how this function is mediated, is not known, or which of the above players are also involved in axon guidance in the CNS. The *in vitro* binding experiments demonstrated between Robo and Dock in *C. elegans* has not been demonstrated with fly or vertebrate forms (Y. Rao, pers. comm.). This does not eliminate the possibility that Dock functions downstream of Robo or converges with a pathway that originates from Robo activation.

However, other work with Dock, or its mammalian homolog Nck, may indicate other instances when it functions downstream of axon guidance. SH2 domains of Dock and Nck were shown to bind to activated Ephrin receptor tyrosine kinases (RTKs; Stein et al. 1998). Likewise, Dock was shown to bind via its SH3 domain to the PXXP domains of the protein tyrosine phosphatase (PTP) 61F (Clemens et al. 1996). Likewise, Nck was shown to interact with proteins involved in the Rho-family GTPase signaling pathways (Quilliam et al. 1996) which are involved in regulating the organisation of the actin

cytoskeleton (Hall 1998). Thus, it is easy to understand that Dock is involved as an intermediate player in axon motility although its role in the Slit repulsion pathway is not known.

7.5 Slit interacts genetically with Integrins

Integrins are classically known as transmembrane receptors involved mostly in cell-matrix, but also some cell-cell events. The possibility of integrins contributing to axon guidance has only been investigated recently (Hoang and Chiba 1998). Here I have demonstrated that Slit interacts genetically with integrins, some more strongly than others.

Of the integrin subunits examined, the α -PS3 and β -PS integrin genes demonstrated the most severe interactions with *slit* and are considered the most important for functioning with Slit. *slit* enhances the *scb* phenotype, while *mys* enhances the *slit* phenotype. It may be possible Slit functions upstream of these integrins or may directly bind them, but further work would need to determine this.

When examining the *scb/slit*; *lamA* +/- triple mutant, a severe *slit*-like phenotype is observed at the midline of the CNS. These results are especially intriguing as Scab is proposed to be a receptor for laminin (Stark et al. 1997) and all three proteins may function as a complex. This, however, cannot exclude the function of the β -PS integrin, which also likely plays a role here. All four are also expressed in the heart and studies examining a putative function there would be interesting.

Although *if* and *mew* demonstrated a mild CNS phenotype when combined with reduced *slit* function, it is likely they do not contribute significantly to Slit-mediated axon guidance, although they are expressed in cells at or near the ventral midline (Hoang and Chiba 1998). Further experiments are required for determining their role in axon guidance.

7.6 Slit, Comm, Robo/Integrins/Dock pathways may intersect downstream

Integrins signal downstream to different factors, resulting in changes in cell shape, motility, cell cycle progression, differentiation and survival. Integrins can also associate

with other membrane proteins to form multireceptor complexes that recruit signaling molecules to the sites of cell-cell or cell-matrix adhesion (Porter and Hogg 1998). Below, I will provide a brief outline of the signaling pathways that integrins are involved in and how Dock and Robo pathways may intersect with intracellular signals.

Integrins can activate various protein tyrosine kinases, such as focal adhesion kinase (FAK), Src-family kinases, Abelson kinase (Abl) and integrin-linked kinase (ILK). Mammalian FAK is activated by most integrins and specifically interacts with the cytoplasmic tail of β -integrins (Giancotti and Ruoslahti 1999). This tyrosine kinase is enhanced by cellular binding to ECM proteins (Schlaepfer and Hunter 1998). DFak56, a *Drosophila* FAK ortholog, was recently cloned in and is expressed in the nervous system from stages 13 to 15 (Fox et al. 1999). Once activated, FAK autophosphorylates, creating a binding site for Src or Fyn to bind via an SH2 domain (Giancotti and Ruoslahti 1999). Src kinase then phosphorylates other cytoplasmic proteins, such as talin and paxillin and p130^{CAS} (Giancotti and Ruoslahti 1999). Talin and paxillin are cytoskeletal proteins that may have signaling potential on their own (Giancotti and Ruoslahti 1999), although paxillin can bind to β -integrins independent of, but to the same site as, FAK (Schaller et al. 1995). p130^{CAS} is a docking protein that recruits the adapter protein Nck (Schlaepfer et al. 1997), thus making a putative connection between Dock (Nck homolog) and the integrin pathway. Both Crk and Nck adapter proteins have been shown to bind to the Son of sevenless (Sos) GDP-GTP exchange factor, which then activates the Ras and ERK mitogen-activated protein kinase (MAPK) pathway (Schlaepfer and Hunter 1998).

In *Drosophila*, a recent study demonstrates a putative link between Calmodulin and Sos function downstream of the Robo pathway (Fritz and VanBerkum 2000). Calmodulin signaling was previously described to be required for axon guidance (VanBerkum and Goodman 1995). While Src is phosphorylating the cytoskeletal components, it is also phosphorylating FAK to create a binding site for Grb2 adapter protein (Giancotti and

Ruoslahti 1999). Grb2 recruits the Sos GDP-GTP exchange factor, which then leads to enhanced GTP exchange on Ras by Sos (Schlaepfer and Hunter 1998). The activation of Ras and the ERK/MAPK pathway is thought to be involved in activating cell proliferation (Hynes 1999), but ERK has also been shown to phosphorylate myosin light chain kinase in fibroblasts (MLCK), which would then influence motility (Schlaepfer and Hunter 1998). MLCK has been shown to be present in neurons of goldfish (Jian et al. 1996), bullfrog (Tokimasa 1995) and cattle (Shimada et al. 1995) and potentially *Drosophila* (Nagano et al. 1998). Experiments have been conducted to test the role of *Drosophila* MLCK in neuronal apoptosis (Nagano et al. 1998), indicating a *Drosophila* MLCK also functions in neurons.

As previously mentioned, integrins also associate with other cis membrane receptors. Activated integrins have been shown to induce autophosphorylation of the EGF receptor by the β -subunit (Moro et al. 1998). This requires activation of receptor kinase activity and prevents the cell from entering apoptosis by triggering activation of the MAPK pathway (Moro et al. 1998). Integrins have also been shown to associate with four-pass transmembrane proteins, known as tetraspanins. These tetraspanins have been shown to link integrins to phosphatidylinositol signaling pathways and thus play a key role in cell motility (Berdichevski et al. 1997). One tetraspanin in *Drosophila*, Late bloomer (Lbm), has been proposed to facilitate integrin-mediated adhesion of FAK and recruit Dock to FAK for signaling (Desai et al. 1999).

Integrins can be present in different affinity states, both in the same and different cell types (Keely et al. 1998). Conformational changes affecting the affinity of an integrin for its ligand are a result of the activity of intracellular proteins that interact with the cytoplasmic region of the integrins (Keely et al. 1998), although the signaling pathways that function here are poorly understood (Hughes and Pfaff 1998). This process is known as "inside-out" signaling. There are a number of proteins that are proposed to be involved in this aspect of integrin function and include: protein kinase C, other protein kinases and

phosphatases, Ras family of GTP-binding proteins and their effectors, ILK, and Rho (Hughes and Pfaff 1998). Thus, an interplay of molecules must involve both activation and modulation of integrin activity.

Slit, Robo and Comm have been shown to interact genetically with a receptor protein tyrosine phosphatase, DPTP10D. This RPTP is expressed only on CNS axons and is shown to also to positively transduce the Robo repulsion activity (Sun et al. 2000). This may provide evidence for the linking of the Robo pathway with other signaling pathway, as RPTPs have been shown to activate Src family kinases and control the integrin-mediated response (Su et al. 1999).

Brief representations of pathways are outlined in Figure 7.1 and Figure 7.2. The objective of introducing these pathways was to provide a model by which further experiments could test possible actions of pathways, and hopefully uncover the transduction cascades involved.

7.7 Slit and Wrapper function in parallel pathways

Wrapper is a transmembrane protein required for glial enwrapping of commissures. *wrapper* mutants develop like wildtype embryos until stage 16, when the MG die and commissures are not properly separated (Noordermeer et al. 1998). *slit* mutants affect the position of MG, but not their differentiation or survival (Sonnenfeld and Jacobs 1994). I observed some *slit*²/*Df*(2R)X58-3 transheterozygous embryos with a partially collapsed nerve cord, while others appear fully collapsed at the midline like *slit*² mutants. It is likely these phenotypes reflect a reduction of *slit* and *wrapper* function in parallel pathways. Although not examined, MG position is likely altered in these transheterozygotes, which would account for the axon tract phenotypes observed.

7.8 Neurexin may indirectly signal to a common Slit-binding RPTP on neurons

Neurexin IV (Nrx IV) is a transmembrane protein localised to septate junctions in epithelial cells that are required to function as barriers. Nrx IV is also expressed by the

Figure 7.1 Selective model of axon guidance involving Slit/Robo, Integrin and Dock signaling pathways that may influence actin cytoskeleton remodeling in axon guidance.

This schematic depicts possible intersection of known pathways working in growth cones. Shown is a selective representation of signaling pathways that may induce actin remodeling in the growth cone. Other intersecting pathways are mentioned in the text. At the centre is activation of integrin proteins by potential ligands Laminin and Slit. Integrins can also be activated by cis membrane proteins, such as tetraspanins. Activated integrins have been shown to signal to a number of different downstream effectors (see text; Giancotti and Ruoslahti 1999), such as FAK and Src, shown here. Phosphorylation of FAK then creates a binding site for Src. Src can then phosphorylate p130^{CAS}, a docking protein that recruits adapter proteins such as Nck, the Dock mammalian homolog. Nck/Dock can in turn interact with Rho-family GTPases, which influence growth cone motility. Rac1 and Cdc42 have been shown to interact with Pak, downstream of which results in growth cone outgrowth. Alternatively, activation of RhoA results in growth cone retraction. Dock has also shown to interact with Misshapen (Msn), which results in cessation of growth cone motility. Activation of Robo signaling by Slit may involve activation of receptor tyrosine phosphatases (RPTPs). RPTPs have been shown to signal downstream to FAK, which may intersect with integrin signaling. Activation of receptor tyrosine kinases (RTKs), a group of proteins that include growth factors, have been shown to signal downstream to Son of sevenless (Sos), resulting in activation of Ras and the ERK/MAPK pathway. In other systems, ERK/MAPK activation then signals through myosin light chain kinase which then influences cell motility. Here, ERK/MAPK is proposed to influence actin remodeling as well, but the downstream effector is not yet known (represented by '?'). As shown, Sos is not only influenced by RTKs but is also activated by Src via Grb2 adapter protein.

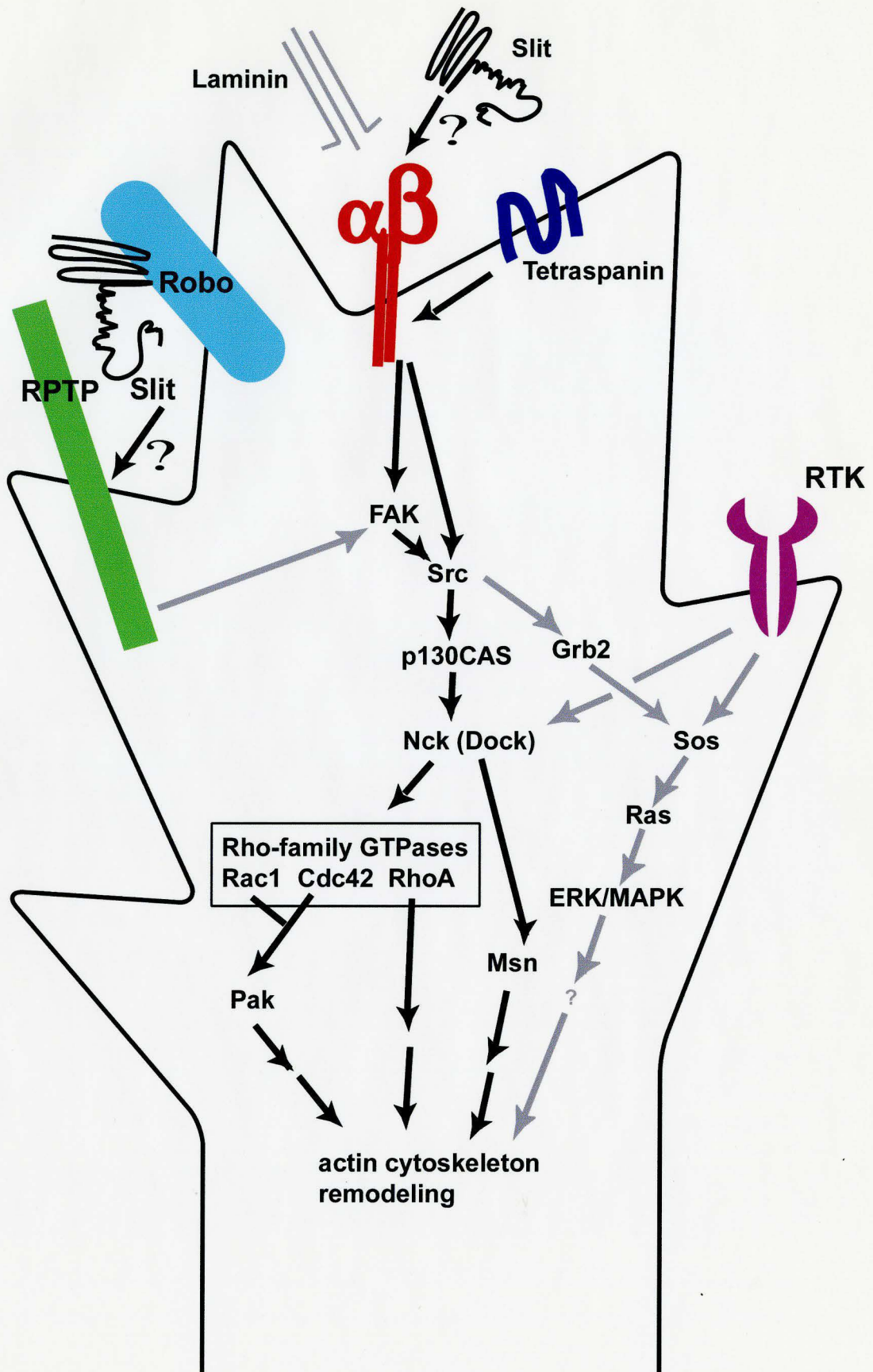
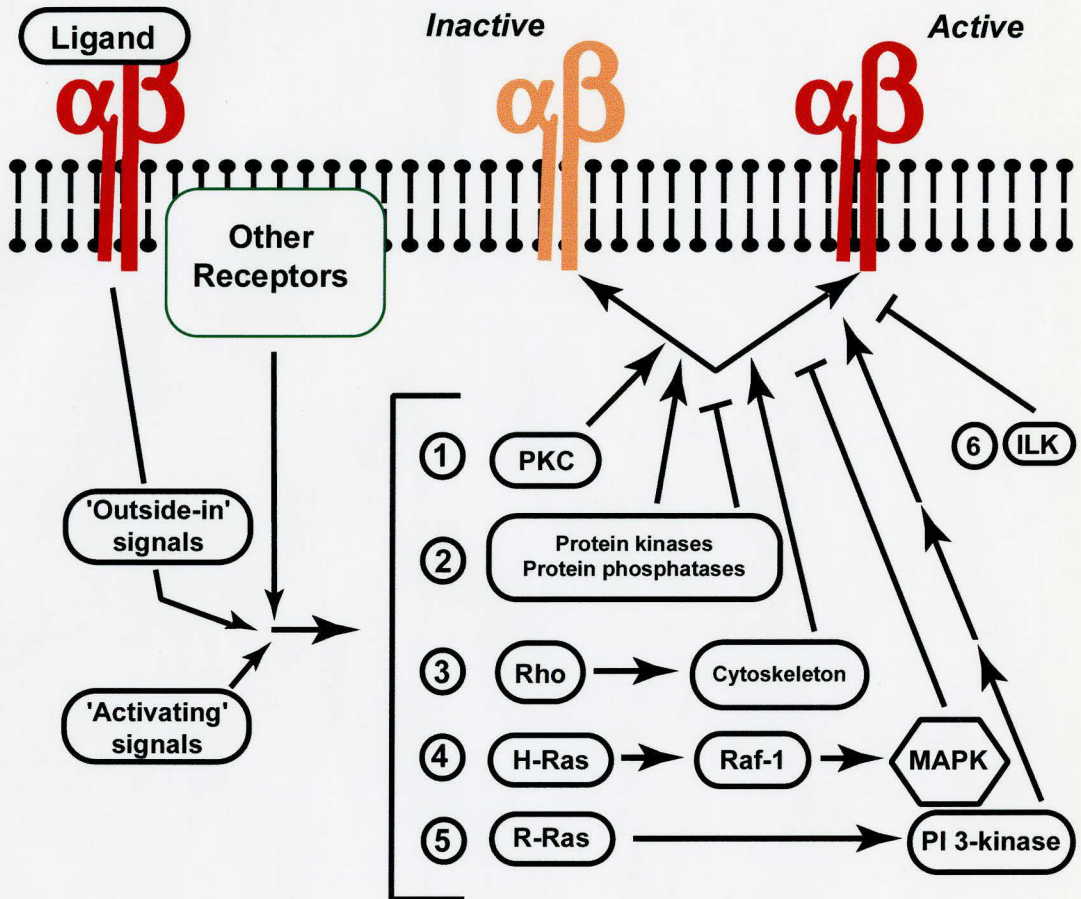


Figure 7.2 Integrin ligand affinity is influenced by cytoplasmic factors.

Integrins are activated by ligands and other receptors present on cells. However, their function is regulated by cytoplasmic factors that influence their ability to bind to their ligands. Depicted here are some cytoplasmic factors that modulate integrin affinity.

Protein kinase C (PKC), protein kinases, cytoskeletal components activated via Rho GTPase, PI 3-kinase activated by R-Ras are some of the factors that induce integrins from the inactive to the active state. In opposition to this, protein phosphatases, MAPK activated from H-Ras via Raf-1, and integrin-linked kinase (ILK) modulate integrin affinity from the active to the inactive state. (Adapted from Hughes and Pfaff 1998).



neuromuscular junction formation (Baumgartner et al. 1996). Nr_x IV was originally characterised as a homolog of mammalian Neurexins but is now considered a member of the Caspr family of proteins. Caspr and Nr_x IV proteins contain Laminin-like G domain, EGF-like domain, fibrinogen-like domain and discoidin-like domain motifs, unlike mammalian neurexins that contain only Laminin-like G domain and EGF-like domain motifs (Missler and Sudhof 1998).

nrx mutants demonstrate occasional midline crossing and lateral displacement of the axon tract in at least one segment. This may indicate loss of adhesion between MG. *slit*; *nrx* mutants display midline crossing and enhanced midline fusion with hypomorphic and severe *slit* alleles, respectively. Reductions in function of two parallel pathways could readily explain these data, ie. Nr_x IV is involved in proper glial adhesion and Slit is an axon guidance molecule, but a reduction in these genes could alter the proper function of their pathways and lead to a CNS phenotype.

Alternatively, Nr_x IV and Slit pathways may intersect. Caspr was shown to associate with Contactin, a cell surface protein that binds to receptor protein tyrosine phosphatases (RPTPs) (Peles et al. 1997). This complex is proposed to facilitate neurite outgrowth. As RPTPs have been shown to be expressed on the surface of growth cones and have been shown recently to interact genetically with Slit (Sun et al. 2000), Nr_x IV may interact with RPTPs with an unknown *Drosophila* Contactin homolog. However, unlike Caspr, which contains an SH3-binding domain in its cytoplasmic region, Nr_x IV contains a PDZ-binding domain. This difference may be fundamental to where they are expressed: Caspr is neuronally expressed, making the SH3-binding domain required for signal transduction of RPTP-binding, whereas Nr_x IV is located on glia. Discs Lost was recently characterised to co-localise with Nr_x IV in the CNS and bind to the cytoplasmic domain of Nr_x IV via PDZ domains (Bhat et al. 1999).

7.9 Toll may conserve its PNS repellent function in the CNS

Maternal Toll is a transmembrane protein originally characterised to be involved in dorsal-ventral pattern formation to direct formation of ventral structures (Hashimoto et al. 1991). In its extracellular region, Toll contains two repeats of a leucine-rich sequence and several cystine residues that participate in disulphide bonds (Hashimoto et al. 1991). Due to its motif composition and localisation at sites of cell-cell interaction, Toll was proposed to promote cellular adhesion via heterotypic interactions (Keith and Gay 1990). Examination in later stages of embryogenesis have isolated roles of zygotic Toll in motoneuron guidance and muscle development (Halfon et al. 1995; Rose et al. 1997; Rose and Chiba 1999). 15% of *Toll* (*Tl*) hemisegments show defects in the number and positioning of RP motoneuron cell bodies and their proper innervation pattern (Halfon et al. 1995). Toll is specifically expressed by a subset of muscle precursors and at sites of muscle insertion into the epidermis (Halfon et al. 1995). *Tl* mutants display duplicated, misinserted or aberrant muscle fiber pattern in almost half of hemisegments (Halfon et al. 1995). Toll was then observed to locally inhibit synapse formation of the RP3 motoneuron on muscle cells that specifically express Toll and needs to be downregulated from their proper targets in order for synapses to be formed (Rose et al. 1997; Rose and Chiba 1999). LRR regions are proposed to mediate this interaction, a response also shown for the Connectin protein (Rose and Chiba 1999).

Toll was also localised to the surface of the MG (Halfon et al. 1995). This function of Toll has not yet been investigated. It is possible that Toll may maintain heterotypic adhesion between glia, consistent with the cell adhesion role proposed by Keith and Gay (1990). However, *Tl* mutants do not display glial positioning or other defects (Halfon et al. 1995). Consistent with its repellent role in the PNS, Toll may function as a midline repellent to axons. Rose et al. (1997) propose that Toll-mediated glia-glia adhesion may function to block growth cones from extending through intermuscular space and aberrantly

synapsing in another location. *slit; Tl* mutant embryos display aberrant midline crossing and lack of separation of commissures. Thus, Toll on MG surface may function in the same way as is suggested in the PNS. Rose et al. (1997) also propose that neurons bear Toll receptors that would enable the repellent signal to be transduced within the growth cone. Defects shown here suggest that Toll may function in repellent signaling, but in a pathway independent of Slit signaling.

7.10 Slit and Masquerade have opposing functions in different pathways

Masquerade (Mas) is a secreted extracellular matrix protein localised in the CNS and at muscle insertions sites in *Drosophila*. It is thought Mas is secreted by midline glia and proteolytically cleaved to release the C-terminal portion of the protein to be distributed on the longitudinal connectives. Likewise, Mas is secreted by the epidermis and localised to sites of muscle insertion. It was also determined that the C-terminus contains the functional domain and the N-terminus acts to promote the processing and trafficking of the C-terminal portion (Murugasu-Oei et al. 1995). Both the N- and C-terminal parts contain cystine residues that participate in disulphide bonds. Studies on cystine knots have implicated them in proper secretion of and heterodimer formation between proteins, not for bioactivity (Sato et al. 1997). The C-terminus also contains the region of homology to serine proteases but Mas does not demonstrate in vivo protease activity due to an amino acid substitution of Gly for Ser. Therefore this domain may easily function to antagonise protease activity (Murugasu-Oei et al. 1995). The action of proteases and their inhibitors have been described to function in growth cone motility and neurite outgrowth (Monard 1988).

Consistent with the above information, matrix proteases would not be regulated and act to destabilise growth cone/matrix interactions in *mas* mutants, leading to repulsion or inhibition of neurite outgrowth. When observing *slit; mas* mutants, phenotypes appear to indicate these proteins function in parallel pathways, but in opposing functions, as Mas

would promote neurite outgrowth while Slit mediates repulsion. Midline crossing in these mutants are a result of reduced *slit* function combined with destabilisation of axon/matrix interaction that have led to pathfinding errors. In *slit; mas* homozygotes, nerve cords appear severely kinked, more severe than observed for *slit* mutants alone. As Mas also functions to stabilise muscle attachments (Murugasu-Oei et al. 1995), an additive effect of *slit*- and *mas*-mediated roles in muscle patterning account for this phenotype.

7.11 Toll and Mas may function together in vivo as a parallel pathway to Slit

Keith and Gay (1990) first describe the similarity of Toll to sequences of platelet glycoprotein 1b (Gp1b), a membrane receptor that binds the secreted serine proteinase thrombin. Interaction between Gp1b and thrombin occurs with the LRR and disulphide bond forming sequences of Gp1b (Harmon and Jamieson 1986). Likewise, Toll may act as a membrane receptor like Gp1b and bind serine proteases in *Drosophila*. Two characterised secreted serine proteases Snake and Easter, are suggested to be candidate ligands for Toll (Keith and Gay 1990). However, *snake* and *easter* are dorsal group genes and are not expressed in the CNS (Tearle and Nusslein-Volhard 1987; Chasan and Anderson 1989). Thus, this leaves open the possibility of yet uncharacterised serine proteases present in the CNS that could interaction with Toll. This postulation also involves the activity of serine protease antagonists, like Mas, that would function to balance protease action. Fusion protein experiments have shown Mas to contain identical cysteine sequence positions as active proteases, positioning being crucial to receptor binding (Murugasu-Oei et al. 1995). Thus, Toll and Mas may function to facilitate axonal outgrowth. As both Toll and Mas are present at muscle insertion sites, their function is likely there as well. In conjunction with proposed Toll function on MG, Toll may act to cleave Mas, leaving the N-terminus of Mas to remain bound to Toll, and the C-terminal portion of Mas to bind to growth cones as they navigate by the MG. As mentioned earlier, neurons may present Toll receptors on their growth cones to signal avoidance for synapse

formation. Alternatively, the presentation of Mas and subsequent signaling of Mas to growth cones may fulfill this avoidance function.

7.12 Slit may not interact with Tenascin proteins

Tenascin is a classical extracellular matrix protein known for its function in axon responses. Tenascins were originally classified to be repulsive glycoproteins but have also shown to promote neurite outgrowth (Faissner 1997; Meiners et al. 1999). These very different responses apparently depend on the spatial expression of the protein and the neuronal cell type (Taylor et al. 1993) as well as the domain of the protein (Faissner 1997; Meiners et al. 1999; Taylor et al. 1993). Vertebrate Tenascin is comprised of four genes but only two of them, *tenascin-C* and *tenascin-R*, are present in the CNS. These two tenascin protein types have EGF domains, FN-III domains and alternatively spliced FN-III domains and a FGN-like domain. The *tenascin-C* protein is a larger protein due to greater numbers of EGF domains and alternatively-spliced FN-III domains (Faissner 1997). In *Drosophila*, there also exist two neuronal forms of tenascin, *tenascin-m* and *tenascin-a*. *Tenascin-a* was the first to be cloned and found to lack the FN-III repeats and FGN-like domain of vertebrate forms but contains a conspicuous cystine-rich sequence (Baumgartner and Chiquet-Ehrismann 1993). *Tenascin-a* protein, found in the nervous system and in the brain, was localised to growing axons and proposed to be involved in axon guidance (Baumgartner and Chiquet-Ehrismann 1993). However, no mutants have yet been isolated for this gene to determine its function. *Tenascin-m* was then cloned and found to encode the first pair-rule gene that acts from outside the cell (Baumgartner et al. 1994). *Tenascin-m*, contains EGF domains, the cystine-rich region of *tenascin-a*, and FN-III repeats but not the FGN domain of vertebrate tenascins (Baumgartner et al. 1994). *Tenascin-m* is localised to commissural and longitudinal axons, in muscle insertion sites and cardiac cells (Baumgartner et al. 1994). Different from the *Tenascin-a* form, *Tenascin-m* contains a RGD sequence that binds to the α -PS2 integrin, *Inflated* (Baumgartner et al. 1994). As

well, no mutants have been isolated for this gene. In attempts to overcome this obvious lack of tenascin gene mutants to work with, I resolved to examining a mutant that maps to the same location as *tenascin-a*, *central body defect (cbd)*, and a deficiency that uncovers *tenascin-m*. *cbd* mutants did not show a mutant CNS phenotype, whereas *tenascin-m* deficient embryos displayed mild defasciculation defects in longitudinal fascicles expressing FasII protein. Thus, Tenascin-m may play a minor role in axon guidance within the CNS. However, whether these proteins interact with Slit is not conclusively known, but likely not, from data shown here. Future work with flies mutated within the loci of these genes will better solidify the conclusions of these data.

7.13 Dlg1 does not function downstream of Slit

Discs-Large (Dlg1) is a cytoplasmic protein also localised to septate junctions like NrX IV (Woods and Bryant 1991). Dlg1 protein contains SH3, HOOK and PDZ domains as structural motifs (Hough et al. 1997). Dlg1, originally identified as a tumor suppressor gene, is thought to be involved in cGMP cycle as a guanylate kinase to control cell proliferation by regulating the supply of guanine nucleotides (Woods and Bryant 1991). Although Dlg1 expression was found to be localised to axon bundles of the CNS, it has been shown here not to function downstream of Slit signaling. However, Dlg1 was also proposed to be involved in localising cytoskeletal and transmembrane proteins (Woods et al. 1996). In particular, Dlg1 was found to properly localise FasII via the PDZ domains in neurons to prepare for synaptogenesis (Thomas et al. 1997). Thus, the neuronal role of Dlg1 may function downstream in neuromuscular junctions (Woods et al. 1996).

7.14 Future Prospects

Since a survey of genetic interactions has been generated, there is a number of experiments that could be conducted to further examine these interactions. First, a backcross of each double mutant line could to the original mutant stock could be conducted to test for dosage contributions to the genetic interaction. These experiments could then be

compared to the double mutant results to better assess the dosage relationship of these interactions. Secondly, you could explore possible protein interactions. Proteins can be isolated by co-immunoprecipitation after expression in S2 cells.

Based on the results of this study, it would be interesting to determine the extent or the nature of the Slit/Integrin genetic interaction. Other genetic tests, such as the GAL4-UAS system could be used as UAS-integrin lines are available, to determine how integrins expressed in different expression patterns in the CNS affect axon guidance. Downstream of integrin signaling, it would be of interest to determine which of the kinases, FAK or others, directly transduce the slit-integrin signal. This can be accomplished when mutations in genes that encode these kinases are isolated and used in genetic crosses. The role of Dock and its downstream effectors would also need to be tested in this system. It would be of interest to determine if Misshapen and Pak are also expressed in CNS neurons and function in a similar way as shown in the eye.

The role of Laminin signaling in the CNS would also need to be investigated further. It has not yet been shown whether *Drosophila* Laminin binds *Drosophila* Slit and Netrin. Mutations isolated in the *lamininB1* and *lamininB2* genes could also be used for genetic crosses to confirm deficiency tests. It would be of interest to determine if the YIGSR sequence of Laminin mediates growth cone repulsion in *Drosophila* and may function in opposition to Netrin.

Finally, it would also be of interest to examine these CNS signaling players in other regions where Slit is expressed, namely muscle insertion sites and in the heart. Some of the genes examined here are also expressed at both sites such as Laminin and the integrins and functions between Slit and these other proteins may be conserved in these areas.

REFERENCES

- Artavanis-Tsakonas, S., Matsuno, K. and Fortini, M. E.** (1995). Notch signaling. *Science* **268**,225-32.
- Battye, R.** (2000). Structure/function analysis of Slit. Ph.D. thesis, McMaster University.
- Battye, R., Stevens, A. and Jacobs, J. R.** (1999). Axon repulsion from the midline of the *Drosophila* CNS requires *slit* function. *Development* **126**,2475-81.
- Baumgartner, S. and Chiquet-Ehrismann, R.** (1993). Tena, a *Drosophila* gene related to tenascin, shows selective transcript localization. *Mech Dev* **40**,165-76.
- Baumgartner, S., Littleton, J. T., Broadie, K., Bhat, M. A., Harbecke, R., Lengyel, J. A., Chiquet-Ehrismann, R., Prokop, A. and Bellen, H. J.** (1996). A *Drosophila* neurexin is required for septate junction and blood-nerve barrier formation and function. *Cell* **87**,1059-68.
- Baumgartner, S., Martin, D., Chiquet-Ehrismann, R., Sutton, J., Desai, A., Huang, I., Kato, K. and Hromas, R.** (1995). The HEM proteins: a novel family of tissue-specific transmembrane proteins expressed from invertebrates through mammals with an essential function in oogenesis. *J Mol Biol* **251**,41-9.
- Baumgartner, S., Martin, D., Hagios, C. and Chiquet-Ehrismann, R.** (1994). Tenm, a *Drosophila* gene related to tenascin, is a new pair-rule gene. *Embo J* **13**,3728-40.
- Berditchevski, F., Toliás, K. F., Wong, K., Carpenter, C. L. and Hemler, M. E.** (1997). A novel link between integrins, transmembrane-4 superfamily proteins (CD63 and CD81), and phosphatidylinositol 4-kinase. *J Biol Chem* **272**,2595-8.
- Bhat, M. A., Izaddoost, S., Lu, Y., Cho, K. O., Choi, K. W. and Bellen, H. J.** (1999). Discs Lost, a novel multi-PDZ domain protein, establishes and maintains epithelial polarity. *Cell* **96**,833-45.
- Boube, M., Benassayag, C., Seroude, L. and Cribbs, D. L.** (1997). Ras1-mediated modulation of *Drosophila* homeotic function in cell and segment identity. *Genetics* **146**,619-28.
- Brose, K., Bland, K. S., Wang, K. H., Arnott, D., Henzel, W., Goodman, C. S., Tessier-Lavigne, M. and Kidd, T.** (1999). Slit proteins bind Robo receptors and have an evolutionarily conserved role in repulsive axon guidance. *Cell* **96**,795-806.
- Brower, D. L., Bunch, T. A., Mukai, L., Adamson, T. E., Wehrli, M., Lam, S., Friedländer, E., Roote, C. E. and Zusman, S.** (1995). Nonequivalent requirements for PS1 and PS2 integrin at cell attachments in *Drosophila*: genetic analysis of the alpha PS1 integrin subunit. *Development* **121**,1311-20.

- Brown, N. H.** (1994). Null mutations in the alpha PS2 and beta PS integrin subunit genes have distinct phenotypes. *Development* **120**,1221-31.
- Bunch, T. A., Graner, M. W., Fessler, L. I., Fessler, J. H., Schneider, K. D., Kerschen, A., Choy, L. P., Burgess, B. W. and Brower, D. L.** (1998). The PS2 integrin ligand tigrin is required for proper muscle function in *Drosophila*. *Development* **125**,1679-89.
- Campos-Ortega, J. A. and Hartenstein, V.** (1985). The Embryonic Development of *Drosophila melanogaster*. 227.
- Chasan, R. and Anderson, K. V.** (1989). The role of *easter*, an apparent serine protease, in organizing the dorsal-ventral pattern of the *Drosophila* embryo. *Cell* **56**,391-400.
- Clemens, J. C., Ursuliak, Z., Clemens, K. K., Price, J. V. and Dixon, J. E.** (1996). A *Drosophila* protein-tyrosine phosphatase associates with an adapter protein required for axonal guidance. *J Biol Chem* **271**,17002-5.
- Crews, S. T., Thomas, J. B. and Goodman, C. S.** (1988). The *Drosophila* single-minded gene encodes a nuclear protein with sequence similarity to the per gene product. *Cell* **52**,143-51.
- Desai, C. J., Garrity, P. A., Keshishian, H., Zipursky, S. L. and Zinn, K.** (1999). The *Drosophila* SH2-SH3 adapter protein Dock is expressed in embryonic axons and facilitates synapse formation by the RP3 motoneuron. *Development* **126**,1527-35.
- Faissner, A.** (1997). The tenascin gene family in axon growth and guidance. *Cell Tissue Res* **290**,331-41.
- FlyBase** (2000). <http://flybase.bio.indiana.edu:7083/>.
- Fogerty, F. J., Fessler, L. I., Bunch, T. A., Yaron, Y., Parker, C. G., Nelson, R. E., Brower, D. L., Gullberg, D. and Fessler, J. H.** (1994). Tigrin, a novel *Drosophila* extracellular matrix protein that functions as a ligand for *Drosophila* alpha PS2 beta PS integrins. *Development* **120**,1747-58.
- Fox, G. L., Rebay, I. and Hynes, R. O.** (1999). Expression of DFak56, a *Drosophila* homolog of vertebrate focal adhesion kinase, supports a role in cell migration in vivo. *Proc Natl Acad Sci U S A* **96**,14978-83.
- Fritz, J. L. and VanBerkum, M. F.** (2000). Calmodulin and son of sevenless dependent signaling pathways regulate midline crossing of axons in the *Drosophila* CNS. *Development* **127**,1991-2000.
- Garcia-Alonso, L., Fetter, R. D. and Goodman, C. S.** (1996). Genetic analysis of Laminin A in *Drosophila*: extracellular matrix containing laminin A is required for ocellar axon pathfinding. *Development* **122**,2611-21.

Garrity, P. A., Rao, Y., Salecker, I., McGlade, J., Pawson, T. and Zipursky, S. L. (1996). *Drosophila* photoreceptor axon guidance and targeting requires the dreadlocks SH2/SH3 adapter protein. *Cell* **85**,639-50.

Giancotti, F. G. and Ruoslahti, E. (1999). Integrin signaling. *Science* **285**,1028-32.

Goodman, C. S. (1996). Mechanisms and molecules that control growth cone guidance. *Annu Rev Neurosci* **19**,341-77.

Goodman, C. S. and Doe, C. Q. (1993). Ch 19: Embryonic development of the *Drosophila* central nervous system. The Development of *Drosophila melanogaster*. Bate, M. and Martinez Arias, A. (eds). 1131-1206.

Gotwals, P. J., Fessler, L. I., Wehrli, M. and Hynes, R. O. (1994). *Drosophila* PS1 integrin is a laminin receptor and differs in ligand specificity from PS2. *Proc Natl Acad Sci U S A* **91**,11447-51.

Grotewiel, M. S., Beck, C. D., Wu, K. H., Zhu, X. R. and Davis, R. L. (1998). Integrin-mediated short-term memory in *Drosophila* [see comments]. *Nature* **391**,455-60.

Halfon, M. S., Hashimoto, C. and Keshishian, H. (1995). The *Drosophila* toll gene functions zygotically and is necessary for proper motoneuron and muscle development. *Dev Biol* **169**,151-67.

Hall (1998). Rho GTPases and the actin cytoskeleton. *Science* **279**,509-514.

Harmon, J. T. and Jamieson, G. A. (1986). The glycoprotein portion of platelet glycoprotein Ib expresses both high and moderate affinity receptor sites for thrombin. A soluble radioreceptor assay for the interaction of thrombin with platelets. *J Biol Chem* **261**,13224-9.

Harris, R., Sabatelli, L. M. and Seeger, M. A. (1996). Guidance cues at the *Drosophila* CNS midline: identification and characterization of two *Drosophila* Netrin/UNC-6 homologs. *Neuron* **17**,217-28.

Hashimoto, C., Gerttula, S. and Anderson, K. V. (1991). Plasma membrane localization of the Toll protein in the syncytial *Drosophila* embryo: importance of transmembrane signaling for dorsal-ventral pattern formation. *Development* **111**,1021-8.

Hidalgo, A. and Booth, G. E. (2000). Glia dictate pioneer axon trajectories in the *Drosophila* embryonic CNS. *Development* **127**,393-402.

Hing, H., Xiao, J., Harden, N., Lim, L. and Zipursky, S. L. (1999). Pak functions downstream of Dock to regulate photoreceptor axon guidance in *Drosophila*. *Cell* **97**,853-63.

Hoang, B. and Chiba, A. (1998). Genetic analysis on the role of integrin during axon guidance in *Drosophila*. *J Neurosci* **18**,7847-55.

- Hocking, A. M., Shinomura, T. and McQuillan, D. J.** (1998). Leucine-rich repeat glycoproteins of the extracellular matrix. *Matrix Biol* **17**,1-19.
- Hoffman, M. P., Nomizu, M., Roque, E., Lee, S., Jung, D. W., Yamada, Y. and Kleinman, H. K.** (1998). Laminin-1 and laminin-2 G-domain synthetic peptides bind syndecan-1 and are involved in acinar formation of a human submandibular gland cell line [published erratum appears in J Biol Chem 1999 Apr 30;274(18):12950]. *J Biol Chem* **273**,28633-41.
- Holmes, G. P., Negus, K., Burridge, L., Raman, S., Algar, E., Yamada, T. and Little, M. H.** (1998). Distinct but overlapping expression patterns of two vertebrate slit homologs implies functional roles in CNS development and organogenesis. *Mech Dev* **79**,57-72.
- Hopker, V. H., Shewan, D., Tessier-Lavigne, M., Poo, M. and Holt, C.** (1999). Growth-cone attraction to netrin-1 is converted to repulsion by laminin-1. *Nature* **401**,69-73.
- Hough, C. D., Woods, D. F., Park, S. and Bryant, P. J.** (1997). Organizing a functional junctional complex requires specific domains of the *Drosophila* MAGUK Discs large. *Genes Dev* **11**,3242-53.
- Hughes, P. E. and Pfaff, M.** (1998). Integrin affinity modulation. *Trends Cell Biol* **8**,359-64.
- Hummel, T., Leifker, K. and Klambt, C.** (2000). The *Drosophila* HEM-2/NAP1 homolog KETTE controls axonal pathfinding and cytoskeletal organization. *Genes Dev* **14**,863-73.
- Hummel, T., Schimmelpfeng, K. and Klambt, C.** (1999a). Commissure formation in the embryonic CNS of *Drosophila*. *Development* **126**,771-9.
- Hummel, T., Schimmelpfeng, K. and Klambt, C.** (1999b). Commissure formation in the embryonic CNS of *Drosophila*. *Dev Biol* **209**,381-98.
- Hynes, R. O.** (1999). Cell adhesion: old and new questions. *Trends Cell Biol* **9**,M33-7.
- Itoh, A., Miyabayashi, T., Ohno, M. and Sakano, S.** (1998). Cloning and expressions of three mammalian homologues of *Drosophila slit* suggest possible roles for Slit in the formation and maintenance of the nervous system. *Brain Res Mol Brain Res* **62**,175-86.
- Jacobs, J. R.** (2000). The midline glia of *Drosophila*: a molecular genetic model for the developmental functions of glia. *Progress in Neurobiology*. In press. .
- Jacobs, J. R. and Goodman, C. S.** (1989). Embryonic development of axon pathways in the *Drosophila* CNS. I. A glial scaffold appears before the first growth cones. *J Neurosci* **9**,2402-11.
- Jian, X., Szaro, B. G. and Schmidt, J. T.** (1996). Myosin light chain kinase: expression in neurons and upregulation during axon regeneration. *J Neurobiol* **31**,379-91.

- Keely, P., Parise, L. and Juliano, R.** (1998). Integrins and GTPases in tumour cell growth, motility and invasion. *Trends Cell Biol* **8**,101-6.
- Keith, F. J. and Gay, N. J.** (1990). The *Drosophila* membrane receptor Toll can function to promote cellular adhesion. *Embo J* **9**,4299-306.
- Kennison, J. A. and Tamkun, J. W.** (1988). Dosage-dependent modifiers of polycomb and antennapedia mutations in *Drosophila*. *Proc Natl Acad Sci U S A* **85**,8136-40.
- Kidd, T., Bland, K. S. and Goodman, C. S.** (1999). Slit is the midline repellent for the robo receptor in *Drosophila*. *Cell* **96**,785-94.
- Kidd, T., Brose, K., Mitchell, K. J., Fetter, R. D., Tessier-Lavigne, M., Goodman, C. S. and Tear, G.** (1998a). Roundabout controls axon crossing of the CNS midline and defines a novel subfamily of evolutionarily conserved guidance receptors. *Cell* **92**,205-15.
- Kidd, T., Russell, C., Goodman, C. S. and Tear, G.** (1998b). Dosage-sensitive and complementary functions of roundabout and commissureless control axon crossing of the CNS midline. *Neuron* **20**,25-33.
- Klambt, C. and Goodman, C. S.** (1991a). The diversity and pattern of glia during axon pathway formation in the *Drosophila* embryo. *Glia* **4**,205-13.
- Klambt, C. and Goodman, C. S.** (1991b). Role of the midline glia and neurons in the formation of the axon commissures in the central nervous system of the *Drosophila* embryo. *Ann N Y Acad Sci* **633**,142-59.
- Klambt, C., Jacobs, J. R. and Goodman, C. S.** (1991). The midline of the *Drosophila* central nervous system: a model for the genetic analysis of cell fate, cell migration, and growth cone guidance. *Cell* **64**,801-15.
- Kolodziej, P. A., Timpe, L. C., Mitchell, K. J., Fried, S. R., Goodman, C. S., Jan, L. Y. and Jan, Y. N.** (1996). frazzled encodes a *Drosophila* member of the DCC immunoglobulin subfamily and is required for CNS and motor axon guidance. *Cell* **87**,197-204.
- Li, H. S., Chen, J. H., Wu, W., Fagaly, T., Zhou, L., Yuan, W., Dupuis, S., Jiang, Z. H., Nash, W., Gick, C., Ornitz, D. M., Wu, J. Y. and Rao, Y.** (1999). Vertebrate slit, a secreted ligand for the transmembrane protein roundabout, is a repellent for olfactory bulb axons. *Cell* **96**,807-18.
- Liang, Y., Annan, R. S., Carr, S. A., Popp, S., Mevissen, M., Margolis, R. K. and Margolis, R. U.** (1999). Mammalian homologues of the *Drosophila* slit protein are ligands of the heparan sulfate proteoglycan glypican-1 in brain. *J Biol Chem* **274**,17885-92.

- Lieber, T., Wesley, C. S., Alcamo, E., Hassel, B., Krane, J. F., Campos-Ortega, J. A. and Young, M. W.** (1992). Single amino acid substitutions in EGF-like elements of Notch and Delta modify *Drosophila* development and affect cell adhesion in vitro. *Neuron* **9**,847-59.
- Lindsley, D. L. and Zimm, G. G.** (1992). The Genome of *Drosophila melanogaster*. 1133.
- MacKrell, A. J., Blumberg, B., Haynes, S. R. and Fessler, J. H.** (1988). The lethal *mysospheroid* gene of *Drosophila* encodes a membrane protein homologous to vertebrate integrin beta subunits. *Proc Natl Acad Sci U S A* **85**,2633-7.
- McCartney, B. M., Kulikauskas, R. M., LaJeunesse, D. R. and Fehon, R. G.** (2000). The neurofibromatosis-2 homologue, Merlin, and the tumor suppressor expanded function together in *Drosophila* to regulate cell proliferation and differentiation. *Development* **127**,1315-24.
- Meiners, S., Mercado, M. L., Nur-e-Kamal, M. S. and Geller, H. M.** (1999). Tenascin-C contains domains that independently regulate neurite outgrowth and neurite guidance. *J Neurosci* **19**,8443-53.
- Missler, M. and Sudhof, T. C.** (1998). Neurexins: three genes and 1001 products. *Trends Genet* **14**,20-6.
- Mitchell, K. J., Doyle, J. L., Serafini, T., Kennedy, T. E., Tessier-Lavigne, M., Goodman, C. S. and Dickson, B. J.** (1996). Genetic analysis of Netrin genes in *Drosophila*: Netrins guide CNS commissural axons and peripheral motor axons. *Neuron* **17**,203-15.
- Monard, D.** (1988). Cell-derived proteases and protease inhibitors as regulators of neurite outgrowth. *Trends Neurosci* **11**,541-4.
- Montell, D. J. and Goodman, C. S.** (1989). *Drosophila* laminin: sequence of B2 subunit and expression of all three subunits during embryogenesis. *J Cell Biol* **109**,2441-53.
- Moro, L., Venturino, M., Bozzo, C., Silengo, L., Altruda, F., Beguinot, L., Tarone, G. and Defilippi, P.** (1998). Integrins induce activation of EGF receptor: role in MAF kinase induction and adhesion-dependent cell survival. *Embo J* **17**,6622-32.
- Mueller, B. K.** (1999). Growth cone guidance: first steps towards a deeper understanding. *Annu Rev Neurosci* **22**,351-88.
- Murugasu-Oei, B., Balakrishnan, R., Yang, X., Chia, W. and Rodrigues, V.** (1996). Mutations in *masquerade*, a novel serine-protease-like molecule, affect axonal guidance and taste behavior in *Drosophila*. *Mech Dev* **57**,91-101.
- Murugasu-Oei, B., Rodrigues, V., Yang, X. and Chia, W.** (1995). Masquerade: a novel secreted serine protease-like molecule is required for somatic muscle attachment in the *Drosophila* embryo. *Genes Dev* **9**,139-54.

- Nagano, M., Suzuki, H., Ui-Tei, K., Sato, S., Miyake, T. and Miyata, Y.** (1998). H-7-induced apoptosis in the cells of a *Drosophila* neuronal cell line through affecting unidentified H-7-sensitive substance(s). *Neurosci Res* **31**,113-21.
- Newman, S. M., Jr. and Wright, T. R.** (1981). A histological and ultrastructural analysis of developmental defects produced by the mutation, *lethal(1)myospheroid*, in *Drosophila melanogaster*. *Dev Biol* **86**,393-402.
- Noordermeer, J. N., Kopczynski, C. C., Fetter, R. D., Bland, K. S., Chen, W. Y. and Goodman, C. S.** (1998). Wrapper, a novel member of the Ig superfamily, is expressed by midline glia and is required for them to ensheath commissural axons in *Drosophila*. *Neuron* **21**,991-1001.
- Nusslein-Volhard, C., Wiechaus, E. and Kluding, H.** (1984). Mutations affecting the pattern of the larval cuticle in *Drosophila melanogaster*. I. Zygotic loci on the second chromosome. *Roux's Arch. Dev. Biol.* **193**,267-282.
- Peles, E., Nativ, M., Lustig, M., Grumet, M., Schilling, J., Martinez, R., Plowman, G. D. and Schlessinger, J.** (1997). Identification of a novel contactin-associated transmembrane receptor with multiple domains implicated in protein-protein interactions. *Embo J* **16**,978-88.
- Porter, J. C. and Hogg, N.** (1998). Integrins take partners: cross-talk between integrins and other membrane receptors. *Trends Cell Biol* **8**,390-6.
- Price, J. V., Savenye, E. D., Lum, D. and Breitkreutz, A.** (1997). Dominant enhancers of Egfr in *Drosophila melanogaster*: genetic links between the Notch and Egfr signaling pathways. *Genetics* **147**,1139-53.
- Quilliam, L. A., Lambert, Q. T., Mickelson-Young, L. A., Westwick, J. K., Sparks, A. B., Kay, B. K., Jenkins, N. A., Gilbert, D. J., Copeland, N. G. and Der, C. J.** (1996). Isolation of a NCK-associated kinase, PRK2, an SH3-binding protein and potential effector of Rho protein signaling. *J Biol Chem* **271**,28772-6.
- Roote, C. E. and Zusman, S.** (1995). Functions for PS integrins in tissue adhesion, migration, and shape changes during early embryonic development in *Drosophila*. *Dev Biol* **169**,322-36.
- Rose, D. and Chiba, A.** (1999). A single growth cone is capable of integrating simultaneously presented and functionally distinct molecular cues during target recognition. *The Journal of Neuroscience* **19**,4899-4906.
- Rose, D., Zhu, X., Kose, H., Hoang, B., Cho, J. and Chiba, A.** (1997). Toll, a muscle cell surface molecule, locally inhibits synaptic initiation of the RP3 motoneuron growth cone in *Drosophila*. *Development* **124**,1561-1571.
- Rothberg, J. M. and Artavanis-Tsakonas, S.** (1992). Modularity of the slit protein. Characterization of a conserved carboxy-terminal sequence in secreted proteins and a motif implicated in extracellular protein interactions. *J Mol Biol* **227**,367-70.

- Rothberg, J. M., Hartley, D. A., Walther, Z. and Artavanis-Tsakonas, S.** (1988). *slit*: an EGF-homologous locus of *D. melanogaster* involved in the development of the embryonic central nervous system. *Cell* **55**,1047-59.
- Rothberg, J. M., Jacobs, J. R., Goodman, C. S. and Artavanis-Tsakonas, S.** (1990). Slit: an extracellular protein necessary for development of midline glia and commissural axon pathways contains both EGF and LRR domains. *Genes Dev* **4**,2169-87.
- Ruan, W., Pang, P. and Rao, Y.** (1999). The SH2/SH3 adaptor protein dock interacts with the Ste20-like kinase misshapen in controlling growth cone motility. *Neuron* **24**,595-605.
- Sato, A., Perlas, E., Ben-Menahem, D., Kudo, M., Pixley, M. R., Furuhashi, M., Hsueh, A. J. and Boime, I.** (1997). Cystine knot of the gonadotropin alpha subunit is critical for intracellular behaviour but not for in vitro biological activity. *Journal of Biological Chemistry* **272**,18098-103.
- Schaller, M. D., Otey, C. A., Hildebrand, J. D. and Parsons, J. T.** (1995). Focal adhesion kinase and paxillin bind to peptides mimicking beta integrin cytoplasmic domains. *J Cell Biol* **130**,1181-7.
- Schlaepfer, D. D., Broome, M. A. and Hunter, T.** (1997). Fibronectin-stimulated signaling from a focal adhesion kinase-c-Src complex: involvement of the Grb2, p130cas, and Nck adaptor proteins. *Mol Cell Biol* **17**,1702-13.
- Schlaepfer, D. D. and Hunter, T.** (1998). Integrin signalling and tyrosine phosphorylation: just the FAKs? *Trends Cell Biol* **8**,151-7.
- Schmid, A., Chiba, A. and Doe, C. Q.** (1999). Clonal analysis of *Drosophila* embryonic neuroblasts: neural cell types, axon projections and muscle targets. *Development* **126**,4653-89.
- Seeger, M., Tear, G., Ferres-Marco, D. and Goodman, C. S.** (1993). Mutations affecting growth cone guidance in *Drosophila*: genes necessary for guidance toward or away from the midline. *Neuron* **10**,409-26.
- Shimada, H., Shimizu, T., Kuwayama, H., Suzuki, M., Nagai, R. and Morii, H.** (1995) Immunocytochemical localization of 155 kDa myosin light chain kinase and myosin heavy chain in bovine brain. *Brain Res* **682**,212-4.
- Simon, M. A., Bowtell, D. D., Dodson, G. S., Laverly, T. R. and Rubin, G. M.** (1991). Ras1 and a putative guanine nucleotide exchange factor perform crucial steps in signaling by the sevenless protein tyrosine kinase. *Cell* **67**,701-716.
- Sonnenfeld, M. J. and Jacobs, J. R.** (1994). Mesectodermal cell fate analysis in *Drosophila* midline mutants. *Mech Dev* **46**,3-13.
- Sonnenfeld, M. J. and Jacobs, J. R.** (1995). Apoptosis of the midline glia during *Drosophila* embryogenesis: a correlation with axon contact. *Development* **121**,569-78.

- Stark, K. A., Yee, G. H., Roote, C. E., Williams, E. L., Zusman, S. and Hynes, R. O.** (1997). A novel alpha integrin subunit associates with betaPS and functions in tissue morphogenesis and movement during *Drosophila* development. *Development* **124**,4583-94.
- Stein, E., Huynh-Do, U., Lane, A. A., Cerretti, D. P. and Daniel, T. O.** (1998). Nck recruitment to Eph receptor, EphB1/ELK, couples ligand activation to c-Jun kinase. *Journal of Biological Chemistry* **273**,1303-8.
- Strutt, D. I., Wiersdorff, V. and Mlodzik, M.** (1995). Regulation of furrow progression in the *Drosophila* eye by cAMP-dependent protein kinase A [see comments]. *Nature* **373**,705-9.
- Su, J., Muranjan, M. and Sap, J.** (1999). Receptor protein tyrosine phosphatase alpha activates Src-family kinases and controls integrin-mediated responses in fibroblasts. *Current Biology* **9**,505-11.
- Sun, Q., Bahri, S., Schmid, A., Chia, W. and Zinn, K.** (2000). Receptor tyrosine phosphatases regulate axon guidance across the midline of the *Drosophila* embryo. *Development* **127**,801-812.
- Taylor, J., Pesheva, P. and Schachner, M.** (1993). Influence of janusin and tenascin on growth cone behavior in vitro. *Journal of Neuroscience Research* **35**,347-362.
- Tear, G., Harris, R., Sutaria, S., Kilomanski, K., Goodman, C. S. and Seeger, M. A.** (1996). commissureless controls growth cone guidance across the CNS midline in *Drosophila* and encodes a novel membrane protein. *Neuron* **16**,501-14.
- Tearle and Nusslein-Volhard, C.** (1987). Tubingen mutants and stock list. **66**,209-269.
- Tessier-Lavigne, M. and Goodman, C. S.** (1996). The molecular biology of axon guidance. *Science* **274**,1123-33.
- Therrien, M., Chang, H. C., Solomon, N. M., Karim, F. D., Wassarman, D. A. and Rubin, G. M.** (1995). KSR, a novel protein kinase required for RAS signal transduction [see comments]. *Cell* **83**,879-88.
- Thomas, J. B., Crews, S. T. and Goodman, C. S.** (1988). Molecular genetics of the single-minded locus: a gene involved in the development of the *Drosophila* nervous system. *Cell* **52**,133-41.
- Thomas, U., Kim, E., Kuhlendahl, S., Koh, Y. H., Gundelfinger, E. D., Sheng, M., Garner, C. C. and Budnik, V.** (1997). Synaptic clustering of the cell adhesion molecule fasciclin II by discs-large and its role in the regulation of presynaptic structure. *Neuron* **19**,787-99.
- Tokimasa, T.** (1995). Effects of myosin light chain kinase inhibitors on delayed rectifier potassium current in bullfrog sympathetic neurons. *Neurosci Lett* **197**,75-7.

- Van Vactor, D. and Flanagan, J. G.** (1999). The middle and the end: slit brings guidance and branching together in axon pathway selection. *Neuron* **22**,649-52.
- VanBerkum, M. F. and Goodman, C. S.** (1995). Targeted disruption of Ca(2+)-calmodulin signaling in *Drosophila* growth cones leads to stalls in axon extension and errors in axon guidance. *Neuron* **14**,43-56.
- Voorberg, J., Fontijn, R., Calafat, J., Janssen, H., van Mourik, J. A. and Pannekoek, H.** (1991). Assembly and routing of von Willebrand factor variants: the requirements for disulfide-linked dimerization reside within the carboxy-terminal 151 amino acids. *J Cell Biol* **113**,195-205.
- Walsh, E. P. and Brown, N. H.** (1998). A screen to identify *Drosophila* genes required for integrin-mediated adhesion. *Genetics* **150**,791-805.
- Wehrli, M., DiAntonio, A., Fearnley, I. M., Smith, R. J. and Wilcox, M.** (1993). Cloning and characterization of alpha PS1, a novel *Drosophila melanogaster* integrin. *Mech Dev* **43**,21-36.
- Wessendorf, L. H., Wehrli, M., DiAntonio, A. and Wilcox, M.** (1992). Genetic interactions with integrins during wing morphogenesis in *Drosophila*. *Cold Spring Harb Symp Quant Biol* **57**,241-8.
- Winberg, M. L., Mitchell, K. J. and Goodman, C. S.** (1998). Genetic analysis of the mechanisms controlling target selection: complementary and combinatorial functions of netrins, semaphorins, and IgCAMs. *Cell* **93**,581-91.
- Woods, D. F. and Bryant, P. J.** (1989). Molecular cloning of the *lethal(1)discs large-1* oncogene of *Drosophila*. *Dev Biol* **134**,222-35.
- Woods, D. F. and Bryant, P. J.** (1991). The *discs-large* tumor suppressor gene of *Drosophila* encodes a guanylate kinase homolog localized at septate junctions. *Cell* **66**,451-64.
- Woods, D. F., Hough, C., Peel, D., Callaini, G. and Bryant, P. J.** (1996). Dlg protein is required for junction structure, cell polarity, and proliferation control in *Drosophila* epithelia. *J Cell Biol* **134**,1469-82.
- Yarnitzky, T. and Volk, T.** (1995). Laminin is required for heart, somatic muscles, and gut development in the *Drosophila* embryo. *Dev Biol* **169**,609-18.
- Yee, G. H. and Hynes, R. O.** (1993). A novel, tissue-specific integrin subunit, beta nu, expressed in the midgut of *Drosophila melanogaster*. *Development* **118**,845-58.
- Yuan, W., Zhou, L., Chen, J. H., Wu, J. Y., Rao, Y. and Ornitz, D. M.** (1999). The mouse SLIT family: secreted ligands for ROBO expressed in patterns that suggest a role in morphogenesis and axon guidance. *Dev Biol* **212**,290-306.

Appendix Figure 1. Genetic crosses for blind screen experiment – X chromosome.

STEP 1

P generation (mate in vial)	NP5/FM7c β ; +; +	x	yw ⁻ /Y; slit ²⁹⁹⁰ /CyO[eng]; +	
			↓	
F1 progeny	NP5/ yw ⁻ ; slit ²⁹⁹⁰ /+; +		yw ⁻ /FM7c β ; slit ²⁹⁹⁰ /+; +	
	FM7c β /Y; slit ²⁹⁹⁰ /+; +		NP5/yw ⁻ ; +/CyO[eng]; +	
	yw ⁻ /FM7c β ; +/CyO[eng]		FM7c β /Y; +/CyO[eng]; +	
	NP5/Y; slit ²⁹⁹⁰ /+; +		NP5/Y; +/CyO[eng]; +	(not viable)

STEP 2

F1 flies (in house)	NP5/yw ⁻ ; slit ²⁹⁹⁰ /+; +	x	FM7c β /Y; slit ²⁹⁹⁰ /+; +	
			↓	
F2 embryos	NP5/FM7c β ; slit ²⁹⁹⁰ /slit ²⁹⁹⁰ ; +		NP5/Y; slit ²⁹⁹⁰ /slit ²⁹⁹⁰ ; +	
	yw ⁻ /FM7c β ; slit ²⁹⁹⁰ /slit ²⁹⁹⁰ ; +		yw ⁻ /Y; slit ²⁹⁹⁰ /slit ²⁹⁹⁰ ; +	
	NP5/FM7c β ; slit ²⁹⁹⁰ /+; +	(x2)*	NP5/Y; slit ²⁹⁹⁰ /+; +	(x2)
	yw ⁻ /FM7c β ; slit ²⁹⁹⁰ /+; +	(x2)	yw ⁻ /Y; slit ²⁹⁹⁰ /+; +	(x2)
	NP5/FM7c β ; +/+		NP5/Y; +/+	
	yw ⁻ /FM7c β ; +/+		yw ⁻ /Y; +/+	

This cross produces embryos of different genotypes, of which 1/16 are double mutant for both genes.

*indicates expected frequency of occurrence; other genotypes lacking adjacent parentheses are only expected to occur 1 time out of 16.

Appendix Figure 2. Genetic crosses for blind screen experiment – 2nd chromosome.

P generation (in house)	yw-; slit ²⁹⁹⁰ /CyO[eng]; +	x	yw-/Y; dock ^{P1} /CyO[eng]; +
		↓	
F1 embryos	yw-; slit ²⁹⁹⁰ /dock ^{P1} ; +		yw-; slit ²⁹⁹⁰ /CyO[eng]; +
	yw-; dock ^{P1} /CyO[eng]; +		yw-; CyO[eng]/CyO[eng]; +

This cross has an expected occurrence of 1/4 of the embryos to be transheterozygous in genotype; meaning, they are deficient in one copy of each gene. An interaction can be demonstrated with reduced gene function, and then compared with a recombinant line.

All genotypes of the F1 generation are possible for both males and females alike.

Appendix Figure 3. Genetic crosses for blind screen experiment – 3rd chromosome.

STEP 1

P generation (in vial)	yw-; slit ²⁹⁹⁰ /CyO[eng]; +	x	yw-/Y; +; lamA/TM3B
		↓	
F1 progeny	yw-; slit ²⁹⁹⁰ /+; lamA/+		yw-; slit ²⁹⁹⁰ /+; +/TM3B
	yw-; +/CyO[eng]; lamA/+		yw-; +/CyO[eng]; +/TM3B

STEP 2

F1 flies (in house)	yw-; slit ²⁹⁹⁰ /+; lamA/+	x	yw-/Y; slit ²⁹⁹⁰ /+; lamA/+
		↓	
F2 progeny*	yw-; slit ²⁹⁹⁰ /slit ²⁹⁹⁰ ; lamA/lamA		yw-; slit ²⁹⁹⁰ /+; lamA/lamA (x2)
	yw-; slit ²⁹⁹⁰ /slit ²⁹⁹⁰ ; lamA/+ (x2)		yw-; +/+; lamA/lamA
	yw-; slit ²⁹⁹⁰ /slit ²⁹⁹⁰ ; +/+		yw-; slit ²⁹⁹⁰ /+; lamA/+ (x4)
	yw-; slit ²⁹⁹⁰ /+; +/+ (x2)		yw-; +/+; lamA/+ (x2)
	yw-; +/+; +/+		

This cross creates a number of genotypes, of which 1/16 is the expected ratio of embryos to be double mutant for both genes. These results can then be further explored in the double mutant stable line.

*All genotypes are representative for both males and females alike.

Appendix Figure 4. Genetic crosses for blind screen experiment – Control crosses.

STEP 1

P generation (in house and vials)	FM7c β /yw-; +; +	x	yw-/Y; slit ²⁹⁹⁰ /CyO[eng]; +
		↓	
F1 progeny	FM7c β /yw-; slit ²⁹⁹⁰ /+; +		FM7c β /Y; slit ²⁹⁹⁰ /+; +
	yw-; slit ²⁹⁹⁰ /+; +		yw-/Y; slit ²⁹⁹⁰ /+; +
	FM7c β /yw-; +/CyO[eng]; +		FM7c β /Y; +/CyO[eng]; +
	yw-; +/CyO[eng]; +		yw-/Y; +/CyO[eng]; +

STEP 2

F1 flies	FM7c β /yw-; slit ²⁹⁹⁰ /+; +	x	FM7c β /Y; slit ²⁹⁹⁰ /+; +
		↓	
F2 embryos	FM7c β /FM7c β ; slit ²⁹⁹⁰ /slit ²⁹⁹⁰		FM7c β /Y; slit ²⁹⁹⁰ /slit ²⁹⁹⁰ ; +
	FM7c β /yw-; slit ²⁹⁹⁰ /slit ²⁹⁹⁰ ; +		yw-/Y; slit ²⁹⁹⁰ /slit ²⁹⁹⁰ ; +
	FM7c β /FM7c β ; slit ²⁹⁹⁰ /+; + (x2)		FM7c β /Y; slit ²⁹⁹⁰ /+; + (x2)
	FM7c β /yw-; slit ²⁹⁹⁰ /+; + (x2)		yw-/Y; slit ²⁹⁹⁰ /+; + (x2)
	FM7c β /FM7c β ; +; +		FM7c β /Y; +; +
	FM7c β /yw-; +; +		yw-; +; +

The initial cross was used to generate F1 flies (in vials) for a second cross, and to stain the F1 progeny. Thus, the first cross was used to generate embryos containing one copy of the X chromosome balancer and *slit*²⁹⁹⁰; the second cross created embryos with the X chromosome balancer and double mutant copy of *slit*²⁹⁹⁰.

Appendix Figure 6 Genetic crosses for stable double mutant fly lines
- create double mutant lines for X chromosome mutant and *slit* allele.

STEP 1

P generation	NP5/FM7c β ; +; +	x	FM7c β /Y; <i>slit</i> ² /CyO[<i>eng</i>]
			↓
F1 progeny	NP5/FM7c β ; <i>slit</i> ² /+		NP5/FM7c β ; +/CyO[<i>eng</i>]
	NP5/Y; <i>slit</i> ² /+		NP5/Y; +/CyO[<i>eng</i>]
	FM7c β ; <i>slit</i> ² /+		FM7c β ; +/CyO[<i>eng</i>]
	FM7c β /Y; <i>slit</i> ² /+		FM7c β /Y; +/CyO[<i>eng</i>]

STEP 2

P generation	*NP5/FM7c β ; <i>slit</i> ² /+ or *NP5/FM7c β ; +/CyO[<i>eng</i>]	x	FM7c β /Y; <i>slit</i> ² /CyO[<i>eng</i>]
			↓
F1 progeny	NP5/FM7c β ; <i>slit</i> ² /CyO[<i>eng</i>]		NP5/FM7c β ; +/CyO[<i>eng</i>]
	NP5/FM7c β ; <i>slit</i> ² /+		NP5/FM7c β ; <i>slit</i> ² / <i>slit</i> ²
	NP5/Y; <i>slit</i> ² /CyO[<i>eng</i>]		NP5/Y; +/CyO[<i>eng</i>]
	NP5/Y; <i>slit</i> ² /+		NP5/Y; <i>slit</i> ² / <i>slit</i> ²
	FM7c β /Y; <i>slit</i> ² /CyO[<i>eng</i>]		FM7c β /Y; +/CyO[<i>eng</i>]
	FM7c β /Y; <i>slit</i> ² /+		FM7c β /Y; <i>slit</i> ² / <i>slit</i> ²
	FM7c β /FM7c β ; <i>slit</i> ² /CyO[<i>eng</i>]		FM7c β /FM7c β ; +/CyO[<i>eng</i>]
	FM7c β /FM7c β ; <i>slit</i> ² /+		FM7c β /FM7c β ; <i>slit</i> ² / <i>slit</i> ²

*used either of these two female genotypes for this cross

STEP 3

P generation NP5/FM7c β ; slit² ? /CyO[eng] x FM7c β /Y; slit²/CyO[eng]

↓

F1 progeny Keep all tubes with curly wing flies.

STEP 4 Complementation Test

NP5/FM7c β ; slit² ? /CyOeng x yw-/Y; slit²/CyO[eng]

If all F1 progeny have curly wings, then you know the 2nd chromosome has the slit allele. You cannot test for complementation on the X chromosome because males are lethal.

Genotypes of double mutant line:

Parental	males	FM7c β /Y; slit ² /CyO[eng]
	females	NP5/FM7c β ; slit ² /CyO[eng]
F1 embryos	NP5/FM7c β ; slit ² /slit ²	NP5/Y; slit ² /slit ²
	NP5/FM7c β ; slit ² /CyO[eng] (x2)	NP5/Y; slit ² /CyO[eng] (x2)
	NP5/FM7c β ; CyO[eng]/CyO[eng]	NP5/Y; CyO[eng]/CyO[eng]
	FM7c β /FM7c β ; slit ² /slit ²	FM7c β /Y; slit ² /slit ²
	FM7c β /FM7c β ; slit ² /CyO[eng] (x2)	FM7c β /Y; slit ² /CyO[eng] (x2)
	FM7c β /Fm7c β ; CyO[eng]/CyO[eng]	FM7c β /Y; CyO[eng]/CyO[eng]

Expected frequency of a hemizygous; slit genotype is 1/16, for double hetero is 1/8, for single hemizygote mutant is 1/16, and for single homozygote mutant is 1/8.

Appendix Figure 7 Genetic crosses for stable double mutant fly lines - create a recombinant chromosome for *slit* and another mutant on the 2nd chromosome.

STEP 1

P generation $yw^-; slit^2/CyO[eng]$ x $yw^-; dockP1/CyO[eng]$

↓

F1 progeny $yw^-; slit^2/dock$ $yw^-; dock/CyO[eng]$
 $yw^-; slit^2/CyO[eng]$ $yw^-; CyO[eng]/CyO[eng]$

STEP 2

P generation $yw^-; slit^2/dock$ x $yw/Y; Sco/CyO[eng]$
 (many pairwise)

↓ (recombination)

F1 progeny $yw^-; slit^2 dock ?^* /CyO[eng]$ $yw^-; Sco/slit^2 dock ?$

STEP 3

P generation pairwise all curly wing flies, non-Sco

$yw^-; slit^2 dock ? /CyO[eng]$ x $yw-/Y; slit dock ? /CyO[eng]$

F1 progeny Keep all tubes with curly wing flies only.

STEP 4 Complementation Test

P generation $yw^-; slit^2 dock ? /CyO[eng]$ x $yw-/Y; dock/CyO[eng]$

P generation $yw^-; slit^2 dock ? /CyO[eng]$ x $yw-/Y; slit^2/CyO[eng]$

You can ensure a line has both genes recombined on the cis chromosome when flies fail to complement the locus of the original mutant stock. Your chances for recombination occurring depend on the distance between the loci.

In embryonic populations you should expect:

1/4 to be double mutant in both genes...	$slit^2 dock/slit^2 dock$
1/2 to be a double heterozygote ...	$slit^2 dock/CyO[eng]$

*"?" denotes a desired recombination event

**Appendix Figure 8 Genetic crosses for stable double mutant fly lines
- create a double mutant line for *slit* and 3rd chromosome balanced marker**

STEP 1

P generation	yw-; slit ² /CyO[eng]	x	yw-/Y; +; D/TM3β
			↓
F1 progeny	yw-; slit ² /+; D/+		yw-; slit ² /+; +/TM3β
	yw-; +/CyO[eng]		yw-; +/CyO[eng]; +/TM3β

STEP 2

P generation	yw-; slit ² /+; D/+	x	yw-/Y; Star/CyO[eng]; D/TM3
			↓
F1 progeny	yw-; slit ² /CyO[eng]; D/TM3		yw-; slit ² /CyO[eng]; D/+
	yw-; slit ² /Star; D/TM3		yw-; slit ² /Star; D/+
	yw-; Star/+; D/TM3		yw-; Star/+; D/+
	yw-; +/CyO[eng]; D/TM3		yw-; +/CyO[eng]; D/+
	yw-; slit²/CyO[eng]; D/D		yw-; slit ² /CyO[eng]; +/TM3
	yw-; slit²/Star; D/D		yw-; slit ² /Star; +/TM3
	yw-; Star/+; D/D		yw-; Star/+; +/TM3
	yw-; +/CyO[eng]; D/D		yw-; +/CyO[eng]; +/TM3

STEP 3

P generation	yw-; slit ² ? /CyO[eng]; D/TM3	x	yw-; Star/CyO[eng]; D/TM3
			↓
F1 progeny	yw-; slit ² ? /CyO[eng]; D/TM3		yw-; Star/slit ² ? ; D/TM3
	yw-; Star/CyO[eng]; D/TM3		

STEP 4

Pairwise $yw^-; slit^2 ? / CyO[eng]; D/TM3$
Keep all tubes with curly wings.

STEP 5 Complementation Test

$yw^-; slit^2 ? / CyO[eng]; D/TM3$ x $yw^-; slit^2 / CyO[eng]$

If all progeny have curly wings, then you have $slit^2$ mutant locus in the stock.

STEP 4

P generation $yw^-; slit^2/CyO; lamA/TM3$ x $yw-/Y; slit^2/CyO[eng]; D/TM3$

↓

If all progeny have curly wings, then mutant slit locus present on 2nd chromosome. Collect males and females with non-Dichaete wings and pairwise.

STEP 5 Complementation Test

P generation $yw^-; slit^2/CyO[eng]$ x $yw/Y; slit^2/CyO[eng]; lamA/TM3$

P generation $yw^-; +; lamA/TM3$ x $yw/Y; slit^2/CyO[eng]; lamA/TM3$

If flies fail to complement the mutant loci of the original stocks, then you have successfully created a stable double mutant fly line.

Genotype of Embryonic Populations

Parental Line males: $yw^-; slit^2/CyO; lamA/TM3$
 females: $yw^-; slit^2/CyO; lamA/TM3$

F1 embryos:

$slit^2/slit^2; lamA/lamA$	$slit^2/CyO; lamA/lamA$ (x2)
$slit^2/slit^2; lamA/TM3$ (x2)	$slit^2/CyO; lamA/TM3$ (x4)
$slit^2/slit^2; TM3/TM3$	$slit^2/CyO; lamA/TM3$ (x2)
$CyO/CyO; lamA/lamA$	
$CyO/CyO; lamA/TM3$ (x2)	
$CyO/CyO; TM3/TM3$	

1/16 of the embryos will be homozygous double mutant or homozygous single mutant for either gene

1/4 will be heterozygous double mutant

1/8 will be homozygous mutant for one gene and heterozygous for the other gene, and vice versa

Appendix Figure 10 Genetics for deficiency crosses

1/4 of embryos from these housed crosses produce the designated genotypes:

a. Slit-Wrapper Cross

i. Cross *slit* and deficiency that uncovers *wrapper* locus

slit/CyO x Df(2R) X58-3/CyO ⇒ *slit* +/ + *wrapper*

ii. Cross *slit* and deficiency that uncovers *robo* and *wrapper* loci

slit/CyO x Df(2R)X58-12/SM5 ⇒ *slit* + +/+ *robo wrapper*

b. Slit-Scab Cross

i. Cross *scab* and *slit* mutants to a deficiency that uncovers *scab* locus

scb/CyO x Df(2R)XTE-18/CyO ⇒ *scb* + / *scb* +

slit/CyO x Df(2R)XTE-18/CyO ⇒ + *slit* / *scb* +

ii. Cross *scab* and *slit* mutants to a deficiency that uncovers both loci

scb/CyO x Df(2R)Jp1/CyO ⇒ *scb* + / *scb slit*

slit/CyO x Df(2R)Jp1/CyO ⇒ + *slit* / *scb slit*

III. Cross *scab* and *slit* mutants to a deficiency that uncovers *slit* locus

scb/CyO x Df(2R)Jp4/CyO ⇒ *scb* + / + *slit*

slit/CyO x Df(2R)Jp4/CyO ⇒ + *slit* / + *slit*

Appendix Figure 11 Genetic crosses for dominant modifier screen

a. Create a triple heterozygote with a gene on the X chromosome

P generation NP5/FM7c β ; +; + x yw-/Y; slit²/CyO[eng]; lamA/TM3
(house)

⇓

F1 embryos	NP5/yw-; slit ² /+; lamA/+	NP5/Y; slit ² /+; lam/+
	NP5/yw-; +/CyO[eng]; +/TM3	NP5/Y; +/CyO[eng]; +/TM3
	NP5/yw-; slit ² /+; +/TM3	NP5/Y; slit ² /+; +/TM3
	NP5/yw-; +/CyO[eng]; lam/+	NP5/Y; +/CyO[eng]; lam/+
	FM7c β /yw-; slit ² /+; lamA/+	FM7c β /Y; slit ² /+; lamA/+
	FM7c β /yw-; +/CyO[eng]; +/TM3	FM7c β /Y; +/CyO[eng]; +/TM3
	FM7c β /yw-; slit ² /+; +/TM3	FM7c β /Y; slit ² /+; +/TM3
	FM7c β /yw-; +/CyO[eng]; lam/+	FM7c β /Y; +/CyO[eng]; lam/+

You would expect 1/16 embryos to be a triple heterozygote.

b. Create a triple heterozygote with a gene on the 2nd chromosome

P generation yw-; robo1/CyOeng x yw-/Y; slit²/CyO[eng]; lamA/TM3
(house)

⇓

F1 embryos	slit ² /robo1; lam/+	slit ² /robo1; +/TM3
	slit ² /CyO; lam/+	slit ² /CyO; +/TM3
	robo1/CyO; lam/+	robo1/CyO; +/TM3
	CyO/CyO; lam/+	CyO/CyO; +/TM3

Expect 1/8 embryos to be a triple heterozygote.

c. Create a triple heterozygous mutant with a gene on the 3rd chromosome

P generation (house)	+	+	Df (3L) AC1/TM3	x	yw/Y; slit ² /CyO[eng]; lamA/TM3
				↓	
F1 embryos	slit ² /+	+	lamA/Df (3L) AC1		+ /CyO[eng]; lamA/Df(3L) AC1
	slit ² /+	+	lamA/TM3		+ /CyO[eng]; lamA/TM3
	slit ² /+	+	Df (3L) AC1		+ /CyO[eng]; Df (3L) AC1/TM3
	slit ² /+	+	TM3/TM3		+ /CyO[eng]; TM3/TM3

Expect 1/8 of embryos to be triple heterozygous mutant.

d. Control crosses for dominant modifier experiment

a. 2nd chromosome loci

P generation (in house)	slit ² /CyO	x	Df(2L)XE-2750/CyO
F1 embryos	slit ² /Df	Df/CyO	slit ² /CyO CyO/CyO

You would expect 1/4 of embryos to be a transheterozygote for the mutant and deficiency.

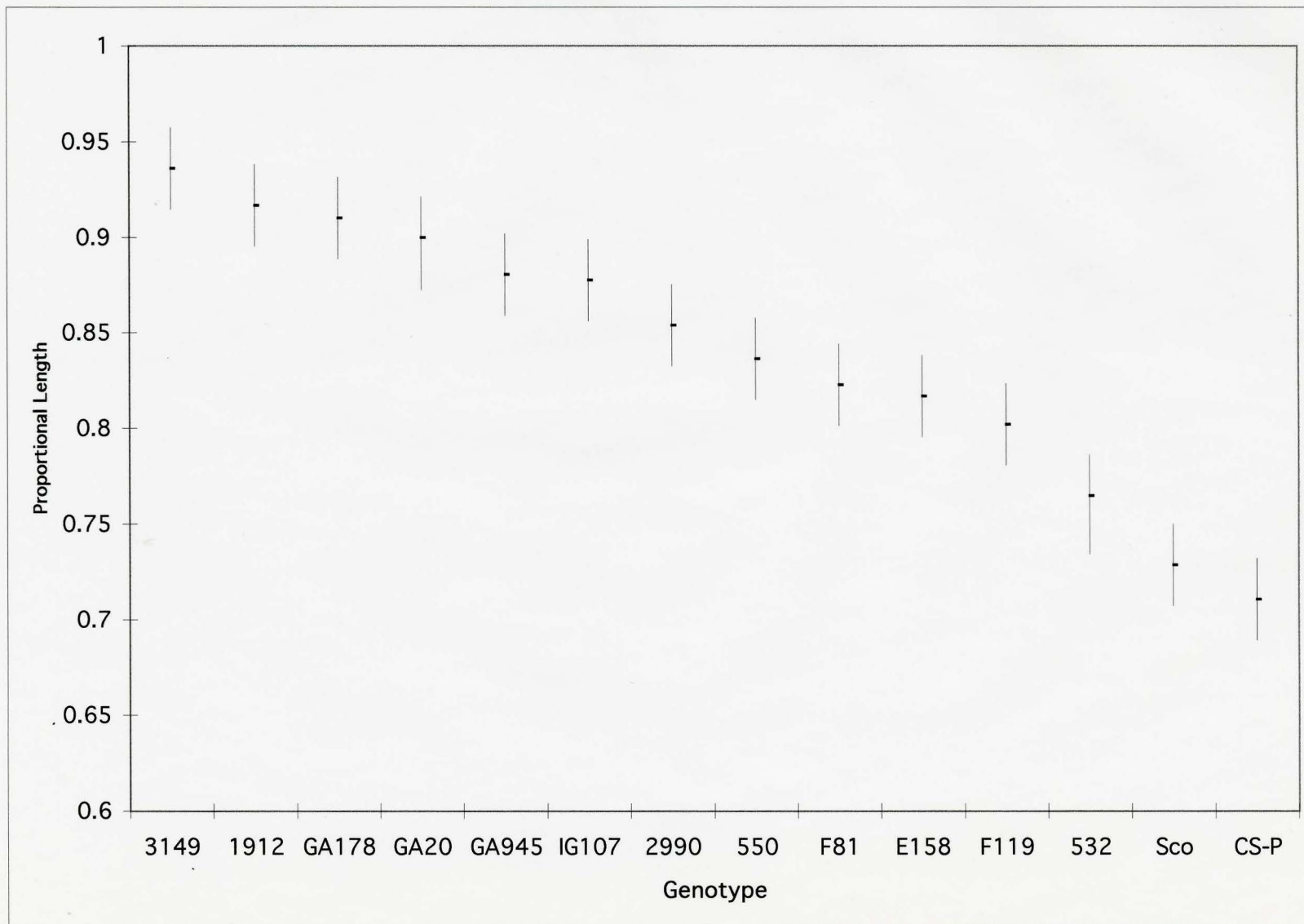
b. 2nd and 3rd chromosome loci

P generation (in house)	slit ² /CyO	x	lamA/TM3
F1 embryos	slit ² /+; lamA/+		slit ² /+; +/TM3
	+ /CyO; lamA/+		+ /CyO; +/TM3

You would expect 1/4 of embryos to be a transheterozygote for both loci.

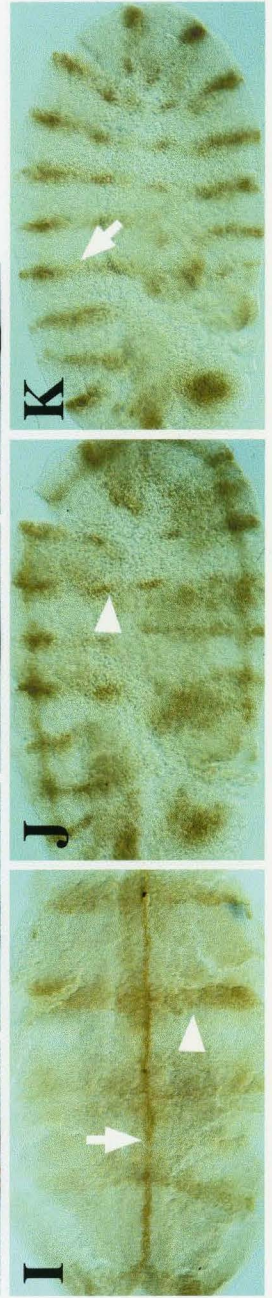
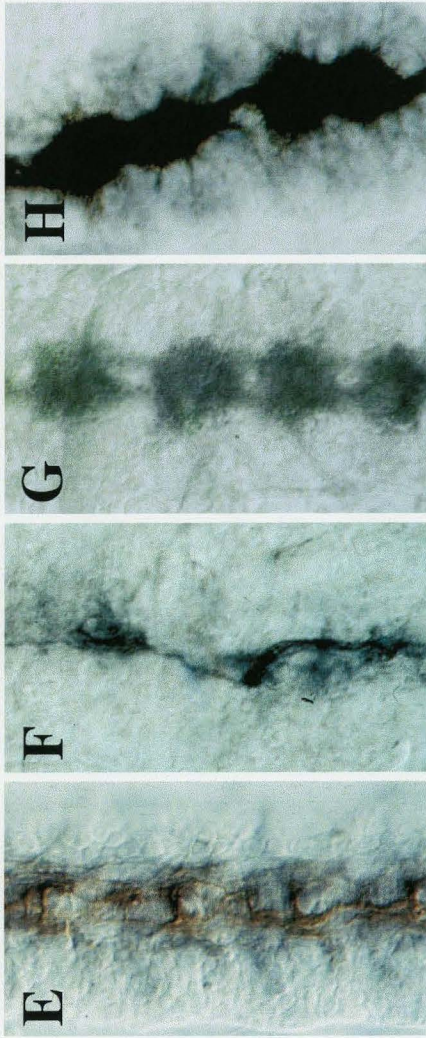
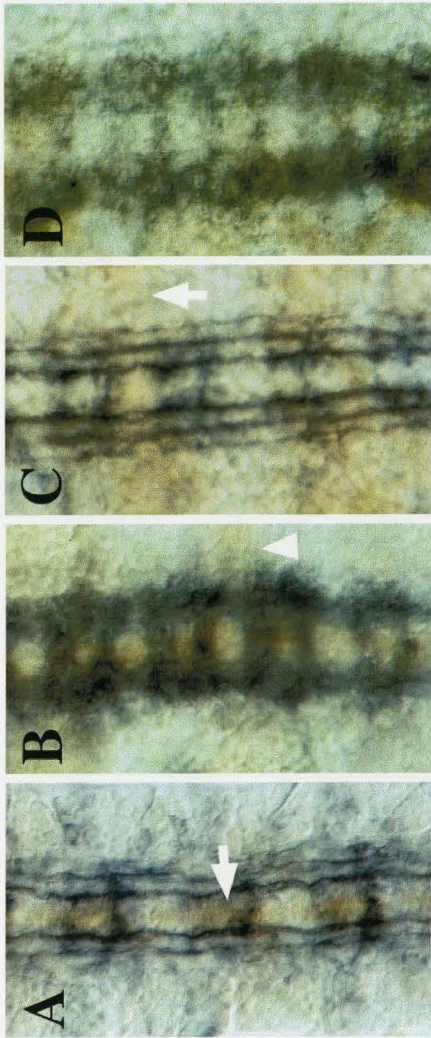
Appendix Figure 12 Upper and lower comparison limits for all *slit* alleles demonstrate some differences between proportional nerve cord lengths.

Nerve cord lengths for all *slit* alleles and control lines Sco/CyO and CS-P were compared to examine potential differences between alleles. Refer to Methods section 2.87 for more details of this analysis. One-Way Analysis of Variance was calculated and determined to have a significance of $p < 0.00001$ (summary table not shown). In attempts to determine differences between pairs of alleles, upper (upper bar) and lower (lower bar) comparison Tukey limits were calculated for each *slit* allele mean (dot). *slit* alleles were considered significantly different if their comparison limits did not overlap.



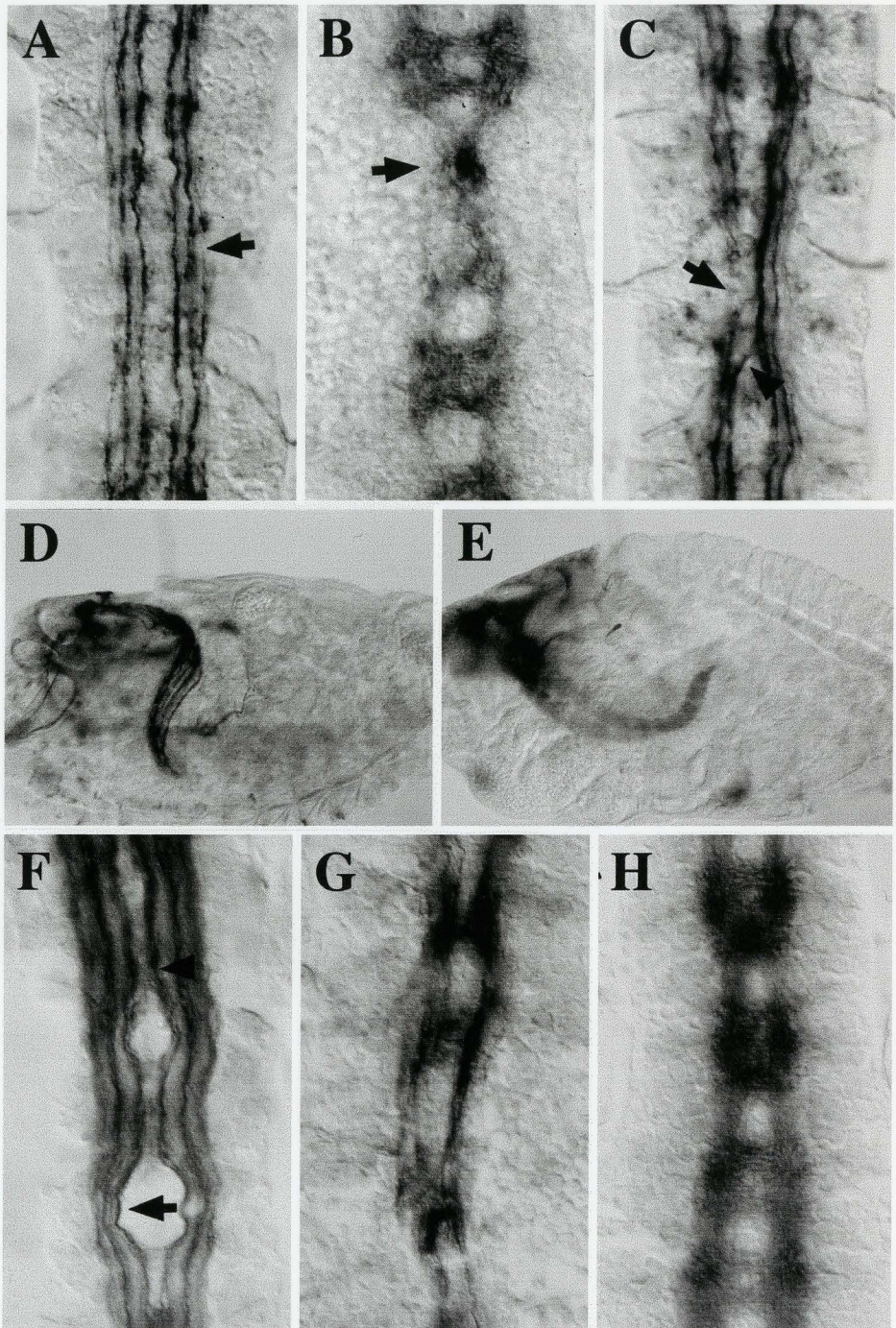
Appendix Figure 13 Control lines demonstrate balancer staining pattern and *slit* only phenotypes.

Frontal views of late stage 16 dissected VNC (A-H) and stage 11 frontal (I) and sagittal (J, K) whole mount embryos. FM7c β balancer lines containing a *ftz-lacZ* reporter demonstrates a near wildtype phenotype (A, B). β -galactosidase staining reveals a *ftz-lacZ* pattern down the midline (arrow, A and I) and parasegmental staining in even-numbered parasegments (arrowhead, B, I and J). CyO[*eng*] balancer line containing an *eng-lacZ* reporter demonstrates a wildtype phenotype (C) and β -galactosidase staining in the anterior-most row of even-numbered parasegments (arrow, C and K). Reporter staining for *ftz* gene becomes less distinguishable by the end of embryogenesis, while that of *eng* remains distinct. FM7c β ; *slit*²⁹⁹⁰/CyO[*eng*] and FM7c β ; *slit*²/CyO[*eng*] lines show only a wildtype phenotype (A, B) or *slit* phenotype when homozygous mutant for *slit*²⁹⁹⁰ (E) or *slit*² (F). Likewise, *slit*²⁹⁹⁰/CyO; *Dichaete* /TM3 and *slit*²/CyO; *Dichaete* /TM3 lines demonstrate a wildtype phenotype (D) or *slit* phenotype when homozygous mutant for *slit*²⁹⁹⁰ (G) or *slit*² (H).



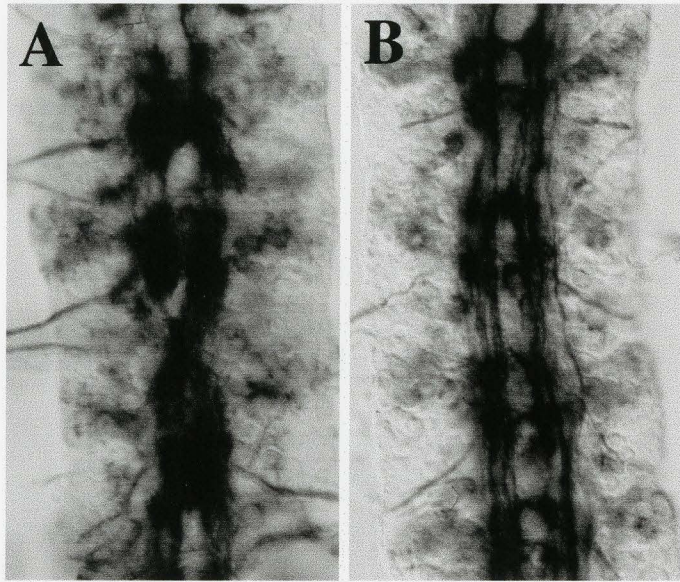
Appendix Figure 14 **Other phenotypes observed in single mutant embryos.**

Frontal views of late stage 16 dissected VNC (A-C, F-H) and sagittal views of stage 17 whole mount embryos (D, E), immunolabelled with mAb 1D4 (A, C, D, F, G) and mAb BP102 (B, E, H). Although a representative proportion of *ifk^{27e}* embryos demonstrate aberrant midline crossing of axons (refer to Figure 3.2M), other embryos (38%, n=39) display only gaps in the lateral fascicle (arrow, A). A majority of these embryos likewise display fuzzy commissures and thinned longitudinal tracts when observed with BP102 (refer to Figure 3.3M), while a less representative group of embryos show a more severely collapsed commissure in some segments (arrow, B). While the majority of *mew^{M6}* embryos display defasciculation and narrowing of the nerve cord (refer to Figure 3.2L), a smaller proportion demonstrate occasional crossing of the medial fascicle (arrowhead) and gaps in some longitudinal axons in that segment (arrow, C). While 22% (n=171) of *scb²* mutants display medial fusion of fascicles (refer to Figure 3.2N), 24% demonstrate a laterally twisted nerve cord (D, E). In 50% of *mys^l* mutants, embryos demonstrate medial fusion of fascicles (Figure 3.2O), near fusion at the midline in some segments (arrowhead, F) with lateral displacement in others (arrow, F), or even yet still severe defasciculation and midline crossing (G). Collapse of the axons tract toward the midline is more obvious in some *mys^l* embryos (H) than observed in others (refer to Figure 3.3O).



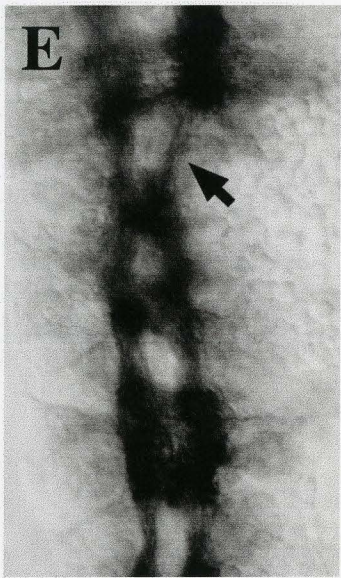
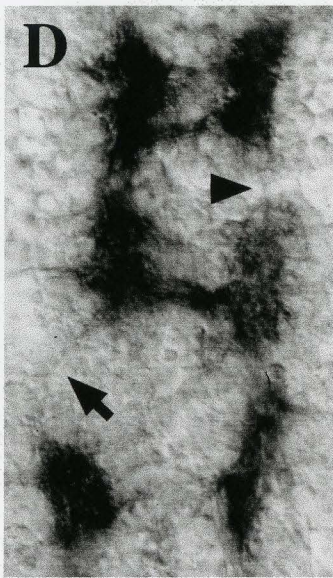
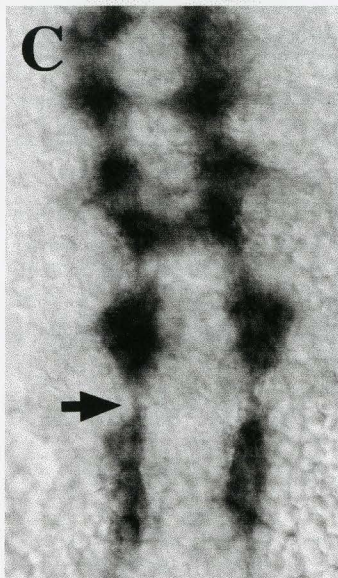
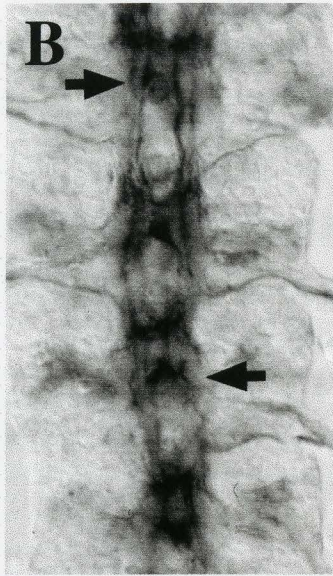
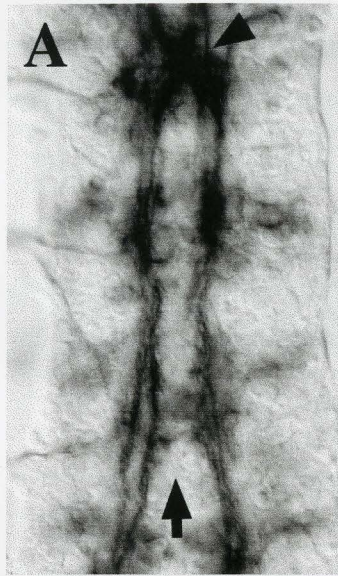
Appendix Figure 15 **Other phenotypes observed with**
***netrin*/FM7c β ; *slit* /CyO[*eng*] stable double mutant fly lines.**

Nerve cords are immunolabelled with mAb 1D4. Reduced copies of *netrin* (Df(1)KA9) and *slit* (*slit*²) results in a range of phenotypes, including those that demonstrate crossovers of all three fascicles (A) to those displaying only weak midline crossovers (arrow, B). The most moderate of these phenotypes is shown in Figure 5.2C. These phenotypes likely represent KA9/FM7c β ; *slit*²/CyO[*eng*] genotype.



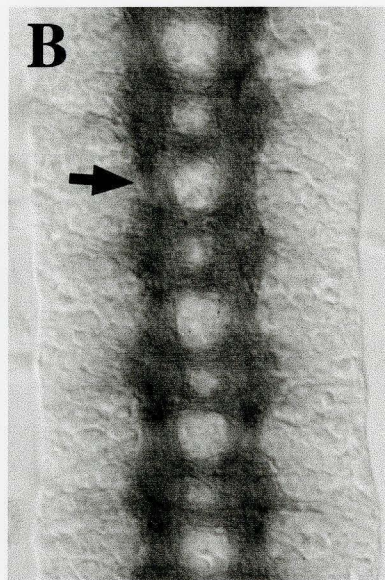
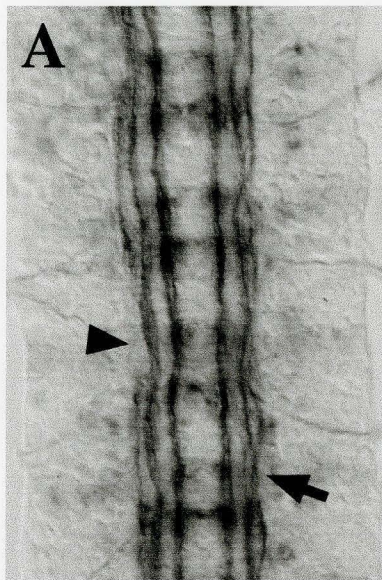
**Appendix Figure 16 Other phenotypes observed in *slit*/CyO;
commissureless/TM3 double mutant fly lines.**

Nerve cords are immunolabelled with mAb 1D4 (A, B) and mAb BP102 (C-E). *slit*²⁹⁹⁰; *comm*^{a490} double mutants produce a phenotype whereby some segments form FasciclinII-positive connections across the midline (refer to Figure 5.3C). *slit*²⁹⁹⁰/CyO; *comm*^{a490} mutants exhibit a similar phenotype, but narrow toward the midline (arrow, A) with occasional crossovers (arrowhead, A). *slit*²⁹⁹⁰/CyO; *comm*^{a490}/TM3 mutants display thin longitudinal tracts with frequently crossing axons across the midline (arrows, B). The phenotypes in A and B represent 38% (n=514) of embryos. Commissure formation is also aberrant in these mutants, as some segments form commissural connections while others do not (refer to Figure 5.3D). *slit*²⁹⁹⁰/CyO; *comm*^{a490} BP102-stained mutants in this collection produce similar phenotypes but display thinner longitudinal connections (arrow, C) or breaks (arrowhead, D) with lateral displacement of the longitudinal tracts (arrow, D). The phenotypes in C and D represent 20.5% (n=356) of embryos. *slit*²⁹⁹⁰/CyO; *comm*^{a490}/TM3 demonstrate a narrowed nerve tract with thinner longitudinals (arrow, E) in 6.5% of embryos.



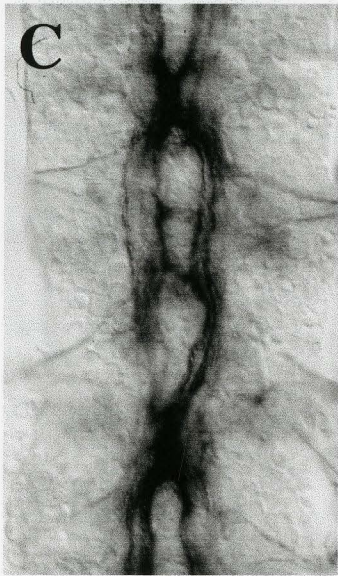
Appendix Figure 17 *robo1¹* and *dock^{P1}* demonstrate a weak genetic interaction in trans.

Nerve cords are immunolabelled with mAb 1D4 (A) and mAb BP102 (B). *robo1¹/dock^{P1}* transheterozygotes demonstrate a weak genetic interaction with 1D4 (A), as the two lateral-most fascicles wander aberrantly between pathways (arrow), with occasional absence of the lateral-most fascicles in some segments (arrowhead). The medial fascicle remains unaltered in these mutants. No apparent mutant phenotype is observed in these transheterozygotes when viewed with BP102 (B).



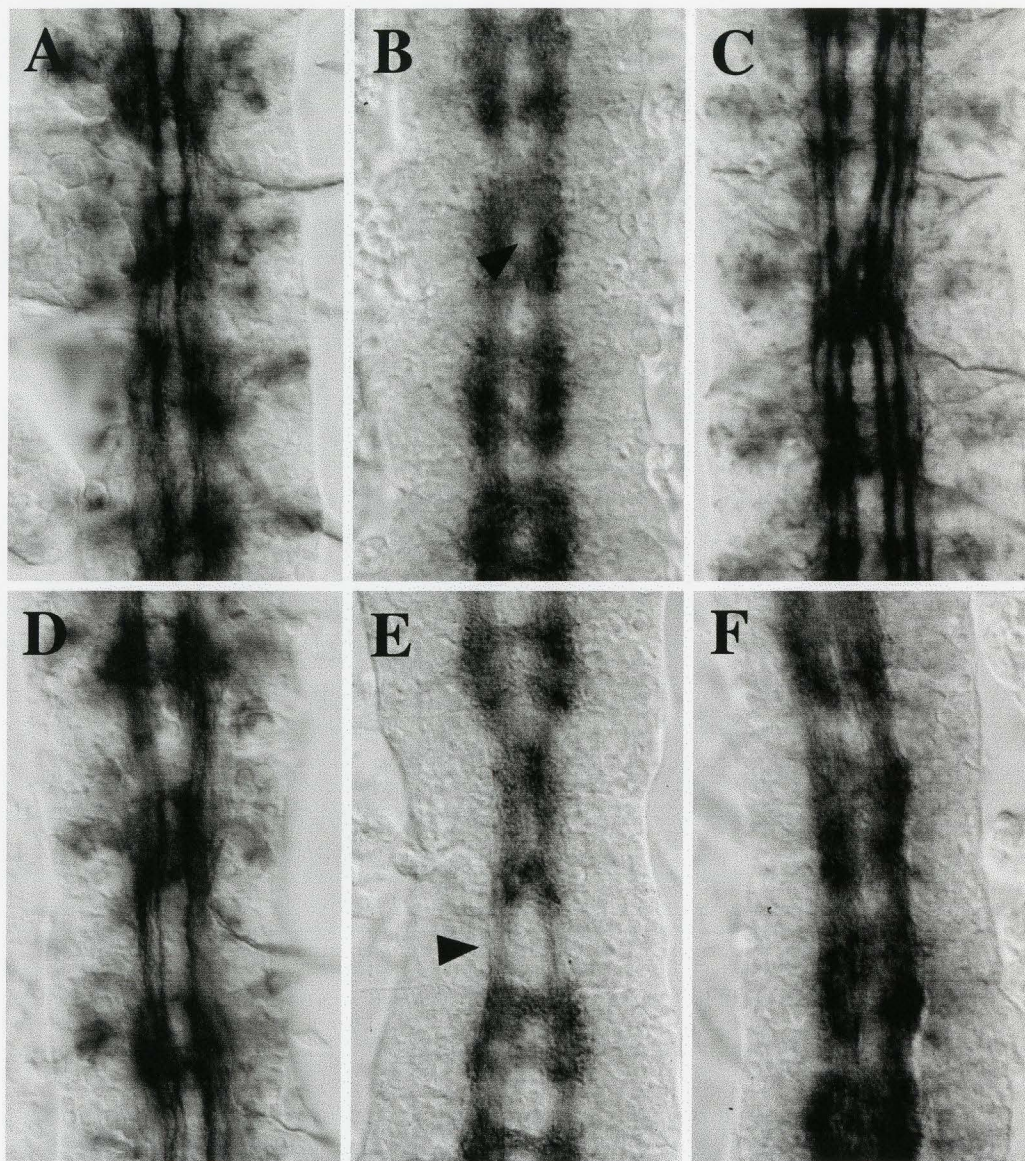
Appendix Figure 18 **Other phenotypes observed in *dreadlocks*,
slit /CyO[eng] stable double mutant fly lines.**

Nerve cords are immunolabelled with mAb 1D4 (A, C) and mAb BP102 (B, D). *dock^{P1}*, *slit²⁹⁹⁰* homozygous recombinants display a collapsed phenotype like that of *slit²⁹⁹⁰* (A). These embryos, however, demonstrate fuzzy commissures (arrow, B) and absent longitudinal connections in some segments (arrowhead, B). *dock^{P1}*, *slit²⁹⁹⁰*/CyO[eng] heterozygous recombinants display a range of crossover severity (compare C to Figure 5.4E) and collapse of commissures (compare D to Figure 5.4F).



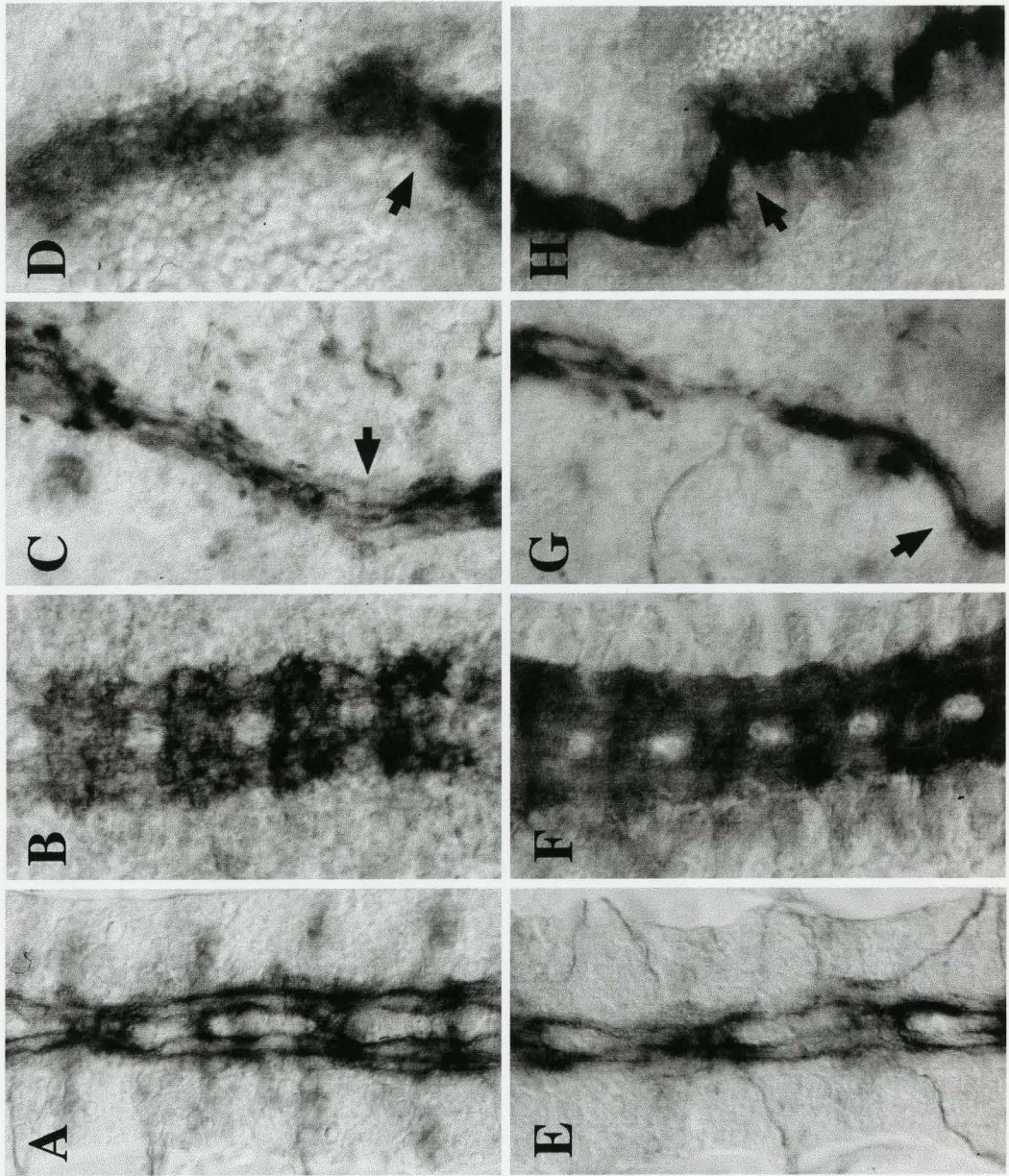
Appendix Figure 19 **Other phenotypes observed in *slit*/CyO;
lamininA/TM3 stable double mutant fly lines.**

Nerve cords are immunolabelled with mAb 1D4 (A, C, D) and mAb BP102 (B, E, F). *slit²⁹⁹⁰/CyO; lamA⁹⁻³²/TM3* mutant embryos demonstrate narrowing of longitudinal axon tracts toward the midline with mAb 1D4 (A) yet commissures remain defined when viewed with BP102 (arrowhead, B) in 18% (n=175) and 16.1% (n=242) of embryos, respectively. *slit²/CyO; lamA⁹⁻³²/TM3* mutants demonstrate midline crossovers in at least one segment (C) but more often in many (refer to Figure 5.5E). These phenotypes are seen in 39.1% (n=197) of embryos. Some of these embryos also display midline narrowing (D). Midline narrowing is often more apparent in BP102-stained *slit²/CyO; lamA⁹⁻³²/TM3*, concurrent with thin longitudinal axon tracts (arrowhead, E). In others (F), midline narrowing is more consistent along the length of the embryo, although not as severe as E. The phenotypes in E and F represent 22.3% (n=278) of embryos.



Appendix Figure 20 **Other phenotypes observed with *slit*/CyO;
masquerade /TM3 stable double mutant fly lines.**

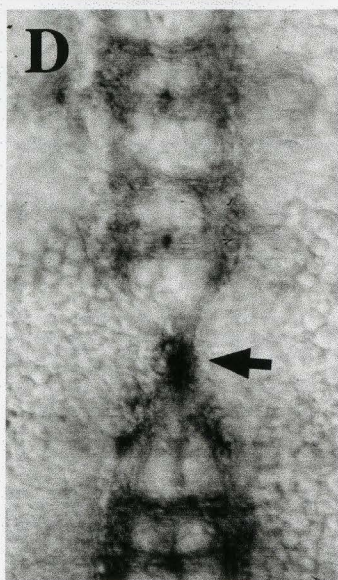
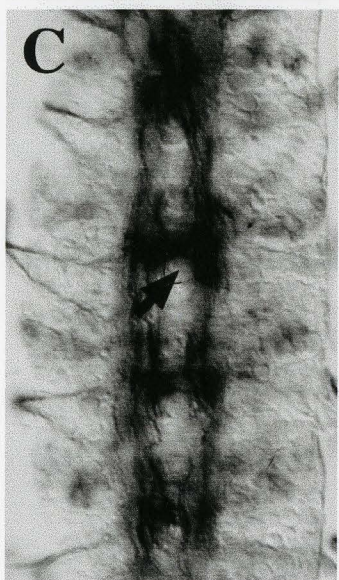
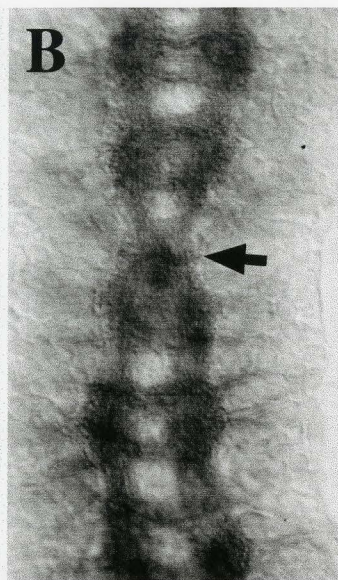
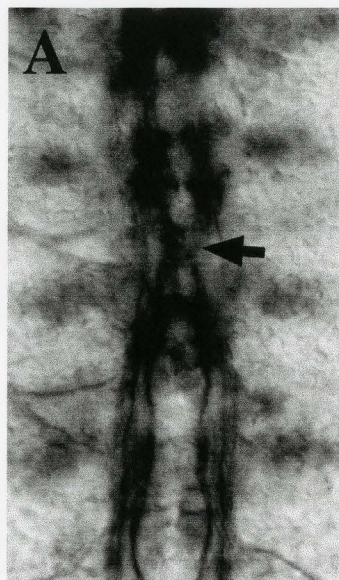
Nerve cords are immunolabelled with mAb 1D4 (A, C, E, H) and mAb BP102 (B, D, G, I). Some *slit*²⁹⁹⁰/CyO; *mas*^{x124}/TM3 mutants display midline crossovers in some segments (A), while other embryos display a fusion of midline fascicles in some segments (refer to Figure 5.7C). These embryos represent 10.3% (n=632) of the collection. Other *slit*²⁹⁹⁰; *mas*^{x124} mutants (likely *slit*²⁹⁹⁰/CyO; *mas*^{x124} and CyO; *mas*^{x124} or only CyO; *mas*^{x124}) have fuzzy commissures (B). These embryos represent 39.4% (n=426) of the collection. *slit*²⁹⁹⁰; *mas*^{x124} homozygotes (C, D) display a *slit*²⁹⁹⁰ phenotype with extreme kinks in the nerve cord (arrows). *slit*²/CyO; *mas*^{x124}/TM3 mutants (E) display a more severe and narrowed midline crossing phenotype than *slit*²⁹⁹⁰/CyO; *mas*^{x124}/TM3 (compare with A). These embryos represent 12.2% (n=662) of the collection. 4.9% (n=313) of BP102-labeled embryos (F) likewise demonstrate a similar fuzzy commissure phenotype as observed in B. *slit*²; *mas*^{x124} homozygous double mutants (G, H) display a *slit*² phenotype and kinks in the nerve cord (arrows) also shown in C and D.



Appendix Figure 21 **Other phenotypes observed by *multiple edematous wings*/FM7cβ; *slit* /CyO[*eng*] stable double mutant fly lines.**

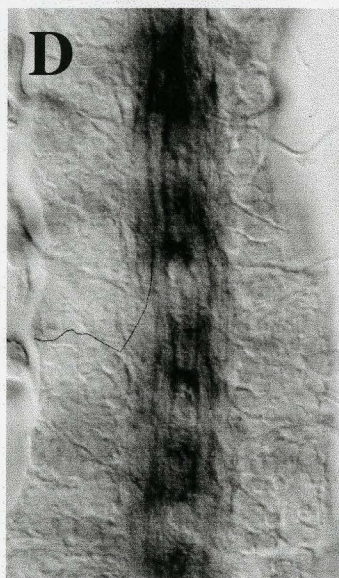
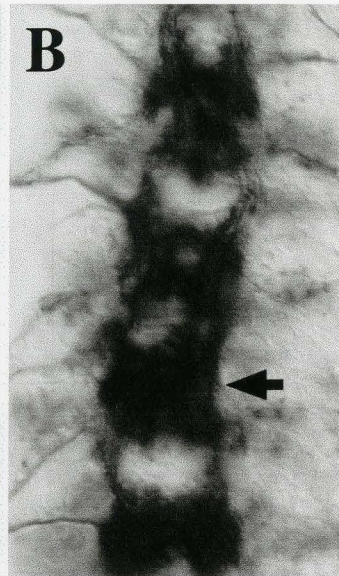
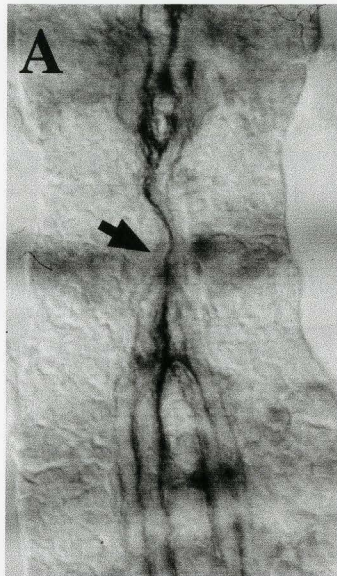
Nerve cords are immunolabelled with mAb 1D4 (A, C) and mAb BP102 (B, D).

mew^{M6}/Y; slit²⁹⁹⁰/CyO[eng] embryos display midline crossing of FasII-positive axons in some embryos (arrow, A) and a more severe midline fusion in others (refer to Figure 5.8C). These embryos represent 8.3% (n=228) of mutants. When viewed with BP102, 14.7% (n=313) of embryos display CNS defects. *mew^{M6}/Y; slit²⁹⁹⁰/CyO[eng]* embryos exhibit a segmental collapse (Figure 5.8D), or a narrowing of the ladder in at least one segment (arrow, B). *mew^{M6}/Y; slit²/CyO[eng]* mutants demonstrate narrowing and more frequent crossing of axons (refer to Figure 5.8E) and weak segmental crossovers (arrow) and occasional midline fusion (C). These phenotypes represent at least 15.1% (n=73) of embryos, although more frequent representation in collections has been observed (see text). *mew^{M6}/Y; slit²⁹⁹⁰/CyO[eng]* mutants (Figure 5.8F) demonstrate a narrowed nerve cord phenotype, or a midline collapse of at least one segment (arrow, D). These embryos represent 5.5% (n=308) of the collection.



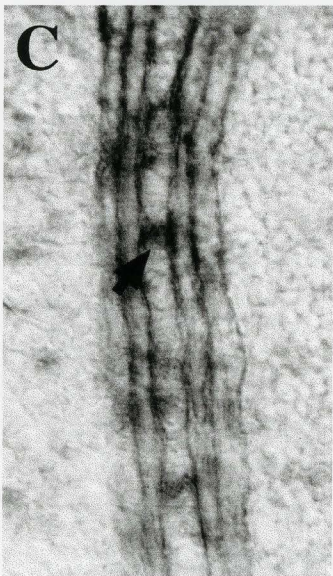
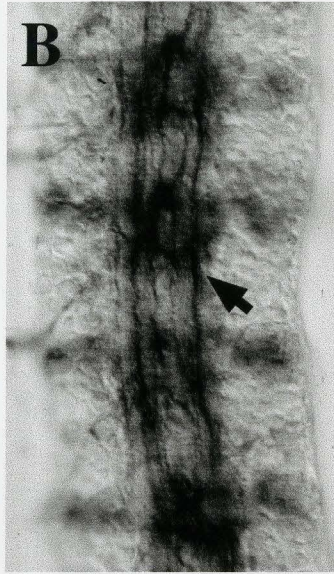
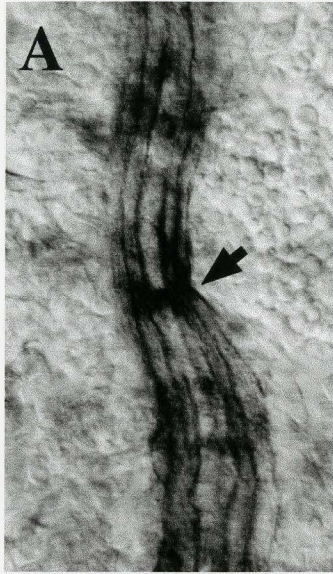
Appendix Figure 22 **Other phenotypes observed in**
***inflated*/FM7cβ; *slit* /Cyo[eng] double mutant fly lines.**

Nerve cords are immunolabelled with mAb 1D4. Some *if^{27e}/Y*; *slit²⁹⁹⁰/CyO[eng]* mutants display fusion of fascicles at the midline (arrow, A) while others show repeated aberrant midline crossing of axons (refer to Figure 5.9B). *if^{27e}/Y*; *slit²/CyO[eng]* mutants display a wide range of defects, from repeated midline crossing of axons (refer to Figure 5.9C), to staining of FasII-positive clumps of axons at the midline (arrow, B), to variable crossing across the midline (C). Only mild crossing of medial fascicles is shown in D and is representative of *if^{27e}/FM7cβ*; *slit²/CyO[eng]*.



Appendix Figure 23 **Other phenotypes observed in**
***myspheroid*/FM7cβ; *slit* /CyO[eng] double mutant fly lines.**

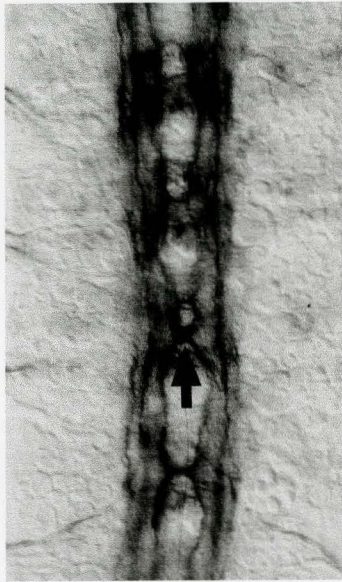
Nerve cords are immunolabelled with mAb 1D4 (A-C) and mAb BP102 (D). Although a strong genetic interaction between *mys^l* and *slit²⁹⁹⁰* produces a phenotype similar to *slit²* mutants (refer to Figure 5.5C), some embryos within that collection demonstrate aberrant midline crossing (arrows, A and B) that are not as severe as *slit²⁹⁹⁰*. These mutants are representative of *mys^l/Y; slit²⁹⁹⁰/CyO[eng]* (A) and *mys^l/FM7cβ; slit²⁹⁹⁰/CyO[eng]* (B) and occur with a frequency of 25% (n=57) in the population. *mys^l/FM7cβ; slit²/CyO[eng]* mutants (5%, n=59) demonstrate weak midline crossing in some segments (arrow, C) as compared to the stronger midline crossing phenotype exhibited by *mys^l/Y; slit²/CyO[eng]* mutants (refer to Figure 5.10C). These embryos displayed midline fusion of one BP102-stained segment (D) in 8.4% (n=177) of mutants.



Appendix Figure 24 **Other phenotypes observed with *slit*/CyO;
Toll /TM3 stable double mutant fly lines.**

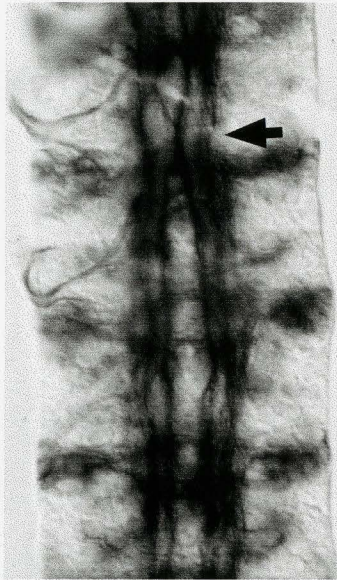
The *slit²⁹⁹⁰/CyO; Tl^{R3}/TM3* genotype is shown, immunolabelled with mAb 1D4. Some embryos demonstrate mild midline crossovers involving the medial fascicle (arrow).

Others (*slit²⁹⁹⁰/CyO; Tl^{R3}*) show a greater severity of midline crossover and fusion (refer to Figure 5.11C). These phenotypes together represent 23.3% (n=257) of the population.



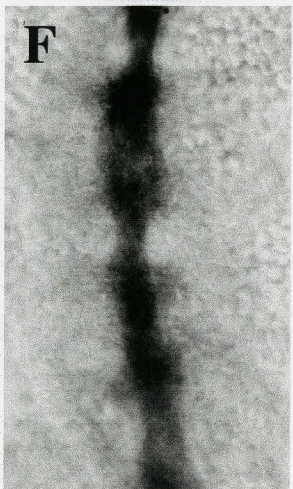
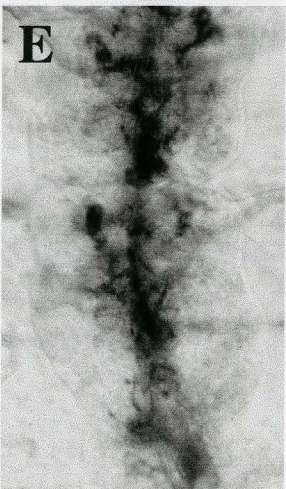
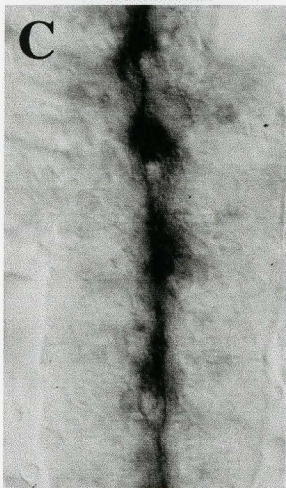
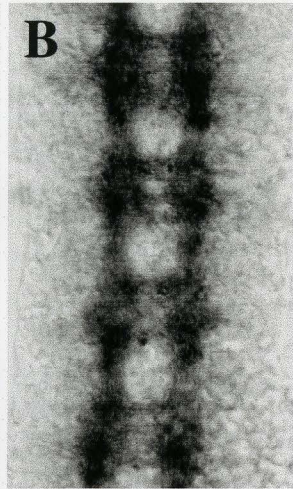
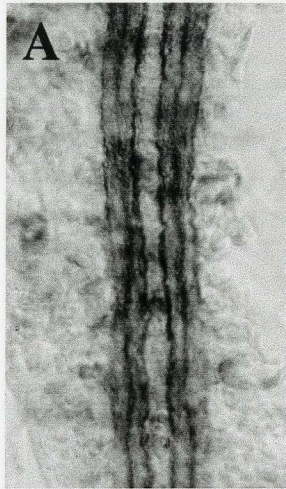
**Appendix Figure 25 Another phenotype observed by *slit*/CyO;
neurexin /TM3 double mutant fly lines.**

The *slit*²⁹⁹⁰/CyO; *nrx*⁴³⁰⁴/TM3 nerve cord is immunolabelled with mAb 1D4. Some mutants demonstrated segmental crossovers (refer to Figure 5.13B) but others demonstrated a fusion of the medial fascicles (arrow) in at least one segment.



Appendix Figure 26 **Immunocytochemical analysis of *central body defect*/FM7c β ; *slit* /CyO[*eng*] stable double mutant fly lines.**

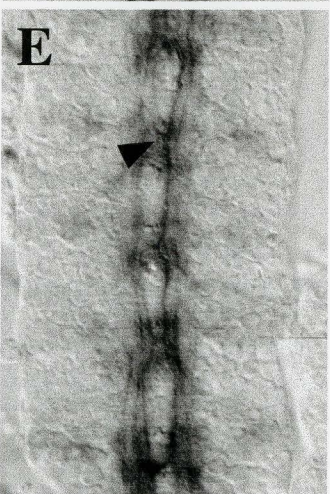
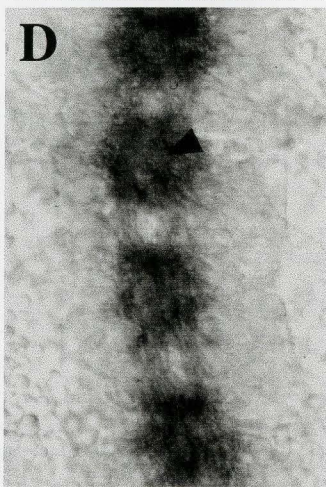
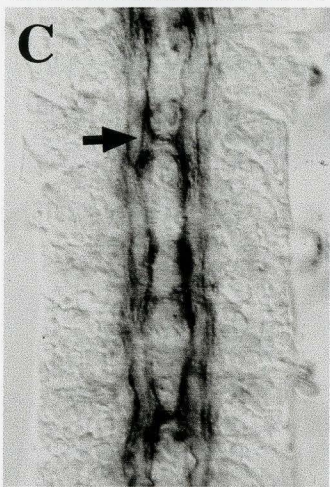
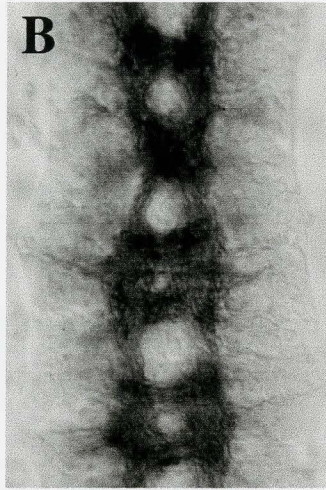
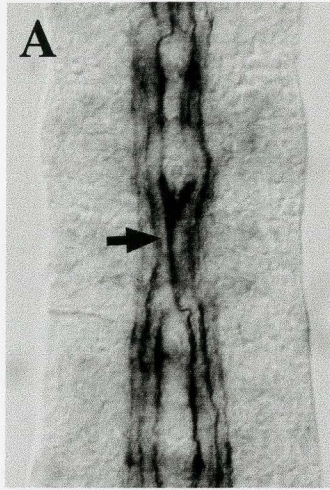
Frontal views of a late stage 16 dissected VNC, immunolabelled with mAb 1D4 (A, C, E) and mAb BP102 (B, D, F). Presumed *cbd*¹ mutants display a nearly wildtype pattern of CNS development (A, B). *cbd*¹; *slit*²⁹⁹⁰ (C, D) and *cbd*¹; *slit*² (E, F) double mutants display phenotypes indistinguishable from *slit*²⁹⁹⁰ and *slit*² mutants, respectively.



Appendix Figure 27 **Other phenotypes observed by *slit/wrapper* genetic interaction.**

Nerve cords are immunolabelled with mAb 1D4 (A, C, E) and mAb BP102 (B, D).

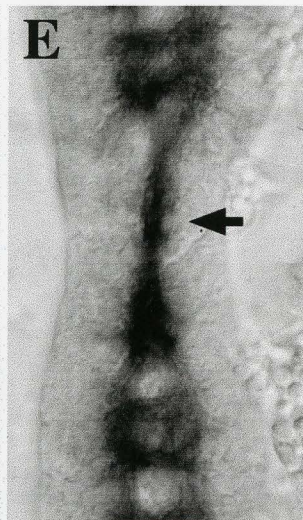
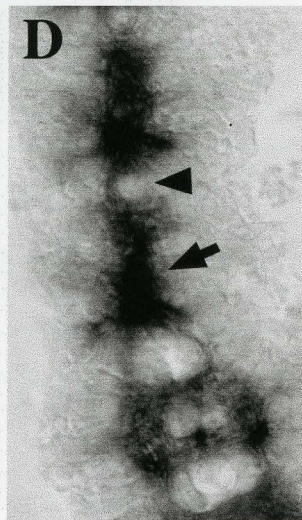
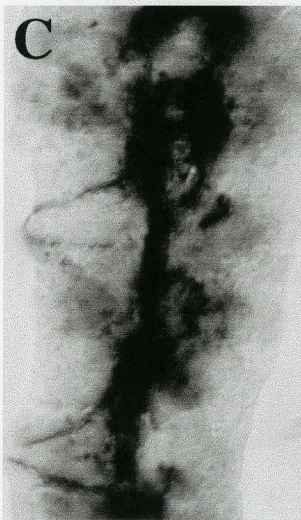
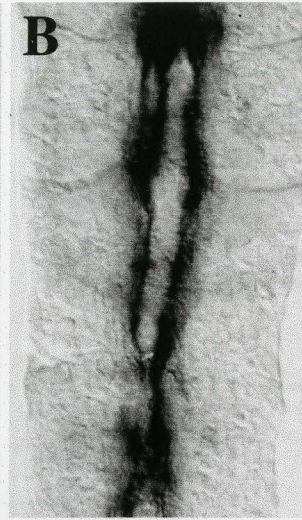
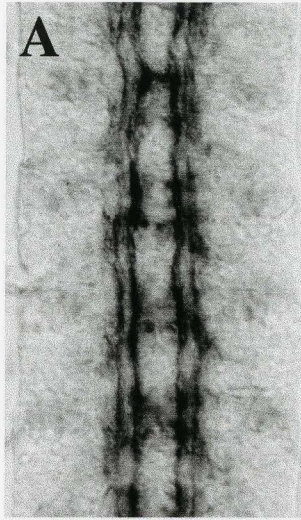
Df(2R)X58-3 uncovers the *wrapper* locus, while Df(2R)X58-12 uncovers the *robo1* and *wrapper* loci. 22% of phenotypic mutants (n=72) in *slit²/Df(2R)X58-3* transheterozygous collection demonstrated a severe *slit*-like phenotype (Figure 6.2A, B) but a larger proportion (78%) demonstrated occasional fusion of medial fascicles at the midline (arrow, A) while other segments appeared wildtype. As a result, these segments look narrowed and some commissures fused (B) when examined with BP102. Likewise, 83.8% of *slit²⁹⁹⁰/Df(2R)X58-3* transheterozygous embryos have mild crossovers in some segments (arrow, C) and a narrowed nerve cord with fuzzy commissures (arrowhead, D). *slit²⁹⁹⁰/Df(2R)X58-12* transheterozygous embryos demonstrate crossovers in most segments (arrowhead, E).



Appendix Figure 28 (A-E)
genetic interactions.

Other phenotypes observed in *scab*

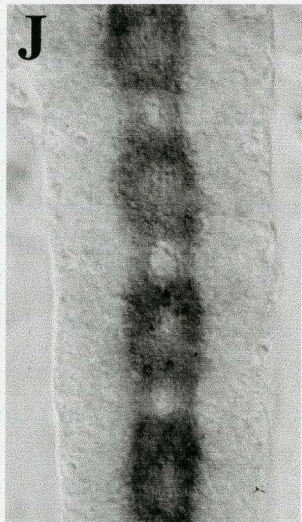
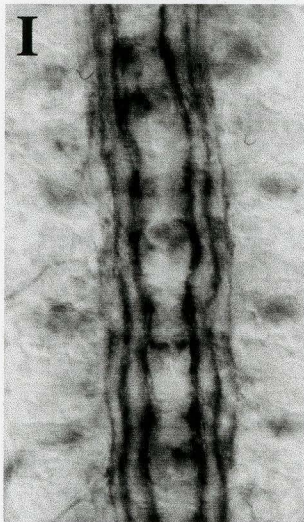
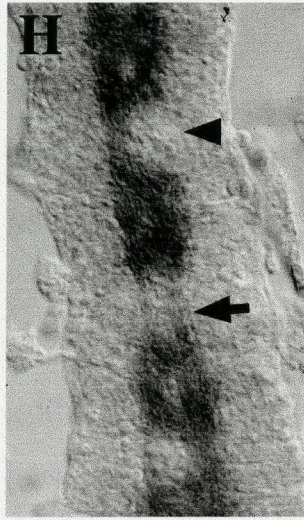
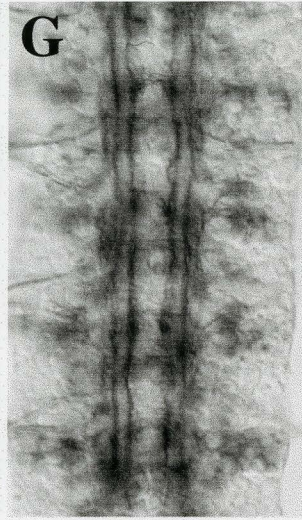
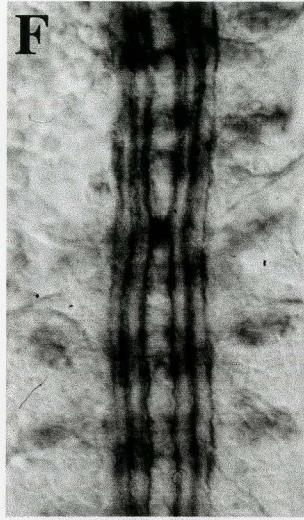
Nerve cords are immunolabelled with mAb 1D4 (A, B) and mAb BP102 (C-E). 50% (n=49) of *scb²/slit²* transheterozygotes display one midline medial fascicle crossover (A), while the remainder 50% demonstrate multiple midline crossovers (Figure 6.3B), crossovers involving at least two fascicles (B) or total midline fusion in some segments (C), although these latter phenotypes were not frequently observed. 40.8% (n=76) of transheterozygotes immunolabelled with BP102 (D) display a collapse of some segments toward the midline (arrow) and thinned or absent longitudinal connections in some segments (arrowhead). In 7.9% of embryos, complete midline fusion was observed in some segments (arrow, E). The majority (51.3%) of embryos, however, demonstrated narrowing toward the midline and poorly separated commissures.



Appendix Figure 28 (F-J)
genetic interactions.

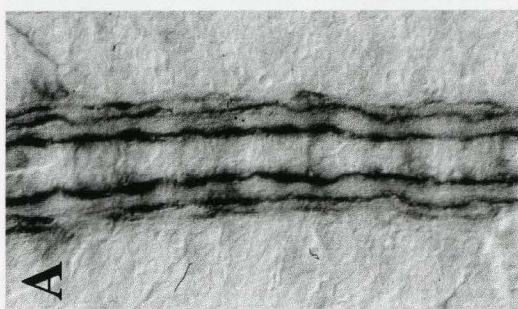
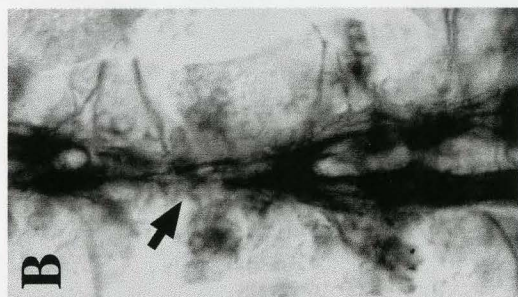
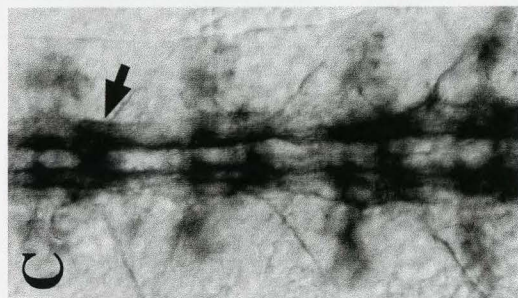
Other phenotypes observed in *scab*

Nerve cords are immunolabelled with mAb 1D4 (F, G, J) and mAb BP102 (H, I, K). Severe *scb²/robo1¹* transheterozygotes (14.5%, n=69) demonstrate midline crossing of axons in some segments (refer to Figure 6.3C), and other embryos display one segmental crossover (F), while others (85.5%) appear near to wildtype although gaps in the lateral fascicle are evident (G). BP102-stained embryos show fuzzy commissures and narrowed nerve cord (refer to Figure 6.4G) but some appear to have more pronounced thinning (arrow, H) or absence (arrowhead, H) of longitudinal axons tracts. Most *scb²/dock^{P1}* transheterozygotes (81.7%, n=77) mostly appear near to wildtype (I), although a significant proportion (18.8%) demonstrate crossovers (refer to Figure 6.4D). *scb²/dock^{P1}* transheterozygotes display defects when visualised with BP102 (refer to Figure 6.3H), others display a narrowed nerve cord and poorly defined commissures (J).



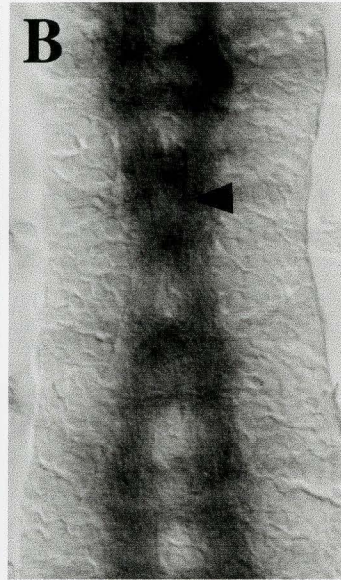
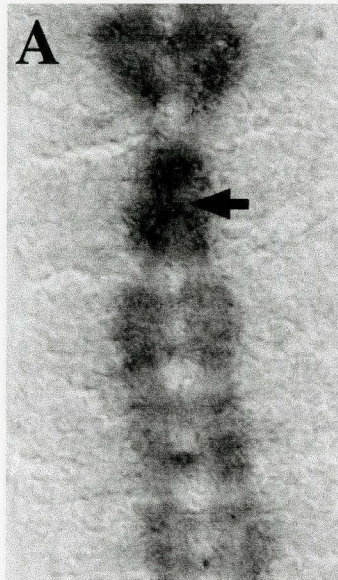
Appendix Figure 29 Other phenotypes observed in *slit/scab* genetic interaction visualised with mAb 1D4.

Frontal views of late stage 16 dissected VNC (A-E) and stage 17 whole mount (F) embryos. 31% (n=139) of *scb²/Df(2R)XTE-18* embryos display midline crossovers (refer to Figure 6.4B), while 69% demonstrate defasciculation and gaps in the lateral fascicle (A). Most *slit²/Df(2R)XTE-18* transheterozygotes (76%) display defasciculation and midline crossovers (refer to Figure 6.4F) but 18% display many crossovers (arrow, B) and 5% demonstrate one midline crossover (arrow, C). Most *scb²/Df(2R)Jp4* transheterozygotes demonstrate frequent midline crossing of FasII-positive fascicles (refer to Figure 6.4C) but some embryos demonstrate less frequent midline crossing (D) or greater narrowing of the VNC (E). These embryos represent 22.7% (n=88) of the population. 11.8% (n=127) of *scb²/Df(2R)Jp1* transheterozygotes display an aberrant midline crossing or fusion of axon bundles in the VNC (refer to Figure 6.4D). Other transheterozygotes (12.6%) in this collection display a twisted VNC that likely also display abnormal midline crossing (F).



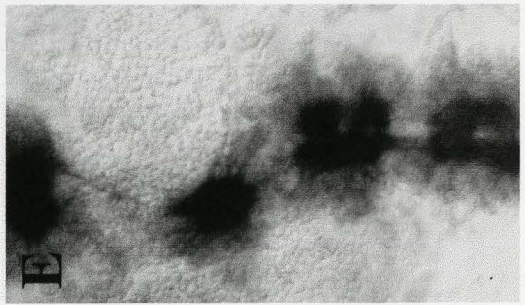
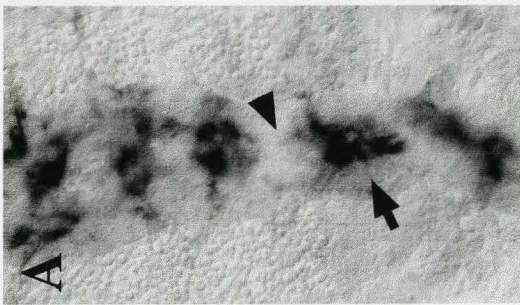
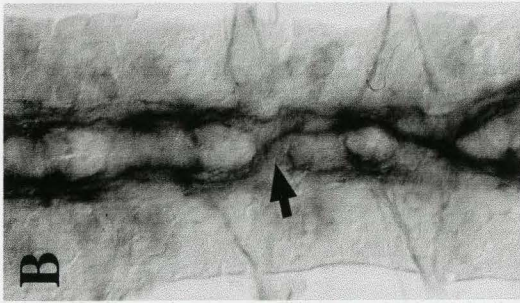
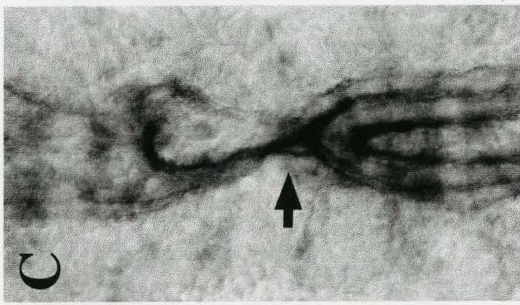
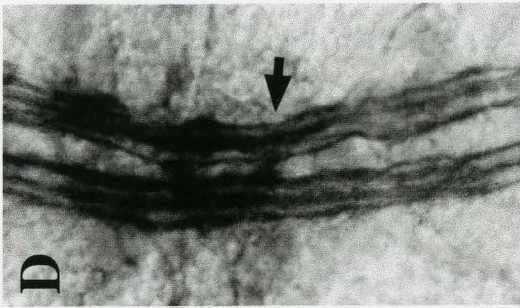
Appendix Figure 30 **Other phenotypes observed in *slit/scab***
genetic interaction visualised with mAb BP102.

Although some *scb²/Df(2R)Jp4* axon tracts display minor commissural and longitudinal defects (refer to Figure 6.4J), some display an obvious segmental collapse toward the midline (arrow, A). These mutants represent 33.9% (n=62) of BP102-stained mutants. Some *scb²/Df(2R)Jp1* mutants (B) were narrow toward the midline in some segments and displayed poorly separated commissures (arrowhead, B), while others displayed narrow, poorly defined commissures and thinned longitudinal tracts (Figure 6.3L).



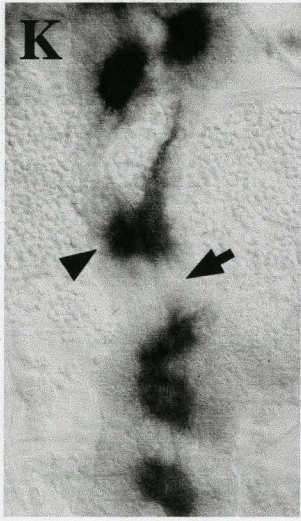
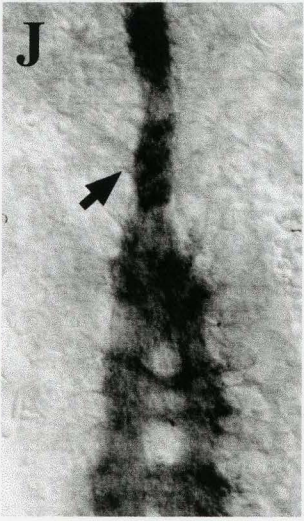
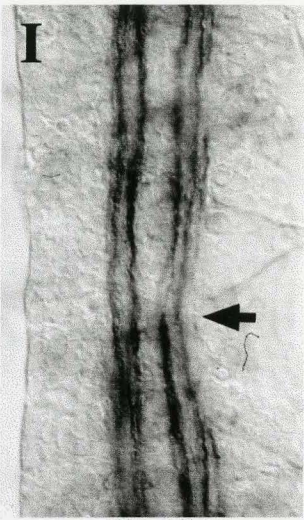
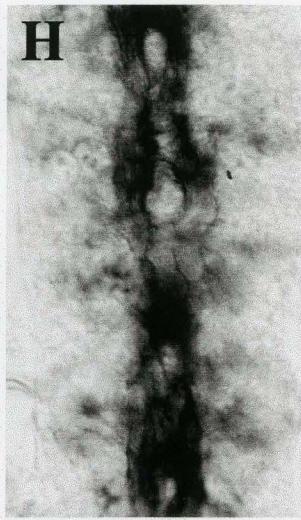
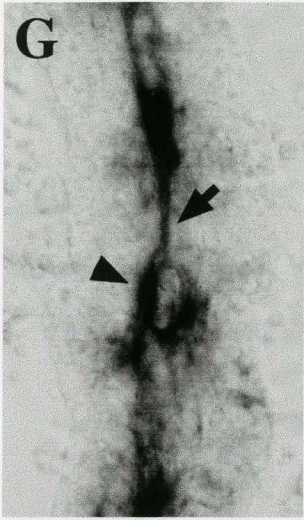
Appendix Figure 31 (A-F) Other phenotypes observed in the triple mutant genetic screen involving the *lamininB1* (Df(2L)Trf-C6R31) locus, *slit* (*slit*²) and *lamininA* (*lama*⁹⁻³²) genes.

Nerve cords are immunolabelled with mAb 1D4 (A-D) and mAb BP102 (E, F). 20% (n=90) of Df(2L)Trf-C6R31/*slit*²; *lama*⁹⁻³²/+ heterozygous mutant embryos from this collection demonstrate crossing and recrossing of medial axon fascicles along the length of the nerve cord (refer to Figure 6.6A). Other embryos in this collection display a range of defects. 17.8% exhibit clumps of FasciclinII-positive axons (arrow, A) and little longitudinal connections between them (arrowhead, A). 16.7% exhibit a range in midline crossovers (arrow, B, C and D) and no collapse toward the midline. With BP102, 6.4% (n=173) of embryos have a narrowed nerve cord and fuzzy commissures (refer to Figure 6.6E). 4.6% of embryos exhibit a phenotype (E) that mirrors the clumps of segmental axons and sparse longitudinal connections observed in A. Others in this group do not show as severe of a midline collapse but display thinned or absent longitudinal tracts (arrow, F).



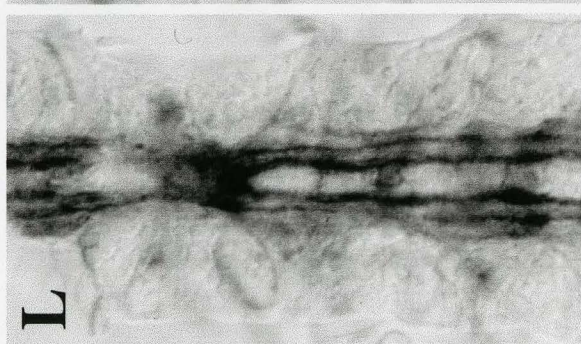
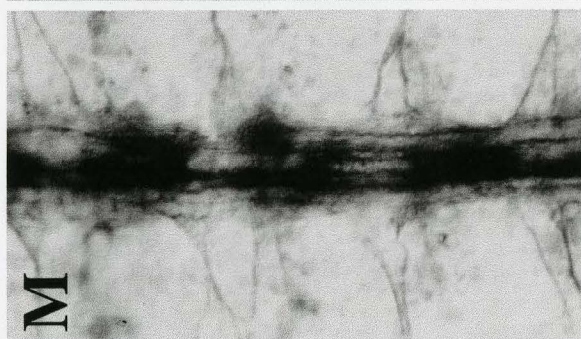
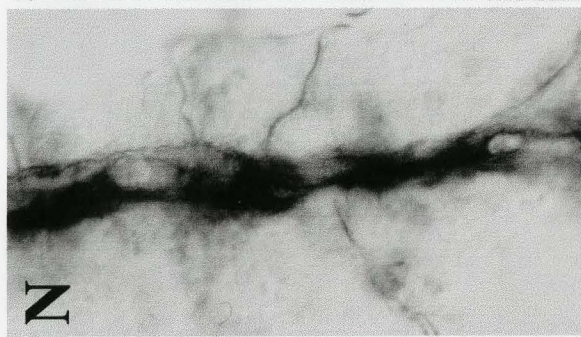
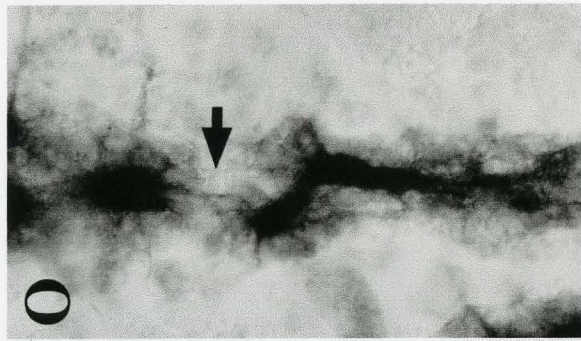
Appendix Figure 31 (G-K) Other phenotypes observed with triple mutant genetic screen involving the lamininB1 (Df(2L)XE-2750) locus, *slit* (*slit*²) and *lamininA* (*lamA*⁹⁻³²) genes.

Nerve cords are immunolabelled with mAb 1D4 (G-I) and mAb BP102 (J, K). Only panel K is not shown at 630x magnification, but rather at 473x. 7.8% (n=129) of embryos from this screen display a phenotype exhibiting midline fusion in some segments and midline crossing of axons in other segments (refer to Figure 6.6B). 10.8% of embryos in this collection (G) demonstrate a more severely fused nerve cord (arrow) with only occasional midline separation (arrowhead). Another 6.2% of embryos (H) display a looping crossover phenotype reminiscent of *robo1*¹ mutants. 27.9% of embryos (I) display nerve cord narrowing in some segments (arrow) and occasional midline crossovers (not shown), similar to Appendix Figure 31D. When observed with BP102, most defects were characterised by a narrowing of the nerve cord and fuzzy commissures in 7.6% (n=276) of embryos (refer to Figure 6.6F). 1.8% observed in this collection displayed midline fusion in some segments (arrow, J). Another phenotype (K) observed in this collection revealed fuzzy commissures (arrowhead) and discontinuous axon tracts (arrow) in 5.8% of embryos.



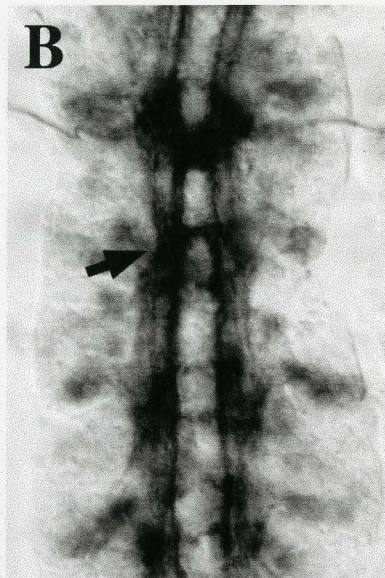
**Appendix Figure 31 (L-O) Other phenotypes observed with
triple mutant genetic screen control cross involving the *slit* (*slit²*) gene and
lamininB1 (Df(2R)XE-2750) locus.**

Nerve cords are immunolabelled with mAb 1D4 (L-N) and mAb BP102 (O). Only panel O is not shown at 630x magnification, but rather at 473x. Although 24.1% (n=87a) of embryos from one transheterozygous collection (ie. *slit²/Df(2R)XE-2750*) demonstrate many midline crossovers (refer to Figure 6.6C), others (41.3%) demonstrate only occasional crossovers (L). In another embryo collection, 13.8% (n=87b) exhibit the phenotype of Figure 6.6C, while others (21.8%) show severe narrowing and medial fusion at the midline (M), or fusion of all fascicles at the midline (N), similar to *slit²* mutants. With BP102, only slight defects are seen in some embryos (refer to Figure 6.6G), while others (O) display a severe collapse of the axon tract at the midline and thinned connections between some segments (arrow).



Appendix Figure 32 Other phenotypes observed with the triple mutant genetic screen involving the *lamininB2* (Df(3L) AC1) locus, *slit* (*slit²*) and *lamininA* (*lamA⁹⁻³²*) genes.

Nerve cords are immunolabelled with mAb 1D4 (A, B) and mAb BP102 (C). 16.9% (n=357) of embryos in this collection displays a phenotype similar to *slit²* mutants (refer to Figure 6.7A), while 21.8% demonstrate a less severe narrowing with crossovers (arrow, A), and 9.2% show no apparent narrowing with crossovers (arrow, B). When observed with BP102, a *slit²* phenotype is observed in 8.1% (n=86) of embryos (refer to Figure 6.7D), while 11.6% display aberrant commissure formation and thinned longitudinal tracts (C).



Appendix Figure 33 **Other phenotypes observed with the triple mutant genetic screen involving the *netrin* (Df(1)NP5) locus, *slit* (*slit*²) and *lamininA* (*lama*⁹⁻³²) genes.**

Nerve cords are immunolabelled with mAb 1D4 (A, B). 2.3% (n=171) of embryos in this heterozygous triple mutant collection displays occasional crossing of axons at the midline (refer to Figure 6.9 A). However, 1.8% display a narrowed nerve cord with medial midline crossovers (A) and 2.3% crossovers involving at least two of the three longitudinal fascicles (arrow, B) in some segments.

